Report No. FAA-RD-76-19

NA-75-180

COPY 1

RD 76/19

APPLICATIONS OF THE SIMULATION MODEL FOR AIR TRAFFIC CONTROL COMMUNICATIONS

J. S. Hunter

D. A. Hsu

NAFEC LIBRARY MAR 7 '77

FEBRUARY 1977

INTERIM REPORT

Document is available to the public through the
National Technical Information Service
Springfield, Virginia 22151

Prepared for

U. S. DEPARTMENT OF TRANSPORTATION

FEDERAL AVIATION ADMINISTRATION

Systems Research & Development Service

Washington, D.C. 20590

NOTICE

This document is disseminated under the sponsorship of the Department of Transportation in the interest of information exchange. The United States Government assumes no liability for its contents or use thereof.

Technical Report Documentation Page

1. Report No.	2. Government Accession No.	3. Recipient's Catalog No.
FAA-RD-76-19		

4. Title and Subtitle	5. Report Date
APPLICATIONS OF THE SIMULATION MODEL FOR AIR TRAFFIC CONTROL COMMUNICATIONS	February 1977
	6. Performing Organization Code
7. Author(s) J. S. Hunter and D.-AHsu	8. Performing Organization Report No. FAA-NA-75-180
9. Performing Organization Name and Address Federal Aviation Administration National Aviation Facilities Experimental Center Atlantic City, New Jersey 08405	10. Work Unit No. (TRAIS)
	11. Contract or Grant No. DOT FA72NA-741
12. Sponsoring Agency Name and Address U.S. Department of Transportation Federal Aviation Administration Systems Research and Development Service Washington, D. C. 20590	13. Type of Report and Period Covered Interim July 1974 - July 1975
	14. Sponsoring Agency Code

15. Supplementary Notes

The analysis reported in this document was performed by the School of Engineering, Princeton University, under DOT/FAA sponsorship, and is the third report under this effort.

16. Abstract

This report contains a review of the GPSS simulation program for air traffic control (ATC) communications, its structure, validation, and applications. The model, constructed using ATC communications data from the New York Center, was checked against ATC communications data from Houston with excellent results. Studies of the applications of the model are described with respect to communications capacity and queuing, the effects of reducing the number of transmissions per transaction, the effects of tone-bursts of different duration, the sensitivity of communication responses to changes in various input variables, etc. The construction of general simulations for sector types, as opposed to individual sectors, is described. (This work may be of special significance to the simulations of oceanic communications performance.) The problems, and some of the progress, in combining sector functions into networks analogous to a communications center are discussed. The multi-dimensional aspects of sector communications are simplified through the construction of new indices. Queuing time analyses and forecasting for ATC communications are reported.

17. Key Words		18. Distribution Statement
ATC Communications	Queing Forecasting	Document is available to the public through the National Technical Information Service, Springfield, Virginia 22151
Simulation	Nonhomogeneous	
Network Modeling	Processes	
Validation		
Sensitivity Analysis		

19. Security Classif. (of this report)	20. Security Classif. (of this page)	21. No. of Pages	22. Price
Unclassified	Unclassified	254	

Form DOT F 1700.7 (8-72) Reproduction of completed page authorized

METRIC CONVERSION FACTORS

Approximate Conversions to Metric Measures

Symbol	When You Know	Multiply by	To Find	Symbol
		LENGTH		
in	inches	*2.5	centimeters	cm
ft	feet	30	centimeters	cm
yd	yards	0.9	meters	m
mi	miles	1.6	kilometers	km
		AREA		
in^2	square inches	6.5	square centimeters	cm^2
ft^2	square feet	0.09	square meters	m^2
yd^2	square yards	0.8	square meters	m^2
mi^2	square miles	2.6	square kilometers	km^2
	acres	0.4	hectares	ha
		MASS (weight)		
oz	ounces	28	grams	g
lb	pounds	0.45	kilograms	kg
	short tons (2000 lb)	0.9	tonnes	t
		VOLUME		
tsp	teaspoons	5	milliliters	ml
Tbsp	tablespoons	15	milliliters	ml
fl oz	fluid ounces	30	milliliters	ml
c	cups	0.24	liters	l
pt	pints	0.47	liters	l
qt	quarts	0.95	liters	l
gal	gallons	3.8	liters	l
ft^3	cubic feet	0.03	cubic meters	m^3
yd^3	cubic yards	0.76	cubic meters	m^3
		TEMPERATURE (exact)		
°F	Fahrenheit temperature	5/9 (after subtracting 32)	Celsius temperature	°C

*1 in = 2.54 (exactly). For other exact conversions and more detailed tables, see NBS Misc. Publ. 286, Units of Weights and Measures, Price $2.25, SD Catalog No. C13.10:286.

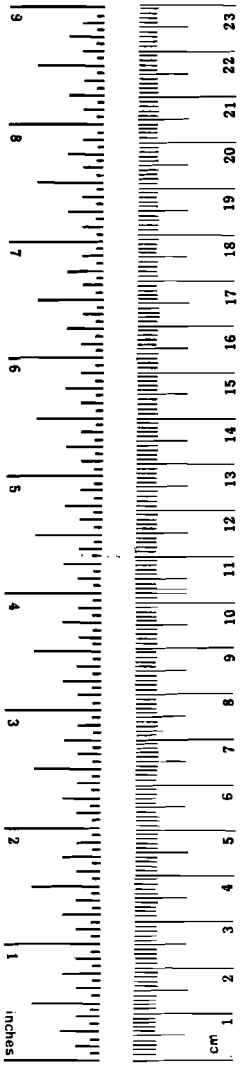

Approximate Conversions from Metric Measures

Symbol	When You Know	Multiply by	To Find	Symbol
		LENGTH		
mm	millimeters	0.04	inches	in
cm	centimeters	0.4	inches	in
m	meters	3.3	feet	ft
m	meters	1.1	yards	yd
km	kilometers	0.6	miles	mi
		AREA		
cm^2	square centimeters	0.16	square inches	in^2
m^2	square meters	1.2	square yards	yd^2
km^2	square kilometers	0.4	square miles	mi^2
ha	hectares (10,000 m^2)	2.5	acres	
		MASS (weight)		
g	grams	0.035	ounces	oz
kg	kilograms	2.2	pounds	lb
t	tonnes (1000 kg)	1.1	short tons	
		VOLUME		
ml	milliliters	0.03	fluid ounces	fl oz
l	liters	2.1	pints	pt
l	liters	1.06	quarts	qt
l	liters	0.26	gallons	gal
m^3	cubic meters	35	cubic feet	ft^3
m^3	cubic meters	1.3	cubic yards	yd^3
		TEMPERATURE (exact)		
°C	Celsius temperature	9/5 (then add 32)	Fahrenheit temperature	°F

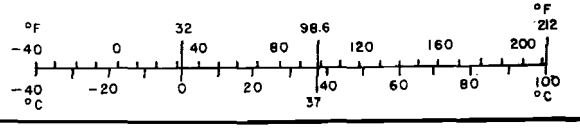

PREFACE

This report, Volume IV of the series on "Modeling Air Traffic Performance Measures," represents the culmination of 3 years investment on the part of the National Aviation Facilities Experimental Center, Federal Aviation Administration and the Transportation Program, Department of Civil Engineering at Princeton University. The initial challenge was to take air traffic communications as recorded on voice tape over the New York Center, and using this raw material to synthesize a statistical-mathematical simulation model that could be put to practical use.

Volume I of this series contains extensive dictionaries and analyses of message elements; Volume II, the initial statistical analyses and early simulation models; Volume III, the construction, validation and initial exercises of the appropriate simulation model.

This volume reviews the simulation model for the New York Air Traffic Control Communications. The validation of the model and the sensitivity of the model to various changes in the input variables is described. The successful use of the model for the Houston Air Traffic Control Communications system is reviewed. Discussions of applications of the model are provided:

(i) for estimating communication capacities for sector types as a function of the aircraft arrival intensity, with particular emphasis on determining when an unstable performance appears,

(ii) for determining the effects of reducing the number of transmissions per transaction,

(iii) for measuring consequences resulting from tone bursts of different lengths.

The model has been used to characterize "general" sector functions (as contrasted with individual sectors). It is anticipated the model may be appropriate for simulating oceanic sector functions. Communication queuing, a response not readily measured in the real world, has been investigated. The many-response character of the communication system has been simplified by the construction of indices. Measures of non-stationary performance are provided along with estimates of the associated probabilities of occurrence. Initial efforts to combine the sector functions into networks are described. Those working on the project believe the present air traffic control simulation model can prove of immediate use, and look forward to its employment.

In the struggle to construct a model descriptive of real world data, many novel theoretical questions arose. The consequence, a happy synergism from the point of view of the university researchers, has been the introduction of several novel statistical tools. Of special mention is the

application of the statistic G, developed by Dr. Der-Ann Hsu, used to test whether the structure of two time series is identical. The use of confidence regions to provide probability statements for the onset of nonstationarity in system performance is, we believe, new. Both these novel applications of statistics should prove widely useful. The study of sector functions has led naturally to the consideration of the ATC Communications as a network, and Markov chain models have been constructed by Mr. Neil W. Polhemus to characterize the aircraft flows in the New York ATC system. This work has stimulated additional theoretical investigations of considerable promise associated with non-homogeneous point process. The subject is of great concern to many transportation scientists.

This project has been a happy coupling of practical problems, real world data, and both the adaptation and development of theory. We give special thanks to Mr. Allen Busch of the FAA for providing cordial, and frank, appraisal and direction to these efforts.

J. Stuart Hunter
Principal Investigator

TABLE OF CONTENTS

		Page
1.	SIMULATION MODEL FOR AIR TRAFFIC CONTROL COMMUNICATIONS	
1.1	Introduction	1-1
1.2	Elements in the Simulation of Air Traffic Control Communications	1-2
1.2.1	Simulation Input Variables	1-2
1.2.2	Simulation Response Variables	1-6
1.3	Validation of the Simulation Model	1-6
1.4	An Application to the Estimation of Sector Communication Capacity	1-7
1.5	Network Analysis	1-7
1.6	Preview of the Following Chapters	1-10
2.	VALIDATION OF A GENERAL SIMULATION MODEL FOR ATC COMMUNICATIONS	
2.1	Introduction	2-1
2.2	Comparison of ATC Communications Performance in New York versus Houston Enroute Sector Functions	2-2
2.2.1	The Data and Their Comparisons	2-2
2.2.2	Analyses of the Number of CT's per Aircraft	2-3
2.3	Validation of Simulations for New York and Houston Sector Functions	2-3
2.4	Summary and Concluding Remarks	2-4
3.	FURTHER APPLICATIONS OF THE SIMULATION MODEL	
3.1	Introduction	3-1
3.2	Estimation of Communications Capacities for New York Sector Functions	3-1
3.2.1	A Theoretical Model for ATC Communications Queuing	3-2
3.2.2	Communications Capacity and Queuing	3-4
3.2.3	Effects of Regulating Communications Transaction Lengths	3-7

TABLE OF CONTENTS (Cont'd)

			Page
	3.2.4	Results of a Simulation Experiment	3-7
	3.2.5	A Special Note on the Capacity of the GN Function	3-12
3.3	Effects of Tone Disturbance upon ATC Communications		3-15
	3.3.1	Simulation Input Variables and the Average Responses	3-15
	3.3.2	Estimation of Average Response at Intermediate Tone Durations	3-16
	3.3.3	Concluding Remarks on the Tone Burst Effect	3-18
3.4	Effects of Changes in Expected Number of TR/CT upon Channel Responses		3-19
	3.4.1	Specification and Estimation of the Transfer Function	3-19
	3.4.2	Results of Simulation Experiments	3-20
3.5	Summary and Concluding Remarks		3-20

4. NETWORK MODELING - NETWORK STRUCTURE, AIRCRAFT ARRIVAL STREAMS, AND SECTOR SEQUENCES

4.1	Introduction		4-1
	4.1.1	Motivation	4-1
	4.1.2	Scope of this Report	4-1
4.2	Network Structure		4-2
	4.2.1	Attributes of the Network	4-2
	4.2.2	Defining Flow on the Network	4-2
4.3	Network Arrivals		4-3
	4.3.1	Arrival Sources	4-3
	4.3.2	Determining Flow Rates on (s, N)	4-3
	4.3.3	Estimation of Arrival Rate Parameters	4-6
	4.3.4	Summary	4-9
4.4	Sector Sequences		4-9
	4.4.1	Definition	4-9
	4.4.2	Initial Distribution of $s_n(0)$	4-10
	4.4.3	Transition Probabilities	4-11
	4.4.4	Estimation of Transition Probabilities	4-14
	4.4.5	Determining the Appropriate Order of Markov Chain	4-16
	4.4.6	Summary	4-17

TABLE OF CONTENTS (Cont'd)

		Page
4.5	Analysis of the New York Enroute Network	4-18
4.5.1	Network Structure	4-18
4.5.2	Modeling Network Arrivals	4-26
4.5.3	Modeling of Traffic Entering Sectors	4-41
4.5.4	Source-Node Transition Probabilities	4-41
4.5.5	Characterization of Sector Sequences	4-46
4.5.6	Relating Sink Attraction Rates to Source Generation Rates	4-62
4.5.7	Summary	4-62
Appendix 4-A	Tabulation of Enroute Sector Traffic	4-64
Appendix 4-B	List of Notations	4-65
Appendix 4-C	References of Chapter 4	4-67
5.	MISCELLANEOUS RELATED STUDIES	
5.1	Introduction	5-1
5.2	Sensitivity Analysis of the Expected ATC Communications Channel Utilization	5-1
5.2.1	Derivation of the Sensitivity Equations	5-2
5.2.2	Concluding Remarks on the Sensitivity Analysis	5-4
5.3	Construction of Operational Indices for ATC Communication Performance	5-4
5.3.1	Some Basic Considerations	5-7
5.3.2	Operational Indices for ATC Communications	5-7
5.3.3	Concluding Remarks on Operational Indices	5-13
5.4	A Transfer Function Model for Aircraft Flows at Adjacent ATC Sectors	5-13
5.4.1	Transfer Functions Representing Dynamic Relationships in a Sequence of Traffic Flow	5-13
5.4.2	Parameterization of the Model	5-15
5.4.3	An Example of Modeling	5-16
5.5	Analysis of New York Eight-Hour Data	5-19
5.6	Queuing Time Analysis and Forecasting for ATC Communications	5-27
5.6.1	Times in System and a Transformation Technique	5-27
5.6.2	Examples from ATC Simulations	5-30

TABLE OF CONTENTS (Cont'd)

	Page
5.6.3 Concluding Remarks on Queuing Time Analysis	5-31
Appendix 5-A References for Section 5.5	5-32
6. CONCLUSIONS AND RECOMMENDATIONS	
6.1 Conclusions	6-1
6.2 Recommendations	6-2

LIST OF TABLES

Table	Title	Page
1.1	Fit of Negative Binomial Distribution to Number of Communications Transactions per Aircraft	1-4
1.2	Average Values of Regression Estimates a_0, a_1 for Gap Lengths in Each Sector Function	1-5
1.3	Transition Matrix from New York Sample Data	1-8
2.1	The Structure of Houston Data	2-5
2.2	Results of Fitting Shifted Negative Binomial Distributions to the Number of Communications Transactions per Aircraft (Houston Individual Sectors)	2-13
2.3	Results of Fitting Shifted Negative Binomial Distributions to the Number of CT/AC (Houston Enroute Functions)	2-17
2.4	Comparison of the Estimates of p and k for Houston and New York Enroute Functions	2-19
2.5	Comparisons of Historical versus Simulated Aircraft Loading Series Generated from Sector Function Simulations (New York Metroplex)	2-20
2.6	Comparison of Historical versus Simulated Channel Utilization Series Generated from Sector Function Simulations (New York Metroplex)	2-21
2.7	Comparison of Historical versus Simulated Aircraft Loading Series Generated from Sector Function Simulations (Houston ARTCC)	2-22
2.8	Comparison of Historical versus Simulated Channel Utilization Series Generated from Sector Function Simulations (Houston ARTCC)	2-23
3.1	Summary Results of the Simulation Experiments for Capacity Study (New York Sector Functions)	3-10
3.2	Estimates of the Communications Capacities for New York Sector Functions	3-13
3.3	$Pr(n_t > k)$ at Various Traffic Densities (LT Sector Function, N.Y. ARTCC)	3-24

LIST OF TABLES (Cont'd)

Table	Title	Page
3.4	$Pr(n_t>k)$ at Various Traffic Densities (LE Sector Function, N.Y. ARTCC)	3-25
3.5	$Pr(n_t>k)$ at Various Traffic Densities (HI Sector Function, N.Y. ARTCC)	3-26
3.6	$Pr(n_t>k)$ at Various Traffic Densities (LC Sector Function, N.Y. Area)	3-27
3.7	$Pr(n_t>k)$ at Various Traffic Densities (LG Sector Function, N.Y. Area)	3-28
3.8	$Pr(n_t>k)$ at Various Traffic Densities (DP Sector Function, N.Y. Area)	3-29
3.9	$Pr(n_t>k)$ at Various Traffic Densities (AD Sector Function, N.Y. Area)	3-30
3.10	$Pr(n_t>k)$ at Various Traffic Densities (AR Sector Function, N.Y. Area)	3-31
3.11	Effects of Tone-Disturbance upon ATC Communications Channels (N.Y. ARTCC, HI Sector Function)	3-32
3.12	Effects of Tone-Disturbance upon ATC Communications Channels (N.Y. ARTCC, LE Sector Function)	3-33
3.13	Effects of Tone-Disturbance upon ATC Communications Channels (N.Y. ARTCC, LT Sector Function)	3-34
3.14	Effects of Tone-Disturbance upon ATC Communications Channels (N.Y. Area, GN Sector Function)	3-35
3.15	Effects of Tone-Disturbance upon ATC Communications Channels (N.Y. Area, LC Sector Function)	3-36
3.16	Effects of Tone-Disturbance upon ATC Communications Channels (N.Y. Area, LG Sector Function)	3-37
3.17	Effects of Tone-Disturbance upon ATC Communications Channels (N.Y. Area, DP Sector Function)	3-38
3.18	Effects of Tone-Disturbance upon ATC Communications Channels (N.Y. Area, AD Sector Function)	3-39

LIST OF TABLES (Cont'd)

Table	Title	Page
3.19	Effects of Tone-Disturbance upon ATC Communications Channels (N.Y. Area, AR Sector Function)	3-40
3.20	Effects of Tone-Disturbance upon ATC Communications Channels (N.Y. ARTCC, HI Sector Function) Average Aircraft Loading	3-41
3.21	Effects of Tone-Disturbance upon ATC Communications Channels (N.Y. ARTCC, HI Sector Function) Average Channel Utilization	3-42
3.22	Effects of Tone-Disturbance upon ATC Communications Channels (N.Y. ARTCC, HI Sector Function) Average Queuing Time	3-43
3.23	Effects of Tone-Disturbance upon ATC Communications Channels (N.Y. ARTCC, LT Sector Function) Average Aircraft Loading	3-44
3.24	Effects of Tone-Disturbance upon ATC Communications Channels (N.Y. ARTCC, LT Sector Function) Average Channel Utilization	3-45
3.25	Effects of Tone-Disturbance upon ATC Communications Channels (N.Y. ARTCC, LT Sector Function) Average Queuing Time	3-46
3.26	Effects of Tone-Disturbance upon ATC Communications Channels (N.Y. ARTCC, LE Sector Function) Average Aircraft Loading	3-47
3.27	Effects of Tone-Disturbance upon ATC Communications Channels (N.Y. ARTCC, LE Sector Function) Average Channel Utilization	3-48
3.28	Effects of Tone-Disturbance upon ATC Communications Channels (N.Y. ARTCC, LE Sector Function) Average Queuing Time	3-49
3.29	Effects of Tone-Disturbance upon ATC Communications Channels (N.Y. Area, GN Sector Function) Average Aircraft Loading	3-50
3.30	Effects of Tone-Disturbance upon ATC Communications Channels (N.Y. Area, GN Sector Function) Average Channel Utilization	3-51

LIST OF TABLES (Cont'd)

Table	Title	Page
3.31	Effects of Tone-Disturbance upon ATC Communications Channels (N.Y. Area, GN Sector Function) Average Queing Time	3-52
3.32	Effects of Tone-Disturbance upon ATC Communications Channels (N.Y. Area , LC Sector Function) Average Aircraft Loading	3-53
3.33	Effects of Tone-Disturbance upon ATC Communications Channels (N.Y. Area , LC Sector Function) Average Channel Utilization	3-54
3.34	Effects of Tone-Disturbance upon ATC Communications Channels (N.Y. Area, LC Sector Function) Average Queuing Time	3-55
3.35	Effects of Tone-Disturbance upon ATC Communications Channels (N.Y. Area, LG Sector Function) Average Aircraft Loading	3-56
3.36	Effects of Tone-Disturbance upon ATC Communications Channels (N.Y. Area , LG Sector Function) Average Channel Utilization	3-57
3.37	Effects of Tone-Disturbance upon ATC Communications Channels (N.Y. Area, LG Sector Function) Average Queuing Time	3-58
3.38	Effects of Tone-Disturbance upon ATC Communications Channels (N.Y. Area, DP Sector Function) Average Aircraft Loading	3-59
3.39	Effects of Tone-Disturbance upon ATC Communications Channels (N.Y. Area, DP Sector Function) Average Channel Utilization	3-60
3.40	Effects of Tone-Disturbance upon ATC Communications Channels (N.Y. Area, DP Sector Function) Average Queuing Time	3-62
3.41	Effects of Tone-Disturbance upon ATC Communications Channels (N.Y. Area , AD Sector Function) Average Aircraft Loading	3-62

LIST OF TABLES (Cont'd)

Table	Title	Page
3.42	Effects of Tone-Disturbance upon ATC Communications Channels (N.Y. Area , AD Sector Function) Average Channel Utilization	3-63
3.43	Effects of Tone-Disturbance upon ATC Communications Channels (N.Y. Area, AD Sector Function) Average Queuing Time	3-64
3.44	Effects of Tone-Disturbance upon ATC Communications Channels (N.Y. Area , AR Sector Function) Average Aircraft Loading	3-65
3.45	Effects of Tone-Disturbance upon ATC Communications Channels (N.Y. Area, AR Sector Function) Average Channel Utilization	3-66
3.46	Effects of Tone-Disturbance upon ATC Communications Channels (N.Y. Area, AR Sector Function) Average Queuing Time	3-67
3.47	Summary Statistics of Simulations for the Study of Tone Disturbance (Duration = 0.0 Seconds)	3-68
3.48	Summary Statistics of Simulations for the Study of Tone Disturbance (Duration = 0.5 Seconds)	3-72
3.49	Summary Statistics of Simulations for the Study of Tone Disturbance (Duration = 1.0 Seconds)	3-76
3.50	Summary Statistics of Simulations for the Study of Tone Disturbance (Duration = 1.5 Seconds)	3-80
3.51	Summary Statistics of Simulations for the Changes in the Expected #TR/CT ($\tilde{K}$=1.0)	3-84
3.52	Summary Statistics of Simulations for the Changes in the Expected #TR/CT ($\tilde{K}$=0.9)	3-88
3.53	Summary Statistics of Simulations for the Changes in the Expected #TR/CT ($\tilde{K}$=0.7)	3-92
3.54	Summary Statistics of Simulations for the Changes in the Expected #TR/CT ($\tilde{K}$=0.5)	3-96

LIST OF TABLES (Cont'd)

Table	Title	Page
3.55	Comparisons of Major Responses at Various Rates of Reduction on #TR/CT (HI Function, N.Y. ARTCC; Expected Traffic Density=60A/HR)	3-23
4.1	Identification of N.Y. Enroute Sectors	4-19
4.2	Traffic from Airports within the New York Region	4-24
4.3	Traffic Breakdown by Class	4-24
4.4	Counts of Departures, Arrivals and Transitions in New York Network	4-27
4.5	Statistics for Arrival and Departure Streams of Major Airports in the New York Region	4-39
4.6	Test Statistics for Poisson Arrivals at Enroute Sectors	4-42
4.7	Estimates of Source-Node Transition Probabilities	4-44
4.8	Tests for Interdependence in Departure Streams	4-47
4.9	New York Enroute Network Transition Counts	4-49
4.10	Arc-arc Transition Matrices with Counts in New York Enroute Network	4-51
5.1	ATC Operational Indices for N.Y. Sector 475 HI at Various Experimental Traffic Densities	5-11
5.2	ATC Operational Indices for Eight N.Y. Sectors at Historical Traffic Densities	5-12

LIST OF ILLUSTRATIONS

Figure	Title	Page
1.1	Schematic Diagram Showing Numbers of Transitions between High Altitude Sectors	1-9
2.1	Estimates of the Parameters of Gamma Distributions Fitted to the Transmission Lengths (New York Data)	2-7
2.2	Estimates of the Parameters of Gamma Distributions Fitted to the Transmission Lengths (Houston Data)	2-8
2.3	Mean versus Standard Deviation of the Transaction Lengths (New York Data)	2-9
2.4	Mean versus Standard Deviation of the Transaction Lengths (Houston Data)	2-10
2.5	Mean versus Standard Deviation of Intertransaction Gap Lengths (New York Data)	2-11
2.6	Mean versus Standard Deviation of the Intertransaction Gap Lengths (Houston Data)	2-12
2.7	Historical Distributions of the Number of Transactions per Aircraft	2-18
3.1	Structure of the Intensity of the ATC Communication Arrivals	3-3
3.2	Lower Bound of the Expected Queuing Time vs C_b (HI Sectors)	3-8
3.3	Channel Utilization as a Function of ac/hr (GN Sectors)	3-14
3.4	Expected Queuing Time as a Function of ac/hr (GN Sectors)	3-14
3.5	Simulated Aircraft Loading Time Series for N.Y. HI Function at 33 A/H and 0.0 Second Tone Duration	3-69
3.6	Simulated Channel Utilization Time Series for N.Y. HI Function at 33 A/H and 0.0 Second Tone Duration	3-70
3.7	Simulated Queue Length Time Series for N.Y. HI Function at 33 A/H and 0.0 Second Tone Duration	3-71
3.8	Simulated Aircraft Loading Time Series for N.Y. HI Function at 33 A/H and 0.5 Second Tone Duration	3-73

LIST OF ILLUSTRATIONS (Cont'd)

Figure	Title	Page
3.9	Simulated Channel Utilization Time Series for N.Y. HI Function at 33 A/H and 0.5 Second Tone Duration	3-74
3.10	Simulated Queue Length Time Series for N.Y. HI Function at 33 A/H and 0.5 Second Tone Duration	3-75
3.11	Simulated Aircraft Loading Time Series for N.Y. HI Function at 33 A/H and 1.0 Second Tone Duration	3-77
3.12	Simulated Channel Utilization Time Series for N.Y. HI Function at 33 A/H and 1.0 Second Tone Duration	3-78
3.13	Simulated Queue Length Time Series for N.Y. HI Function at 33 A/H and 1.0 Second Tone Duration	3-79
3.14	Simulated Aircraft Loading Time Series for N.Y. HI Function at 33 A/H and 1.5 Second Tone Duration	3-81
3.15	Simulated Channel Utilization Time Series for N.Y. HI Function at 33 A/H and 1.5 Second Tone Duration	3-82
3.16	Simulated Queue Length Time Series for N.Y. HI Function at 33 A/H and 1.5 Second Tone Duration	3-83
3.17	Original Probability Function of TR/CT (New York HI Function)	3-21
3.18	The Weighting Function ($\tilde{K}$=0.9)	3-21
3.19	The New Distribution ($\tilde{K}$=0.9)	3-21
3.20	The Weighting Function ($\tilde{K}$=0.7)	3-22
3.21	The New Distribution ($\tilde{K}$=0.7)	3-22
3.22	The Weighting Function ($\tilde{K}$=0.5)	3-22
3.23	The New Distribution ($\tilde{K}$=0.5)	3-22
3.24	Simulated Aircraft Loading Time Series for N.Y. HI Function at 60 A/H and $\tilde{K}$=1.0	3-85
3.25	Simulated Channel Utilization Time Series for N.Y. HI Function at 60 A/H and $\tilde{K}$=1.0	3-86

LIST OF ILLUSTRATIONS (Cont'd)

Figure	Title	Page
3.26	Simulated Queue Length Time Series for N.Y. HI Function at 60 A/H and $\tilde{K}$=1.0	3-87
3.27	Simulated Aircraft Loading Time Series for N.Y. HI Function at 60 A/H and $\tilde{K}$=0.9	3-89
3.28	Simulated Channel Utilization Time Series for N.Y. HI Function at 60 A/H and $\tilde{K}$=0.9	3-90
3.29	Simulated Queue Length Time Series for N.Y. HI Function at 60 A/H and $\tilde{K}$=0.9	3-91
3.30	Simulated Aircraft Loading Time Series for N.Y. HI Function at 60 A/H and $\tilde{K}$=0.7	3-93
3.31	Simulated Channel Utilization Time Series for N.Y. HI Function at 60 A/H and $\tilde{K}$=0.7	3-94
3.32	Simulated Queue Length Time Series for N.Y. HI Function at 60 A/H and $\tilde{K}$=0.7	3-95
3.33	Simulated Aircraft Loading Time Series for N.Y. HI Function at 60 A/H and $\tilde{K}$=0.5	3-97
3.34	Simulated Channel Utilization Time Series for N.Y. HI Function at 60 A/H and $\tilde{K}$=0.5	3-98
3.35	Simulated Queue Length Time Series for N.Y. HI Function at 60 A/H and $\tilde{K}$=0.5	3-99
4.1	ATC Network Diagram	4-4
4.2	Sample ATC Network	4-13
4.3	One-step Transition Matrix	4-13
4.4	The New York ARTCC (1969)	4-20
4.5	New York ARTCC Sector Control Boundaries - High Altitude	4-21
4.6	New York ARTCC Sector Control Boundaries - Low Altitude and Low Transitional (4-19-68)	4-22
4.7	Node-node Incidence Matrix in New York Enroute Network	4-23

LIST OF ILLUSTRATIONS (Cont'd)

Figure	Title	Page
4.8	Schematic Diagram of Enroute Network Traffic Flow	4-25
4.9	Histogram of Interdeparture Times at EWR	4-31
4.10	Histogram of Interarrival Times at EWR	4-32
4.11	Histogram of Interdeparture Times at JFK	4-33
4.12	Histogram of Interarrival Times at JFK	4-34
4.13	Histogram of Interdeparture Times at LGA	4-35
4.14	Histogram of Interarrival Times at LGA	4-36
4.15	Histogram of Interdeparture Times at PHL	4-37
4.16	Histogram of Interarrival Times at PHL	4-38
4.17	Plot of Conditional Uncertainties in Sector Sequences	4-50
5.1	Elasticity Measure η_θ (N.Y. HI Function)	5-5
5.2	Elasticity Measure η_k (N.Y. HI Function)	5-5
5.3	Elasticity Measure η_p (N.Y. HI Function)	5-6
5.4	Operational Index I_a for Aircraft Loading Time Series	5-9
5.5	Operational Index I_b for Channel Utilization	5-9
5.6	Operational Index I_c for Queuing Time	5-10
5.7	A Traffic Stream Through two ATC Sectors	5-14
5.8	Application of the Impulse Response Function	5-14
5.9	Aircraft Loading Time Series for N.Y. LC Sector 513 and DP Sector 535	5-17
5.10	Eight-Hour Aircraft Loading Time Series for N.Y. LC Sector 515	5-20
5.11	Plot of Cumulative Arrival Count vs. Time for LC Sector 515	5-22

LIST OF ILLUSTRATIONS (Cont'd)

Figure	Title	Page
5.12	Plot of Arrival Count in Twenty-Minute Intervals for LC Sector 515	5-22
5.13	Plot of Cumulative Departure Count Versus Time for LC Sector 515	5-23
5.14	Plot of Departure Count in Twenty-Minute Intervals for LC Sector 515	5-23
5.15	Scatter Plot of Pairs of Consecutive Headways in LC Sector 515 Arrival Stream	5-25
5.16	Log Survivor Function for Headways in LC Sector 515 Arrival Stream	5-25
5.17	Scatter Plot of Pairs of Consecutive Headways in LC Sector 515 Departure Stream	5-26
5.18	Log Survivor Function for Headways in LC Sector 515 Departure Stream	5-26

CHAPTER 1

SIMULATION MODEL FOR AIR TRAFFIC CONTROL COMMUNICATIONS

1.1 Introduction

In the continuing effort to construct a useful model for Air Traffic Control (ATC) Communications, the results of data analyses and the construction, validation and applications of a simulation model have been described in detail in the reports:

Modeling Air Traffic Performance Measures

Volume I: Message Element Analyses and Dictionaries

(Report No. FAA-RD-73-147,I)

Volume II: Initial Data Analyses and Simulations

(Report No. FAA-RD-73-147,II)

Simulation Model for New York Air Traffic Control Communications

(Report No. FAA-RD-74-203)

Data used in these reports for modeling ATC communications were collected from the New York area, during a 2-hour peak traffic period, on April 30, 1969. Message contents, origins, frequences and time durations of voice communications transmissions were analyzed and reported in full detail in volume I. Extensive analyses of communication data, on each of the elements comprising the ATC performance, were described in volume II.

In the third volume the structure of a simulation model, based on the New York data file, was described and its generalization presented through the use of various master equations and tables. Validation of the simulation model was performed by comparing generated responses with their historical counterparts through the use, in part, of newly developed statistical techniques. The results of comparisons indicated that the simulation model did operate satisfactorily not only for individual sectors but for sector types as well. Applications of the simulation model were also reported in the third volume. One special example concerns the determination of communications capacity for HI sectors, a study of interest to those investigating oceanic air traffic. The value of the simulation model was especially demonstrated in a study of communications queuing, that is, the frequency and length of time a pilot must wait before he can use the communication channel. There is no direct measure of communications queuing available in the historical data. Other related studies were also presented on the subjects: (i) response coupling; (ii) air traffic control network capacities; (iii) sequential structure of the intercommunication gap lengths; and (iv) the applications of Sichel distribution for number of transmissions (TR) per communications transaction (CT).

Although the studies outlined above are available, to prepare readers for a further discussion in this volume, we now briefly review some terminology and concepts.

1.2 Elements in the Simulation of Air Traffic Control Communications

It is appropriate to describe briefly the characteristics of the ATC communications system. The air space within an airport region is divided into a number of "sectors," each with its own controller. For instance, the New York area contains 101 separate sectors. These sectors are divided into 12 different sector functions, namely, Low Altitude Transitional (LT), Low Altitude Enroute (LE), High Altitude Enroute (HI), Clearance Delivery (CD), Ground Control (GN), Local Control (LC), Local and Ground Control (LG), Approach Control, Non-Radar (AP), Radar Departure Control (DP), Radar Arrival Control (AR), Radar Arrival and Departure Control (AD), and Radar Advisory Position (RA). The sector functions are partitioned into three distinct groups: enroute sectors (LT, LE, HI), tower cab sectors (CD, GN, LC, LG, AP) and IFR room sectors (DP, AR, AD, RA).

Within a sector, and using only a single communication channel, a number of communications are made between the controller and each aircraft pilot within that sector's jurisdiction. A completed conversation between an aircraft in a sector and the controller is termed a "communications transaction" or "CT." Each CT is composed of separate "transmissions" or "TR's" which are made alternatively by pilot and controller. Each TR in turn contains one or more "message elements" or "ME's." Volume I contains extensive dictionaries, listing the ME's comprising individual TR's along with statistics characterizing their time duration and frequency.

1.2.1 Simulation Input Variables

The first input variable required by the simulation model is the aircraft arrival stream entering a sector. It was found that a Poisson process described the pattern of aircraft arrival to a sector adequately for most sectors in the New York area. A Poisson process is the one in which the number of occurrences of an event (e.g. the aircraft arrival) in a unit of time can be represented by the probability model

$$p(j) = e^{-\theta} \cdot \theta^{j} / j! \qquad (1.1)$$

where $p(j)$ is the probability of j occurrences, θ is the arrival rate and $j=0, 1, 2, \ldots$ is the number of aircraft arrivals observed in each time unit.

For each of the aircraft assigned to the control sector, the number of communications transactions (CT's) associated with this aircraft becomes the second input variable. From the analyses presented in volume II, chapter 4, a negative binomial distribution was shown adequate

in describing this variable. In mathematical form, this distribution is

$$p(r) = \binom{k+r-1}{k-1} p^k \quad (1-p)^r, \; r=0,1,2,\ldots (0<p<1), \tag{1.2}$$

where p and k are parameters and p(r) is the probability of r+m CT's per aircraft where m=2 for the enroute sectors and m=1 for others. A master table for the values of p and k estimated from the New York data for each of the sector types is given in table 1.1. Table 1.1 also indicates the χ^2 test statistic for a lack of fit test. The significant lack of fit observed on the LC and AR sectors, indicating the inappropriateness of the negative binomial model, is due to the nonhomogeneous performance of individual sectors within the function. Further discussion on this issue will be given later in this volume.

The third variable requiring specification is the time length between two consecutive CT's for the same aircraft, termed intercommunication gap lengths. The actual procedure for generating this variable for the simulations is complicated. It is determined using two parameters a_o and a_1 relating the intercommunication gap length to the number of CT's per aircraft. A master table for the values of a_o and a_1 is given in table 1.2 for each of the sector types.

An important input variable for a simulation is the length of CT. This variable is a function of the number of TR's per CT and transmission length (TR length). Unfortunately, the number of TR per CT is too irregular to be fitted by any simple mathematical model, and therefore histograms compiled from historical data are used to provide this variable in the simulations. For the second variable, TR length, the gamma distribution proved adequate for representation. This distribution is

$$f(t) = \frac{1}{\lambda^{\alpha}\Gamma(\alpha)} t^{\alpha-1} e^{-t/\lambda} \qquad \begin{array}{l} 0<t<\infty \\ \alpha>0 \;,\; \lambda>0 \end{array} \tag{1.3}$$

where t is the TR length, and α and λ are parameters. In order to determine the values of α and λ for each of the sector types, two simultaneous master equations, relating the values of α and λ to the aircraft arrival rate, were compiled. The following two equations apply to all sectors specified: (The CD, AP and RA sector functions are exceptions due to their small numbers and unique behavior).

$$\begin{array}{lll} \text{(i)} & \alpha \cdot \lambda = 3.70 - 0.0158\,\theta & \text{(General)} \\ & \quad\;\; = 2.97 - 0.0042\,\theta & \text{(LC)} \\ \text{(ii)} & (\alpha - 1)\,\lambda = 2.0 & \text{(General)} \\ & (\alpha - 1)\,\lambda = 1.7 & \text{(GN)} \\ & (\alpha - 1.13)\,\lambda = 1.72 & \text{(DP)} \\ & (\alpha - 1.5)\;\;\lambda = 1.0 & \text{(AD)} \end{array} \tag{1.4}$$

Table 1.1 Fit of Negative Binomial Distribution to Number of Communications Transactions per Aircraft

Sector Function	No. Obs.	$m^{\dagger}$	$\hat{p}$	$\hat{k}$	Degrees of Freedom	χ^2
LT	514	2	0.41	2.36	14	21.07
LE	498	2	0.46	2.30	12	13.89
HI	379	2	0.58	4.03	11	4.14
CD	200	1	0.94	15.87	4	8.30
GN	905	1	0.41	0.88	10	16.15
LC	1075	1	0.71	6.83	11	125.49*
LG	128	1	0.69	6.83	8	10.78
AP	49	1	0.63	2.63	5	7.02
DP	252	1	0.88	30.45	10	7.27
AD	88	1	0.58	4.85	9	8.28
AR	225	1	0.43	4.54	16	33.46*
RA	95	1	0.46	3.01	10	7.72

* Significant lack of fit at the 0.01 level.

† To be comparable to a variable from the negative binomial distribution, subtract m from the actual number of CT/AC.

Table 1.2 Average Values of Regression Estimates a_0, a_1 for Gap Lengths in Each Sector Function

Sector Function		$\bar{a}_0$	$\bar{a}_1$	Sector Function		$\bar{a}_0$	$\bar{a}_1$
LT	(12)*	4.903	-0.109	LG	(5)	4.919	-0.028
LE	(11)	5.579	-0.164	AP	(4)	4.671	0.069
HI	(9)	5.184	-0.083	DP	(6)	4.415	-0.046
CD	(4)	5.600	-0.171	AD	(12)	4.646	-0.048
GN	(13)	4.180	0.162	AR	(6)	4.583	-0.065
LC	(16)	4.673	-0.024	RA	(3)	4.902	-0.048

* Value in the parenthesis indicates the number of sectors in the function specified.

Once again Θ is the expected number of aircraft arrivals per hour. A pair of parameter values α and λ can be obtained, given Θ, by solving these two equations. Altogether, seven input parameters, Θ, p, k, a_o, a_1, α and λ are required to initiate a simulation, plus the appropriate histogram for the number of TR/CT.

1.2.2 Simulation Response Variables

In addition to these input variables, three major responses are generated from each of the simulation exercises. They are (i) channel utilization; (ii) aircraft loading; and (iii) communications queuing. Channel utilization (CU) is defined as the proportion of time the single communication channel is utilized. Usually in our analysis, the channel utilization is computed for each 60-second interval. The time series thus compiled is then used for further analysis. The second response, aircraft loading, is defined as the number of aircraft in a sector at a given time point. As in the case of channel utilization, this response is also averaged for each 60-seconds to form a time series. The third response, not available in the historical records, is of special interest. There are two aspects to this response. One is the number of aircraft waiting to converse with the controller (or conversely, the number of aircraft the controller has to converse with but cannot because he is occupied by other aircraft) at a given time point. The other aspect is the time length an aircraft waits to converse with the controller (the converse also applies) for each CT attempted. These two aspects, the number of waiting aircraft and the queue time, provide information supplementary to the other in the analysis of queuing status. In the simulation 60-second averages of the number of aircraft waiting to converse are compiled as a time series.

1.3 Validation of the Simulation Model

Validation of the simulation model was performed by comparing the generated responses, namely, the aircraft loading and the channel utilization, compiled as time series, with their corresponding historical time series. A test procedure designed to detect the difference of two time series with respect to their structural parameters (the mean, autocorrelation and error variance) was employed to do the comparison more rigorously. Two test statistics were used in this comparison procedure. One is the test statistic $\bar{G}(\underset{\sim}{\psi},\gamma)$ distributed as a χ^2 variable and useful for comparing two time series with respect to their estimated autoregressive parameters and error variances. The other is a test statistic distributed as Student's t appropriate for testing the difference in means of two autocorrelated time series.

Results of validation of the simulation exercise on the individual sector basis (the seven initiating parameters given are unique to the sector being simulated), using typical sectors from each of the eight types of control function considered, were shown in chapter 3 of volume III

for the responses: aircraft loading series and the channel utilization series separately. The resulting statistics indicate that the simulation model successfully reconstructed the dynamic responses of concern. Another simulation exercise on the HI sector type, in which all the seven initiating parameters were obtained from master tables and equations descriptive of the functions, was also examined and shown satisfactory. A continuing study on the validation of sector type simulations for other sector functions is presented in chapter 2 of this volume.

1.4 An Application to the Estimation of Sector Communication Capacity

The simulation model was exercised for sector 475 HI, a representative enroute sector, in an experiment in changing traffic density. The aircraft arrival rate per hour was increased gradually from a level equal to the historical record to, finally, a level constrained by the ceiling of communication channel capacity. Graphs of the generated response time series, the aircraft loading series, the channel utilization series and, most important, the queue lengths series, were presented, in volume III, chapter 4, for each of the traffic densities tried. The onset of the operation instability, or an explosive status, was clearly seen by the sudden leap in the level of the queue length series. The aircraft loading series revealed similar behavior. In addition to this eye inspection of the response series, a test statistic useful for detecting nonstationarity of a time series model was used to indicate the operational instability (unstable or overloaded performance) observed from the aircraft loading series. A continuing discussion on the simulation experiments for communications capacities will be given in chapter 3 of this volume.

1.5 Network Analyses

In order to construct a simulation model that is applicable to a whole airport region, it is necessary to examine the patterns of transfer of aircraft from one sector to another in addition to the within sector characteristics. The historical movements of aircraft between sectors were followed and the numbers of aircraft transferring between all pairs of sectors determined. These observed transitions were then summarized by sector function and are shown in a transition matrix in table 1.3.

More detailed information on the patterns of movement of aircraft between separate sectors was presented in a number of schematic diagrams obtained from further analyses of the data. Figure 1.1 shows an example of one of the schematic diagrams of transitions between various sectors. This work is an extension of the studies on the networks of routes between sectors initially reported upon in chapter 7 of volume II.

Table 1.3 Transition Matrix from New York Sample Data

	Enroute			Tower Cab					IFR Room			
From \ To	LT	LE	HI	CD	GN	LC	LG	AP	DP	AD	AR	RA
LT	184	88	72	0	0	0	0	0	0	7	162	0
LE	31	159	53	0	0	0	2	17	0	16	60	0
HI	79	79	104	0	0	0	0	0	0	0	0	0
CD	0	0	0	0	151	22	0	0	0	0	0	0
GN	0	0	0	40	7	354	0	0	0	0	0	0
LC	11	0	1	0	351	11	0	3	192	25	5	21
LG	0	13	0	0	0	0	2	3	0	10	0	0
AP	4	3	0	0	0	12	10	0	0	0	1	0
DP	159	48	0	0	0	3	0	0	0	1	5	1
AD	4	22	0	0	0	19	9	2	6	1	2	0
AR	1	1	0	0	0	289	0	0	6	2	167	8
RA	1	0	0	0	0	44	0	0	0	0	2	7

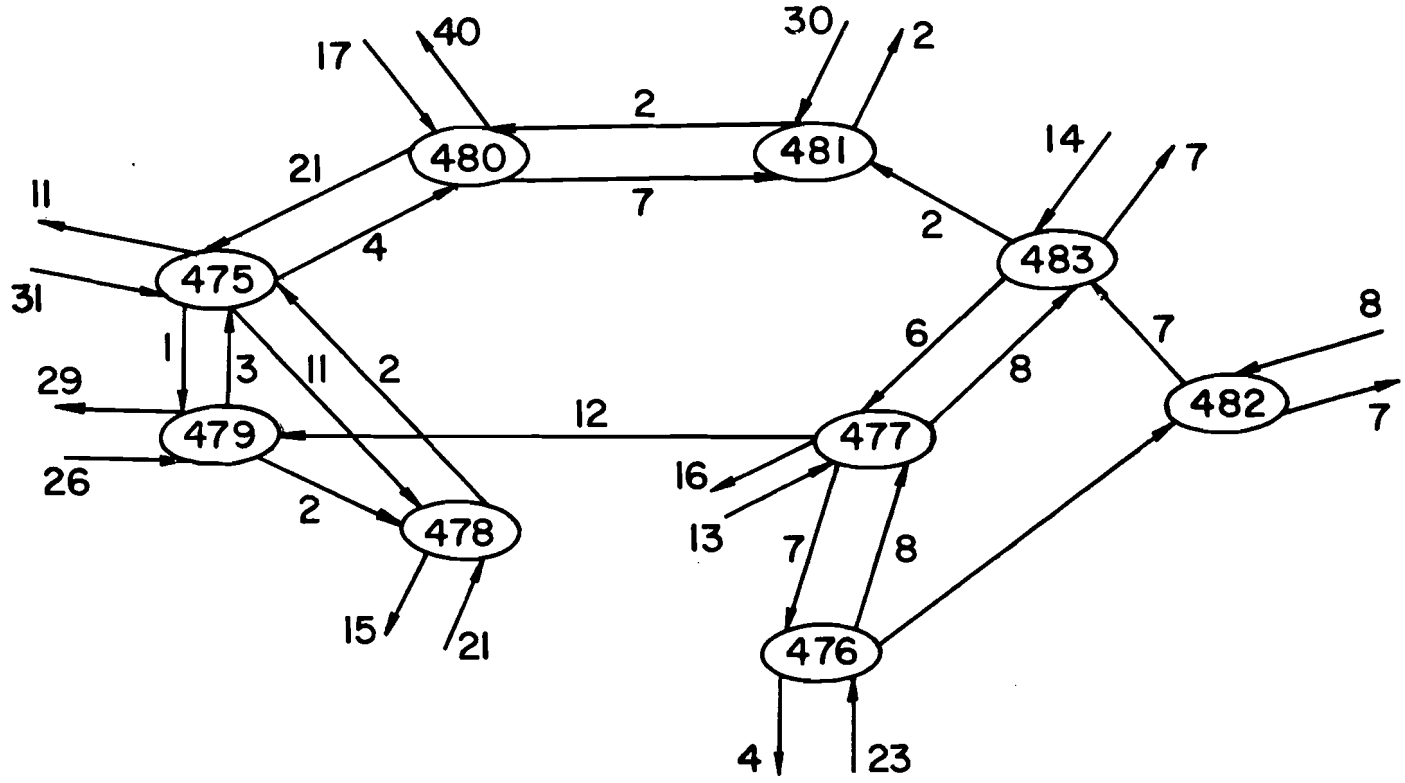

Figure 1.1 Schematic Diagram Showing Numbers of Transitions between High Altitude Sectors

An important network problem presented by the study of sector transitions is the determination of system capacity, given the structure of individual sectors. An initial formulation of the ATC system in network terminology was discussed in chapter 5, section 5.3, of the third volume, and maximum flow algorithms were applied to a sample network. In the present volume a more complete network model that includes the network arrival streams, the formulation of the network structure, and the construction of transition patterns is presented in chapter 4.

1.6 Preview of the Following Chapters

The present volume continues the effort presented in the earlier three volumes listed at the beginning of this chapter, and summarized in the previous sections. One objective is to generalize the framework of the simulation model for adaption to various sector types and geographical characteristics. Further validation on the model for sector type simulations has been accomplished. Applications have been extended to studies on: (i) sector type communication capacities; (ii) effects of a tone-burst scheme for aircraft identification, proposed by FCC; and finally (iii) the influence of hypothesized changes in the number of TR/CT. An extensive analysis of N.Y. ARTCC network structure -- the theoretical formulation, empirical modeling, and tests -- is also discussed in this volume as an initial step toward network simulation modeling. This network framework can hopefully be useful to the study of ATC performance in ocean areas.

In chapter 2 of this volume we first review the sector type simulations defined in the third volume and perform the simulation exercises for nine out of the 12 sector types in N.Y. area. Results indicate that the model can work adequately for all of these sector types given a slight modification on one or two of the input parameters, for some of the sector types. The simulation model is further extended and adapted for distinct geographic characteristics. Using the Houston enroute sector groups as an example, a comparison of various key input parameters for New York versus Houston data has been made to determine which of the input variables should be adjusted. No basic changes in the structure of the simulation model proved necessary. Simulations on Houston sector types are also validated.

Several applications of the sector type simulation model are demonstrated and described in chapter 3. The subjects included are: (i) the estimation of sector type communication capacities for the New York sectors; (ii) the effects of a proposed tone-burst scheme designed to enforce the air traffic control performance; and (iii) the influence of a change in the expected number of TR/CT. The first subject is an extension of the work presented in chapter 4 of the third volume, while the second subject is an interesting realistic exercise of the simulation model. In the latter case, a spline fitting method is used to generate a complete average response surface for the major variables studied. For

the last subject mentioned, an exponential weighting function is used to "improve" the input variable available as historical histograms.

Chapter 4 provides a more complete network model discussing the mathematical model for aircraft arrival streams to the network as well as the second order Markov model for the transition pattern of the aircraft transferring from one sector to another. Extensive network data analysis is given to examine the adequacy of the postulated model.

Miscellaneous related studies are presented in chapter 5. Subjects included are: (i) sensitivity analysis of the expected channel utilization; (ii) the construction of operational indices for ATC performance; (iii) transfer function models for aircraft flows at adjacent sectors; (iv) modeling long-term time series for the inputs and responses of an ATC system; and (v) queuing time forecasting in the ATC communication system.

The last chapter summarizes the conclusions and recommendations made in previous chapters and sections.

CHAPTER 2

VALIDATION OF A GENERAL SIMULATION MODEL FOR ATC COMMUNICATIONS

2.1 Introduction

In simulation modeling, we note that a model, useful in studying responses for a complicated system, can work appropriately only when an adequate set of input variables is provided. All simulation models are constrained to be simplifications of reality. Thus they require input rich in information extracted from both the structure and history of the system. In the ATC simulation model constructed to date, the simulation system starts with seven initiating parameters plus a histogram (for the distribution of #TR/CT). No further inputs are used, or required, to exercise the present model. Subsequent close study has shown that the responses derived from the simulation appear to depend only on those components which can be specified by the seven input parameters. To have included in the ATC simulation program all the details descriptive of an individual ATC sector is logically untenable and computationally too cumbersome.

The ATC simulation procedure consists of two stages: (i) structure and data analysis; and (ii) verification and exercise of the (GPSS) computer program. These two stages are equally important. The ATC structure and data analysis have been described in full detail in volumes I and II. The computer model was explained and illustrated in detail in the third volume, and summarized in chapter 1 of this volume.

In these previous studies, the structure of the simulation model, and the corresponding derivation and use of the initiating parameters, was established and verified using information from individual sectors. The next step of the simulation development was then to construct a useful "general" sector representative of a function. First of all, this required the input parameters extracted from historical data of all the sectors performing a particular function. These are now available as "master tables" and "master equations." From the discussion given in the beginning paragraph of this chapter, a "general" simulation is therefore possible. However, validations are required to examine the usefulness of the "general" model.

The validation of the simulation model for individual sectors was straightforward, since the individual sector data was in hand. However, the validation of the simulation model for sector function encounters the problem of non-homogeneity of performance amongst the individual sectors performing that function. In a few cases, responses provided by the sector function model did not agree well with the corresponding responses for the individual sectors. After much study it was discovered that modest changes in only one or two of the function simulation parameters were required to bring the function and sector responses into compliance. Thus,

although the simulations provided by the function parameters may not always provide response time series sufficiently similar to those available from the individual sectors, the function simulations remain valuable. Further function simulations proved very useful in extension to geographical areas other than New York.

In section 2.2 of this chapter, the data collected from Houston ARTCC (consisting exclusively of the LT, LE and HI enroute sectors) are analyzed and compared against the results with the New York enroute sectors. A great similarity between the regions exists. The only exception in the performance of these two distinct geographical areas concerns the variable #CT/AC. A straight extension of the simulation model to the Houston sector functions is made using entire "master kit" borrowed from N.Y. ARTCC, except for the parameters p and k corresponding to the Houston variable #CT/AC. Results of the validation of this performance presented in section 2.3 indicate the adequacy of the general simulation model for both the N.Y. and Houston areas. The inference that the simulation model is appropriate to geographical areas other than New York is thus sustained.

2.2 Comparison of ATC Communications Performance in New York versus Houston Enroute Sector Functions

In this section ATC communications data collected from 32 New York enroute sectors and 23 Houston enroute sectors are compared. Results of the analyses indicate that the only major difference between New York and Houston ATC communications is with the distribution of the number of communications transactions per aircraft (#CT/AC).

2.2.1 The Data and Their Comparisons

The data of New York sectors were collected and described in volume II for a 2-hour period (20/00/00 - 22/00/00 GMT on April 30, 1969. The Houston data were also recorded for 2-hour periods, and furthermore, repeated for the same sector at different times in a day and/or the same time at different dates. The sampling periods spread between February 17, 1971, and March 5, 1971. Altogether 109 distinct sets of 2-hour data are available. Detailed description of the data structure is given in table 2.1.

Four important variables: (i) transmission lengths; (ii) transaction lengths; (iii) intertransaction gap lengths and (iv) number of CT's per aircraft are analyzed and compared for Houston versus New York enroute sectors. Gamma distributions were fitted to the transmission length data and their parameters estimated. The scatter diagrams of these parameter estimates are shown in figures 2.1 and 2.2 for New York and Houston enroute sectors, respectively. A striking similarity between these two diagrams is observed. Their locations, dispersions and the relationships between the estimates $\hat{\alpha}$ and $\hat{\lambda}$ for both regions are almost identical. Similar comparisons for transaction lengths, as well as the

intertransaction gap lengths are given in figures 2.3 - 2.6. The similarities observed are again remarkable.

However, the distributions of the number of communication transactions per aircraft appear to be different for the LT and HI functions in these two distinct geographical areas.

2.2.2 Analyses of the Number of CT's per Aircraft

Negative binomial distributions were fitted to the Houston data for the number of CT's per aircraft. Details of the parameter estimates for each of the 109 sets of records are displayed in table 2.2. Results from fitting the distribution to the data compiled by sector functions are shown in table 2.3. Histograms of the number of CT's per aircraft are shown for the Houston data in contrast to those of the New York, in figure 2.7. A further list of the estimates of p and k and the expected values is given in table 2.4 for both the Houston and New York data.

In these tables and figures, the nonhomogeneous behavior observed from the Houston HI sectors in the run codes 194H - 217H versus the remainder (data represented by the last 10 run codes were collected from two controller sectors at different periods of time) suggested the separation of the Houston HI sector function into two subgroups. The shapes of the distribution functions and the estimates of p and k, particularly the mean value of the distributions, for these two subgroups, are apparently distinct. A careful inspection of table 2.4 indicates that except for the LE function, the p and k values for N.Y. sectors are different from those of the Houston sectors. A rigorous statistical test for the comparison of two negative binomial variables is complicated and not presented here. For the purpose in hand we consider the distributions to be different and correspondingly adjust the specification of parameter values in the simulations for Houston sector functions as shown in the next section.

2.3 Validation of Simulations for New York and Houston Sector Functions

A general ATC simulation for New York HI sector function has been demonstrated in Chapter 3 of Volume III. In the simulation mentioned, input parameters were generated from various master tables and equations compiled for the N.Y. area . To further explore the general simulation for other sector functions, techniques developed for the comparison of two time series, with respect to their stochastic structures, are again applied to detect possible differences in essential structure between the generated time series responses and their historical counterparts. Since the historical responses can only be observed for individual sectors, not for a sector function as a whole, comparisons of time series generated from a function simulation versus historical time series of individual sectors within the function were carried out in the following fashion. A function simulation using parameters determined by master tables and

equations was first executed and validated against responses observed from a single representative sector within a function. Significant discrepancies, if any, between the simulated and historical responses, were then studied, and adjustment made on the value of the input function simulation parameters. Some individual sectors, exclusively in the terminal sector functions, necessitated adjustments on either the #TR/CT or #CT/AC input variables. With these occasional adjustments, the simulations for a sector function produced responses satisfactorily similar to the historical time series of an individual sector. Results of the final validations of the simulations of nine sector functions of N.Y. area are displayed in tables 2.5 and 2.6.

The master tables and equations compiled from the New York data were then used to perform function simulations for the Houston enroute sector functions. The only changes required in the master tables were the values of p and k, for the distributions of the number of CT's per aircraft. The new values of p and k were estimated from the Houston data. The simulation model gave a surprisingly good performance as seen from the results of validation tests shown in tables 2.7 and 2.8. This suggests the general applicability of the simulation procedure for sector functions in areas other than New York.

Complete statistical tables and figures generated from the New York and Houston simulation programs for the validations of function simulations were compiled along with the historical time series of the individual sectors having been compared. This material is now available in a NAFEC-Princeton University Interim Report (PU-36).

2.4 Summary and Concluding Remarks

A previous simulation model adequate for mimicking the dynamic behavior of an individual ATC sector has been generalized and applied to the function simulations for both New York and Houston areas. Studies on the verifications indicated that the "general" simulation model is rich in information and convenient for use in extensions to varied studies. Only one or two sensitive variables, mostly likely the distributions of #TR/CT or #CT/AC, need to be adjusted in order to extend the simulations to other geographical areas. Much effort is saved by concentrating on tuning one or two input parameters, instead of reconstructing a new model, for the simulations of ATC communications in different geographical areas, as well as for distinct types of simulation studies.

Future experience with more extensive data collected from various environments, such as the ATC systems in the ocean areas, will certainly help develop the present model into an even more mature form.

Table 2.1 The Structure of Houston Data

Sector Identification					Function	Date M/D/Y	Time from	Time to
0100H	HDG	ZHU	1-2R	BFM	LE	021771	160000	180000
0101H	HDG	ZHU	1-2R	BFM	LE	021871	160000	180000
0102H	HDG	ZHU	1-2R	BFM	LE	021971	160000	180000
0104H	HDG	ZHU	1-6R	MOB	LE	022571	210000	230000
0105H	HDG	ZHU	1-6R	MOB	LE	022671	150000	170000
0106H	HDG	ZHU	1-6R	MOB	LE	030171	180000	200000
0107H	HDG	ZHU	1-18R	LCH	LE	022571	210000	230000
0108H	HDG	ZHU	1-18R	LCH	LE	022671	210000	230000
0111H	HDG	ZHU	1-18R	LCH	LE	030471	210000	230000
0112H	HDG	ZHU	1-20R	AEX	LE	021771	190000	210000
0113H	HDG	ZHU	1-20R	AEX	LE	021871	190000	210000
0114H	HDG	ZHU	1-20R	AEX	LE	021971	190000	210000
0116H	HDG	ZHU	1-20R	AEX	LE	030471	210000	230000
0117H	HDG	ZHU	1-8R	MSY/E	LT	021771	160000	180000
0118H	HDG	ZHU	1-8R	MSY/E	LT	021871	160000	180000
0119H	HDG	ZHU	1-8R	MSY-E	LT	021971	160000	180000
0120H	HDG	ZHU	1-8R	MSY/E	LT	030471	210000	230000
0121H	HDG	ZHU	1-8R	MSY/E	LT	030471	150000	170000
0123H	HDG	ZHU	1-12R	MCB	LT	022571	180000	200000
0124H	HDG	ZHU	1-12R	MCB	LT	022671	180000	200000
0126H	HDG	ZHU	1-12R	MCB	LT	030171	210000	230000
0128H	HDG	ZHU	114LR	MSY/SW	LT	022271	220000	000000
0129H	HDG	ZHU	114LR	MSY/SW	LT	022471	220000	000000
0130H	HDG	ZHU	114LR	MSY/SW	LT	030571	150000	170000
0131H	HDG	ZHU	114LR	MSY/SW	LT	030571	180000	200000
0132H	HDG	ZHU	124RR	BPT	LT	022371	150000	170000
0133H	HDG	ZHU	124RR	BPT	LT	022571	150000	170000
0134H	HDG	ZHU	124RR	BPT	LT	030171	150000	170000
0135H	HDG	ZHU	124RR	BPT	LT	030271	150000	170000
0136H	HDG	ZHU	124RR	BPT	LT	030271	180000	200000
0137H	HDG	ZHU	124RR	BPT	LT	030271	210000	230000
0138H	HDG	ZHU	124RR	BPT	LT	030371	150000	170000
0139H	HDG	ZHU	124RR	BPT	LT	030371	180000	200000
0140H	HDG	ZHU	124RR	BPT	LT	030371	210000	230000
0141H	HDG	ZHU	1-26R	HOU/N	LT	022571	180000	200000
0142H	HDG	ZHU	1-26R	HOU/N	LT	022671	180000	200000
0143H	HDG	ZHU	1-26R	HOU/N	LT	030171	180000	200000
0144H	HDG	ZHU	1-26R	HOU/N	LT	030271	150000	170000
0145H	HDG	ZHU	1-26R	HOU/N	LT	030271	180000	200000
0146H	HDG	ZHU	1-26R	HOU/N	LT	030271	210000	230000
0147H	HDG	ZHU	1-26R	HOU/N	LT	030371	150000	170000
0148H	HDG	ZHU	1-26R	HOU/N	LT	030371	180000	200000
0149H	HDG	ZHU	1-26R	HOU/N	LT	030371	210000	230000
0150H	HDG	ZHU	1-30R	HOU/SW	LT	021771	220000	000000
0151H	HDG	ZHU	1-30R	HOU-SW	LT	021871	220000	000000
0152H	HDG	ZHU	1-30R	HOU/SW	LT	021971	220000	000000
0153H	HDG	ZHU	1-30R	HOU/SW	LT	030271	150000	170000
0154H	HDG	ZHU	1-30R	HOU/SW	LT	030271	180000	200000
0155H	HDG	ZHU	1-30R	HOU/SW	LT	030271	210000	230000
0156H	HDG	ZHU	1-30R	HOU/SW	LT	030371	150000	170000
0157H	HDG	ZHU	1-30R	HOU/SW	LT	030371	180000	200000
0158H	HDG	ZHU	1-30R	HOU/SW	LT	030371	210000	230000
0159H	HDG	ZHU	1-32R	HOU/NW	LT	022371	150000	170000
0160H	HDG	ZHU	1-32R	HOU/NW	LT	022571	150000	170000
0161H	HDG	ZHU	1-32R	HOU/NW	LT	030171	150000	170000

Table 2.1 The Structure of Houston Data (cont.)

Sector Identification					Function	Date M/D/Y	Time from	Time to
0162H	HDG	ZHU	1-32R	HOU/NW	LT	030271	150000	170000
0163H	HDG	ZHU	1-32R	HOU/NW	LT	030271	180000	200000
0164H	HDG	ZHU	1-32R	HOU/NW	LT	030271	210000	230000
0165H	HDG	ZHU	1-32R	HOU/NW	LT	030371	150000	170000
0166H	HDG	ZHU	1-32R	HOU/NW	LT	030371	180000	200000
0167H	HDG	ZHU	1-32R	HOU/NW	LT	030371	210000	230000
0170H	HDG	ZHU	2-17R	SKF	LT	022571	180000	230000
0171H	HDG	ZHU	2-17R	SKF	LT	022671	180000	200000
0172H	HDG	ZHU	2-17R	SKF	LT	030171	180000	200000
0173H	HDG	ZHU	2-19R	SAT	LT	021771	190000	210000
0174H	HDG	ZHU	2-19R	SAT	LT	021871	220000	000000
0175H	HDG	ZHU	2-19R	SAT	LT	021971	190000	210000
0176H	HDG	ZHU	2-19R	SAT	LT	030471	210000	230000
0177H	HDG	ZHU	2-19R	SAT	LT	030571	150000	170000
0179H	HDG	ZHU	223LR	BCS	LT	022271	220000	000000
0180H	HDG	ZHU	223LR	BCS	LT	022371	210000	230000
0181H	HDG	ZHU	223LR	BCS	LT	022471	190000	210000
0183H	HDG	ZHU	228LR	MTA	LT	021771	220000	000000
0184H	HDG	ZHU	228LR	MTA	LT	021871	190000	210000
0185H	HDG	ZHU	228LR	MTA	LT	021971	220000	000000
0187H	HDG	ZHU	228LR	MTA	LT	030571	150000	170000
0188H	HDG	ZHU	228PR	AUS	LT	022271	160000	180000
0189H	HDG	ZHU	228PR	AUS	LT	022371	180000	200000
0190H	HDG	ZHU	228PR	AUS	LT	022471	160000	180000
0191H	HDG	ZHU	228PR	AUS	LT	030471	210000	230000
0192H	HDG	ZHU	228PR	AUS	LT	030571	150000	170000
0194H	HDG	ZHU	3-7R	MOB	HI	022271	160000	180000
0195H	HDG	ZHU	3-7R	MOB	HI	022371	180000	200000
0196H	HDG	ZHU	3-7R	MOB	HI	022471	160000	180000
0197H	HDG	ZHU	3-7R	MOB	HI	030571	150000	170000
0198H	HDG	ZHU	3-9R	MSY/HI	HI	022371	150000	170000
0199H	HDG	ZHU	3-9R	MSY/HI	HI	022571	150000	170000
0202H	HDG	ZHU	3-9R	MSY/HI	HI	030571	150000	170000
0203H	HDG	ZHU	3-13R	LCH/HI	HI	022271	190000	210000
0206H	HDG	ZHU	3-13R	LCH/HI	HI	030471	180000	200000
0207H	HDG	ZHU	3-15R	AEX/HI	HI	030571	180000	200000
0208H	HDG	ZHU	3-15R	AEX/HI	HI	022271	190000	210000
0209H	HDG	ZHU	3-15R	AEX-HI	HI	022371	210000	230000
0210H	HDG	ZHU	3-15R	AEX/HI	HI	022471	190000	210000
0212H	HDG	ZHU	3-15R	AEX/HI	HI	030471	210000	230000
0213H	HDG	ZHU	3-19R	HOU/HI	HI	022671	210000	230000
0215H	HDG	ZHU	3-19R	HOU/HI	HI	030471	180000	200000
0216H	HDG	ZHU	3-19R	HOU/HI	HI	030471	210000	230000
0217H	HDG	ZHU	3-19R	HOU/HI	HI	030571	180000	200000
0218H	HDG	ZHU	321LR	AUS/HI	HI	022271	190000	210000
0219H	HDG	ZHU	321LR	AUS/HI	HI	022671	150000	170000
0220H	HDG	ZHU	321LR	AUS/HI	HI	022671	210000	230000
0221H	HDG	ZHU	321LR	AUS/HI	HI	030471	210000	230000
0222H	HDG	ZHU	321LR	AUS/HI	HI	030571	150000	170000
0223H	HDG	ZHU	325RR	SAT/HI	HI	022571	210000	230000
0224H	HDG	ZHU	325RR	SAT/HI	HI	022671	210000	230000
0225H	HDG	ZHU	325RR	SAT-HI	HI	030171	210000	230000
0226H	HDG	ZHU	325RR	SAT/HI	HI	030471	210000	230000
0227H	HDG	ZHU	325RR	SAT/HI	HI	030571	150000	170000

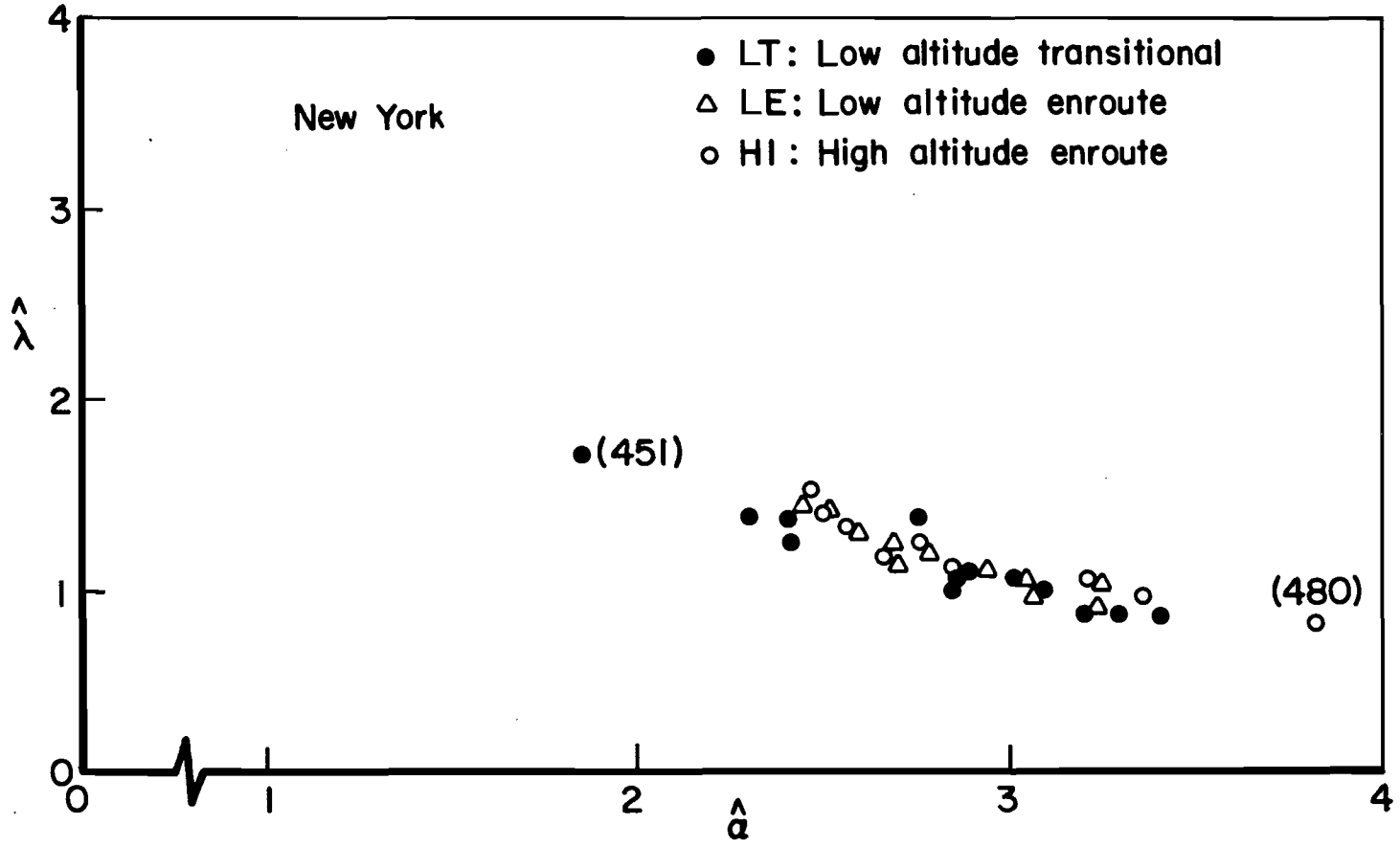

Figure 2.1 Estimates of the Parameters of Gamma Distributions Fitted to the Transmission Lengths (New York Data)

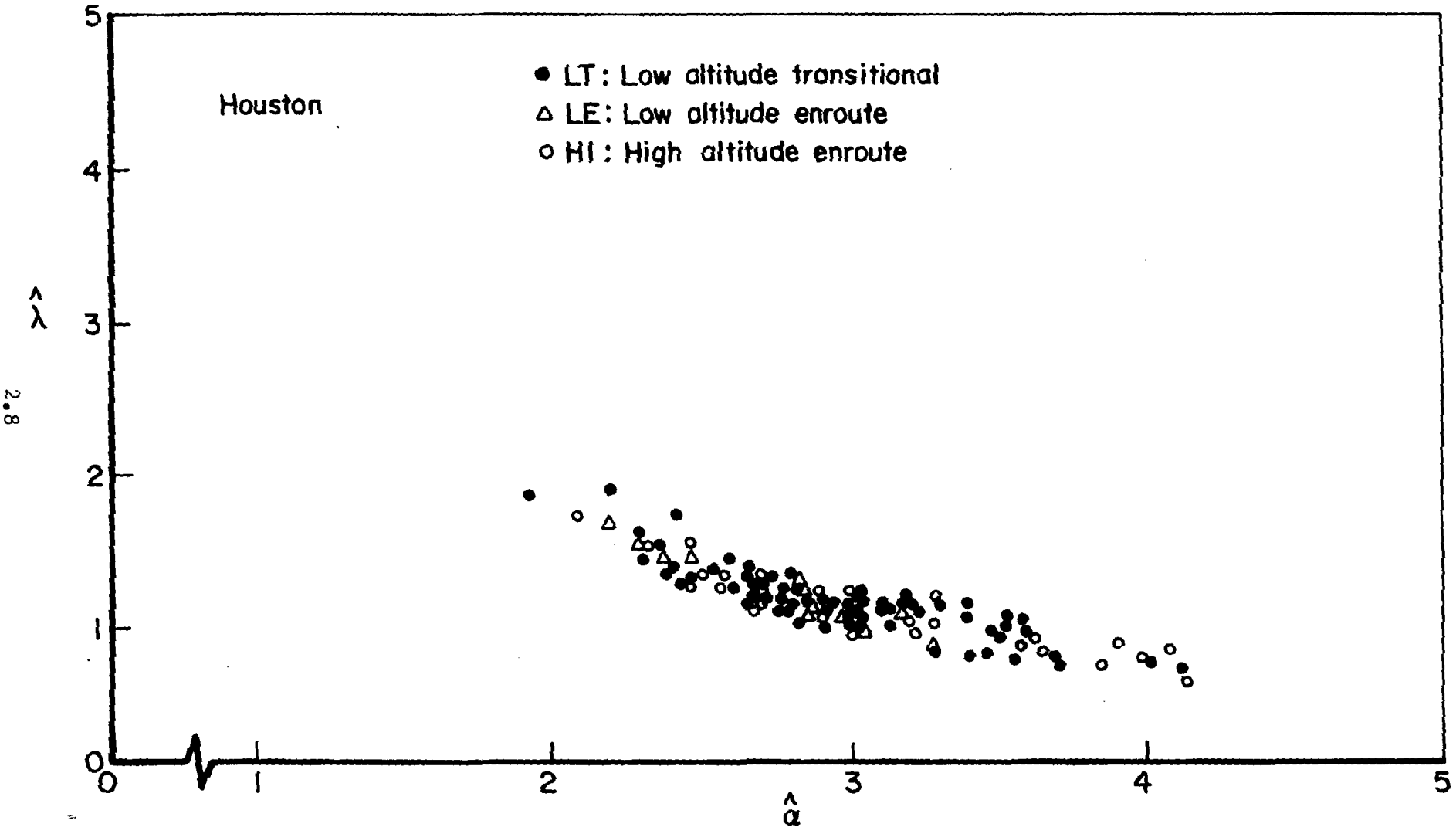

Figure 2.2 Estimates of the Parameters of Gamma Distributions Fitted to the Transmission Lengths (Houston Data)

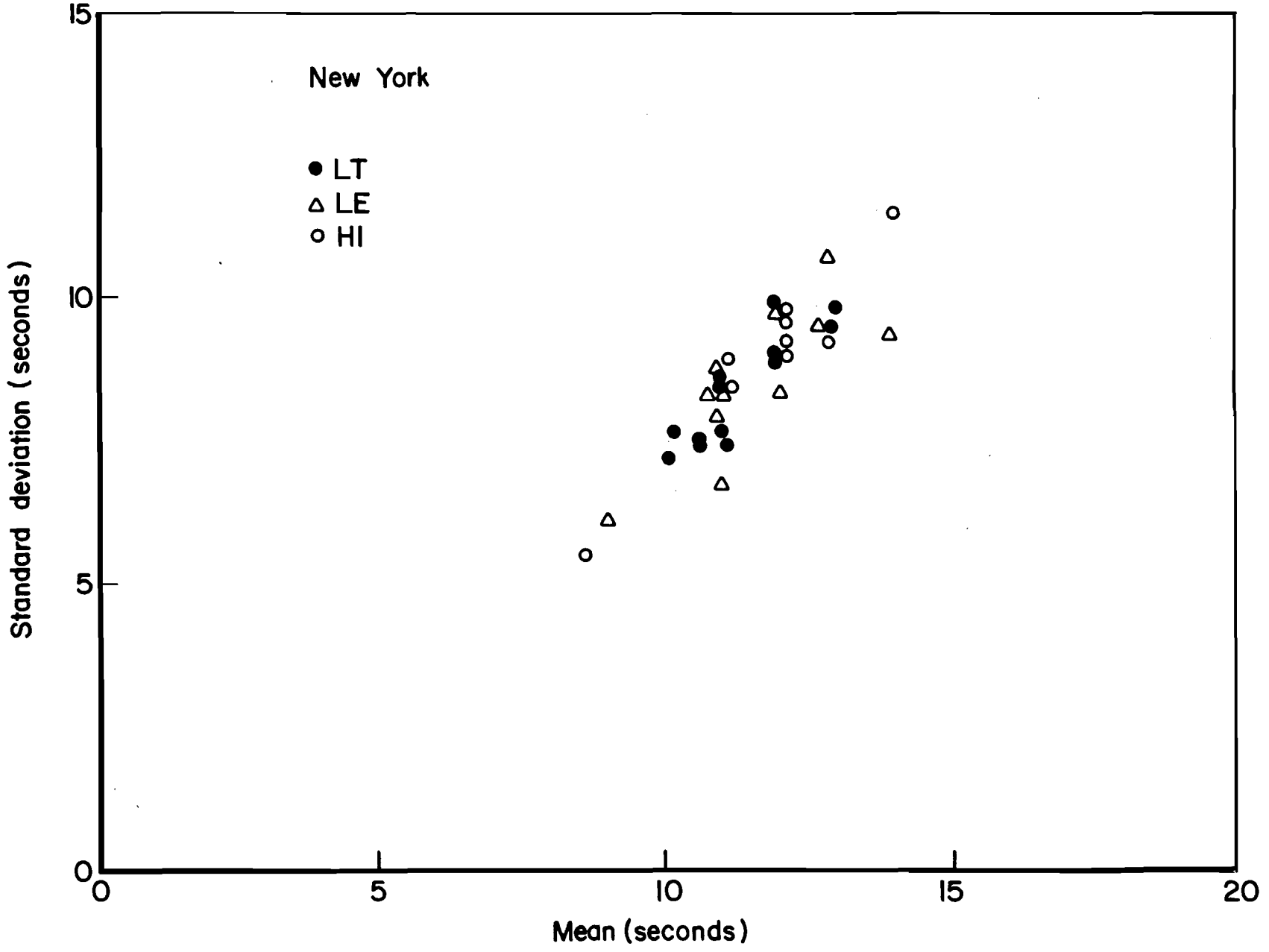

Figure 2.3 Mean versus Standard Deviation of the Transaction Lengths (New York)

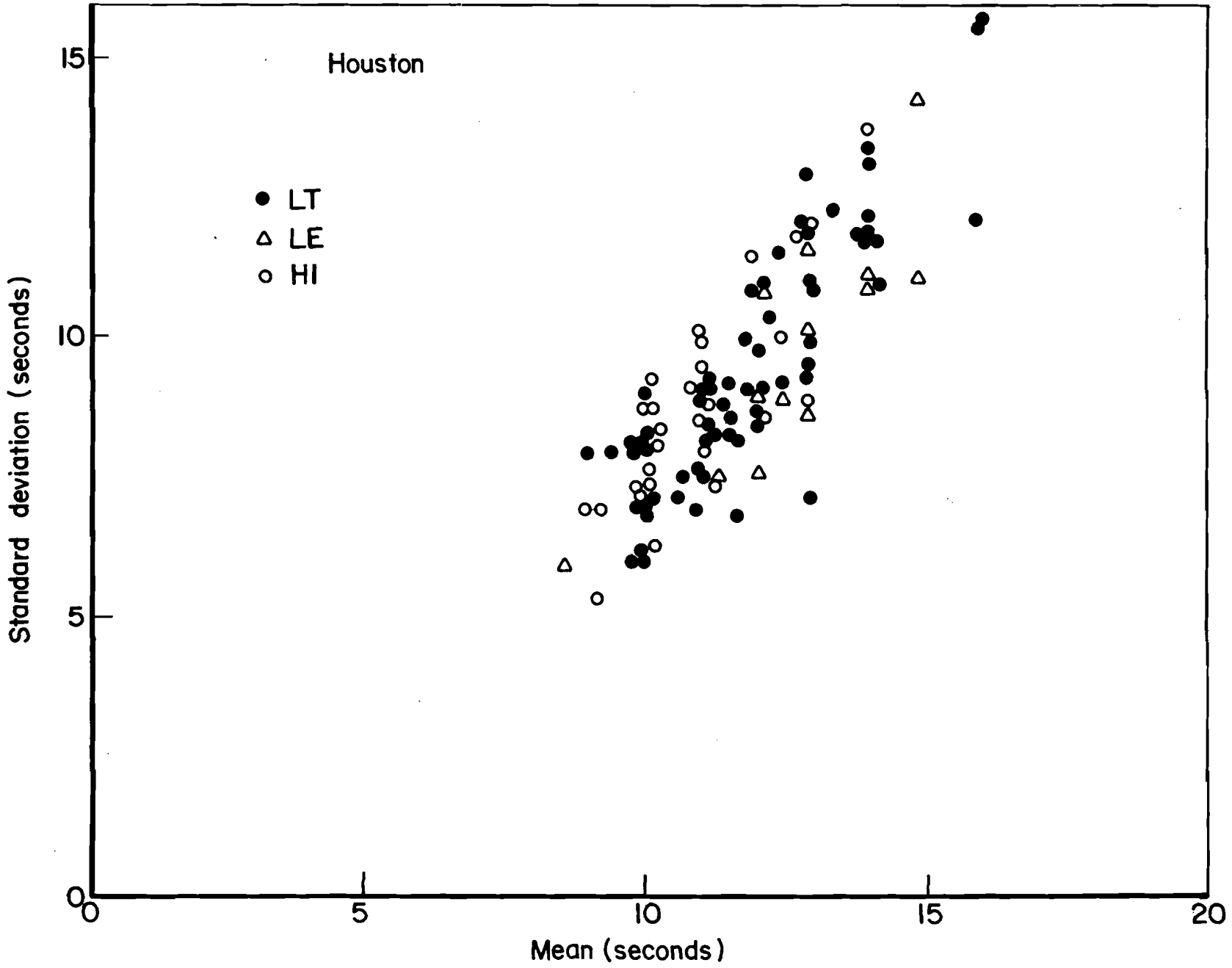

Figure 2.4 Mean versus Standard Deviation of the Transaction Lengths (Houston Data)

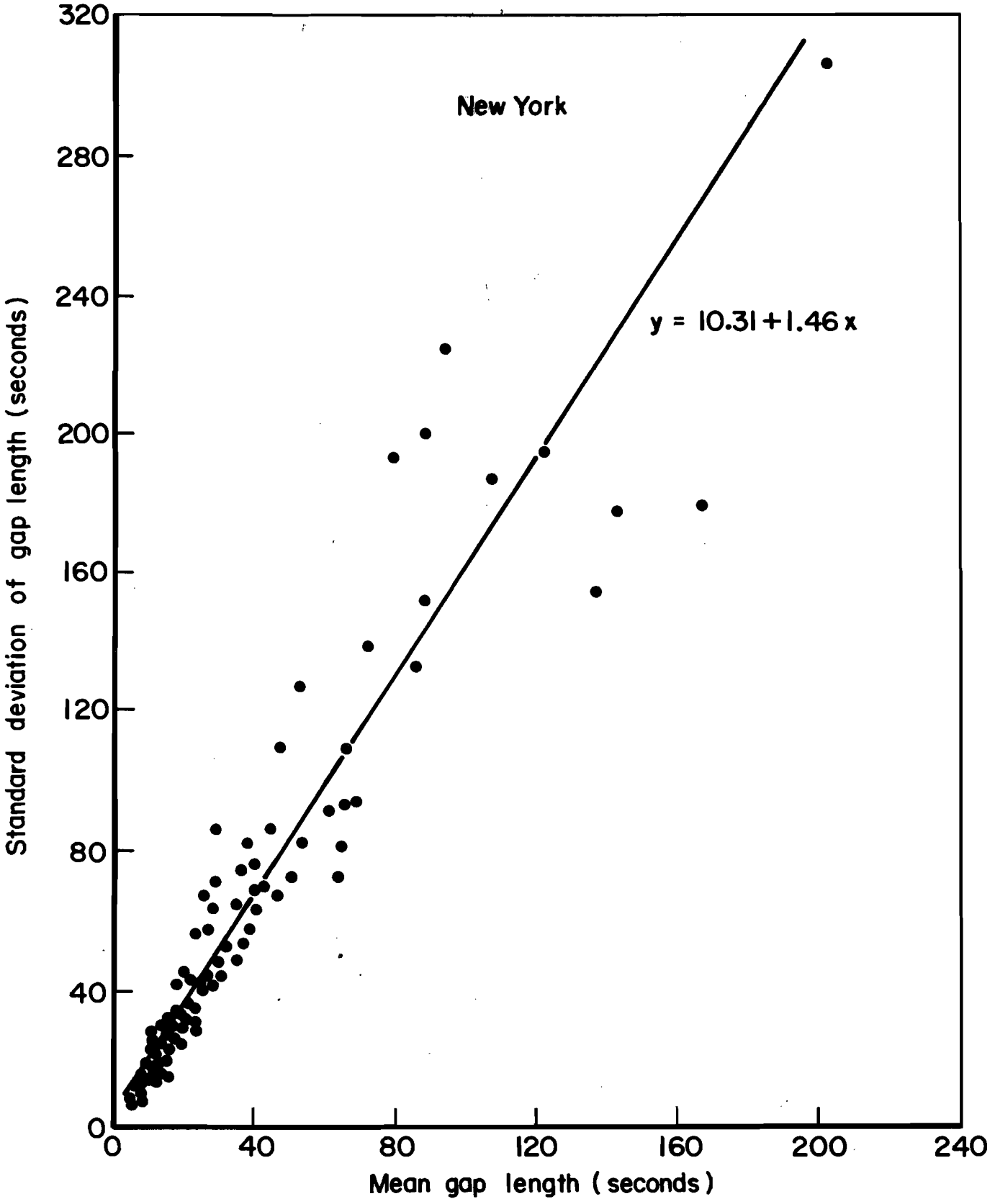

Figure 2.5 Mean vs Standard Deviation of Intertransaction Gap Lengths (New York Data)

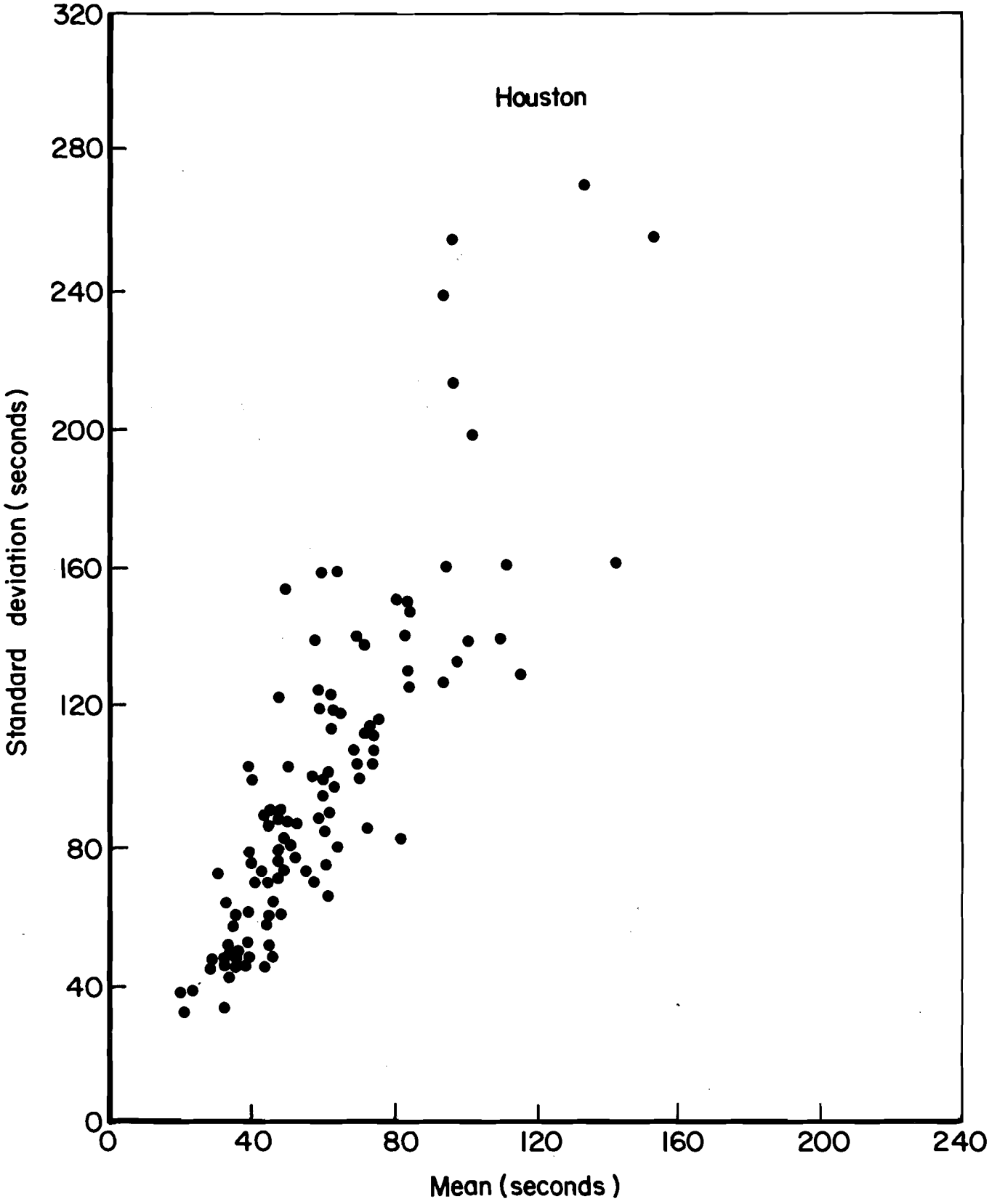

Figure 2.6 Mean versus Standard Deviation of the Intertransaction Gap Lengths (Houston Data)

Table 2.2 Results of Fitting Shifted Negative Binomial Distributions to the Number of Communications Transactions per Aircraft (Houston Individual Sectors)

Sector ID			No. Obs.	$\hat{p}$	$\hat{k}$	No. Adj.	d.f.	χ^2
100H	LE	BFM	7	0.41	1.91	0	3	1.76
101H	LE	BFM	19	0.55	2.80	0	5	6.72
102H	LE	BFM	22	0.33	1.09	0	5	3.99
104H	LE	MOB	15	0.47	2.95	0	6	4.05
105H	LE	MOB	10	0.27	1.25	0	4	3.43
106H	LE	MOB	39	0.81	17.11	5	8	8.03
107H	LE	LCH	22	0.53	3.78	0	6	9.72
108H	LE	LCH	12	0.42	2.54	0	6	4.62
111H	LE	LCH	35	0.78	20.32	5	9	10.31
112H	LE	AEX	20	0.64	5.08	0	6	4.57
113H	LE	AEX	22	0.29	1.35	0	7	4.48
114H	LE	AEX	26	0.42	2.29	0	7	7.62
116H	LE	AEX	17	0.37	1.08	0	4	7.19
117H	LT	MSY/E	23	0.60	2.36	0	4	13.38*
118H	LT	MSY/E	27	0.90	21.85	1	5	2.57
119H	LT	MSY/E	18	0.81	8.15	0	4	5.00
120H	LT	MSY/E	21	0.52	3.02	0	6	2.20
121H	LT	MSY/E	18	0.85	5.04	0	2	2.02
123H	LT	MCB	20	0.57	4.07	0	6	5.63
124H	LT	MCB	19	0.48	2.50	0	5	3.60
126H	LT	MCB	24	0.36	1.60	0	7	6.78
128H	LT	MSY/SW	25	0.76	4.72	0	3	8.17
129H	LT	MSY/SW	20	0.56	2.53	0	4	2.10
130H	LT	MSY/SW	21	0.32	1.34	0	6	2.52
131H	LT	MSY/SW	41	0.83	15.33	2	7	4.69
132H	LT	BPT	19	0.90	24.67	0	5	3.88
133H	LT	BPT	19	0.61	3.65	0	5	4.21
134H	LT	BPT	16	0.66	4.67	0	4	4.48
135H	LT	BPT	15	0.37	1.97	0	6	3.94
136H	LT	BPT	14	0.64	6.15	0	4	7.24

Table 2.2 Results of Fitting Shifted Negative Binomial Distributions to the Number of Communications Transactions per Aircraft (cont.) (Houston Individual Sectors)

Sector ID	No. Obs.	$\hat{p}$	$\hat{k}$	No. Adj.	d.f.	χ^2
137H LT BPT	28	0.92	34.38	1	5	4.86
138H LT BPT	21	0.50	2.47	0	5	5.30
139H LT BPT	24	0.64	2.42	0	3	0.77
140H LT BPT	13	0.86	16.21	0	4	1.73
141H LT HOU/N	25	0.42	1.85	0	6	8.95
142H LT HOU/N	20	0.73	5.97	0	4	5.21
143H LT HOU/N	29	0.61	3.60	0	5	12.13
144H LT HOU/N	25	0.63	4.90	0	6	7.89
145H LT HOU/N	33	0.68	6.54	0	7	7.99
146H LT HOU/N	28	0.73	6.62	0	5	3.26
147H 1t HOU/N	12	0.60	2.92	0	3	2.36
148H LT HOU/N	17	0.83	13.78	0	5	7.62
149H LT HOU/N	24	0.56	2.18	0	4	3.61
150H LT HOU/SW	19	0.38	1.62	0	6	6.78
151H LT HOU/SW	29	0.93	29.94	0	5	2.02
152H LT HOU/SW	22	0.65	4.88	0	5	1.76
153H LT HOU/SW	33	0.53	2.73	0	6	7.47
154H LT HOU/SW	26	0.75	5.59	0	4	2.08
155H LT HOU/SW	28	0.77	6.00	0	4	2.31
156H LT HOU/SW						
157H LT HOU/SW	19	0.46	2.26	0	5	2.51
158H LT HOU/SW	27	0.82	12.40	1	5	6.72
159H LT HOU/NW	38	0.70	10.80	4	8	10.74
160H LT HOU/NW	28	0.61	3.86	0	6	3.44
161H LT HOU/NW	23	0.40	2.39	0	8	5.97
162H LT HOU/NW	25	0.55	3.43	0	6	8.78
163H LT HOU/NW	18	0.61	2.23	0	3	3.84
164H LT HOU/NW	24	0.46	2.73	0	7	4.76
165H LT HOU/NW						
166H LT HOU/NW	17	0.48	1.88	0	4	7.16
167H LT HOU/NW	14	0.85	16.71	0	4	1.33
170H LT SKF	28	0.52	2.53	0	5	9.50
171H LT SKF	24	0.60	3.35	0	5	1.73

Table 2.2 Results of Fitting Shifted Negative Binomial Distributions to the Number of Communications Transactions per Aircraft (cont.) (Houston Individual Sectors)

Sector ID			No. Obs.	$\hat{p}$	$\hat{k}$	No. Adj	d.f.	χ^2
172H	LT	SKF	27	0.48	2.60	0	6	5.81
173H	LT	SAT	17	0.34	1.23	0	5	6.84
174H	LT	SAT	18	0.75	10.14	0	5	4.50
175H	LT	SAT	19	0.68	3.97	0	4	2.46
176H	LT	SAT	20	0.67	6.09	0	6	2.94
177H	LT	SAT	30	0.75	10.75	3	7	11.22
179H	LT	8CS	18	0.79	9.75	0	5	4.25
180H	LT	8CS	12	0.75	8.64	0	4	2.12
181H	LT	8CS	22	0.35	1.86	0	7	5.62
183H	LT	MTA	21	0.68	3.84	0	4	2.17
184H	LT	MTA	37	0.43	1.57	0	6	4.46
185H	LT	MTA	18	0.54	2.52	0	4	11.07
187H	LT	MTA	12	0.37	1.45	0	4	5.59
188H	LT	AUS	11	0.46	2.50	0	4	2.38
189H	LT	AUS	13	0.55	3.29	0	4	4.48
190H	LT	AUS	23	0.76	4.49	0	3	3.63
191H	LT	AUS	19	0.58	2.51	0	4	4.02
192H	LT	AUS	39	0.85	16.30	4	6	5.60
194H	HI	MOB	34	0.70	3.54	0	4	16.54*
195H	HI	MOB	23	0.48	1.58	0	4	4.95
196H	HI	MOB	27	0.43	1.02	0	4	2.99
197H	HI	MOB	34	0.45	1.08	0	4	7.20
198H	HI	MSY/HI	25	0.41	0.58	0	3	3.60
199H	HI	MSY/HI	36	0.57	1.76	0	4	2.30
202H	HI	MSY/HI	40	0.53	1.53	0	4	3.71
203H	HI	LCH/HI	13	0.22	0.54	0	3	6.94
206H	HI	LCH/HI	32	0.84	19.86	2	6	4.32
207H	HI	AEX/HI	23	0.24	1.11	0	7	8.30
208H	HI	AEX/HI	33	0.47	1.45	0	5	2.25
209H	HI	AEX/HI	20	0.67	2.98	0	3	1.47
210H	HI	AEX/HI	29	0.46	1.46	0	5	2.91
212H	HI	AEX/HI	33	0.48	1.46	0	5	10.43

Table 2.2 Results of Fitting Shifted Negative Binomial Distributions to the Number of Communications Transactions per Aircraft (cont.) (Houston Individual Sectors)

Sector ID			No. Obs.	$\hat{p}$	$\hat{k}$	No. Adj.	d.f.	χ^2
213H	HI	HOU/HI	15	0.61	1.38	0	2	4.45
215H	HI	HOU/HI	20	0.61	2.31	0	4	9.72
216H	HI	HOU/HI	31	0.80	4.73	0	3	5.58
217H	HI	HOU/HI	27	0.43	1.31	0	5	9.19
218H	HI	AUS/HI	54	0.93	29.25	4	5	2.00
219H	HI	AUS/HI	18	0.25	1.21	0	7	6.30
220H	HI	AUS/HI	29	0.66	4.22	0	5	12.76
221H	HI	AUS/HI	28	0.57	3.07	0	5	6.39
222H	HI	AUS/HI	21	0.18	0.55	0	6	24.91*
223H	HI	SAT/HI						
224H	HI	SAT/HI	17	0.37	3.51	0	9	14.90
225H	HI	SAT/HI	19	0.29	1.59	0	7	8.06
226H	HI	SAT/HI	33	0.31	1.95	0	10	16.71
227H	HI	SAT/HI	20	0.69	6.11	0	5	5.03

* Significant at the 0.01 level

Table 2.3 Results of Fitting Shifted Negative Binomial Distributions to the Number of CT/AC (Houston Enroute Functions)

Sector Function	No. Obs.	$\hat{p}$	$\hat{k}$	No. Adj.	d.f.	χ^2
LE	206	0.42	2.01	0	11	10.42
LI	1412	0.56	2.98	0	12	9.30
HI	704	0.36	1.14	0	13	33.46*
HI Group 1 (194H-217H)	482	0.51	1.59	0	9	8.63
HI Group 2 (218H-227H)	222	0.31	1.41	0	13	26.37

* Significant at the 0.01 level

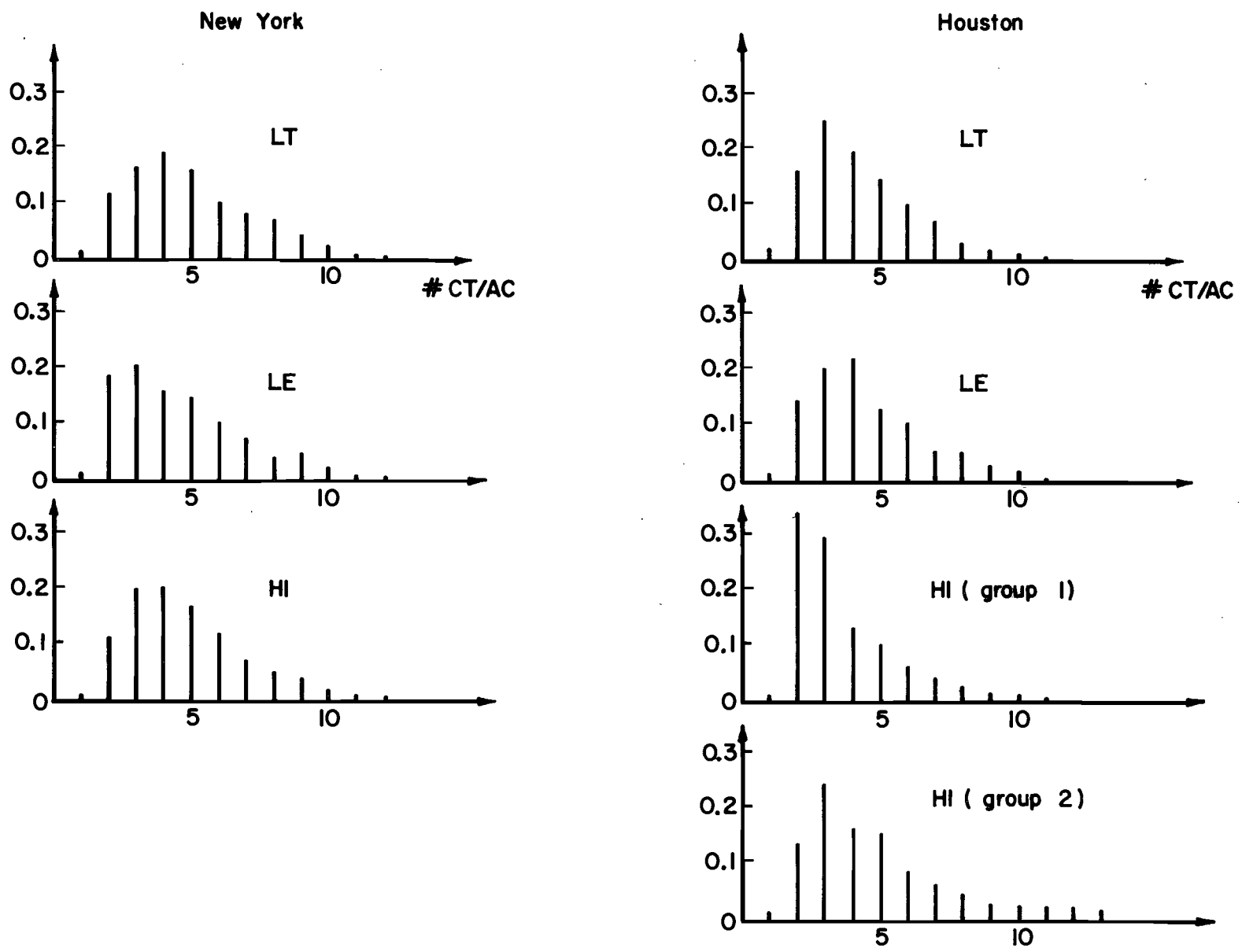

Figure 2.7 Historical Distributions of the Number of Transactions per Aircraft

Table 2.4 Comparison of the Estimates of p and k for Houston and New York Enroute Functions

	Houston			New York		
	$\hat{p}$	$\hat{k}$	E(X)*	$\hat{p}$	$\hat{k}$	E(X)
LE	0.42	2.01	4.7757	0.46	2.30	4.7000
LT	0.56	2.98	4.3414	0.41	2.36	5.3961
HI (group 1)	0.51	1.59	3.5276	0.58	4.03	4.9183
HI (group 2)	0.31	1.41	5.1384			

$$^{*}E(X) = \hat{k}\left(\frac{1}{\hat{p}} - 1\right) + m$$

Table 2.5 Comparison of Historical versus Simulated Aircraft Loading Series Generated from Sector Function Simulations (New York Metroplex)

Sector Function	Series	$\hat{\mu}$	$\hat{\phi}_1$	$\hat{\phi}_2$	$\hat{\sigma}^2$	t^a	$G(\underset{\sim}{0},1)^b$
LT	Historical (453LT)	4.4988	1.1131	-0.2015	0.5884	-0.7027	1.9051
	Simulated	3.7909	1.1379	-0.2363	0.4313		
LE	Historical (464LE)	5.4113	1.1533	-0.2511	0.6567	0.3245	0.6908
	Simulated	5.7026	1.1416	-0.3038	0.7000		
HI	Historical (475HI)	4.4104	1.2874	-0.4048	0.5655	0.7049	1.0887
	Simulated	4.9354	1.1647	-0.3319	0.6849		
GN	Historical (504GN)	2.4156	0.9155	-0.0698	0.5360	0.3682	1.6614
	Simulated	2.6585	1.1470	-0.2833	0.5362		
LC	Historical (510LC)	6.3220	0.9737	-0.1314	0.5271	-0.2922	4.3406
	Simulated	6.0167	1.1618	-0.2510	0.8592		
LG	Historical (524LG)	2.9971	1.2741	-0.3681	0.4132	-0.0460	0.2286
	Simulated	2.9472	1.2740	-0.3446	0.4607		
DP	Historical (534DP)	1.8776	0.9404	-0.2310	0.3680	1.8743	5.3551
	Simulated	2.8147	1.1990	-0.3514	0.5868		
AD	Historical (543AD)	1.3789	1.2273	-0.3855	0.2247	1.1687	3.4071
	Simulated	2.0835	1.1577	-0.2600	0.3558		
AR	Historical (553AR)	3.3706	1.0482	-0.0891	0.4028	-0.1142	1.8212
	Simulated	3.1905	1.2261	-0.3093	0.3791		

[a] $t_{.005}(200) = 2.6$

[b] $\frac{1}{2}\chi^2_{.01}(3) = 5.6$

Table 2.6 Comparison of Historical versus Simulated Channel Utilization Series Generated from Sector Function Simulations (New York Metroplex)

Sector Function	Series	$\hat{\mu}$	$\hat{\phi}_1$	$\hat{\phi}_2$	$\hat{\sigma}^2$	t_a	$G(\underset{\sim}{0},1)^b$
LT	Historical (453LT)	0.4939	0.1303	0.2064	0.0510	-0.7299	2.4383
	Simulated	0.4534	0.3496	0.1231	0.0689		
LE	Historical (464LE)	0.4806	0.3763	0.1823	0.0542	1.3919	0.4348
	Simulated	0.5837	0.4587	0.1259	0.0638		
HI	Historical (475HI)	0.5740	0.3502	0.1485	0.0491	-0.8195	0.9569
	Simulated	0.5177	0.4932	0.1022	0.0593		
GN	Historical (504GN)	0.4964	0.5094	0.0667	0.0742	-1.6846	1.4124
	Simulated	0.3691	0.2920	0.1570	0.0795		
LC	Historical (510LC)	0.5595	0.2194	0.0407	0.0470	-2.2771	2.0329
	Simulated	0.4463	0.4568	0.0586	0.0484		
LG	Historical (524LG)	0.3096	0.2989	0.2286	0.0520	-0.1488	0.6368
	Simulated	0.2992	0.4112	0.1625	0.0616		
DP	Historical (534DP)	0.4379	0.2513	0.2124	0.0441	0.6749	5.6940*
	Simulated	0.4846	0.5330	0.0438	0.0741		
AD	Historical (543AD)	0.5760	0.3171	0.1153	0.0840	-2.9322*	1.7839
	Simulated	0.3366	0.4808	0.1480	0.0726		
AR	Historical (553AR)	0.5521	0.3268	0.1879	0.0574	-0.1614	0.9875
	Simulated	0.5396	0.5003	0.1434	0.0588		

[a] $t_{.005}(200) = 2.6$

[b] $\frac{1}{2}\chi^2_{.01}(3) = 5.6$

Table 2.7 Comparison of Historical versus Simulated Aircraft Loading Series Generated from Sector Function Simulations (Houston ARTCC)

Sector Function	Series	$\hat{\mu}$	$\hat{\phi}_1$	$\hat{\phi}_2$	$\hat{\sigma}^2$	t^a	$G(\underset{\sim}{0},1)^b$
LE	Historical (LE107H)	4.3157	1.1472	-0.1994	0.2471	-1.3858	4.7444
	Simulated	3.0292	1.2237	-0.3926	0.3359		
LT	Historical (LT145H)	3.2067	1.2395	-0.3017	0.2959	-1.3546	2.6192
	Simulated	2.0489	1.1751	-0.3557	0.3374		
HI	Historical (HI226H)	3.0424	1.2056	-0.2268	0.2782	-0.1192	4.2715
	Simulated	2.7642	1.2418	-0.3599	0.3723		

[a] $t_{.005}(200) = 2.6$

[b] $\frac{1}{2}\chi^2_{.01}(3) = 5.6$

Table 2.8 Comparison of Historical versus Simulated Channel Utilization Series Generated from Sector Function Simulations (Houston ARTCC)

Sector Function	Series	$\hat{\mu}$	$\hat{\phi}_1$	$\hat{\phi}_2$	$\hat{\sigma}^2$	t^a	$G(\underset{\sim}{0},1)^b$
LE	Historical (LE107H)	.2642	.1861	.0901	.0529	.5767	2.0493
	Simulated	.2934	.4425	.0102	.0601		
LT	Historical (LT145H)	.3066	.2926	.1344	.0543	-.4998	0.8263
	Simulated	.2799	.4150	-.0080	.0603		
HI	Historical (HI226H)	.3046	.3924	.2049	.504[illegible]	.1511	0.3541
	Simulated	.3151	.3176	.2039	.0578		

[a] $t_{.005}(200) = 2.6$

[b] $\frac{1}{2}\chi^2_{.01}(3) = 5.6$

CHAPTER 3

FURTHER APPLICATIONS OF THE SIMULATION MODEL

3.1 Introduction

In the evolution of the ATC simulation model, several considerations have guided the technical developments:

(i) the structure of the simulation procedure should be general, but adaptive to specific applications as well,

(ii) the formulation of the computer program should be simple, but allow additional details to be added.

Experience gained from many exercises, and the feedback from comparisons against historical data have resulted in many modifications of the simulation model. The simulation has been extended from the one appropriate to individual sectors to a general simulation for sector functions without requiring extra computational effort. Applications, either for hypothesized changes of the system, or for the study of events with practical significance should continue to contribute to additional generalizations and understanding of the simulation model.

In this chapter three different applications of the simulation model are presented to illustrate the usefulness of the model. In section 3.2 a continuing study of estimating communications capacities for sector functions is described and results analyzed in conjunction with some conventional queuing models. Section 3.3 is devoted to the exploration of the effects of a proposed FCC regulation concerning tone burst identification of privately owned transmitters, for ATC air/ground communications. Various response surfaces are constructed on the two causal factors: the tone duration and traffic density, from the results of simulation experimentation and spline extropolations. In section 3.4 a hypothesized change in the distribution of #TR/CT using a smooth weighting function is investigated and results analyzed.

3.2 Estimation of Communications Capacities for New York Sector Functions

As earlier demonstrated in the report volume III, chapter 4, techniques useful for detecting nonstationarity of the response time series can be used to measure capacities of communication channels. In order to gain more insights about the mechanism which determines the communication capacity and to explore the effects of regulating input variables (e.g. the transaction lengths, communication arrival streams, etc.), some well-known results from the conventional queuing theory are discussed in this section and information particularly important for the design of simulation experiments gathered.

In the following discussions we first compare the ATC communication queuing with a theoretical model of Poisson arrival streams and general service time distributions. Effects of the nonhomogeneity of communication arrivals upon queuing are then discussed. Influences of the variance reduction of communications transaction lengths are studied and results presented. Finally, a simulation experiment for estimating sector function communications capacities is described and results tabulated for practical use.

3.2.1 A Theoretical Model for ATC Communications Queuing

In chapter 2 of report volume III, an exponential model was analyzed and verified for intercommunication gap lengths. It was demonstrated that the parameter values descriptive of the gap length associated with a specific aircraft were a function of the number of transactions made by the aircraft. By further assuming independence between individual gap lengths, a theoretical model for the communication arrivals to an ATC communication channel can be formulated. To explain:

(i) For a single aircraft, arrivals to the communications channel follow a homogeneous Poisson process. The value of the arrival intensity (i.e. the value of the Poisson parameter λ_i for the ith aircraft) is determined by the number of communication transactions associated with this aircraft.

(ii) When there are many aircraft handled by a controller at one time, and within a moderate short time length where no aircraft enters or leaves the sector, the combined communication arrival stream is still homogeneous Poisson. The intensity of this combined process is equal to the sum of the intensities of all aircraft presently in the sector (i.e. $\lambda^*=\Sigma\lambda_i$).

(iii) Whenever an aircraft enters or leaves the sector, the intensity of the combined communication arrival stream λ^* changes depending on the number of aircraft staying in the sector and their associated communication intensities. From a simple simulation experiment it was found that λ^* follows a second order autoregressive model, when data based on per-minute averages were examined. In fact, the values of λ^* follow the so-called immigration-death process. (For reference, see Cox and Miller: The Theory of Stochastic Processes, 1966, John Wiley Co.)

A schematic presentation of the process described above is given in figure 3.1. From the time plot for λ^*, the communication arrival intensity for the combined process, one can see differences between the arrival stream to an ATC communication channel and those provided by the conventional assumption of a homogeneous Poisson process which has a constant λ^* throughout the entire time period.

As has been discussed in earlier chapters, the communication transaction lengths are gamma variables (for the transmission lengths) compounded with a distribution for the number of transmissions per communication

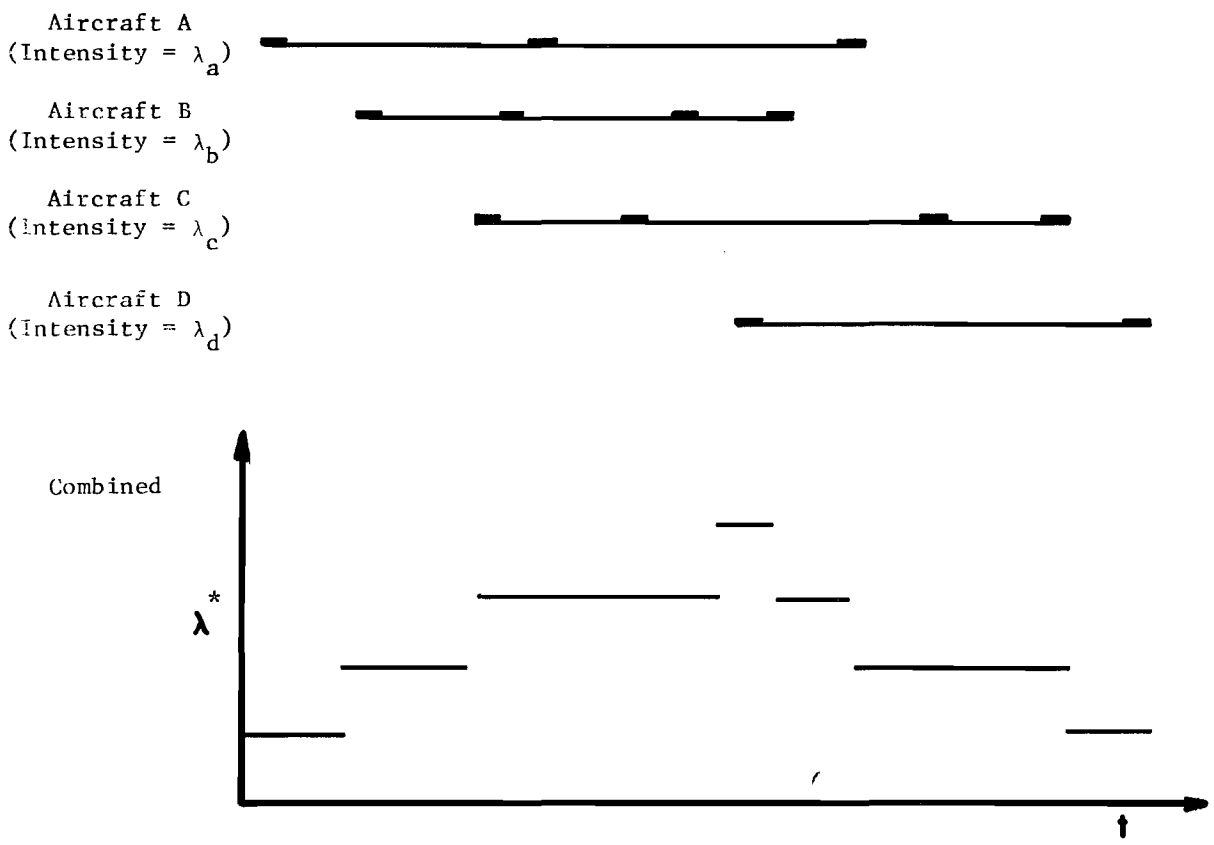

▬ = time interval during which a transaction is in process;

$\lambda_.$ = intensity associated with the aircraft specified;

λ^* = sum of intensities of individual aircraft in the sector.

Figure 3.1 Structure of the Intensity of the ATC Communication Arrivals

transaction. In the literature of queuing theory, the compounded distribution is called the service time distribution. Combining a non-homogeneous Poisson arrival stream with the distribution of transaction lengths, a complete queuing model for the ATC communications is specified.

Although analytic solutions to such models are difficult to attain, this formulation is helpful in providing insights about the queuing properties of communication transactions. Particularly, solutions to a model consisting of a homogeneous Poisson arrival and a general service time distribution can be considered as providing lower bounds to the expected queuing times and queue sizes. These lower bounds are useful for selecting ranges for simulation experiments.

3.2.2 Communications Capacity and Queuing

It can be shown that the expected channel utilization, expressed by number of seconds per hour, is

$$E(CU) = \Theta[E(TR)][E(\#TR/CT)][E(\#CT/AC)]$$

$$= \Theta[\ b_o - b_1\Theta][\tau][k(\frac{1}{p} - 1) + m] \qquad (3.1)$$

where

E = Expectation Operator

Θ = the number of aircraft arrivals per hour;

b_o, b_1 : the parameters used to relate E(TR) with Θ;

τ : the expected number of transmissions per CT;

k, p, m : parameters in the distribution of #CT/AC;

A straightforward determination of the sector communication capacity is to set E(CU) equal to 3600 seconds x 0.85, the physical limitation for the period of 1 hour, and then to solve the Equation (3.1) for Θ. In other words, the value of Θ which satisfies the equation:

$$\Theta(b_o - b_1\Theta) = 3600\ (0.85)\cdot\tau^{-1}\cdot\ [k(\frac{1}{p} - 1) + m]^{-1} \qquad (3.2)$$

is the maximum number of aircraft arrivals theoretically allowed.

We now turn to a discussion of queuing associated with Equation (3.2). Let us hypothesize that one is able to stablize the communication arrivals to an ATC communication channel such that the intensity λ^* stays constant over a fairly long period of time. The results of conventional queuing theory can now be used to explore the nature of the communication capacity.

It is well-known in the literature of queuing theory, that the expected queuing time for an M/G/1 model (the system consists of a

Poisson arrival stream, a general service time distribution, and a single server), in a long run equilibrium, is

$$E(Q) = \text{expected queuing time}$$

$$= \frac{1}{\lambda^*} \left[\rho + \frac{\rho^2(1+C_b^2)}{2(1-\rho)} \right] - \text{expected service time} \qquad (3.3)$$

where

λ^* : parameter of the homogeneous (after stabilization, in our case) Poisson arrival process;

ρ : a traffic intensity (= mean service time/mean inter-arrival time);

C_b : the coefficient of variation of the service time distribution (= standard deviation/mean).

One interesting fact is that ρ is equal to E(CU)/3600. This can be seen from the following algebraic manipulations. Let us write

(i) $\rho = \dfrac{\text{mean service time}}{\text{mean communication interarrival time}}$

(ii) mean service time = mean communication transaction length = $E(TR) \cdot E(\#TR/CT) = (b_o - b_1\Theta) \cdot \tau$

(iii) mean communication interarrival time = $\frac{1}{\lambda^*}$ = $3600/[\Theta \cdot E(\#CT/AC)] = 3600 . \Theta^{-1} \; [k(\frac{1}{p} - 1)+m]^{-1}$

Substituting (ii) and (iii) into (i), one finds

$$\rho = \Theta \cdot (b_o - b_1\Theta) \cdot \tau \cdot [k(\frac{1}{p} - 1)+m]/3600$$

$$= E(CU)/3600 \qquad (3.4)$$

Q.E.D.

Furthermore, since

$$\lambda^* = \Theta[k(\frac{1}{p} - 1)+m]/3600 \qquad (3.5)$$

the ρ can be expressed as

$$\rho = \lambda^* \cdot (b_o - b_1\Theta) \cdot \tau \qquad (3.6)$$

From Equation (3.4) one may see that, to find the value of Θ which gives $\rho = 0.85$, one has to refer, once again to Equation(3.2). Now let us denote the solution value of Θ in Equation(3.2)by $\tilde{\Theta}$. The complete formula for E(Q), when $\rho = 0.85$, is thus

$$E(Q) = \frac{1}{\tilde{\lambda}^*}\left[\tilde{\rho} + \frac{\tilde{\rho}^2 (1+C_b^2)}{2(1-\tilde{\rho})}\right] - (b_0 - b_1\tilde{\Theta})\tau \qquad (3.7)$$

where

$$\tilde{\lambda}^* = \tilde{\Theta}[k(\frac{1}{p} - 1) + m]/3600$$

$$\tilde{\rho} = \tilde{\lambda}^*(b_o - b_1\tilde{\Theta})\tau \quad (=0.85 \text{ in our case})$$

An illustration of the calculation of E(Q) for HI sectors is given below.

From previous reports volume II and III, the parameter estimates from an HI sector function are as follows:

$b_o = 3.70$	$p = 0.58$
$b_1 = 0.0158$	$m = 2$
$\tau = 3.56$	$C_b = 0.8054$
$k = 4.03$	

Substituting these values into Equation (3.2), one obtains

$$\begin{aligned}\theta(3.70 - 0.0158\theta) &= 3600\ (0.85)\ (3.56)^{-1}\ [4.03(0.724)+2]^{-1} \\ &= 3600\ (0.85)\ (0.281)\ (0.203) \\ &= 174.85\end{aligned}$$

The above equation can be rewritten as

$$\theta^2 - 234.18\theta + 11066.46 = 0$$

Thus, $\tilde{\Theta} = 65.675 \approx 66$

The second root of $\tilde{\theta}$ is ignored because the value of E(CU) is higher than 3600x0.85. The figure of 66 is thus the theoretical maximum number of aircraft allowed to enter an average HI sector, per hour, without exploding the system. This does not mean that one may actually load this many aircraft into the channel at the specified rate. Another important response, the communications queuing times, which is also closely related to the aircraft arrival rate, should be simultaneously considered.

It must be emphasized that the expected queuing time for an ATC communication channel, which has a nonhomogeneous Poisson arrival stream,

is still unknown to us. A lower bound of this expected queuing time can be calculated from Equation (3.7). Again, by substituting all estimates of the parameters of concern into Equation (3.7), we obtain

$$\tilde{\lambda}^* = \tilde{\Theta}\ [k(\frac{1}{p} - 1) + m]/3600$$
$$= 66\ [4.03(0.724) + 2]/3600$$
$$= 0.09$$

Thus,

$$E(Q) = (0.09)^{-1}\ [0.85 + \frac{(0.85)^2(1+0.65)}{2(1-0.85)}] -$$
$$[3.70 - (0.0158)66](3.56)$$
$$= 44.10 \text{ (seconds)}$$

This lower bound for E(Q) indicates that when an HI sector channel is loaded at 66 aircraft per hour, the average queuing time per communication is at least 44.10 seconds. Comparing this result with a simulation result previously reported in volume III, chapter 4, we found that the actual average queuing time was equal to 56.82 seconds, where 50 aircraft were loaded per hour. Clearly the expected queuing time derived from a hypothesized homogeneous Poisson process, in particular, the M/G/1 model, is indeed too small but it is still valid if viewed as a lower bound.

3.2.3 Effects of Regulating Communications Transaction Lengths

One interesting problem related to the study of communication capacity concerns how much improvement in queuing can be anticipated if one is able to reduce the variability of the communication transaction lengths. Although a precise solution to this problem is still unavailable, the effects of regulating transaction lengths can be elucidated by studying the shifts of the lower bound of the expected queuing time, E(Q), at different values of C_b, the coefficient of variation of the transaction lengths. Using the same example as in the preceding section, with $\rho = 0.85$, we compute the E(Q) at various values of C_b, ranging from 0 to 1. The results are displayed in figure 3.2. From this plot one may see the lower bound of 44.10 seconds has dropped to the level of 26.74 seconds when C_b is reduced from its present value of 0.8 to 0.0. This is a reduction of 39 per cent. In general, regulating the transaction lengths will help reduce queuing times, particularly under heavy traffic situations.

3.2.4 Results of a Simulation Experiment

ATC communications simulations for New York and Houston ARTCC sector functions were validated and results reported in chapter 2.

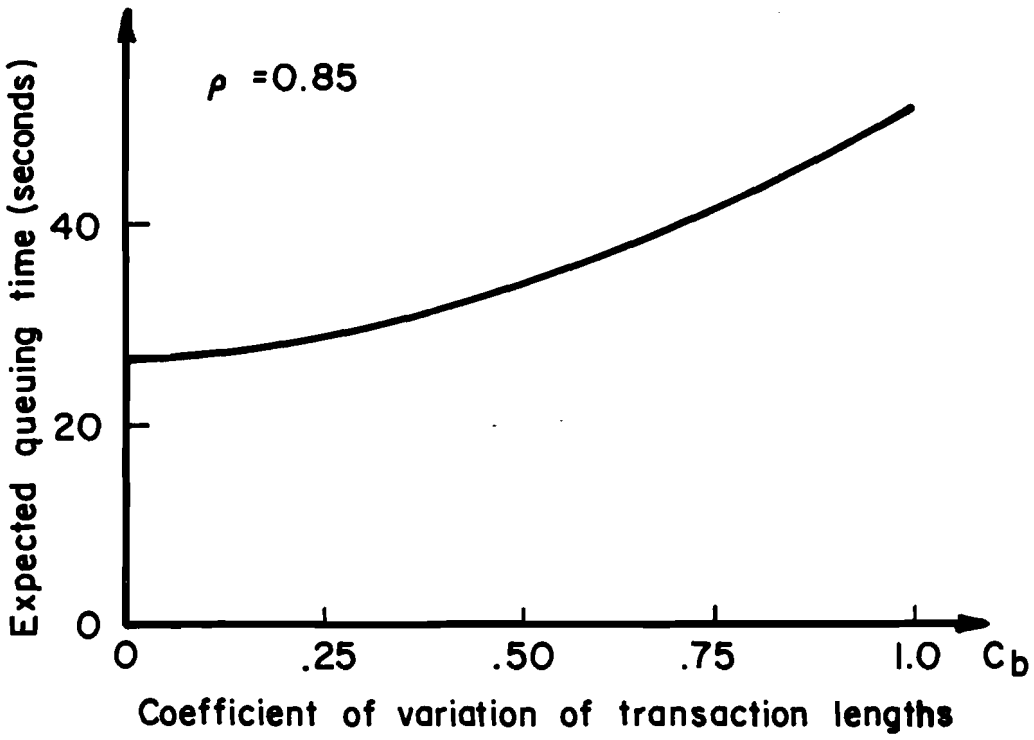

Figure 3.2 Lower Bound of the Expected Queuing Time vs C_b (HI Sectors)

Making use of this verified model, we proceeded to estimate the communications capacities by varying the expected number of aircraft arrivals per hour in a sequence of simulation exercises. The capacity measurements were made by simultaneously considering the following five variables:

(i) Average aircraft loading, $\bar{n}_t$;

(ii) Average channel utilization, $\bar{c}_t$;

(iii) Average queuing time per communication transaction, $\bar{Q}_t$;

(iv) The degree of nonstationarity measured from the time series of n_t, denoted by $Pr(\xi>1)$;

(v) The probability of n_t being larger than a critical value k, denoted by $Pr(n_t>k)$.

Capacity estimates through experimentation with the simulation model were obtained for eight different sector functions, namely, LT, LE, HI, LC, LG, DP, AD, and AR. Details of these experiments are given below. A special study on the sector function GN, using an analytical formula, is presented later in this subsection.

For all simulation runs actually performed, the three rules listed below were followed:

(i) The simulation is run for a period of 1-hour (simulation time) before any record is taken; this is to eliminate the effects of initial conditions.

(ii) The pseudo random numbers used are kept identical whenever possible for the simulations of the same sector function.

(iii) For each of the computer runs of 2-hour simulation time the three major responses: the aircraft loading (n_t), the channel utilization (c_t), and the queue lengths (q_t) are recorded as time series, on the basis of 60-second averages.

Our simulation experiments for exploring the communications capacities were performed in an iterative fashion as described below. An initial traffic density was selected, usually being equal to or slightly higher than the value observed from the historical data. The experimentation with the simulation model is then carried out by increasing the expected number of aircraft arrivals per hour until the average channel utilization generated reached 0.85.

Summary statistics of the responses of concern are furnished in table 3.1 (where the "bar" on the top of the variable means "averaged over the 2-hour data"). The nonstationarity detection measure $Pr(\xi>1)$, where $\xi = \hat{\phi}_1 + \hat{\phi}_2$, which has been described in the report volume III, chapter 4, was applied to the simulated aircraft loading time series, n_t. The numerical results of this measure under various experimental

Table 3.1 Summary Results of the Simulation Experiments for Capacity Study (New York Sector Functions)

Sector Function	Traffic Density (#ac/hr) Expected	Actual	$\bar{n}_t$	$\bar{c}_t$	$\bar{Q}_t$ (sec.)	$Pr(\xi>1)$
LT	40	40	6.628	.689	17.247	.0031
	45	44	7.401	.775	23.273	.0038
	55	49	10.204	.844	46.112	.0262*
LE	35	39	5.852	.591	13.357	.0001
	45	44	7.669	.636	24.660	.0057
	55	58	9.362	.748	30.638	.0092
	70	68	16.458	.857	81.866	.0696*
HI	45	52	8.216	.728	21.017	.0000
	50	57	9.555	.800	28.629	.0032
	60	68	16.640	.869	89.104	.3749*
LC	85	74	11.652	.760	23.953	.0018
	100	93	26.157	.877	120.406	.0298*
	110	101	45.195	.877	265.149	.3001*
LG	80	77	10.995	.730	24.531	.0095
	90	93	15.079	.786	46.835	.0357*
	100	108	20.097	.822	72.632	.4555*
DP	50	44	6.137	.686	19.205	.0034
	55	50	6.895	.745	21.293	.0032
	60	56	8.059	.807	28.792	.0015
	70	66	12.573	.875	62.698	.0590*

Table 3.1 Summary Results of the Simulation Experiments for Capacity Study (New York Sector Functions) (cont.)

Sector Function	Traffic Density (#ac/hr) Expected	Actual	$\bar{n}_t$	$\bar{c}_t$	$\bar{Q}_t$ (sec.)	$Pr(\xi>1)$
AD	40	34	4.089	.603	13.532	.0017
	45	42	4.694	.665	15.514	.0000
	50	43	5.865	.714	25.307	.0040
	60	56	7.095	.773	33.039	.0007
	70	67	11.781	.873	76.798	.0796*
AR	35	34	6.443	.780	27.855	.0037
	40	42	9.079	.873	49.853	.0153*

*Indicating critical conditions

conditions are displayed in the last column of table 3.1. In this study we use $Pr(\xi>1) = 0.01$ as a critical point which seems sensible, although somewhat arbitrary, for the detection of the onset of an unstable operation. From the results displayed in table 3.1, capacities of each control function in N.Y. metroplex were decided and listed in table 3.2. Additional measurements of the operational instability, expressed by the probability $Pr(n_t>k)$, projecting from the fitted AR(2) process, where k is a predetermined value, are listed in tables 3.3-3.10 for each of the eight functions studied. Tables containing detailed statistics computed from the simulated data, as well as the time series plots of the major responses are compiled and available as a separate interim report (PU-37).

3.2.5 A special Note on the Capacity of the GN Function

Because of the low average value on the number of CT's per aircraft (=2.27) and the relatively high speed of decrease on the expected transmission length (expected TR length = 3.70 - 0.0158·(expected number of aircraft arrivals per hour)), the GN function has an extraordinarily large communications capacity. Due to the limitation of the storage space in a computer, a simulation experiment is difficult to carry out for this control function. Nevertheless, an analytic approximation to the ATC channel model is available for the estimation of the capacity. Formulas useful for this purpose are sketched below. Related numerical results are displayed in figures 3.3 and 3.4. From these graphs $\Theta = 180$ aircraft arrivals/hour seem to be a moderate estimate of the capacity of the GN function.

Analysis of the GN function capacity:

$E(\#CT/AC) = k(\frac{1}{p} - 1) + m = 0.88(2.439 - 1) + 1 = 2.2663$

$E(\#TR/CT) = 3.4695$

$E(TR) = 3.70 - 0.0158\Theta, \qquad C_b = 0.99 - (\Theta - 50)\ 0.005$

Additional Conditions:

(i) TR Length on average ≥ 2.0
(ii) $0.7 \leq C_b \leq 0.99$

$$\rho = \Theta\ E(TR)E(\#TR/CT)E(\#CT/AC)/3600$$

$$\lambda = 2.2663\ \Theta/3600$$

$$E(Q) = \frac{1}{\lambda}\left[\rho + \frac{\rho^2\ (1+C_b^2)}{2(1-\rho)}\right] - E(TR\ \ )\ 3.4695$$

Both ρ and E(Q) are plotted on graphs for various traffic densities (#ac/hr).

Table 3.2 Estimates of the Communications Capacities for New York Sector Functions

Sector Function	Expected Capacity (# aircraft/hour)	Conservative Capacity+ (# aircraft/hour)
LT	50	41
LE	55	46
HI	50	41
GN	180*	163
LC	90	78
LG	85	73
DP	60	50
AD	60	50
AR	37	29

* Estimated from an analytic solution,

\+ Conservative Capacity = Expected Capacity - 1.282(Expected Capacity)$^{0.5}$.

= 90% confidence range

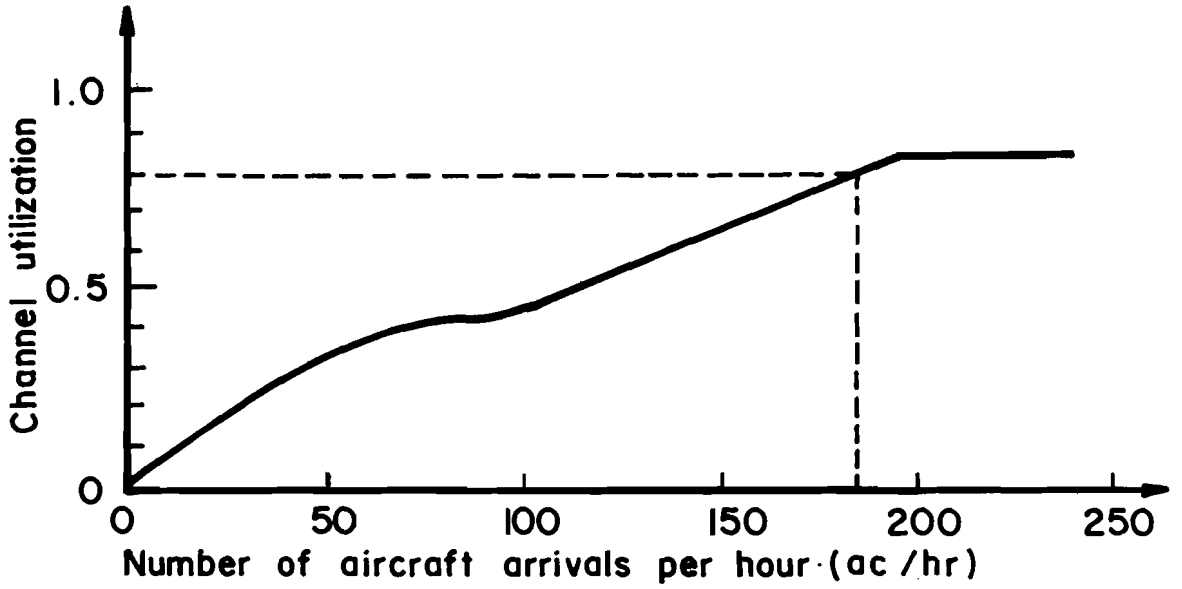

Figure 3.3 Channel Utilization as a Function of ac/hr (GN Sectors)

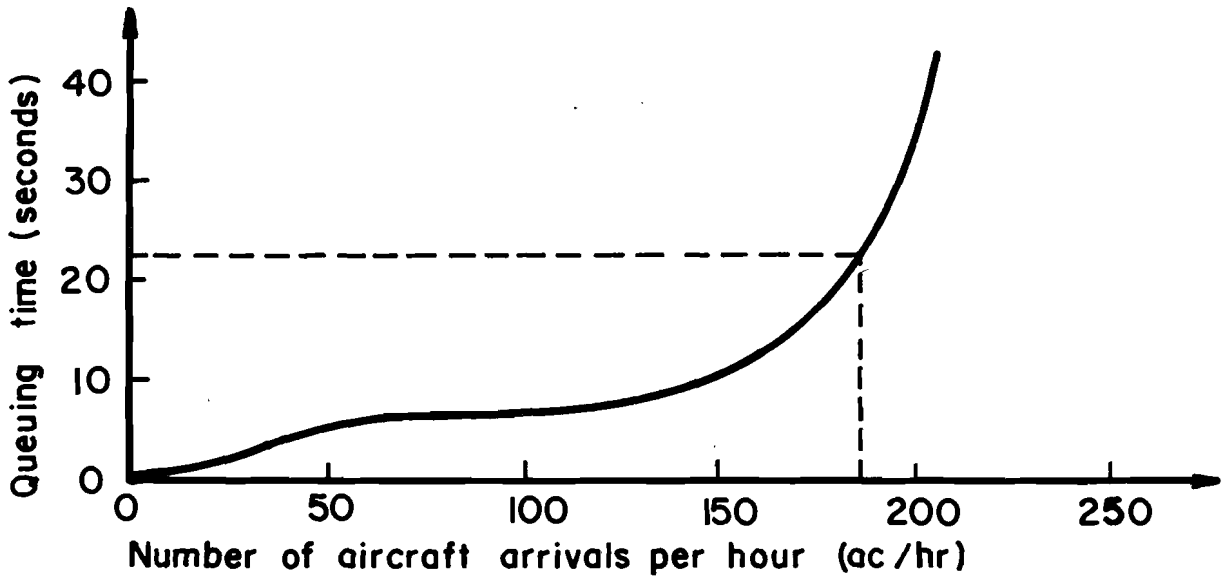

Figure 3.4 Expected Queuing Time as a Function of ac/hr (GN Sectors)

3.3 Effects of Tone Disturbance upon ATC Communications

This section describes the results of simulation experiments designed to show the effect of the proposed FCC regulation concerning tone burst identification of privately owned transmitters on air traffic control (ATC) air/ground communications. The nine functions subjected to investigation are: HI, LE, LT, GN, LC, LG, DP, AD and AR selected from the N.Y. area. The results for a particular function demonstrate the effect that the proposed regulation, if implemented, will have upon communications in a typical sector within that function. The complete results for each function are contained in 20 pages of tables and graphs, thereby giving a total of 180 pages of output. In this report only a complete set of material for HI function is included for illustration. Instead, the summary statistics and spline extropolated response surfaces for each of the nine sector functions are presented. A complete collection of the material related to this study is available as a NAFEC-Princeton University Interim Report (PU-39).

3.3.1 Simulation Input Variables and the Average Responses

In this study, a simulation experiment is characterized by two basic input parameters, namely, tone duration and expected aircraft arrival rate per hour. In the present study, simulation experiments were conducted at tone durations of 0, .5, 1, and 1.5 seconds. A tone burst appeared at the beginning and end of each pilot-initiated transmission. Since only a negligible number of transmissions last for more than 30 seconds, no attempt was made to incorporate tone bursts at intervals of 30 seconds within the main body of a transmission as proposed by FCC. Hence, the effect of the tone burst was to increase the length of pilot-initiated transmissions by 0, 1, 2, or 3 seconds. Average aircraft arrival rates per hour for each of the typical sectors involved in table 2.5, estimated from data collected in 1969, were used in each simulation conducted for this study. In addition, all the remaining parameters were obtained from master equations and tables. Thus a total of four 2-hour experiments were performed for each of the nine sector functions. The results of each experiment were originally displayed on four pages of output consisting of one summary page followed by three graphs exhibiting the dynamic behavior of communications during the 2-hour observation period. However, only a grand summary of all simulations is presented for each of the sector functions as shown in tables 3.11 - 3.19. (A sample of the raw tables and graphs is given at the end of this chapter.)

From a careful inspection of the tables, one is not intrigued by the fact that the average number of aircraft in sector n_t increases with increasing tone duration at constant aircraft arrival rate. In practice, it might be expected that pilots and controllers will alter the flow of information to compensate for the additional burden imposed upon the channel by long tone burst lengths rather than resort to such measures as speed control, stacking, etc. On the other hand, the simulation program was developed from data collected in a normal busy working environment

rather than a crisis situation. As a result, it does not presently provide for compensation via alteration of information flow, and so the time interval of an aircraft's being in the sector increases with increasing tone burst duration. Thus, the simulation results must be interpreted under the assumption that the amount of ATC information flow between an aircraft and ground is independent of tone burst length. Succinctly stated, system degradation due to increasing tone durations must be reflected by the three response variables, number of aircraft in sector, channel state, and aircraft queuing state, or a reduction in the quality and/or quantity of ATC air/ground information flow. In this study, the degradation is displayed by changes in the three response variables. However, this is not to say that degradation in terms of information flow cannot be incorporated into the simulation software. Obviously, once a mechanism of compensation by alteration of information flow is specified, the possibility of incorporation arises. In fact, the development of the present ATCC simulation program was undertaken for the purpose of studying the effect that such variations from normal operating conditions have on communications.

3.3.2 Estimation of Average Response at Intermediate Tone Durations

Since the GPSS program can execute simulations for only integer number of seconds of transmission length, the four trials for each of the sector function simulation experiments, at the tone durations of 0.0, 0.5, 1.0 and 1.5 seconds, are all one can perform within this programming restriction. Nevertheless, for tone durations falling between these four points, a polynomial spline can be used to interpolate the four average response points obtained from the simulation exercises. At a traffic density specified (for instance, for the N.Y. HI sector function the expected traffic density is specified as 33 aircraft arrivals per hour), a cubic polynomial curve which relates the average response (y) with the tone duration (x) can be written as

$$y = c_0 + c_1 x + c_2 x^2 + c_3 x^3 \tag{3.8}$$

where c_0, c_1, c_2 and c_3 are constant parameters to be determined from a spline fitting procedure. Since now we have four observations on y and x and the same number of unknown parameters, the spline equation can be completely specified by solving four simultaneous equations each expressing a value of y by its corresponding value of x, in the polynomial function. Values other than the multiples of 0.5-second tone duration can then substitute the variable x in Equation (3.8), and the values of y determined.

On the other hand, for a given tone duration, but varied traffic density, another spline can be specified, estimated and combined with the one just described. Making use of the values displayed in table 3.1, in which different traffic densities were imposed upon the sector function

simulations with a zero tone duration, a spline with three parameters as expressed below is adequate for relating the response to the expected traffic density:

$$y = d_1 z + d_2 z^2 + d_3 z^3 \tag{3.9}$$

where y is the average response results from a simulation run and z is the expected traffic density (number of aircraft arrivals/hour). Again, using three pairs of moderate values of y and z, from table 3.1, one can completely determine the parameters in the polynomial function considered. For values of z other than those actually tried the corresponding values of y can be interpolated.

Furthermore, a convenient method useful for combining the two splines discussed above to form a complete surface of y for various combinations of x and z is described below. Assume that the values of y at different values of x are proportionally invariant at every value of z, i.e. the ratio

$$\frac{y}{c_0} = 1 + \frac{c_1}{c_0} x + \frac{c_2}{c_0} x^2 + \frac{c_3}{c_0} x^3 \tag{3.10}$$

remains constant for all values of z. Let y_0 denote the value of y when the tone duration is equal to zero, i.e. $x = 0$, and the traffic density is equal to z_0, $(y_0 = d_1 z_0 + d_2 z^2_0 + d_3 z^3_0)$. Then the value of y for a given tone duration x and the traffic density z_0 can be computed in the following way:

$$y = y_0 \left(1 + \frac{c_1}{c_0} x + \frac{c_2}{c_0} x^2 + \frac{c_3}{c_0} x^3\right) \tag{3.11}$$

Through the use of this procedure a complete <u>average</u> response surface was constructed and tabulated for each of the three responses: aircraft loading, channel utilization and the queuing time per communication transaction. Totally nine sets of three-tables were compiled for each of the nine functions investigated (see tables 3.20 - 3.46).

For practical use of these tables two special notes are made below. First, in occasional cases the polynomial functions determined were found having negative slope in certain range of the values of the driving variable. To remedy this difficulty a horizontal straight line was used to replace the portion of valley-like curve. Second, the average channel utilization rate over the 2-hour observation period was assumed upper bounded by fractions in the neighborhood of 0.85, due to the common pauses that occur during the ebb and flow of human conversations. For convenience, all values which were originally greater than 0.85 were reduced to 0.85, thereby to indicate the existence of an unstable channel status under unduly heavy demands for conversations. The tabulated values of aircraft loading and queuing time corresponding to a 0.85 channel rate

are in fact providing the very lower bounds to the responses expected from a real situation represented by the combination of tone duration and traffic density.

Several extra simulations were executed to provide checks on the accuracy of the spline projected response surface. Results are summarized as follows:

Case (i): New York HI function
Θ = 20 aircraft arrivals per hour, tone duration = 1.0 second
Simulated responses: $(\bar{n}_t, \bar{c}_t, \bar{Q}_t) = (3.88, 0.48, 7.31)$
Projected responses: $(\bar{n}_t, \bar{c}_t, \bar{Q}_t) = (3.85, 0.39, 8.01)$

Case (ii): New York LT Function
Θ = 20 aircraft arrivals per hour; tone duration = 1.0 second
Simulated responses: $(\bar{n}_t, \bar{c}_t, \bar{Q}_t) = (3.39, 0.53, 11.45)$
Projected responses: $(\bar{n}_t, \bar{c}_t, \bar{Q}_t) = (2.50, 0.56, 13.24)$

Case (iii): New York AR function
Θ = 10 aircraft arrivals per hour; tone duration = 1.0 second
Simulated responses: $(\bar{n}_t, \bar{c}_t, \bar{Q}_t) = (1.25, 0.30, 3.83)$
Projected responses: $(\bar{n}_t, \bar{c}_t, \bar{Q}_t) = (1.90, 0.32, 9.78)$

Impressions obtained from an inspection of these results appear to be in favor of an acceptance of the spline projections as convenient, and low cost, approximations to the responses desired.

3.3.3 Concluding Remarks on the Tone Burst Effect

From an inspection of the tables provided, it is found that the range of percentage increases in average channel utilization for all nine sector functions is 11 to 18 for a tone burst length of .5 second and 35 to 54 for 1.5-second bursts. The corresponding ranges of percentage increases in average queuing time are 28 to 80 and 138 to 475. This leads us to believe that implementation of the proposed FCC regulation may severely impact the ability of the agency to provide adequate air traffic control service unless some way is found to prevent tone identification procedures from extending the duration of pilot-initiated transmissions.

A sample set of tables and graphs for HI sector function, from which tables 3.11 - 3.19 were constructed is appended to this chapter (see tables 3.47 - 3.50 and figures 3.5 - 3.16).

3.4 Effects of Changes in Expected Number of TR/CT upon Channel Responses

From studies performed to date, it was found that among the major inputs to the simulation model the number of TR/CT is the variable most difficult to describe using conventional statistical models. Historical histograms were therefore suggested to be used as inputs to the simulation programs. Furthermore, nonhomogeneity of this variable was found to exist among individual sectors within a function. All these facts indicate the flexibility or adaptability of this variable to varied environments. We suspect that, for improving the ATC performance in the future, the number of TR/CT could be the first candidate subjected to modifications.

In this section, without specifying detailed changes in the communicational technology, we hypothesize a transfer function, which transfers an old distribution into a new distribution, to express the improvement due to a change in the ATC method and/or facilities. The effects on various responses are then studied through simulation experiments.

3.4.1 Specification and Estimation of the Transfer Function

Let the old distribution of #TR/CT be denoted by p(j), while the new one by p*(j); in both cases j = 1,2,3, ... The transfer function w(x), which maps p(j) into p*(j) and reduces the expected value to a proportion, $\tilde{K}$, of the original level, is the function satisfying the following conditions:

(i) $$\sum_{j=1}^{\infty} p^*(j) = \sum_{j=1}^{\infty} w(j)p(j) = 1;$$

(ii) $$\sum_{j=1}^{\infty} jp^*(j) = \sum_{j=1}^{\infty} j\, w(j)p(j) = \tilde{K} \sum_{j=1}^{\infty} j\, p(j) \qquad (3.12)$$

The first condition is to assure that p*(j) is a probability function and the second is to "shift" the expected level to a new point.

A transfer function useful for #TR/CT is the one which can be written as:

$$w(x) = a\, e^{-x/b}, \qquad 0 < x < \infty \qquad (3.13)$$

where a and b are constants to be determined by the two conditions given in Equation (3.12). This function means that, in order to reduce the average level of the variable to a given point, the frequencies at the lower range of the variable are to be increased while those at the higher range decreased. The shifts of the weights are of an exponential form. This appears to be an efficient way of improving the responses.

3.4.2 Results of Simulation Experiments

To investigate the effects of this shift in the expected value of #TR/CT upon the responses of concern, a simulation experiment for N.Y. HI function was carried out using distributions determined by Equations (3.13) and (3.12). For a given distribution of #TR/CT, as shown in figure 3.17, the function $w(x)$ and the new distribution $p^*(j)$ are shown in figures 3.18 - 3.23 for $\tilde{K}$ = 0.9, 0.7, and 0.5. The resulting distributions of $p^*(j)$ were then used as inputs to the simulation exercises, at a traffic density equal to 60 aircraft arrivals per hour. The computer outputs for the four trials are provided in tables 3.51 - 3.54 and figures 3.24 - 3.35 and appended to this chapter. A summary table (table 3.55) is given for the review of the average responses. Significant improvements in the responses are observed for each of the decrements on the value of $\tilde{K}$. The explosive status in the case of $\tilde{K}$ = 1.0 has been transferred to a normal operation due to a 30 per cent reduction on the #TR/CT (for $\tilde{K}$=0.7). This result will be useful for the future design for system improvement.

3.5 Summary and Concluding Remarks

In this chapter three applications of the simulation model have been discussed; namely, the estimation of sector function communications capacities, the evaluation of the effects of tone disturbance, and an illustration of influence of changes in expected number of TR/CT. All three applications provide valuable information for the future design for system improvement. These examples also suggest the general applicability of the simulation model to various studies.

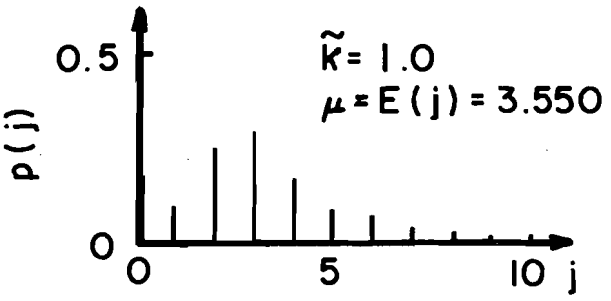

Figure 3.17 Original Probability Function of TR/CT (New York HI Function)

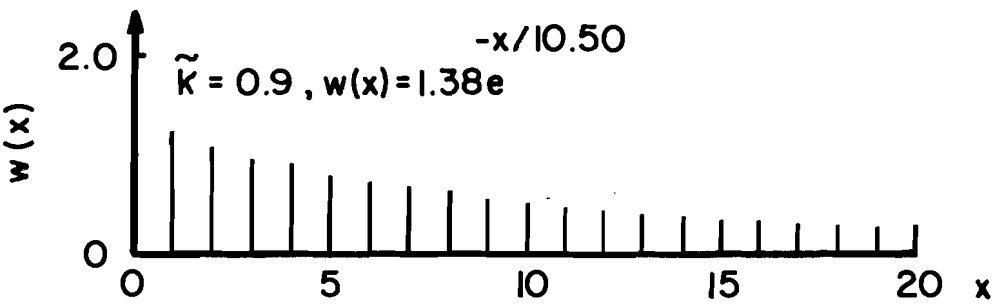

Figure 3.18 The Weighting Function ($\tilde{k}$=0.9)

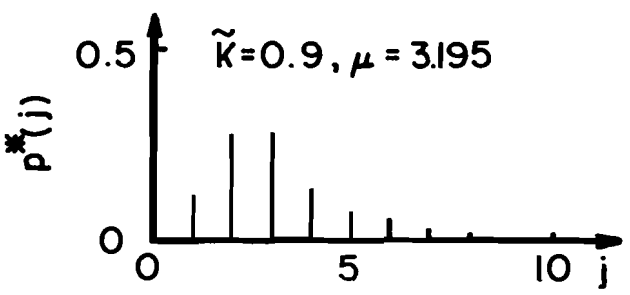

Figure 3.19 The New Distribution ($\tilde{k}$=0.9)

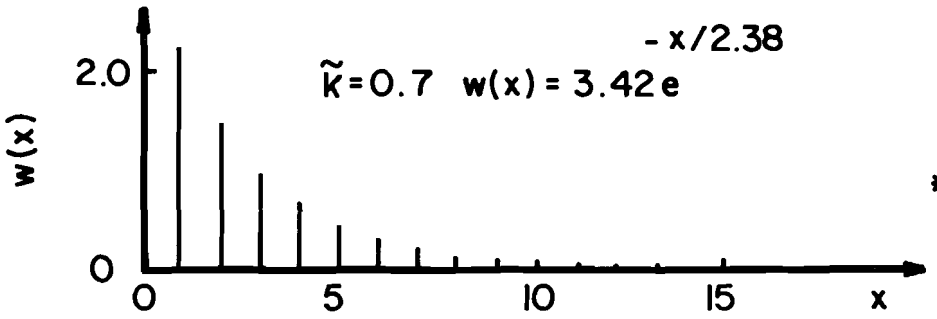

Figure 3.20 The Weighting Function ($\tilde{k}=0.7$)

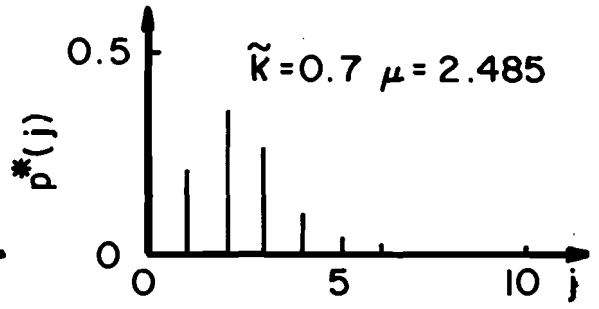

Figure 3.21 The New Distribution ($\tilde{k}=0.7$)

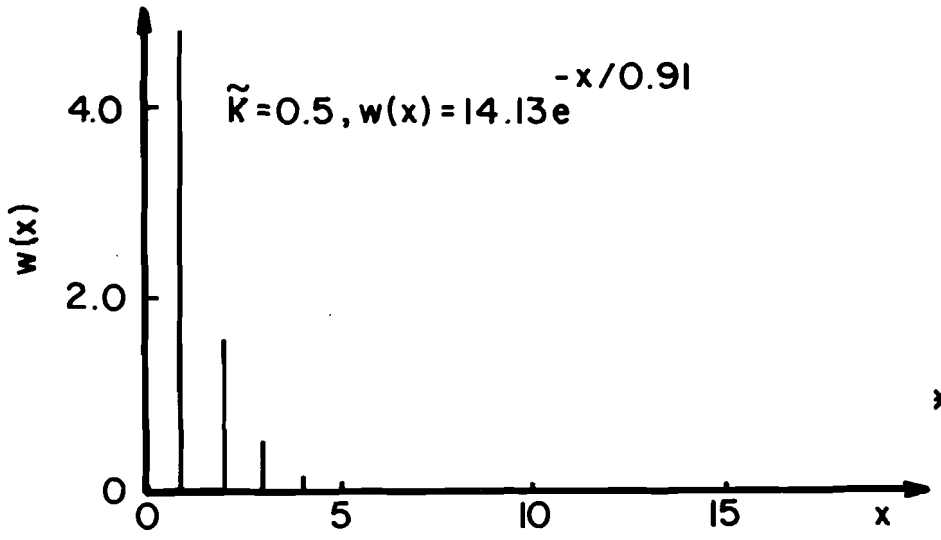

Figure 3.22 The Weighting Function ($\tilde{k}=0.5$)

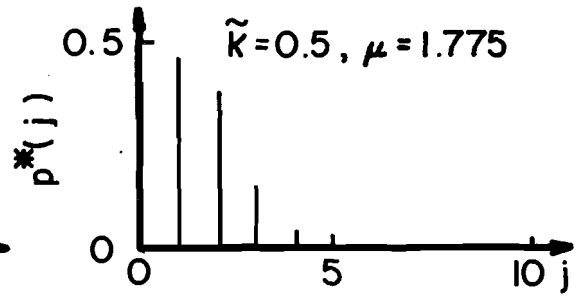

Figure 3.23 The New Distribution ($\tilde{k}=0.5$)

Table 3.55 Comparisons of Major Responses at Various Rates of Reduction on #TR/CT

(HI Function, N.Y. ARTCC; Expected Traffic Density=60A/HR)

	$\tilde{K}^{*} = 1.$	$\tilde{K} = 0.9$	$\tilde{K} = 0.7$	$\tilde{K} = 0.5$
$\bar{n}_t$	16.640	13.447	10.260	9.343
$\bar{c}_t$	0.869	0.824	0.669	0.475
$\bar{Q}_t$ (sec.)	89.104	46.511	12.222	4.670
$Pr(\xi>1)$	0.3749	0.090	0.003	0.000

* $\tilde{K}$ = (New average #TR/CT) / (Old average #TR/CT)

Table 3.3 $Pr(n_t > k)$ at Various Traffic Densities
(LT Sector Function, N.Y. ARTCC)

k	40A/HR	45A/HR	55A/HR
10	0.1219	0.1359	0.5225
11	.0653	.0641	.4121
12	.0316	.0259	.3082
13	.0138	.0090	.2178
14	.0054	.0026	.1450
15	.0019	.0007	.0906
16	.0006	.0001	.0531
17	.0002	.0000	.0291
18	.0000	.0000	.0149
19	.0000	.0000	.0071
20	.0000	.0000	.0032
21	.0000	.0000	.0013
22	.0000	.0000	.0005
23	.0000	.0000	.0002
24	.0000	.0000	.0001
25	.0000	.0000	.0000
$\hat{\phi}_1$	1.2470	1.1598	1.2819
$\hat{\phi}_2$	-0.3352	-0.2603	-0.3349
$\hat{\sigma}^2$	0.9489	0.7989	0.8894
$\hat{\mu}$	6.6280	7.4010	10.2040

*A/HR = expected number of aircraft arrivals per hour

Table 3.4 $Pr(n_t > k)$ at Various Traffic Densities

(LE Sector Function, N.Y. ARTCC)

k	35A/HR	45A/HR	55A/HR	70A/HR
10	0.0107	0.2131	0.4203	0.8786
11	.0021	.1278	.3026	.8382
12	.0003	.0697	.2026	.7899
13	.0000	.0344	.1255	.7341
14	.0000	.0154	.0717	.6716
15	.0000	.0062	.0376	.6039
16	.0000	.0022	.0181	.5329
17	.0	.0007	.0080	.4608
18	.0	.0002	.0032	.3900
19	.0	.0001	.0012	.3227
20	.0	.0000	.0004	.2607
21	.0	.0	.0001	.2055
22	.0	.0	.0	.1579
23	.0	.0	.0	.1182
24	.0	.0	.0	.0861
25	.0	.0	.0	.0611
26	.0	.0	.0	.0421
27	.0	.0	.0	.0282
28	.0	.0	.0	.0184
29	.0	.0	.0	.0116
30	.0	.0	.0	.0071
31	.0	.0	.0	.0043
32	.0	.0	.0	.0025
33	.0	.0	.0	.0014
34	.0	.0	.0	.0008
35	.0	.0	.0	.0004
36	.0	.0	.0	.0002
37	.0	.0	.0	.0001
38	.0	.0	.0	.0
$\hat{\phi}_1$	1.1417	1.1516	1.1946	1.0966
$\hat{\phi}_2$	-0.3038	-0.2154	-0.2637	-0.1283
$\hat{\sigma}^2$	0.6882	0.8377	0.9945	1.6658
$\hat{\mu}$	5.8520	7.6690	9.3620	16.4580

Table 3.5 $P_r(n_t>k)$ at Various Traffic Densities

(HI Sector Function, N.Y. ARTCC)

k	45A/HR	50A/HR	60A/HR
10	0.1934	0.4380	0.6733
11	0.0884	0.3059	0.6485
12	0.0332	0.1953	0.6232
13	0.0101	0.1132	0.5972
14	0.0025	0.0592	0.5709
15	0.0005	0.0279	0.5442
16	0.0001	0.0118	0.5173
17	0.0000	0.0045	0.4904
18	0.0000	0.0015	0.4634
19	0.0000	0.0005	0.4367
20	0.0000	0.0001	0.4102
21	0.0000	0.0000	0.3842
22	0.0000	0.0000	0.3586
23	0.0000	0.0000	0.3337
24	0.0	0.0	0.3095
25	0.0	0.0	0.2861
26	0.0	0.0	0.2635
27	0.0	0.0	0.2419
28	0.0	0.0	0.2213
29	0.0	0.0	0.2018
30	0.0	0.0	0.1833
31	0.0	0.0	0.1659
32	0.0	0.0	0.1496
33	0.0	0.0	0.1344
34	0.0	0.0	0.1204
35	0.0	0.0	0.1073
36	0.0	0.0	0.0954
37	0.0	0.0	0.0844
38	0.0	0.0	0.0744
39	0.0	0.0	0.0654
40	0.0	0.0	0.0572
$\hat{\phi}_1$	1.1522	1.1942	1.3581
$\hat{\phi}_2$	-0.3326	-0.2906	-0.3626
$\hat{\sigma}^2$	0.9532	1.0674	1.2398
$\hat{\mu}$	8.2160	9.5550	16.6400

Table 3.6 $Pr(n_t > k)$ at Various Traffic Densities

(LC Sector Function, N.Y. Area)

k	85A/HR	100A/HR	110A/HR
10	0.6708	0.9992	0.9973
11	0.5693	0.9985	0.9965
12	0.4629	0.9973	0.9956
13	0.3591	0.9951	0.9945
14	0.2648	0.9915	0.9931
15	0.1850	0.9857	0.9915
16	0.1222	0.9769	0.9894
17	0.0761	0.9638	0.9870
18	0.0446	0.9453	0.9841
19	0.0246	0.9199	0.9807
20	0.0127	0.8866	0.9767
21	0.0062	0.8443	0.9720
22	0.0028	0.7927	0.9665
23	0.0012	0.7323	0.9602
24	0.0005	0.6640	0.9530
25	0.0002	0.5898	0.9447
26	0.0001	0.5123	0.9353
27	0.0000	0.4343	0.9247
28	0.0	0.3588	0.9128
29	0.0	0.2885	0.8996
30	0.0	0.2254	0.8850
31	0.0	0.1710	0.8689
32	0.0	0.1258	0.8514
33	0.0	0.0897	0.8323
34	0.0	0.0619	0.8118
35	0.0	0.0413	0.7987
36	0.0	0.0267	0.7662
37	0.0	0.0167	0.7414
38	0.0	0.0101	0.7152
39	0.0	0.0059	0.6878
40	0.0	0.0033	0.6593
$\hat{\phi}_1$	1.2824	1.2551	1.1921
$\hat{\phi}_2$	-0.3747	-0.3035	-0.2008
$\hat{\sigma}^2$	1.5563	1.7169	2.2231
$\hat{\mu}$	11.6520	26.1570	45.1950

Table 3.7 $Pr(n_t > k)$ at Various Traffic Densities
(LG Sector Function, N.Y. Area)

k	80A/HR	90A/HR	100A/HR
10	0.6048	0.8072	0.6560
11	0.4995	0.7571	0.6413
12	0.3943	0.7007	0.6263
13	0.2963	0.6389	0.6112
14	0.2113	0.5733	0.5958
15	0.1426	0.5056	0.5804
16	0.0908	0.4377	0.5648
17	0.0545	0.3716	0.5491
18	0.0308	0.3092	0.5333
19	0.0163	0.2517	0.5175
20	0.0081	0.2005	0.5016
21	0.0038	0.1561	0.4857
22	0.0017	0.1187	0.4699
23	0.0007	0.0882	0.4541
24	0.0003	0.0639	0.4384
25	0.0001	0.0452	0.4228
26	0.0	0.0311	0.4073
27	0.0	0.0209	0.3919
28	0.0	0.0137	0.3767
29	0.0	0.0087	0.3617
30	0.0	0.0054	0.3469
31	0.0	0.0033	0.3324
32	0.0	0.0019	0.3181
33	0.0	0.0011	0.3040
34	0.0	0.0006	0.2903
35	0.0	0.0003	0.2768
36	0.0	0.0001	0.2636
37	0.0	0.0001	0.2508
38	0.0	0.0	0.2383
39	0.0	0.0	0.2262
40	0.0	0.0	0.2144
$\hat{\phi}_1$	1.2028	1.2828	1.1654
$\hat{\phi}_2$	-0.2747	-0.3242	-0.1671
$\hat{\sigma}^2$	1.4232	1.8864	1.7836
$\hat{\mu}$	10.9950	15.0790	20.0970

Table 3.8 $Pr(n_t > k)$ at Various Traffic Densities

(DP Sector Function, N.Y. Area)

k	50A/HR	55A/HR	60A/HR	70A/HR
10	0.0491	0.0551	0.2082	0.7094
11	0.0187	0.0173	0.1091	0.6321
12	0.0060	0.0043	0.0494	0.5490
13	0.0017	0.0008	0.0193	0.4636
14	0.0004	0.0001	0.0064	0.3800
15	0.0001	0.0000	0.0018	0.3016
16	0.0000	0.0000	0.0004	0.2314
17	0.0000	0.0000	0.0001	0.1715
18	0.0000	0.0	0.0	0.1225
19	0.0	0.0	0.0	0.0843
20	0.0	0.0	0.0	0.0558
21	0.0	0.0	0.0	0.0355
22	0.0	0.0	0.0	0.0217
23	0.0	0.0	0.0	0.0127
24	0.0	0.0	0.0	0.0072
25	0.0	0.0	0.0	0.0039
26	0.0	0.0	0.0	0.0020
27	0.0	0.0	0.0	0.0010
28	0,0	0,0	0,0	0,0005
29	0.0	0.0	0.0	0.0002
30	0.0	0.0	0.0	0.0001
31	0.0	0.0	0.0	0.0
$\hat{\phi}_1$	1.1326	1.0023	1.1631	1.2635
$\hat{\phi}_2$	-0.2413	-0.1155	-0.2796	-0.3009
$\hat{\sigma}^2$	0.8606	0.7180	0.9139	1.1208
$\hat{\mu}$	6.1370	6.8950	8.0590	12.5730

Table 3.9 $Pr(n_k > k)$ at Various Traffic Densities

(AD Sector Function, N.Y. Area)

k	40A/HR	45A/HR	50A/HR	60A/HR	70A/HR
10	0.0001	0.0000	0.0374	0.1380	0.6211
11	0.0000	0.0000	0.0135	0.0715	0.5538
12	0.0	0.0	0.0041	0.0329	0.4850
13	0.0	0.0	0.0011	0.0134	0.4165
14	0.0	0.0	0.0002	0.0048	0.3506
15	0.0	0.0	0.0	0.0015	0.2889
16	0.0	0.0	0.0	0.0004	0.2328
17	0.0	0.0	0.0	0.0001	0.1833
18	0.0	0.0	0.0	0.0	0.1410
19	0.0	0.0	0.0	0.0	0.1059
20	0.0	0.0	0.0	0.0	0.0775
21	0.0	0.0	0.0	0.0	0.0554
22	0.0	0.0	0.0	0.0	0.0385
23	0.0	0.0	0.0	0.0	0.0261
24	0.0	0.0	0.0	0.0	0.0173
25	0.0	0.0	0.0	0.0	0.0111
26	0.0	0.0	0.0	0.0	0.0070
27	0.0	0.0	0.0	0.0	0.0042
28	0.0	0.0	0.0	0.0	0.0025
29	0.0	0.0	0.0	0.0	0.0014
30	0.0	0.0	0.0	0.0	0.0008
31	0.0	0.0	0.0	0.0	0.0004
32	0.0	0.0	0.0	0.0	0.0002
33	0.0	0.0	0.0	0.0	0.0001
34	0.0	0.0	0.0	0.0	0.0001
35	0.0	0.0	0.0	0.0	0.0
$\hat{\phi}_1$	1.0631	1.1136	1.2060	1.2472	1.3505
$\hat{\phi}_2$	-0.2108	-0.3297	-0.3123	-0.3715	-0.3769
$\hat{\sigma}^2$	0.5605	0.4908	0.7561	1.0602	1.0876
$\hat{\mu}$	4.0890	4.6940	5.8650	7.0950	11.7810

Table 3.10 $Pr(n_t > k)$ at Various Traffic Densities

(AR Sector Function. N.Y. Area)

k	35A/HR	40A/HR
10	0.0991	0.3952
11	0.0496	0.2896
12	0.0222	0.1996
13	0.0088	0.1289
14	0.0031	0.0777
15	0.0010	0.0437
16	0.0003	0.0229
17	0.0001	0.0111
18	0.0000	0.0050
19	0.0000	0.0021
20	0.0000	0.0008
21	0.0000	0.0003
22	0.0000	0.0001
23	0.0000	0.0000
$\hat{\phi}_1$	1.3244	1.3496
$\hat{\phi}_2$	-0.4000	-0.4073
$\hat{\sigma}^2$	0.6743	0.8047
$\hat{\mu}$	6.4430	9.0790

Table 3.11

Effects of Tone-Disturbance upon ATC Communications Channels

(N.Y. ARTCC, III Sector Function)

Traffic Density = 33 Aircraft Arrivals/Hour

Response	Tone Duration (seconds)			
	0.0	0.5	1.0	1.5
$\bar{n}_t$	5.579	5.982	6.497	6.933
$\bar{c}_t$	0.529	0.611	0.685	0.755
$\bar{Q}_t$ (sec)	9.146	16.448	21.251	29.576

$\bar{n}_t$ = average aircraft loading per second

$\bar{c}_t$ = average channel utilization

$\bar{Q}_t$ = average queuing time.

Table 3.12

Effects of Tone-Disturbance upon ATC Communications Channels

(N.Y. ARTCC, LE Sector Function)

Traffic Density = 35 Aircraft Arrivals/Hour

Response	Tone Duration (seconds)			
	0.0	0.5	1.0	1.5
$\bar{n}_t$	5.852	6.228	7.313	9.300
$\bar{c}_t$	0.591	0.676	0.766	0.859
$\bar{Q}_t$ (sec)	13.357	21.016	40.303	76.829

$\bar{n}_t$ = average aircraft loading per second

$\bar{c}_t$ = average channel utilization

$\bar{Q}_t$ = average queuing time.

Table 3.13

Effects of Tone-Disturbance upon ATC Communications Channels

(N.Y. ARTCC, LT Sector Function)

Traffic Density = 29 Aircraft Arrivals/Hour

Response	Tone Duration (seconds)			
	0.0	0.5	1.0	1.5
$\bar{n}_t$	4.257	4.692	4.875	5.320
$\bar{c}_t$	0.545	0.616	0.700	0.770
$\bar{Q}_t$ (sec)	9.410	15.683	19.368	28.148

$\bar{n}_t$ = average aircraft loading per second

$\bar{c}_t$ = average channel utilization

$\bar{Q}_t$ = average queuing time.

Table 3.14

Effects of Tone-Disturbance upon ATC Communications Channels

(N.Y. Area, GN Sector Function)

Traffic Density = 43 Aircraft Arrivals/Hour

Response	Tone Duration (seconds)			
	0.0	0.5	1.0	1.5
$\bar{n}_t$	2.374	2.496	2.608	2.763
$\bar{c}_t$	0.289	0.340	0.388	0.436
$\bar{Q}_t$ (sec)	3.830	6.145	10.091	13.246

$\bar{n}_t$ = average aircraft loading per second

$\bar{c}_t$ = average channel utilization

$\bar{Q}_t$ = average queuing time.

Table 3.15

Effects of Tone-Disturbance upon ATC Communications Channels

(N.Y. Area, LC Sector Function)

Traffic Density = 42 Aircraft Arrivals/Hour

Response	Tone Duration (seconds)			
	0.0	0.5	1.0	1.5
$\bar{n}_t$	5.905	6.275	6.644	7.291
$\bar{c}_t$	0.454	0.537	0.609	0.700
$\bar{Q}_t$ (sec.)	6.689	8.540	13.484	22.656

$\bar{n}_t$ = average aircraft loading per second

$\bar{c}_t$ = average channel utilization

$\bar{Q}_t$ = average queuing time.

Table 3.16

Effects of Tone-Disturbance upon ATC Communications Channels

(N.Y. Area, LG Sector Function)

Traffic Density = 25 Aircraft Arrivals/Hour

Response	Tone Duration (seconds)			
	0.0	0.5	1.0	1.5
$\bar{n}_t$	2.990	2.998	3.240	3.606
$\bar{c}_t$	0.306	0.354	0.405	0.453
$\bar{Q}_t$ (sec.)	7.232	10.944	20.381	24.628

$\bar{n}_t$ = average aircraft loading per second

$\bar{c}_t$ = average channel utilization

$\bar{Q}_t$ = average queuing time.

Table 3.17

Effects of Tone-Disturbance upon ATC Communications Channels

(N.Y. Area, DP Sector Function)

Traffic Density = 25 Aircraft Arrivals/Hour

Response	Tone Duration (seconds)			
	0.0	0.5	1.0	1.5
$\bar{n}_t$	3.295	3.565	3.907	4.191
$\bar{c}_t$	0.469	0.535	0.591	0.660
$\bar{Q}_t$ (sec.)	10.288	13.884	19.099	28.000

$\bar{n}_t$ = average aircraft loading per second

$\bar{c}_t$ = average channel utilization

$\bar{Q}_t$ = average queuing time.

Table 3.18

Effects of Tone-Disturbance upon ATC Communications Channels

(N.Y. Area, AD Sector Function)

Traffic Density = 16 Aircraft Arrivals/Hour

Response	Tone Duration (seconds)			
	0.0	0.5	1.0	1.5
$\bar{n}_t$	1.592	1.602	1.741	1.813
$\bar{c}_t$	0.240	0.271	0.304	0.337
$\bar{Q}_t$ (sec.)	4.779	6.398	9.981	11.390

$\bar{n}_t$ = average aircraft loading per second

$\bar{c}_t$ = average channel utilization

$\bar{Q}_t$ = average queuing time.

Table 3.19

Effects of Tone-Disturbance upon ATC Communications Channels

(N.Y. Area , AR Sector Function)

Traffic Density = 22 Aircraft Arrivals/Hour

Response	Tone Duration (seconds)			
	0.0	0.5	1.0	1.5
$\bar{n}_t$	2.892	3.151	3.469	3.780
$\bar{c}_t$	0.527	0.585	0.644	0.712
$\bar{Q}_t$ (sec.)	11.232	15.087	21.512	27.277

$\bar{n}_t$ = average aircraft loading per second

$\bar{c}_t$ = average channel utilization

$\bar{Q}_t$ = average queuing time.

Table 3.20

EFFECTS OF TONE-DISTURBANCE UPON ATC COMMUNICATIONS CHANNELS

(N.Y. ARTCC, HI SECTOR FUNCTION)

AVERAGE AIRCRAFT LOADING

A/H	TONE DURATION (SECONDS)														
	0.0	0.1	0.2	0.3	0.4	0.5	0.6	0.7	0.8	0.9	1.0	1.1	1.2	1.3	1.4
20.	3.31	3.35	3.39	3.44	3.49	3.55	3.61	3.67	3.73	3.79	3.85	3.91	3.97	4.02	4.07
25.	4.14	4.18	4.24	4.30	4.36	4.44	4.51	4.59	4.66	4.74	4.82	4.89	4.96	5.03	5.09
30.	5.02	5.07	5.14	5.21	5.29	5.38	5.47	5.56	5.65	5.75	5.84	5.93	6.02	6.10	6.17
33.	5.58	5.64	5.71	5.80	5.88	5.98	6.08	6.18	6.29	6.39	6.50	6.60	6.69	6.78	6.86
35.	5.97	6.04	6.12	6.20	6.30	6.40	6.51	6.62	6.73	6.84	6.95	7.06	7.16	7.26	7.34
40.	7.03	7.11	7.20	7.30	7.42	7.54	7.66	7.79	7.92	8.06	8.18	8.31	8.43	8.54	8.64
45.	8.21	8.31	8.41	8.53	8.67	8.81	8.95	9.11	9.26	9.41	9.56	9.71	9.85	9.98	10.10
50.	9.55	9.66	9.78	9.92	10.08	10.24	10.41	10.59	10.77	10.95	11.12	11.29	11.46	11.61	11.75

Table 3.21

EFFECTS OF TONE-DISTURBANCE UPON ATC COMMUNICATIONS CHANNELS

(N.Y. ARTCC, HI SECTOR FUNCTION)

AVERAGE CHANNEL UTILIZATION

A/H	TONE DURATION (SECONDS)														
	0.0	0.1	0.2	0.3	0.4	0.5	0.6	0.7	0.8	0.9	1.0	1.1	1.2	1.3	1.4
20.	0.30	0.31	0.32	0.33	0.34	0.35	0.35	0.36	0.37	0.38	0.39	0.40	0.40	0.41	0.42
25.	0.39	0.40	0.41	0.42	0.44	0.45	0.46	0.47	0.48	0.49	0.50	0.51	0.52	0.53	0.54
30.	0.48	0.49	0.51	0.52	0.54	0.55	0.56	0.58	0.59	0.60	0.62	0.63	0.64	0.65	0.67
33.	0.53	0.55	0.56	0.58	0.60	0.61	0.63	0.64	0.66	0.67	0.68	0.70	0.71	0.73	0.74
35.	0.56	0.58	0.60	0.62	0.63	0.65	0.67	0.68	0.70	0.71	0.73	0.75	0.76	0.78	0.79
40.	0.65	0.67	0.69	0.71	0.73	0.75	0.77	0.79	0.80	0.82	0.84	0.85	0.85	0.85	0.85
45.	0.73	0.75	0.77	0.80	0.82	0.84	0.85	0.85	0.85	0.85	0.85	0.85	0.85	0.85	0.85
50.	0.80	0.83	0.85	0.85	0.85	0.85	0.85	0.85	0.85	0.85	0.85	0.85	0.85	0.85	0.85

Table 3.22

EFFECTS OF TONE-DISTURBANCE UPON ATC COMMUNICATIONS CHANNELS

(N.Y. ARTCC, HI SECTOR FUNCTION)

AVERAGE QUEUING TIME

A/H	TONE DURATION (SECONDS)														
	0.0	0.1	0.2	0.3	0.4	0.5	0.6	0.7	0.8	0.9	1.0	1.1	1.2	1.3	1.4
20.	3.45	4.18	4.81	5.34	5.80	6.20	6.57	6.91	7.25	7.62	8.01	8.46	8.98	9.59	10.31
25.	5.01	6.07	6.98	7.75	8.42	9.00	9.53	10.03	10.53	11.06	11.63	12.28	13.04	13.92	14.96
30.	7.31	8.87	10.19	11.32	12.29	13.14	13.92	14.65	15.38	16.14	16.98	17.93	19.03	20.33	21.85
33.	9.14	11.09	12.75	14.16	15.38	16.44	17.41	18.33	19.24	20.20	21.25	22.44	23.82	25.43	27.33
35.	10.59	12.85	14.76	16.40	17.81	19.04	20.16	21.22	22.28	23.39	24.60	25.98	27.58	29.45	31.65
40.	15.08	18.29	21.02	23.35	25.36	27.12	28.71	30.22	31.73	33.31	35.04	37.00	39.27	41.94	45.08
45.	21.01	25.49	29.30	32.54	35.34	37.79	40.01	42.12	44.21	46.41	48.83	51.56	54.73	58.44	62.81
50.	28.62	34.73	39.91	44.33	48.14	51.48	54.51	57.37	60.23	63.22	66.51	70.24	74.55	79.61	85.57

Table 3.23

EFFECTS OF TONE-DISTURBANCE UPON ATC COMMUNICATIONS CHANNELS

(N.Y. ARTCC, LT SECTOR FUNCTION)

AVERAGE AIRCRAFT LOADING

A/H	TONE DURATION (SECONDS)														
	0.0	0.1	0.2	0.3	0.4	0.5	0.6	0.7	0.8	0.9	1.0	1.1	1.2	1.3	1.4
20.	2.18	2.25	2.31	2.35	2.38	2.41	2.43	2.45	2.46	2.48	2.50	2.53	2.56	2.61	2.66
25.	3.31	3.42	3.50	3.56	3.61	3.65	3.68	3.71	3.74	3.76	3.79	3.83	3.89	3.95	4.04
29.	4.26	4.39	4.49	4.58	4.64	4.69	4.73	4.77	4.80	4.83	4.87	4.93	4.99	5.08	5.18
30.	4.49	4.63	4.74	4.83	4.90	4.95	4.99	5.03	5.06	5.10	5.14	5.20	5.27	5.36	5.47
35.	5.63	5.80	5.94	6.05	6.14	6.20	6.26	6.30	6.34	6.39	6.44	6.51	6.60	6.71	6.85
40.	6.63	6.83	7.00	7.13	7.23	7.30	7.37	7.42	7.47	7.53	7.59	7.67	7.77	7.90	8.07
45.	7.40	7.63	7.81	7.96	8.07	8.16	8.23	8.29	8.34	8.40	8.47	8.56	8.68	8.83	9.01

Table 3.24

EFFECTS OF TONE-DISTURBANCE UPON ATC COMMUNICATIONS CHANNELS

(N.Y. ARTCC, LT SECTOR FUNCTION)

AVERAGE CHANNEL UTILIZATION

A/H	TONE DURATION (SECONDS)														
	0.0	0.1	0.2	0.3	0.4	0.5	0.6	0.7	0.8	0.9	1.0	1.1	1.2	1.3	1.4
20.	0.43	0.44	0.45	0.46	0.48	0.49	0.50	0.52	0.53	0.54	0.56	0.57	0.58	0.59	0.60
25.	0.50	0.51	0.52	0.53	0.55	0.56	0.58	0.59	0.61	0.62	0.64	0.65	0.67	0.68	0.69
29.	0.54	0.56	0.57	0.58	0.60	0.62	0.63	0.65	0.67	0.68	0.70	0.72	0.73	0.75	0.76
30.	0.56	0.57	0.58	0.60	0.61	0.63	0.65	0.66	0.68	0.70	0.72	0.73	0.75	0.76	0.77
35.	0.62	0.63	0.65	0.66	0.68	0.70	0.72	0.74	0.76	0.78	0.79	0.81	0.83	0.85	0.85
40.	0.69	0.70	0.72	0.74	0.76	0.78	0.80	0.82	0.84	0.85	0.85	0.85	0.85	0.85	0.85
45.	0.77	0.79	0.81	0.83	0.85	0.85	0.85	0.85	0.85	0.85	0.85	0.85	0.85	0.85	0.85

Table 3.25

EFFECTS OF TONE-DISTURBANCE UPON ATC COMMUNICATIONS CHANNELS

(N.Y. ARTCC, LT SECTOR FUNCTION)

AVERAGE QUEUING TIME

A/H	TONE DURATION (SECONDS)														
	0.0	0.1	0.2	0.3	0.4	0.5	0.6	0.7	0.8	0.9	1.0	1.1	1.2	1.3	1.4
20.	6.43	7.68	8.69	9.51	10.17	10.72	11.20	11.64	12.11	12.62	13.24	13.99	14.92	16.08	17.51
25.	7.84	9.37	10.60	11.60	12.41	13.07	13.66	14.20	14.77	15.40	16.15	17.06	18.20	19.62	21.35
29.	9.41	11.24	12.72	13.91	14.88	15.68	16.38	17.03	17.71	18.47	19.36	20.47	21.83	23.53	25.61
30.	9.88	11.81	13.36	14.61	15.63	16.47	17.20	17.89	18.60	19.40	20.34	21.50	22.94	24.72	26.90
35.	12.90	15.41	17.44	19.07	20.40	21.50	22.45	23.35	24.28	25.32	26.55	28.06	29.93	32.26	35.11
40.	17.24	20.60	23.31	25.50	27.27	28.74	30.02	31.22	32.46	33.84	35.49	37.51	40.02	43.12	46.94
45.	23.27	27.79	31.46	34.41	36.80	38.78	40.51	42.13	43.80	45.67	47.89	50.62	54.00	58.19	63.34

Table 3.26

EFFECTS OF TONE-DISTURBANCE UPON ATC COMMUNICATIONS CHANNELS

(N.Y. ARTCC, LE SECTOR FUNCTION)

AVERAGE AIRCRAFT LOADING

A/H	TONE DURATION (SECONDS)														
	0.0	0.1	0.2	0.3	0.4	0.5	0.6	0.7	0.8	0.9	1.0	1.1	1.2	1.3	1.4
20.	3.12	3.13	3.16	3.20	3.25	3.32	3.40	3.50	3.61	3.75	3.90	4.07	4.26	4.47	4.70
25.	4.01	4.03	4.07	4.12	4.19	4.27	4.38	4.50	4.65	4.82	5.02	5.23	5.48	5.75	6.05
30.	4.93	4.95	4.99	5.06	5.14	5.25	5.38	5.53	5.71	5.92	6.16	6.43	6.73	7.06	7.43
35.	5.85	5.88	5.93	6.00	6.10	6.23	6.38	6.57	6.78	7.03	7.31	7.63	7.99	8.38	8.82
40.	6.77	6.80	6.86	6.94	7.06	7.20	7.38	7.60	7.84	8.13	8.46	8.83	9.24	9.70	10.20
45.	7.67	7.70	7.77	7.87	8.00	8.16	8.36	8.60	8.89	9.21	9.58	10.00	10.47	10.99	11.56
50.	8.54	8.58	8.65	8.76	8.90	9.08	9.31	9.58	9.89	10.25	10.67	11.13	11.65	12.23	12.87
55.	9.36	9.40	9.48	9.60	9.76	9.96	10.21	10.50	10.85	11.24	11.70	12.21	12.78	13.41	14.11

Table 3.27

EFFECTS OF TONE-DISTURBANCE UPON ATC COMMUNICATIONS CHANNELS

(N.Y. ARTCC, LE SECTOR FUNCTION)

AVERAGE CHANNEL UTILIZATION

A/H	TONE DURATION (SECONDS)														
	0.0	0.1	0.2	0.3	0.4	0.5	0.6	0.7	0.8	0.9	1.0	1.1	1.2	1.3	1.4
20.	0.50	0.52	0.53	0.55	0.56	0.58	0.59	0.61	0.62	0.64	0.65	0.67	0.68	0.70	0.72
25.	0.55	0.56	0.58	0.59	0.61	0.62	0.64	0.66	0.67	0.69	0.71	0.73	0.74	0.76	0.78
30.	0.57	0.59	0.61	0.62	0.64	0.66	0.67	0.69	0.71	0.72	0.74	0.76	0.78	0.80	0.81
35.	0.59	0.61	0.62	0.64	0.66	0.68	0.69	0.71	0.73	0.75	0.77	0.78	0.80	0.82	0.84
40.	0.61	0.63	0.64	0.66	0.68	0.70	0.72	0.73	0.75	0.77	0.79	0.81	0.83	0.85	0.85
45.	0.64	0.65	0.67	0.69	0.71	0.73	0.75	0.77	0.78	0.80	0.82	0.84	0.85	0.85	0.85
50.	0.68	0.70	0.72	0.74	0.76	0.78	0.80	0.82	0.84	0.85	0.85	0.85	0.85	0.85	0.85
55.	0.75	0.77	0.79	0.81	0.83	0.85	0.85	0.85	0.85	0.85	0.85	0.85	0.85	0.85	0.85

Table 3.28

EFFECTS OF TONE-DISTURBANCE UPON ATC COMMUNICATIONS CHANNELS

(N.Y. ARTCC, LE SECTOR FUNCTION)

AVERAGE QUEUING TIME

A/H	TONE DURATION (SECONDS)														
	0.0	0.1	0.2	0.3	0.4	0.5	0.6	0.7	0.8	0.9	1.0	1.1	1.2	1.3	1.4
20.	7.63	8.13	8.79	9.64	10.70	12.01	13.58	15.44	17.62	20.14	23.03	26.31	30.01	34.16	38.78
25.	9.54	10.16	10.99	12.05	13.38	15.01	16.97	19.30	22.02	25.17	28.78	32.89	37.51	42.70	48.47
30.	11.45	12.19	13.18	14.46	16.05	18.01	20.36	23.16	26.42	30.20	34.54	39.46	45.02	51.24	58.17
35.	13.35	14.23	15.38	16.87	18.73	21.01	23.76	27.02	30.83	35.24	40.29	46.04	52.52	59.78	67.86
40.	19.38	20.64	22.32	24.47	27.18	30.49	34.47	39.20	44.73	51.13	58.46	66.80	76.20	86.73	98.46
45.	24.66	26.26	28.40	31.14	34.58	38.79	43.87	49.88	56.92	65.06	74.40	85.01	96.97	*****	*****
50.	28.61	30.47	32.95	36.13	40.12	45.01	50.89	57.87	66.03	75.48	86.31	98.62	*****	*****	*****
55.	30.63	32.63	35.28	38.69	42.96	48.20	54.50	61.97	70.72	80.83	92.43	*****	*****	*****	*****

Table 3.29

EFFECTS OF TONE-DISTURBANCE UPON ATC COMMUNICATIONS CHANNELS

(N.Y. AREA, 3N SECTOR FUNCTION)

AVERAGE AIRCRAFT LOADING

A/H	TONE DURATION (SECONDS)														
	0.0	0.1	0.2	0.3	0.4	0.5	0.6	0.7	0.8	0.9	1.0	1.1	1.2	1.3	1.4
43.	2.36	2.39	2.42	2.44	2.46	2.48	2.51	2.53	2.55	2.57	2.60	2.62	2.65	2.68	2.71

Table 3.30

EFFECTS OF TONE-DISTURBANCE UPON ATC COMMUNICATIONS CHANNELS

(N.Y. AREA, 3N SECTOR FUNCTION)

AVERAGE CHANNEL UTILIZATION

A/H	TONE DURATION (SECONDS)														
	0.0	0.1	0.2	0.3	0.4	0.5	0.6	0.7	0.8	0.9	1.0	1.1	1.2	1.3	1.4
43.	0.29	0.30	0.31	0.32	0.33	0.34	0.35	0.36	0.37	0.38	0.39	0.40	0.41	0.41	0.42

Table 3.31

EFFECTS OF TONE-DISTURBANCE UPON ATC COMMUNICATIONS CHANNELS

(N.Y. AREA, GN SECTOR FUNCTION)

AVERAGE QUEUING TIME

A/H	TONE DURATION (SECONDS)														
	0.0	0.1	0.2	0.3	0.4	0.5	0.6	0.7	0.8	0.9	1.0	1.1	1.2	1.3	1.4
43.	3.81	4.03	4.39	4.87	5.45	6.12	6.85	7.63	8.43	9.25	10.04	10.81	11.53	12.18	12.74

Table 3.32

EFFECTS OF TONE-DISTURBANCE UPON ATC COMMUNICATIONS CHANNELS

(N.Y. AREA , IC SECTOR FUNCTION)

AVERAGE AIRCRAFT LOADING

A/H	TONE DURATION (SECONDS) 0.0	0.1	0.2	0.3	0.4	0.5	0.6	0.7	0.8	0.9	1.0	1.1	1.2	1.3	1.4
30.	4.22	4.28	4.34	4.39	4.44	4.48	4.53	4.58	4.63	4.68	4.75	4.82	4.90	4.99	5.09
40.	5.62	5.71	5.78	5.85	5.91	5.98	6.04	6.10	6.17	6.24	6.33	6.42	6.53	6.65	6.79
42.	5.90	5.99	6.07	6.14	6.21	6.27	6.34	6.41	6.48	6.56	6.64	6.74	6.85	6.98	7.13
50.	6.97	7.08	7.17	7.25	7.33	7.41	7.49	7.57	7.65	7.74	7.85	7.96	8.09	8.24	8.42
60.	8.31	8.43	8.54	8.64	8.74	8.83	8.92	9.02	9.12	9.23	9.35	9.49	9.65	9.82	10.03
70.	9.65	9.79	9.92	10.04	10.14	10.25	10.36	10.47	10.58	10.71	10.85	11.01	11.20	11.40	11.64
80.	10.98	11.15	11.29	11.43	11.55	11.67	11.79	11.92	12.05	12.20	12.36	12.54	12.75	12.98	13.25
85.	11.65	11.82	11.98	12.12	12.25	12.38	12.51	12.64	12.78	12.94	13.11	13.30	13.52	13.77	14.06
90.	15.42	15.65	15.85	16.04	16.22	16.39	16.56	16.73	16.92	17.12	17.35	17.61	17.90	18.23	18.61
95.	20.22	20.52	20.79	21.03	21.26	21.49	21.71	21.94	22.18	22.45	22.75	23.09	23.47	23.90	24.40
100.	26.16	26.54	26.89	27.21	27.51	27.80	28.08	28.38	28.70	29.04	29.43	29.86	30.36	30.92	31.56

Table 3.33

EFFECTS OF TONE-DISTURBANCE UPON ATC COMMUNICATIONS CHANNELS

(N.Y. AREA , LC SECTOR FUNCTION)

AVERAGE CHANNEL UTILIZATION

A/H	TONE DURATION (SECONDS) 0.0	0.1	0.2	0.3	0.4	0.5	0.6	0.7	0.8	0.9	1.0	1.1	1.2	1.3	1.4
30.	0.35	0.37	0.38	0.39	0.40	0.41	0.43	0.44	0.45	0.46	0.47	0.48	0.50	0.51	0.52
40.	0.44	0.46	0.47	0.49	0.50	0.52	0.53	0.55	0.56	0.57	0.59	0.60	0.62	0.64	0.65
42.	0.45	0.47	0.49	0.51	0.52	0.54	0.55	0.57	0.58	0.59	0.61	0.62	0.64	0.66	0.68
50.	0.52	0.54	0.56	0.58	0.59	0.61	0.63	0.64	0.66	0.67	0.69	0.71	0.73	0.75	0.77
60.	0.59	0.61	0.63	0.65	0.67	0.69	0.71	0.73	0.75	0.77	0.79	0.81	0.83	0.85	0.85
70.	0.66	0.68	0.71	0.73	0.75	0.78	0.80	0.82	0.84	0.85	0.85	0.85	0.85	0.85	0.85
80.	0.72	0.75	0.78	0.81	0.83	0.85	0.85	0.85	0.85	0.85	0.85	0.85	0.85	0.85	0.85
85.	0.76	0.79	0.82	0.85	0.85	0.85	0.85	0.85	0.85	0.85	0.85	0.85	0.85	0.85	0.85
90.	0.80	0.83	0.85	0.85	0.85	0.85	0.85	0.85	0.85	0.85	0.85	0.85	0.85	0.85	0.85
95.	0.84	0.85	0.85	0.85	0.85	0.85	0.85	0.85	0.85	0.85	0.85	0.85	0.85	0.85	0.85
100.	0.85	0.85	0.85	0.85	0.85	0.85	0.85	0.85	0.85	0.85	0.85	0.85	0.85	0.85	0.85

Table 3.34

EFFECTS OF TONE-DISTURBANCE UPON ATC COMMUNICATIONS CHANNELS

(N.Y. AREA , LC SECTOR FUNCTION)

AVERAGE QUEUING TIME

A/H	TONE DURATION (SECONDS)														
	0.0	0.1	0.2	0.3	0.4	0.5	0.6	0.7	0.8	0.9	1.0	1.1	1.2	1.3	1.4
30.	4.78	4.90	5.09	5.35	5.68	6.10	6.60	7.20	7.90	8.71	9.63	10.67	11.84	13.15	14.59
40.	6.37	6.54	6.79	7.13	7.58	8.13	8.80	9.60	10.53	11.61	12.84	14.23	15.79	17.53	19.45
42.	6.69	6.87	7.13	7.49	7.96	8.54	9.24	10.08	11.06	12.19	13.48	14.94	16.58	18.41	20.43
50.	9.90	10.16	10.55	11.09	11.78	12.64	13.68	14.92	16.37	18.05	19.96	22.12	24.54	27.24	30.24
60.	13.91	14.28	14.83	15.58	16.56	17.76	19.23	20.97	23.01	25.36	28.05	31.09	34.49	38.29	42.50
70.	17.93	18.40	19.11	20.08	21.33	22.89	24.78	27.03	29.65	32.68	36.14	40.05	44.44	49.34	54.76
80.	21.94	22.52	23.39	24.58	26.11	28.02	30.33	33.08	36.29	40.00	44.23	49.02	54.40	60.38	67.02
85.	23.95	24.59	25.53	26.83	28.50	30.58	33.10	36.10	39.61	43.66	48.28	53.51	59.37	65.91	73.15
90.	48.48	49.76	51.68	54.30	57.68	61.89	67.00	73.07	80.17	88.37	97.72	*****	*****	*****	*****
95.	80.38	82.51	85.69	90.02	95.63	*****	*****	*****	*****	*****	*****	*****	*****	*****	*****
100.	*****	*****	*****	*****	*****	*****	*****	*****	*****	*****	*****	*****	*****	*****	*****

Table 3.35

EFFECTS OF TONE-DISTURBANCE UPON ATC COMMUNICATIONS CHANNELS

(N.Y. AREA , L3 SECTOR FUNCTION)

AVERAGE AIRCRAFT LOADING

A/H	TONE DURATION (SECONDS)														
	0.0	0.1	0.2	0.3	0.4	0.5	0.6	0.7	0.8	0.9	1.0	1.1	1.2	1.3	1.4
20.	2.61	2.61	2.61	2.61	2.61	2.61	2.64	2.68	2.72	2.77	2.83	2.88	2.95	3.01	3.08
25.	2.99	2.99	2.99	2.99	2.99	3.00	3.03	3.07	3.12	3.18	3.24	3.31	3.38	3.45	3.53
30.	3.33	3.33	3.33	3.33	3.33	3.34	3.37	3.42	3.47	3.54	3.60	3.68	3.76	3.84	3.93
40.	3.99	3.99	3.99	3.99	3.99	4.00	4.04	4.10	4.16	4.24	4.32	4.41	4.50	4.60	4.70
50.	4.84	4.84	4.84	4.84	4.84	4.85	4.90	4.97	5.05	5.14	5.24	5.35	5.46	5.58	5.71
60.	6.12	6.12	6.12	6.12	6.12	6.14	6.21	6.29	6.39	6.51	6.63	6.77	6.91	7.07	7.22
70.	8.09	8.09	8.09	8.09	8.09	8.11	8.20	8.32	8.45	8.60	8.77	8.95	9.14	9.34	9.55
80.	10.99	10.99	10.99	10.99	10.99	11.02	11.15	11.30	11.48	11.69	11.91	12.16	12.42	12.69	12.97
90.	15.08	15.08	15.08	15.08	15.08	15.12	15.29	15.50	15.75	16.03	16.34	16.68	17.03	17.41	17.79

Table 3.36

EFFECTS OF TONE-DISTURBANCE UPON ATC COMMUNICATIONS CHANNELS

(N.Y. AREA , LG SECTOR FUNCTION)

AVERAGE CHANNEL UTILIZATION

A/H	TONE DURATION (SECONDS)														
	0.0	0.1	0.2	0.3	0.4	0.5	0.6	0.7	0.8	0.9	1.0	1.1	1.2	1.3	1.4
20.	0.25	0.26	0.27	0.28	0.28	0.29	0.30	0.31	0.32	0.33	0.33	0.34	0.35	0.36	0.37
25.	0.31	0.32	0.32	0.33	0.34	0.35	0.36	0.37	0.38	0.39	0.40	0.42	0.42	0.43	0.44
30.	0.36	0.37	0.38	0.39	0.40	0.41	0.42	0.44	0.45	0.46	0.47	0.48	0.50	0.51	0.52
40.	0.45	0.46	0.48	0.49	0.50	0.52	0.53	0.55	0.56	0.58	0.59	0.61	0.62	0.64	0.65
50.	0.53	0.55	0.56	0.58	0.60	0.61	0.63	0.65	0.67	0.69	0.70	0.72	0.74	0.75	0.77
60.	0.60	0.62	0.64	0.66	0.68	0.70	0.72	0.74	0.76	0.78	0.80	0.82	0.84	0.85	0.85
70.	0.67	0.69	0.71	0.73	0.75	0.78	0.80	0.82	0.84	0.85	0.85	0.85	0.85	0.85	0.85
80.	0.73	0.75	0.77	0.80	0.82	0.84	0.85	0.85	0.85	0.85	0.85	0.85	0.85	0.85	0.85
90.	0.79	0.81	0.83	0.85	0.85	0.85	0.85	0.85	0.85	0.85	0.85	0.85	0.85	0.85	0.85

Table 3.37

EFFECTS OF TONE-DISTURBANCE UPON ATC COMMUNICATIONS CHANNELS

(N.Y. AREA , IG SECTOR FUNCTICN)

AVERAGE QUEUING TIME

A/H	TONE DUPATICN (SECCNDS)														
	0.0	0.1	0.2	0.3	0.4	0.5	0.6	0.7	0.8	0.9	1.0	1.1	1.2	1.3	1.4
20.	5.79	5.79	5.87	6.53	7.52	8.76	10.18	11.71	13.29	14.85	16.30	17.60	18.65	19.40	19.77
25.	7.23	7.23	7.33	8.16	9.39	10.94	12.72	14.64	16.62	18.56	20.38	21.99	23.31	24.25	24.72
30.	8.80	8.80	8.93	9.94	11.44	13.32	15.49	17.83	20.23	22.60	24.81	26.78	28.38	29.52	30.09
40.	11.95	11.95	12.11	13.48	15.52	18.08	21.02	24.20	27.46	30.67	33.68	36.34	38.52	40.07	40.84
50.	15.10	15.10	15.30	17.03	19.61	22.84	26.56	30.56	34.69	38.74	42.54	45.91	48.66	50.62	51.59
60.	18.24	18.24	18.49	20.58	23.69	27.60	32.09	36.93	41.91	46.81	51.40	55.47	58.80	61.16	62.34
70.	21.39	21.39	21.68	24.13	27.78	32.36	37.62	43.30	49.14	54.88	60.27	65.04	68.94	71.71	73.09
80.	24.53	24.53	24.87	27.68	31.87	37.12	43.16	49.67	56.37	62.95	69.13	74.61	79.08	82.26	83.84
90.	46.84	46.84	47.48	52.85	60.84	70.87	82.39	94.83	*****	*****	*****	*****	*****	*****	*****

Table 3.38

EFFECTS OF TONE-DISTURBANCE UPON ATC COMMUNICATIONS CHANNELS

(N.Y. AREA, DP SECTOR FUNCTION)

AVERAGE AIRCRAFT LOADING

A/H	TONE DURATION (SECONDS)														
	0.0	0.1	0.2	0.3	0.4	0.5	0.6	0.7	0.8	0.9	1.0	1.1	1.2	1.3	1.4
15.	2.19	2.21	2.25	2.28	2.32	2.37	2.41	2.46	2.50	2.55	2.59	2.64	2.68	2.72	2.75
20.	2.76	2.80	2.84	2.88	2.93	2.99	3.04	3.10	3.16	3.22	3.27	3.33	3.38	3.43	3.47
25.	3.29	3.34	3.39	3.44	3.50	3.56	3.63	3.70	3.77	3.84	3.91	3.97	4.03	4.09	4.14
30.	3.81	3.86	3.92	3.98	4.05	4.12	4.20	4.28	4.36	4.44	4.52	4.59	4.67	4.73	4.79
35.	4.33	4.39	4.45	4.52	4.60	4.69	4.77	4.86	4.95	5.05	5.14	5.22	5.30	5.38	5.45
40.	4.88	4.94	5.01	5.09	5.18	5.28	5.38	5.48	5.58	5.68	5.78	5.88	5.97	6.06	6.14
45.	5.47	5.54	5.62	5.71	5.81	5.92	6.03	6.14	6.26	6.37	6.49	6.60	6.70	6.80	6.88
50.	6.14	6.21	6.31	6.41	6.52	6.64	6.76	6.89	7.02	7.15	7.28	7.40	7.51	7.62	7.72
55.	6.89	6.98	7.09	7.20	7.33	7.46	7.60	7.74	7.89	8.03	8.18	8.31	8.44	8.56	8.67

Table 3.39

EFFECTS OF TONE-DISTURBANCE UPON ATC COMMUNICATIONS CHANNELS

(N.Y. AREA, DP SECTOR FUNCTION)

AVERAGE CHANNEL UTILIZATION

A/H	TONE DURATION (SECONDS)														
	0.0	0.1	0.2	0.3	0.4	0.5	0.6	0.7	0.8	0.9	1.0	1.1	1.2	1.3	1.4
15.	0.34	0.35	0.36	0.37	0.38	0.39	0.40	0.40	0.41	0.42	0.43	0.44	0.45	0.46	0.47
20.	0.41	0.43	0.44	0.45	0.46	0.47	0.48	0.49	0.50	0.51	0.52	0.53	0.54	0.55	0.57
25.	0.47	0.48	0.50	0.51	0.52	0.53	0.55	0.56	0.57	0.58	0.59	0.60	0.62	0.63	0.64
30.	0.52	0.53	0.55	0.56	0.58	0.59	0.60	0.61	0.63	0.64	0.65	0.66	0.68	0.69	0.71
35.	0.56	0.57	0.59	0.61	0.62	0.64	0.65	0.66	0.67	0.69	0.70	0.72	0.73	0.75	0.76
40.	0.60	0.62	0.63	0.65	0.67	0.68	0.69	0.71	0.72	0.74	0.75	0.77	0.78	0.80	0.82
45.	0.64	0.66	0.68	0.69	0.71	0.73	0.74	0.76	0.77	0.79	0.80	0.82	0.84	0.85	0.85
50.	0.69	0.71	0.73	0.75	0.77	0.78	0.80	0.82	0.83	0.85	0.85	0.85	0.85	0.85	0.85
55.	0.74	0.77	0.79	0.81	0.83	0.85	0.85	0.85	0.85	0.85	0.85	0.85	0.85	0.85	0.85

Table 3.40

EFFECTS OF TONE-DISTURBANCE UPON ATC COMMUNICATIONS CHANNELS

(N.Y. AREA , DP SECTOR FUNCTION)

AVERAGE QUEUING TIME

A/H	TONE DURATION (SECONDS)														
	0.0	0.1	0.2	0.3	0.4	0.5	0.6	0.7	0.8	0.9	1.0	1.1	1.2	1.3	1.4
15.	6.64	7.08	7.52	7.98	8.45	8.95	9.50	10.10	10.76	11.50	12.32	13.23	14.25	15.39	16.66
20.	8.51	9.08	9.65	10.23	10.84	11.48	12.19	12.95	13.80	14.75	15.80	16.97	18.28	19.74	21.36
25.	10.29	10.98	11.66	12.37	13.10	13.88	14.73	15.66	16.69	17.83	19.10	20.52	22.10	23.86	25.82
30.	12.01	12.81	13.62	14.44	15.29	16.21	17.20	18.28	19.48	20.81	22.29	23.95	25.80	27.86	30.15
35.	13.72	14.64	15.56	16.49	17.47	18.52	19.65	20.88	22.25	23.77	25.47	27.36	29.47	31.83	34.44
40.	15.46	16.50	17.53	18.58	19.69	20.86	22.14	23.53	25.08	26.79	28.70	30.83	33.21	35.86	38.81
45.	17.27	18.43	19.58	20.76	22.00	23.31	24.73	26.29	28.02	29.93	32.07	34.45	37.11	40.07	43.36
50.	19.20	20.49	21.77	23.08	24.45	25.92	27.50	29.23	31.15	33.28	35.65	38.30	41.25	44.55	48.20
55.	21.29	22.72	24.14	25.59	27.11	28.73	30.49	32.41	34.53	36.89	39.53	42.46	45.74	49.39	53.45

Table 3.41

EFFECTS OF TONE-DISTURBANCE UPON ATC COMMUNICATIONS CHANNELS

(N.Y. AREA, AD SECTOR FUNCTION)

AVERAGE AIRCRAFT LOADING

A/H	TONE DURATION (SECONDS)														
	0.0	0.1	0.2	0.3	0.4	0.5	0.6	0.7	0.8	0.9	1.0	1.1	1.2	1.3	1.4
10.	1.01	1.01	1.01	1.01	1.01	1.01	1.03	1.05	1.06	1.08	1.10	1.12	1.13	1.14	1.15
16.	1.59	1.59	1.59	1.59	1.59	1.60	1.63	1.65	1.68	1.71	1.74	1.77	1.79	1.80	1.81
20.	1.98	1.98	1.98	1.98	1.98	1.99	2.02	2.06	2.09	2.13	2.17	2.20	2.23	2.25	2.26
25.	2.48	2.48	2.48	2.48	2.48	2.49	2.53	2.57	2.62	2.66	2.71	2.75	2.78	2.81	2.82
30.	2.99	2.99	2.99	2.99	2.99	3.01	3.05	3.10	3.16	3.21	3.27	3.32	3.36	3.39	3.40
35.	3.52	3.52	3.52	3.52	3.52	3.55	3.60	3.66	3.72	3.79	3.85	3.91	3.96	3.99	4.01
40.	4.09	4.09	4.09	4.09	4.09	4.11	4.18	4.25	4.32	4.40	4.47	4.54	4.59	4.64	4.66
45.	4.69	4.69	4.69	4.69	4.69	4.72	4.79	4.87	4.96	5.05	5.13	5.21	5.27	5.32	5.35

Table 3.42

EFFECTS OF TONE-DISTURBANCE UPON ATC COMMUNICATIONS CHANNELS

(N.Y. AREA , AD SECTOR FUNCTION)

AVERAGE CHANNEL UTILIZATION

A/H	TONE DURATION (SECONDS)														
	0.0	0.1	0.2	0.3	0.4	0.5	0.6	0.7	0.8	0.9	1.0	1.1	1.2	1.3	1.4
10.	0.15	0.15	0.15	0.16	0.16	0.16	0.17	0.17	0.18	0.18	0.18	0.19	0.19	0.20	0.20
16.	0.24	0.25	0.25	0.26	0.26	0.27	0.28	0.28	0.29	0.30	0.30	0.31	0.32	0.32	0.33
20.	0.30	0.31	0.32	0.33	0.33	0.34	0.35	0.36	0.37	0.38	0.38	0.39	0.40	0.41	0.42
25.	0.38	0.39	0.40	0.41	0.42	0.43	0.44	0.45	0.46	0.47	0.49	0.50	0.51	0.52	0.53
30.	0.46	0.47	0.48	0.50	0.51	0.52	0.53	0.54	0.56	0.57	0.58	0.60	0.61	0.62	0.63
35.	0.53	0.55	0.56	0.57	0.59	0.60	0.62	0.63	0.65	0.66	0.68	0.69	0.71	0.72	0.74
40.	0.60	0.62	0.63	0.65	0.66	0.68	0.70	0.71	0.73	0.75	0.76	0.78	0.80	0.81	0.83
45.	0.66	0.68	0.70	0.72	0.73	0.75	0.77	0.79	0.81	0.82	0.84	0.85	0.85	0.85	0.85

Table 3.43

EFFECTS OF TONE-DISTURBANCE UPON ATC COMMUNICATIONS CHANNELS

(N.Y. AREA AD SECTOR FUNCTION)

AVERAGE QUEUING TIME

A/H	TONE DURATION (SECONDS)														
	0.0	0.1	0.2	0.3	0.4	0.5	0.6	0.7	0.8	0.9	1.0	1.1	1.2	1.3	1.4
10.	2.87	2.87	2.95	3.17	3.47	3.84	4.25	4.69	5.14	5.58	5.98	6.34	6.62	6.81	6.88
16.	4.78	4.78	4.93	5.28	5.78	6.40	7.09	7.83	8.58	9.31	9.98	10.57	11.04	11.35	11.48
20.	6.13	6.13	6.31	6.77	7.41	8.20	9.09	10.03	10.99	11.93	12.79	13.55	14.15	14.55	14.72
25.	7.88	7.88	8.12	8.71	9.54	10.55	11.69	12.91	14.14	15.34	16.46	17.43	18.20	18.72	18.93
30.	9.71	9.71	10.00	10.73	11.75	12.99	14.40	15.90	17.42	18.90	20.27	21.46	22.42	23.05	23.32
35.	11.59	11.59	11.95	12.82	14.03	15.52	17.20	18.99	20.81	22.57	24.21	25.64	26.77	27.54	27.85
40.	13.53	13.53	13.95	14.96	16.38	18.12	20.07	22.16	24.29	26.35	28.26	29.93	31.25	32.14	32.51
45.	15.51	15.51	15.99	17.15	18.78	20.77	23.01	25.41	27.84	30.21	32.40	34.31	35.83	36.85	37.27

Table 3.44

EFFECTS OF TONE-DISTURBANCE UPON ATC COMMUNICATIONS CHANNELS

(N.Y. AREA , AR SECTOR FUNCTION)

AVERAGE AIRCRAFT LOADING

A/H	TONE DURATION (SECONDS)														
	0.0	0.1	0.2	0.3	0.4	0.5	0.6	0.7	0.8	0.9	1.0	1.1	1.2	1.3	1.4
10.	1.58	1.61	1.63	1.66	1.69	1.73	1.76	1.79	1.83	1.86	1.90	1.93	1.97	2.00	2.04
15.	2.07	2.11	2.14	2.18	2.22	2.26	2.30	2.35	2.40	2.44	2.49	2.54	2.58	2.63	2.67
20.	2.62	2.66	2.70	2.75	2.80	2.85	2.91	2.96	3.02	3.08	3.14	3.20	3.26	3.31	3.37
22.	2.89	2.94	2.98	3.04	3.09	3.15	3.21	3.27	3.34	3.40	3.47	3.53	3.60	3.66	3.72
25.	3.40	3.45	3.51	3.57	3.64	3.71	3.78	3.85	3.93	4.00	4.08	4.16	4.23	4.30	4.38
30.	4.61	4.68	4.76	4.84	4.93	5.03	5.12	5.22	5.33	5.43	5.53	5.64	5.74	5.84	5.94
35.	6.44	6.54	6.65	6.76	6.89	7.02	7.16	7.30	7.44	7.58	7.73	7.87	8.01	8.15	8.29
40.	9.03	9.22	9.37	9.53	9.71	9.89	10.08	10.28	10.48	10.69	10.89	11.09	11.29	11.49	11.68

Table 3.45

EFFECTS OF TONE-DISTURBANCE UPON ATC COMMUNICATIONS CHANNELS

(N.Y. AREA, AR SECTOR FUNCTION)

AVERAGE CHANNEL UTILIZATION

A/H	TONE DURATION (SECONDS)														
	0.0	0.1	0.2	0.3	0.4	0.5	0.6	0.7	0.8	0.9	1.0	1.1	1.2	1.3	1.4
10.	0.26	0.27	0.27	0.28	0.28	0.29	0.30	0.30	0.31	0.31	0.32	0.33	0.33	0.34	0.35
15.	0.38	0.39	0.39	0.40	0.41	0.42	0.43	0.43	0.44	0.45	0.46	0.47	0.48	0.49	0.50
20.	0.49	0.50	0.51	0.52	0.53	0.54	0.55	0.56	0.57	0.58	0.59	0.60	0.62	0.63	0.64
22.	0.53	0.54	0.55	0.56	0.57	0.58	0.60	0.61	0.62	0.63	0.64	0.66	0.67	0.68	0.70
25.	0.59	0.60	0.61	0.63	0.64	0.65	0.67	0.68	0.69	0.70	0.72	0.73	0.75	0.76	0.78
30.	0.69	0.70	0.72	0.73	0.75	0.76	0.78	0.79	0.81	0.82	0.84	0.85	0.85	0.85	0.85
35.	0.78	0.80	0.81	0.83	0.85	0.85	0.85	0.85	0.85	0.85	0.85	0.85	0.85	0.85	0.85
40.	0.85	0.85	0.85	0.85	0.85	0.85	0.85	0.85	0.85	0.85	0.85	0.85	0.85	0.85	0.85

Table 3.46

EFFECTS OF TONE-DISTURBANCE UPON ATC COMMUNICATIONS CHANNELS

(N.Y. AREA, AR SECTOR FUNCTION)

AVERAGE QUEUING TIME

A/H	TONE DURATION (SECONDS)														
	0.0	0.1	0.2	0.3	0.4	0.5	0.6	0.7	0.8	0.9	1.0	1.1	1.2	1.3	1.4
10.	5.11	5.29	5.57	5.93	6.37	6.86	7.39	7.97	8.56	9.17	9.78	10.37	10.94	11.48	11.97
15.	7.66	7.94	8.36	8.90	9.55	10.29	11.09	11.95	12.84	13.76	14.67	15.56	16.42	17.22	17.95
20.	10.21	10.58	11.14	11.87	12.73	13.71	14.79	15.93	17.13	18.34	19.55	20.74	21.89	22.96	23.94
22.	11.23	11.64	12.26	13.05	14.01	15.09	16.27	17.53	18.84	20.17	21.51	22.82	24.08	25.25	26.33
25.	11.57	11.99	12.63	13.45	14.43	15.54	16.76	18.06	19.41	20.78	22.16	23.51	24.80	26.01	27.12
30.	16.04	16.62	17.51	18.64	20.00	21.54	23.23	25.03	26.90	28.81	30.72	32.59	34.38	36.06	37.60
35.	27.85	28.87	30.40	32.37	34.73	37.41	40.34	43.47	46.72	50.03	53.34	56.59	59.71	62.63	65.29
40.	49.85	51.67	54.41	57.94	62.16	66.96	72.21	77.80	83.61	89.54	95.47	*****	*****	*****	*****

Table 3.47 Summary Statistics of Simulations for the Study of Tone Disturbance (Duration = 0.0 Seconds)

INPUT PARAMETERS - SECTOR FUNCTION HT TONE DURATION = 0.0 SECONDS

(1) AIRCRAFT INTERARRIVAL TIMES: EXPONENTIAL WITH MEAN = 109.089 SECONDS
(2) TRANSACTIONS PER AIRCRAFT: SHIFTED NEGATIVE BINOMIAL WITH K = 4.029 AND P = 0.579
(3) TRANSMISSIONS PER TRANSACTION: EMPIRICAL DISTRIBUTION
(4) TRANSMISSIONS LENGTHS: GAMMA WITH P = 0.8484 AND ALPHA = 2.6969
(NOTE: GAMMA PARAMETERS DETERMINED FROM EXPECTED ARRIVAL RATE)
(5) INTERCOMMUNICATION GAP LENGTHS ARE A FUNCTION OF TRANSACTIONS PER AIRCRAFT

SIMULATION RESPONSE - 2 HOUR ANALYSIS

(1) SECTOR AIRCRAFT LOADING
NUMBER OF AIRCRAFT IDENTIFIED IN SECTOR = 78
AVERAGE NUMBER OF AIRCRAFT PER SECOND = 5.579
MAXIMUM NUMBER OF AIRCRAFT PER SECOND = 10

(2) COMMUNICATIONS CHANNEL LOADING
AVERAGE CHANNEL UTILIZATION = .529
TOTAL NUMBER OF TRANSACTIONS = 342
AVERAGE LENGTH OF TRANSACTIONS = 11.152 SECONDS
TOTAL NUMBER OF PILOT TRANSMISSIONS = 581

(3) CHANNEL QUEUEING EFFECTS
AVERAGE TIME IN QUEUE = 9.146 SECONDS
AVERAGE TIME EXCLUDING ZERO ENTRIES = 16.550 SECONDS
TOTAL ENTRIES INTO QUEUE = 342
NUMBER OF ZERO ENTRIES (NON-WAITING) = 153
PERCENT OF ZERO ENTRIES = 44.7
AVERAGE NUMBER OF AIRCRAFT IN QUEUE = .434
MAXIMUM NUMBER OF AIRCRAFT IN QUEUE = 6

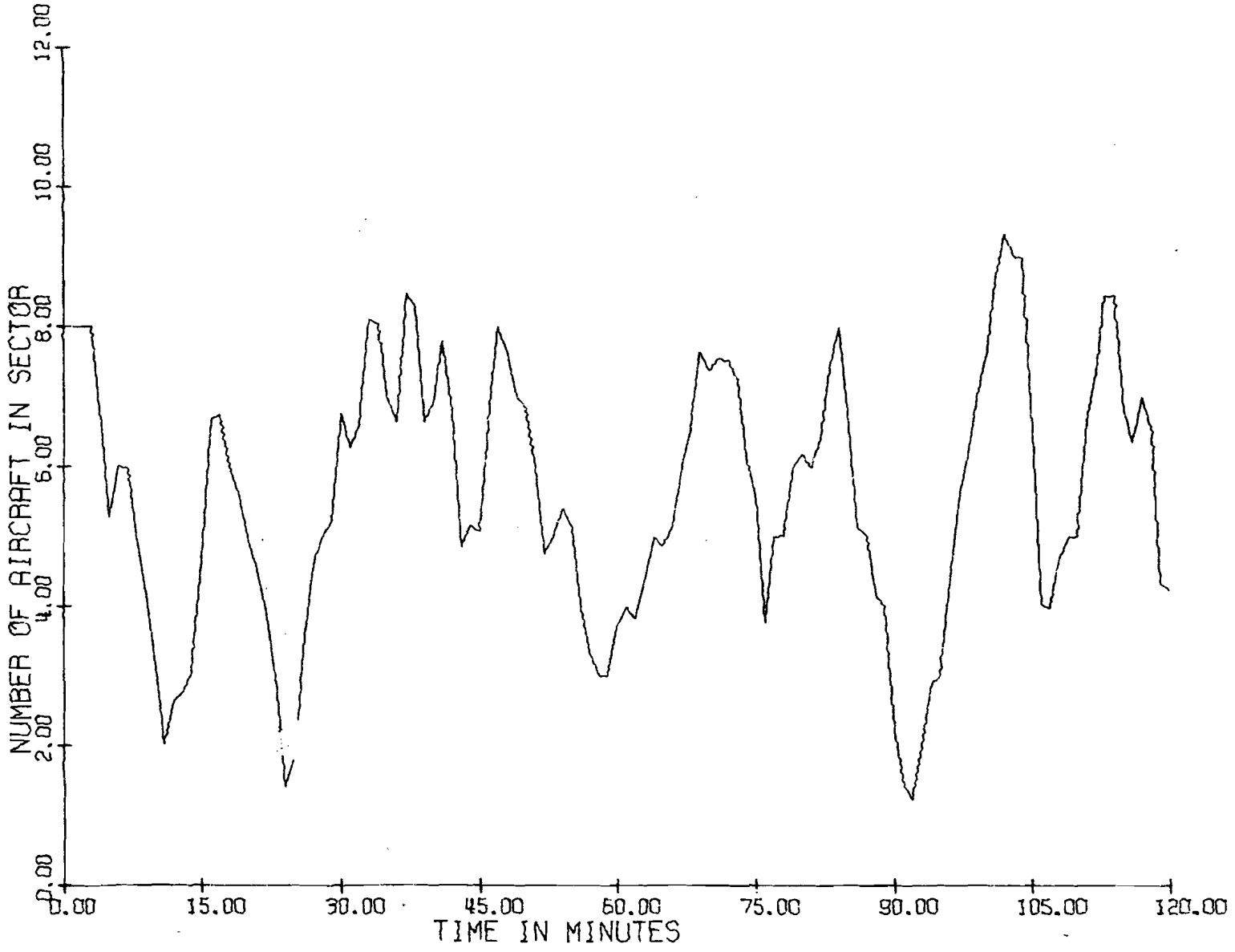

Figure 3.5 Simulated Aircraft Loading Time Series for N.Y. HI Function at 33 A/H and 0.0 Second Tone Duration

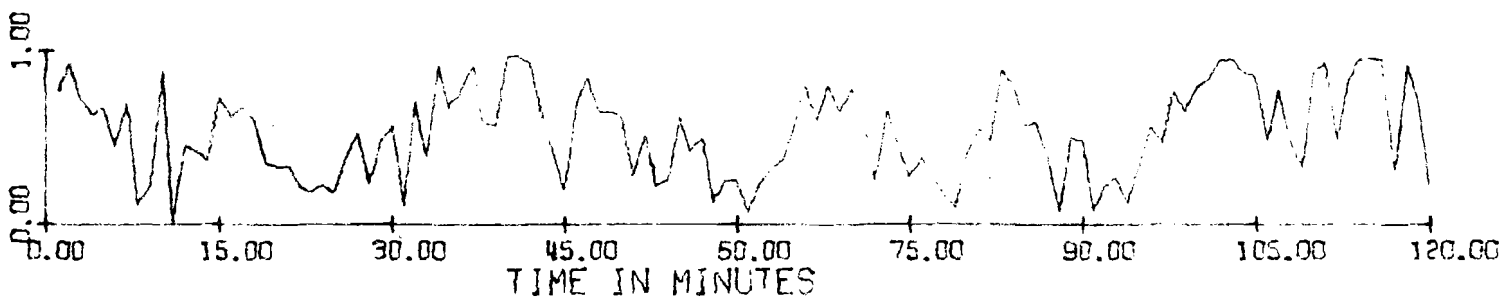

Figure 3.6 Simulated Channel Utilization Time Series for N.Y. HI Function at 33 A/H and 0.0 Second Tone Duration

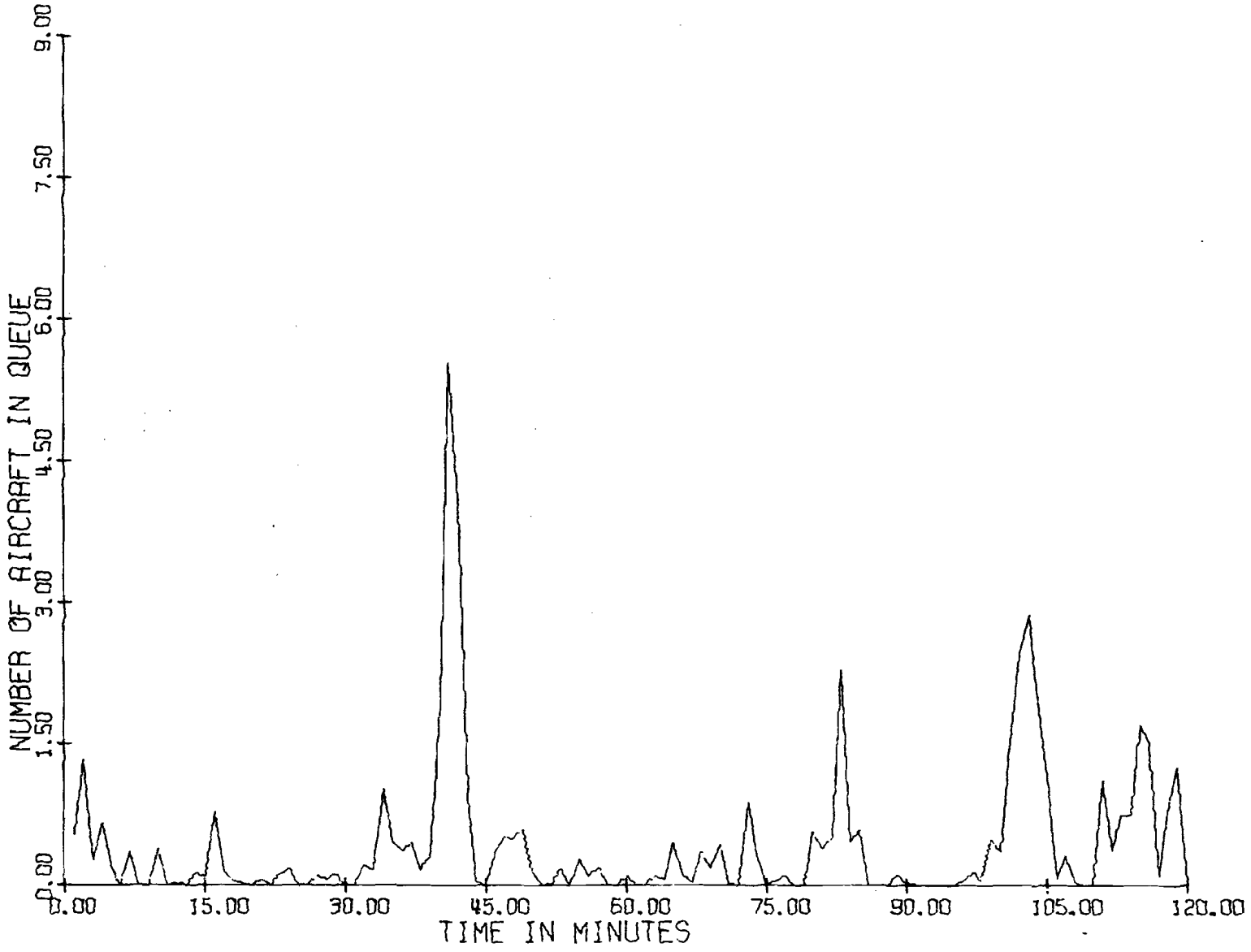

Figure 3.7 Simulated Queue Length Time Series for N.Y. HI Function at 33 A/H and 0.0 Second Tone Duration

Table 3.48 Summary Statistics of Simulations for the Study of Tone Disturbance (Duration = 0.5 Seconds)

INPUT PARAMETERS - SECTOR FUNCTION HI TONE DURATION = 0.5 SECONDS

(1) AIRCRAFT INTERARRIVAL TIMES: EXPONENTIAL WITH MEAN = 109.089 SECONDS
(2) TRANSACTIONS PER AIRCRAFT: SHIFTED NEGATIVE BINOMIAL WITH K = 4.029 AND P = 0.579
(3) TRANSMISSIONS PER TRANSACTION: EMPIRICAL DISTRIBUTION
(4) TRANSMISSIONS LENGTHS: GAMMA WITH P = 0.8484 AND ALPHA = 2.6969
(NOTE: GAMMA PARAMETERS DETERMINED FROM EXPECTED ARRIVAL RATE)
(5) INTERCOMMUNICATION GAP LENGTHS ARE A FUNCTION OF TRANSACTIONS PER AIRCRAFT

SIMULATION RESPONSE - 2 HOUR ANALYSIS

(1) SECTOR AIRCRAFT LOADING
NUMBER OF AIRCRAFT IDENTIFIED IN SECTOR = 78
AVERAGE NUMBER OF AIRCRAFT PER SECOND = 5.982
MAXIMUM NUMBER OF AIRCRAFT PER SECOND = 10

(2) COMMUNICATIONS CHANNEL LOADING
AVERAGE CHANNEL UTILIZATION = .611
TOTAL NUMBER OF TRANSACTIONS = 343
AVERAGE LENGTH OF TRANSACTIONS = 12.834 SECONDS
TOTAL NUMBER OF PILOT TRANSMISSIONS = 582

(3) CHANNEL QUEUEING EFFECTS
AVERAGE TIME IN QUEUE = 16.448 SECONDS
AVERAGE TIME EXCLUDING ZERO ENTRIES = 23.805 SECONDS
TOTAL ENTRIES INTO QUEUE = 343
NUMBER OF ZERO ENTRIES (NON-WAITING) = 106
PERCENT OF ZERO ENTRIES = 30.9
AVERAGE NUMBER OF AIRCRAFT IN QUEUE = .783
MAXIMUM NUMBER OF AIRCRAFT IN QUEUE = 5

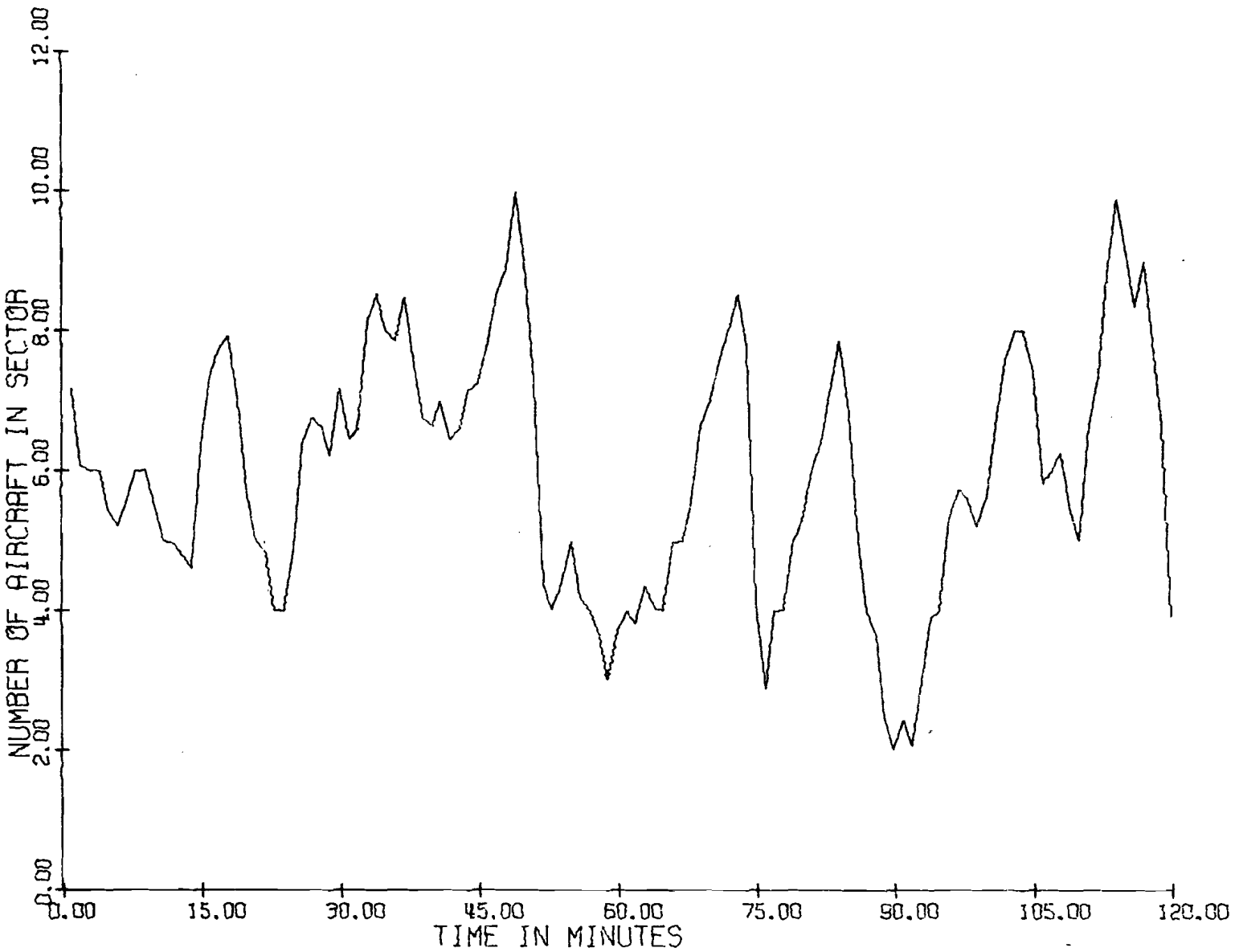

Figure 3.8 Simulated Aircraft Loading Time Series for N.Y. HI Function at 33 A/H and 0.5 Second Tone Duration

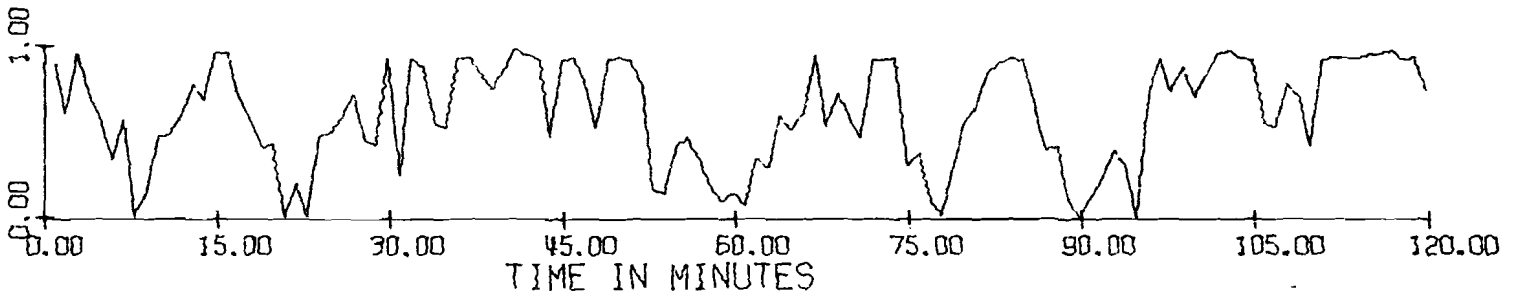

Figure 3.9 Simulated Channel Utilization Time Series for N.Y. HI Function at 33 A/H and 0.5 Second Tone Duration

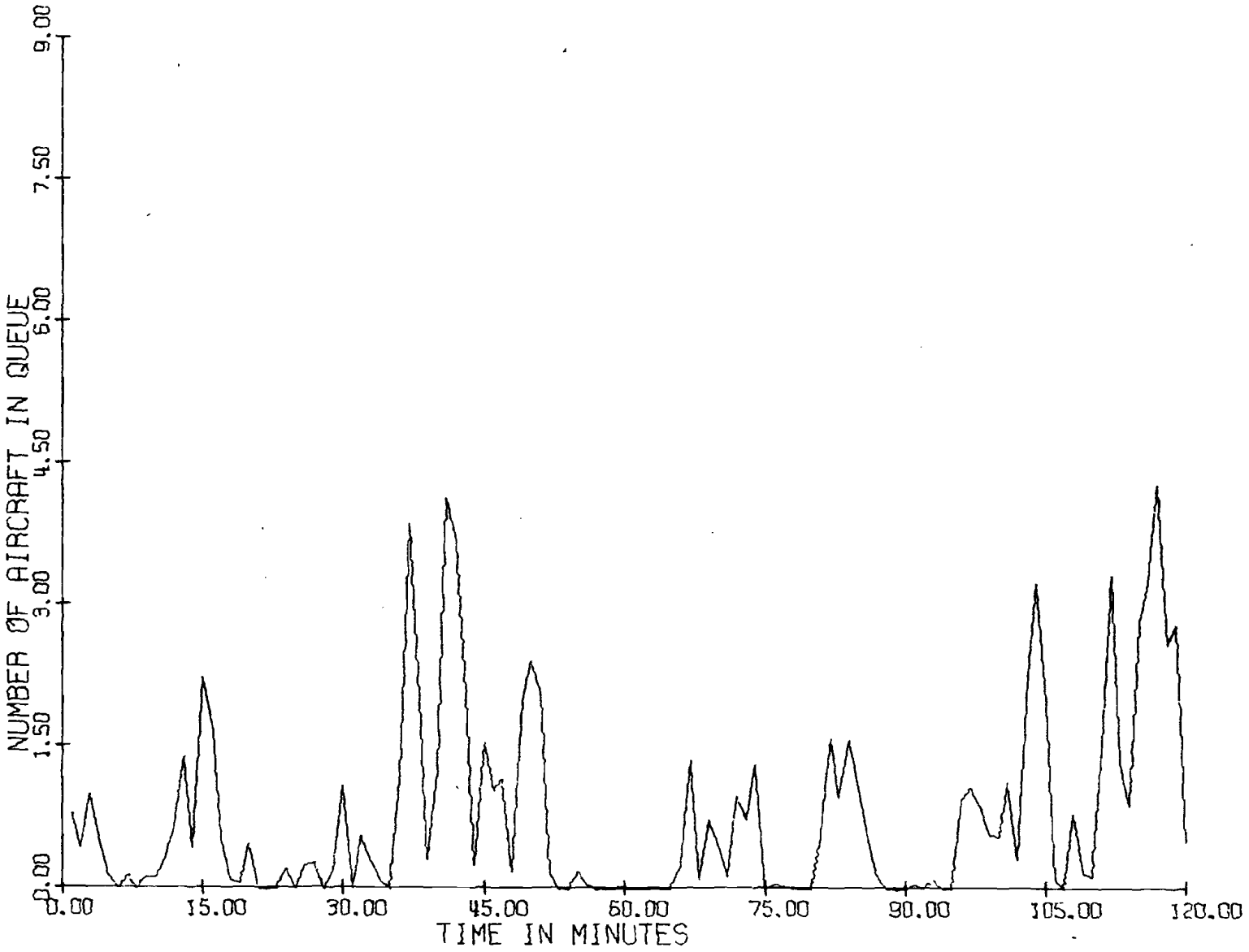

Figure 3.10 Simulated Queue Length Time Series for N.Y. HI Function at 33 A/H and 0.5 Second Tone Duration

Table 3.49 Summary Statistics of Simulations for the Study of Tone Disturbance (Duration = 1.0 Seconds)

INPUT PARAMETERS - SECTOR FUNCTION HI TONE DURATION = 1.0 SECONDS

(1) AIRCRAFT INTERARRIVAL TIMES: EXPONENTIAL WITH MEAN = 109.089 SECONDS
(2) TRANSACTIONS PER AIRCRAFT: SHIFTED NEGATIVE BINOMIAL WITH K = 4.029 AND P = 0.579
(3) TRANSMISSIONS PER TRANSACTION: EMPIRICAL DISTRIBUTION
(4) TRANSMISSIONS LENGTHS: GAMMA WITH B = 0.8484 AND ALPHA = 2.6969
(NOTE: GAMMA PARAMETERS DETERMINED FROM EXPECTED ARRIVAL RATE)
(5) INTERCOMMUNICATION GAP LENGTHS ARE A FUNCTION OF TRANSACTIONS PER AIRCRAFT

SIMULATION RESPONSE - 2 HOUR ANALYSIS

(1) SECTOR AIRCRAFT LOADING
NUMBER OF AIRCRAFT IDENTIFIED IN SECTOR = 79
AVERAGE NUMBER OF AIRCRAFT PER SECOND = 6.497
MAXIMUM NUMBER OF AIRCRAFT PER SECOND = 10

(2) COMMUNICATIONS CHANNEL LOADING
AVERAGE CHANNEL UTILIZATION = .685
TOTAL NUMBER OF TRANSACTIONS = 343
AVERAGE LENGTH OF TRANSACTIONS = 14.397 SECONDS
TOTAL NUMBER OF PILOT TRANSMISSIONS = 574

(3) CHANNEL QUEUEING EFFECTS
AVERAGE TIME IN QUEUE = 21.251 SECONDS
AVERAGE TIME EXCLUDING ZERO ENTRIES = 29.188 SECONDS
TOTAL ENTRIES INTO QUEUE = 342
NUMBER OF ZERO ENTRIES (NON-WAITING) = 93
PERCENT OF ZERO ENTRIES = 27.1
AVERAGE NUMBER OF AIRCRAFT IN QUEUE = 1.009
MAXIMUM NUMBER OF AIRCRAFT IN QUEUE = 5

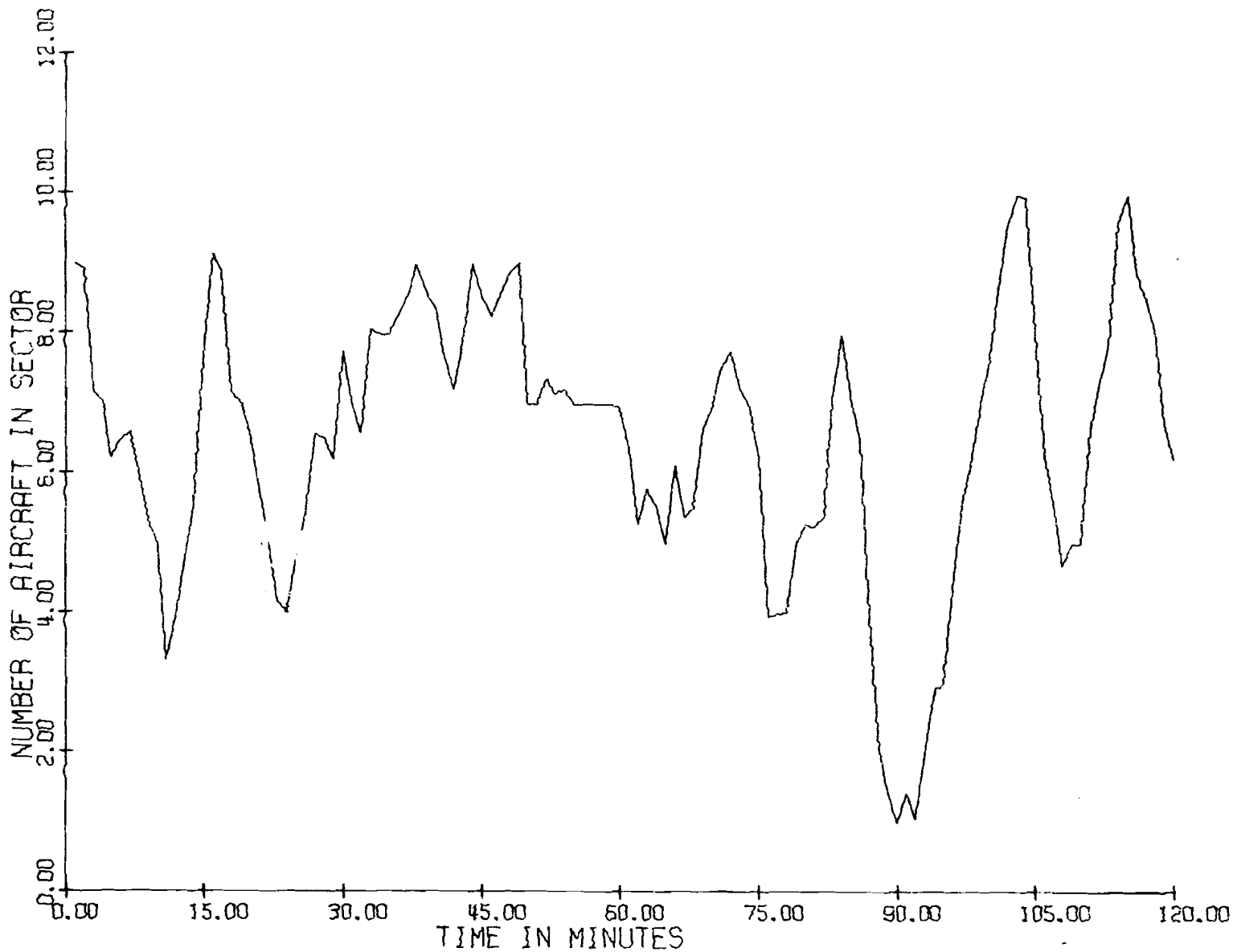

Figure 3.11 Simulated Aircraft Loading Time Series for N.Y. HI Function at 33 A/H and 1.0 Second Tone Duration

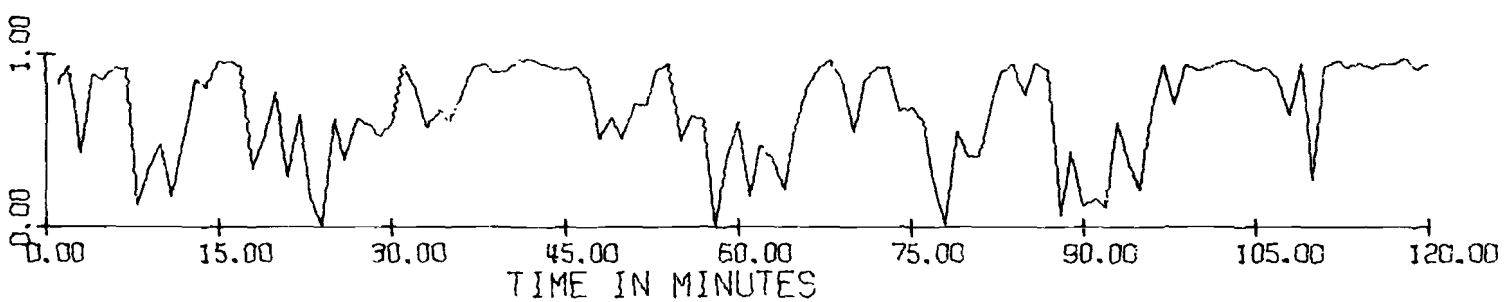

Figure 3.12 Simulated Channel Utilization Time Series for N.Y. HI Function at 33 A/H and 1.0 Second Tone Duration

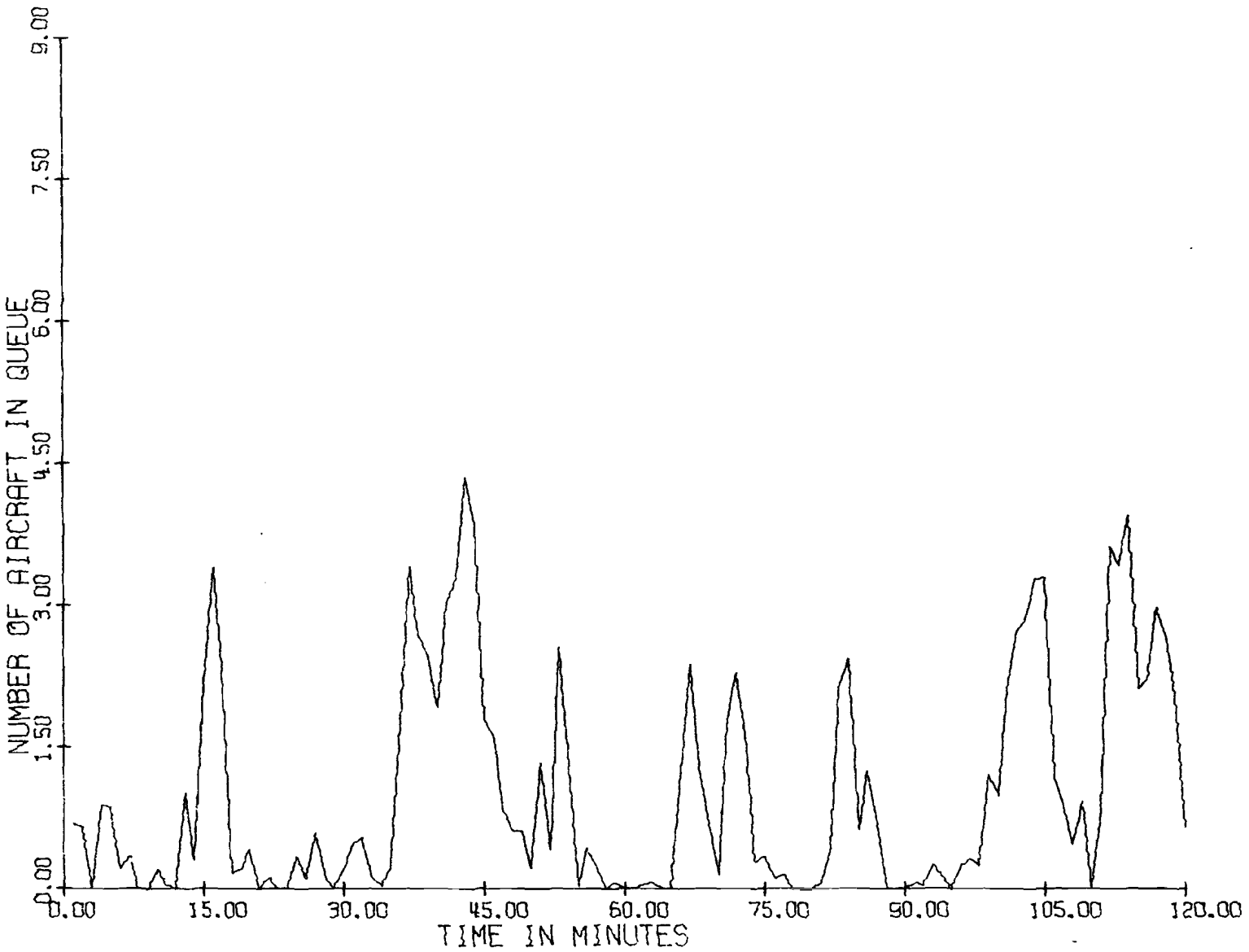

Figure 3.13 Simulated Queue Length Time Series for N.Y. HI Function at 33 A/H and 1.0 Second Tone Duration

Table 3.50 Summary Statistics of Simulations for the Study of Tone Disturbance (Duration = 1.5 Seconds)

INPUT PARAMETERS - SECTOR FUNCTION HI TONE DURATION = 1.5 SECONDS

(1) AIRCRAFT INTERARRIVAL TIMES: EXPONENTIAL WITH MEAN = 109.089 SECONDS
(2) TRANSACTIONS PER AIRCRAFT: SHIFTED NEGATIVE BINOMIAL WITH K = 4.029 AND P = 0.579
(3) TRANSMISSIONS PER TRANSACTION: EMPIRICAL DISTRIBUTION
(4) TRANSMISSIONS LENGTHS: GAMMA WITH P = 0.8484 AND ALPHA = 2.6969
(NOTE: GAMMA PARAMETERS DETERMINED FROM EXPECTED ARRIVAL RATE)
(5) INTERCOMMUNICATION GAP LENGTHS ARE A FUNCTION OF TRANSACTIONS PER AIRCRAFT

SIMULATION RESPONSE - 2 HOUR ANALYSIS

(1) SECTOR AIRCRAFT LOADING
NUMBER OF AIRCRAFT IDENTIFIED IN SECTOR = 80
AVERAGE NUMBER OF AIRCRAFT PER SECOND = 6.933
MAXIMUM NUMBER OF AIRCRAFT PER SECOND = 11

(2) COMMUNICATIONS CHANNEL LOADING
AVERAGE CHANNEL UTILIZATION = .755
TOTAL NUMBER OF TRANSACTIONS = 342
AVERAGE LENGTH OF TRANSACTIONS = 15.895 SECONDS
TOTAL NUMBER OF PILOT TRANSMISSIONS = 559

(3) CHANNEL QUEUEING EFFECTS
AVERAGE TIME IN QUEUE = 29.576 SECONDS
AVERAGE TIME EXCLUDING ZERO ENTRIES = 38.360 SECONDS
TOTAL ENTRIES INTO QUEUE = 345
NUMBER OF ZERO ENTRIES (NON-WAITING) = 79
PERCENT OF ZERO ENTRIES = 22.9
AVERAGE NUMBER OF AIRCRAFT IN QUEUE = 1.417
MAXIMUM NUMBER OF AIRCRAFT IN QUEUE = 7

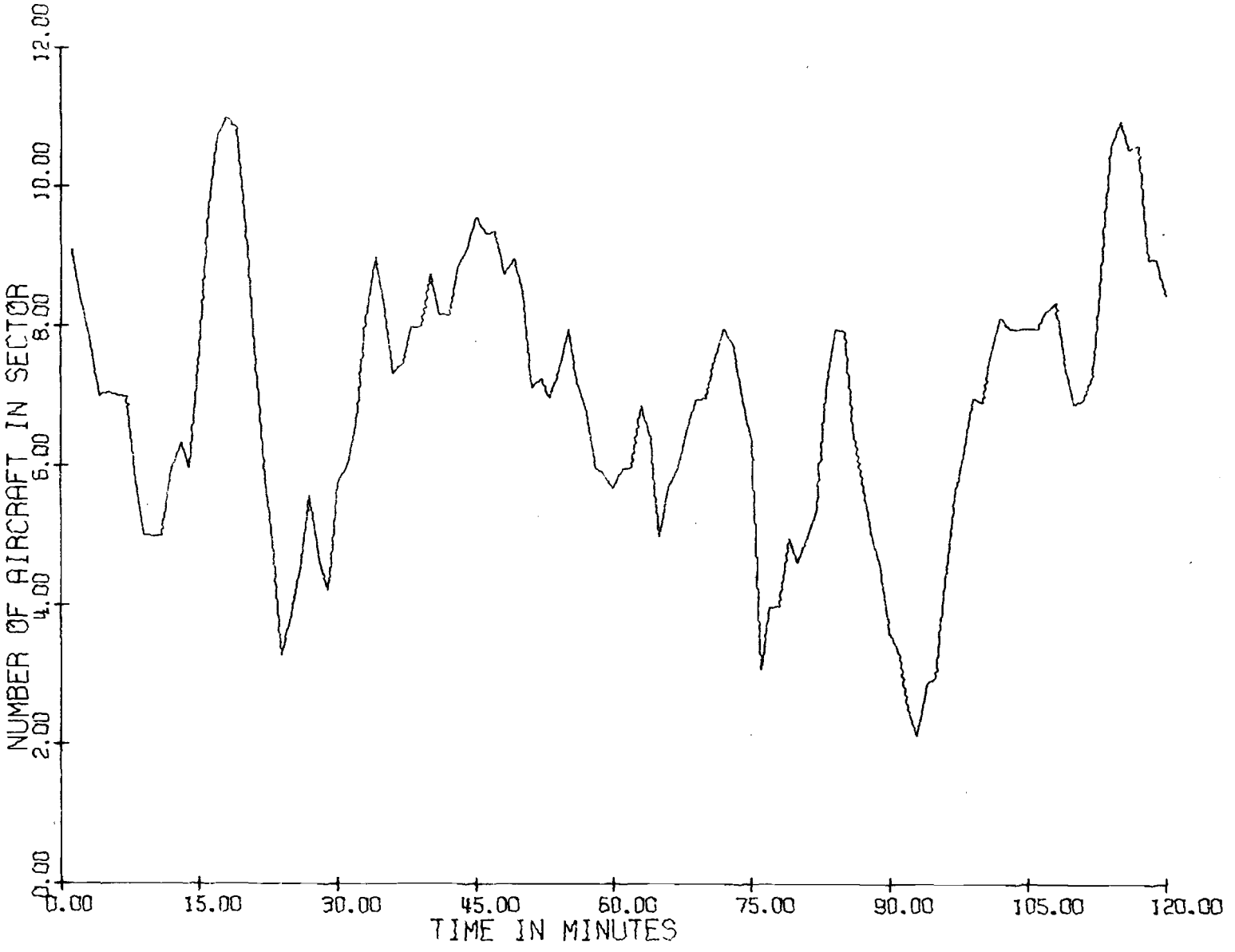

Figure 3.14 Simulated Aircraft Loading Time Series for N.Y. HI Function at 33 A/H and 1.5 Second Tone Duration

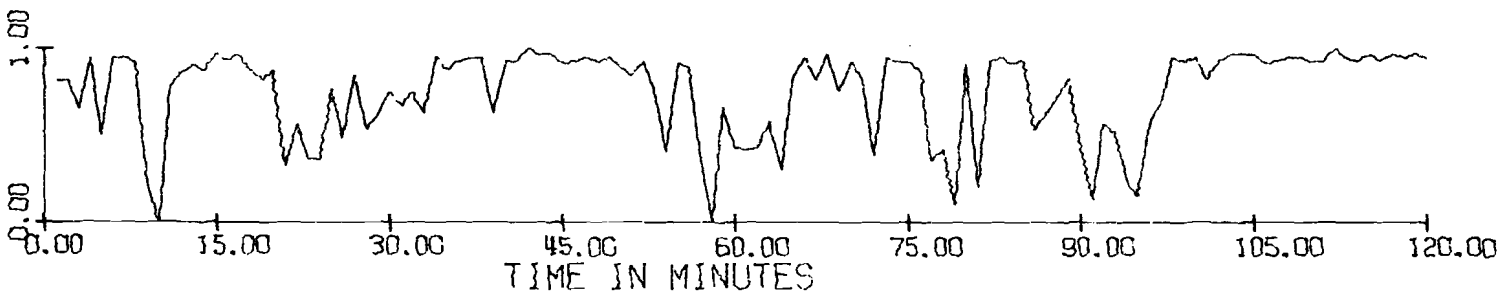

Figure 3.15 Simulated Channel Utilization Time Series for N.Y. HI Function at 33 A/H and 1.5 Second Tone Duration

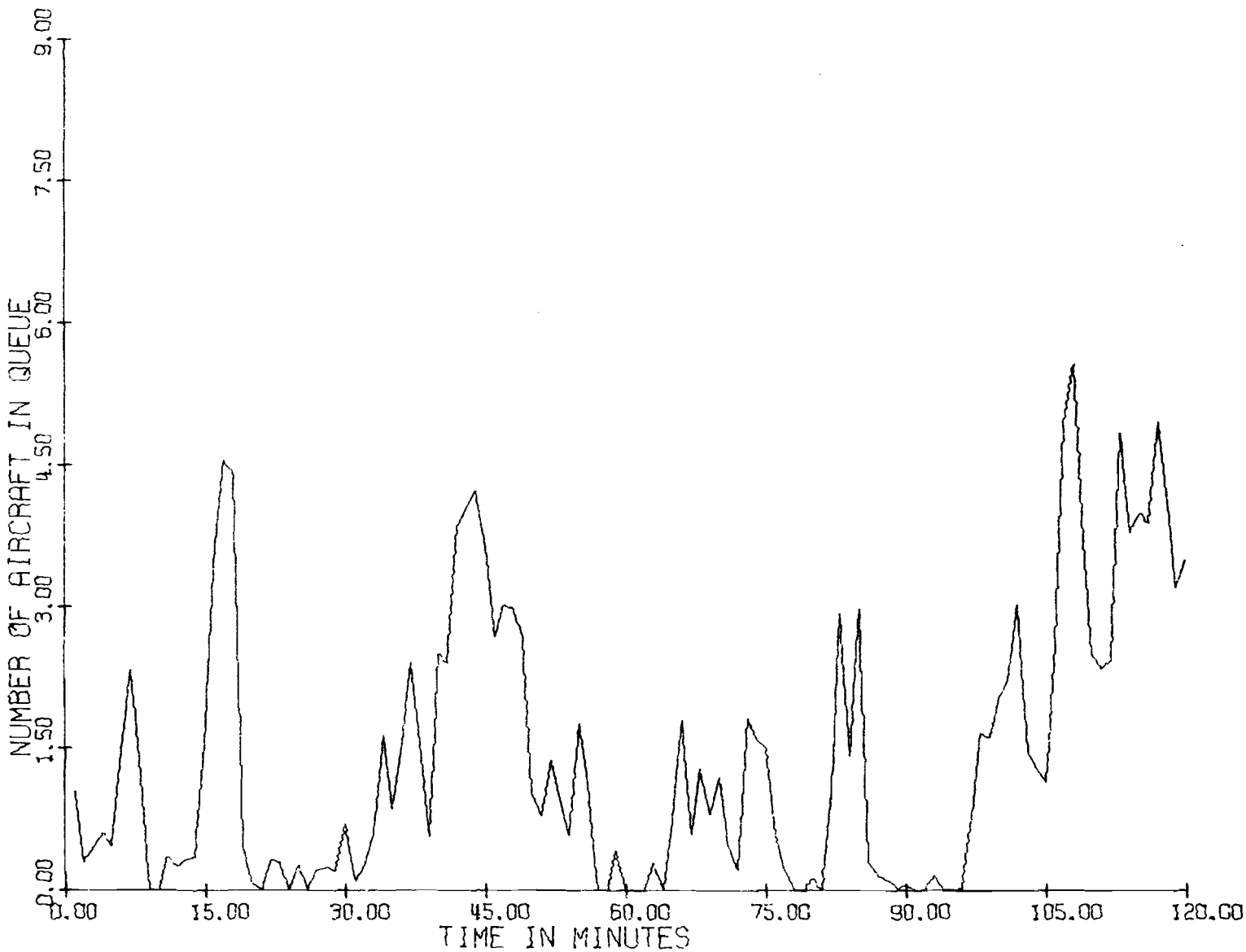

Figure 3.16 Simulated Queue Length Time Series for N.Y. HI Function at 33 A/H and 1.5 Second Tone Duration

Table 3.51 Summary Statistics of Simulations for the Changes in the Expected #TR/CT ($\tilde{K}$=1.0)

INPUT PARAMETERS - SECTOR FUNCTION HI

(1) AIRCRAFT INTERARRIVAL TIMES: EXPONENTIAL WITH MEAN = 60.000 SECONDS
(2) TRANSACTIONS PER AIRCRAFT: SHIFTED NEGATIVE BINOMIAL WITH K = 4.029 AND P = 0.579
(3) TRANSMISSIONS PER TRANSACTION: EMPIRICAL DISTRIBUTION
(4) TRANSMISSIONS LENGTHS: GAMMA WITH P = 1.3297 AND ALPHA = 3.6595
(NOTE: GAMMA PARAMETERS DETERMINED FROM EXPECTED ARRIVAL RATE)
(5) INTERCOMMUNICATION GAP LENGTHS ARE A FUNCTION OF TRANSACTIONS PER AIRCRAFT

SIMULATION RESPONSE - 2 HOUR ANALYSIS

(1) SECTOR AIRCRAFT LOADING
NUMBER OF AIRCRAFT IDENTIFIED IN SECTOR = 153 ACTUAL AIRCRAFT ARRIVALS IN TWO HOURS = 135
AVERAGE NUMBER OF AIRCRAFT PER SECOND = 16.640
MAXIMUM NUMBER OF AIRCRAFT PER SECOND = 35

(2) COMMUNICATIONS CHANNEL LOADING
AVERAGE CHANNEL UTILIZATION = .869
TOTAL NUMBER OF TRANSACTIONS = 659
AVERAGE LENGTH OF TRANSACTIONS = 9.504 SECONDS

(3) CHANNEL QUEUEING EFFECTS
AVERAGE TIME IN QUEUE = 89.104 SECONDS
AVERAGE TIME EXCLUDING ZERO ENTRIES = 93.809 SECONDS
TOTAL ENTRIES INTO QUEUE = 678
NUMBER OF ZERO ENTRIES (NON-WAITING) = 34
PERCENT OF ZERO ENTRIES = 5.0
AVERAGE NUMBER OF AIRCRAFT IN QUEUE = 8.390
MAXIMUM NUMBER OF AIRCRAFT IN QUEUE = 25

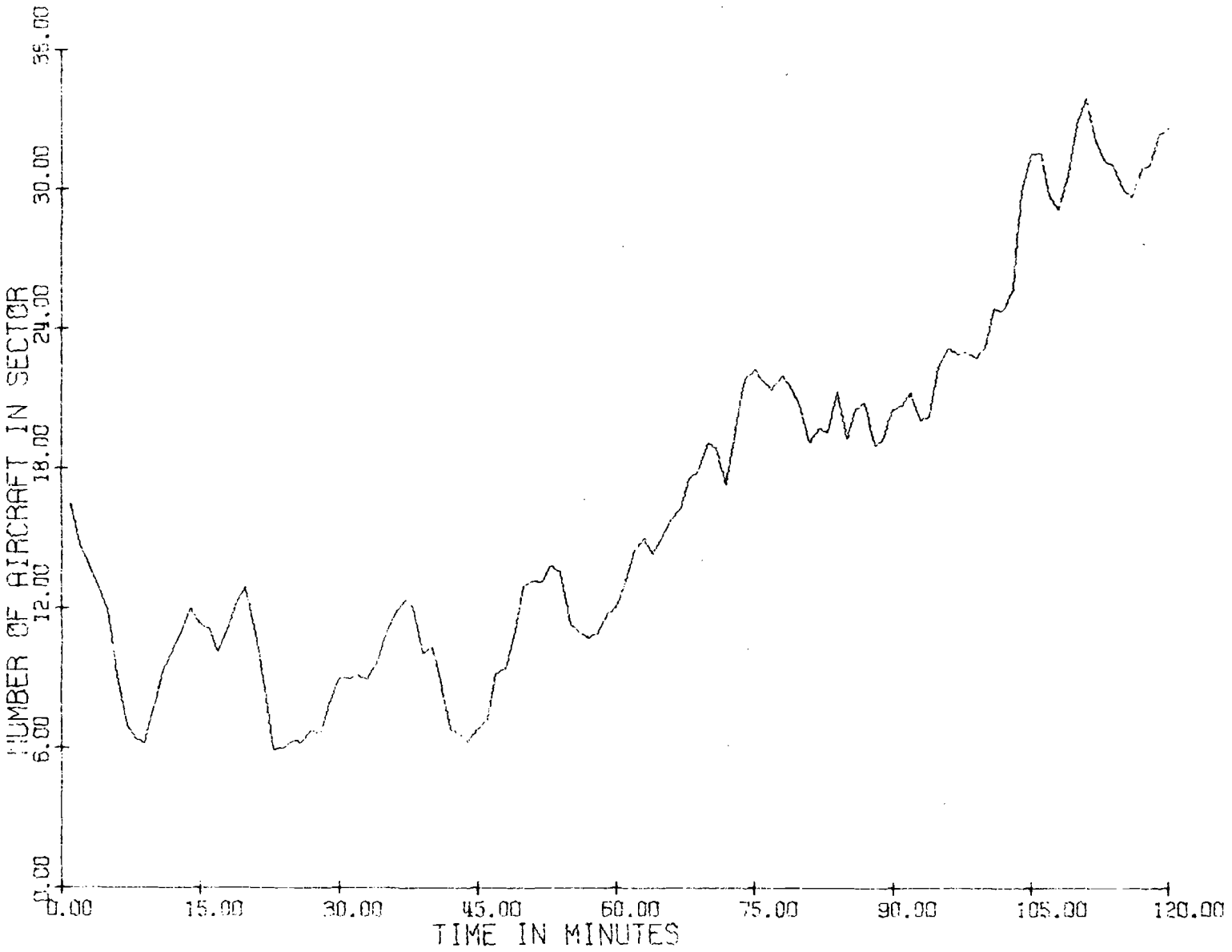

Figure 3.24 Simulated Aircraft Loading Time Series for N.Y. HI Function at 60 A/H and $\tilde{K}$=1.0

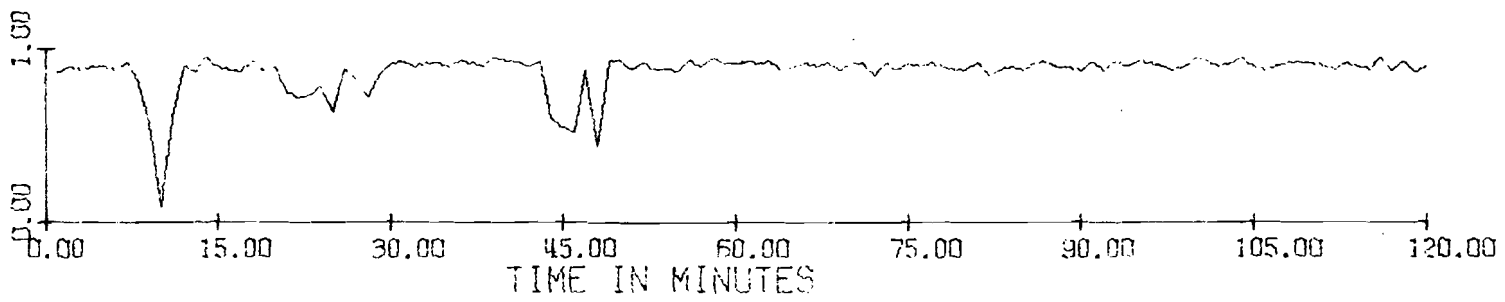

Figure 3.25 Simulated Channel Utilization Time Series for N.Y. HI Function at 60 A/H and $\tilde{K}$=1.0

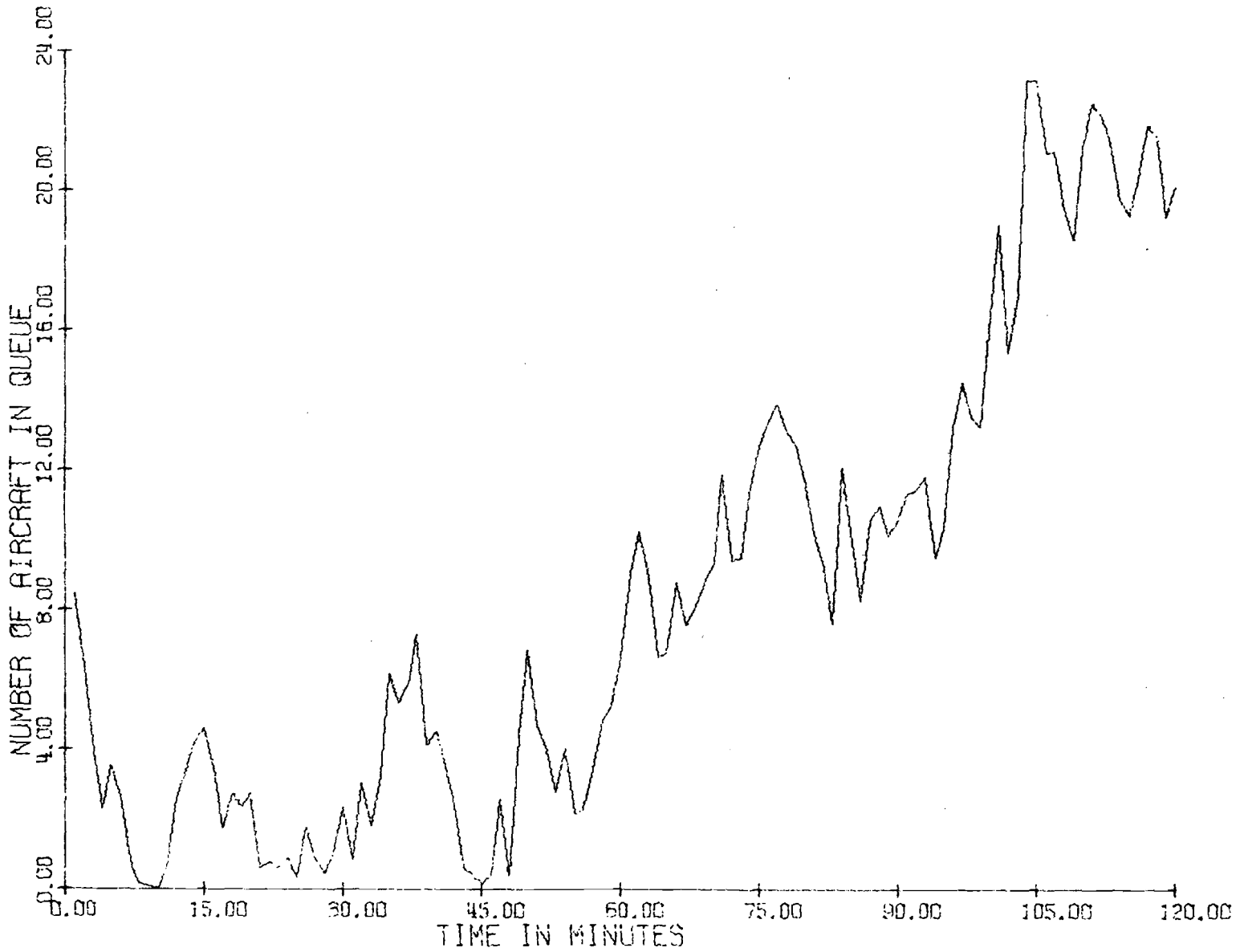

Figure 3.26 Simulated Queue Length Time Series for N.Y. HI Function at 60 A/H and $\bar{K}$=1.0

Table 3.52 Summary Statistics of Simulations for the Changes in the Expected #TR/CT ($\tilde{K}$=0.9)

INPUT PARAMETERS - SECTOR FUNCTION HI

(1) AIRCRAFT INTERARRIVAL TIMES: EXPONENTIAL WITH MEAN = 60.000 SECONDS
(2) TRANSACTIONS PER AIRCRAFT: SHIFTED NEGATIVE BINOMIAL WITH K = 4.029 AND P = 0.579
(3) TRANSMISSIONS PER TRANSACTION: EMPIRICAL DISTRIBUTION
(4) TRANSMISSIONS LENGTHS: GAMMA WITH P = 1.3297 AND ALPHA = 3.6595
(NOTE: GAMMA PARAMETERS DETERMINED FROM EXPECTED ARRIVAL RATE)
(5) INTERCOMMUNICATION GAP LENGTHS ARE A FUNCTION OF TRANSACTIONS PER AIRCRAFT

SIMULATION RESPONSE - 2 HOUR ANALYSIS

(1) SECTOR AIRCRAFT LOADING
NUMBER OF AIRCRAFT IDENTIFIED IN SECTOR = 151
AVERAGE NUMBER OF AIRCRAFT PER SECOND = 13.447
MAXIMUM NUMBER OF AIRCRAFT PER SECOND = 25

(2) COMMUNICATIONS CHANNEL LOADING
AVERAGE CHANNEL UTILIZATION = .824
TOTAL NUMBER OF TRANSACTIONS = 689
AVERAGE LENGTH OF TRANSACTIONS = 8.620 SECONDS

(3) CHANNEL QUEUEING EFFECTS
AVERAGE TIME IN QUEUE = 46.511 SECONDS
AVERAGE TIME EXCLUDING ZERO ENTRIES = 52.212 SECONDS
TOTAL ENTRIES INTO QUEUE = 696
NUMBER OF ZERO ENTRIES (NON-WAITING) = 76
PERCENT OF ZERO ENTRIES = 10.9
AVERAGE NUMBER OF AIRCRAFT IN QUEUE = 4.496
MAXIMUM NUMBER OF AIRCRAFT IN QUEUE = 17

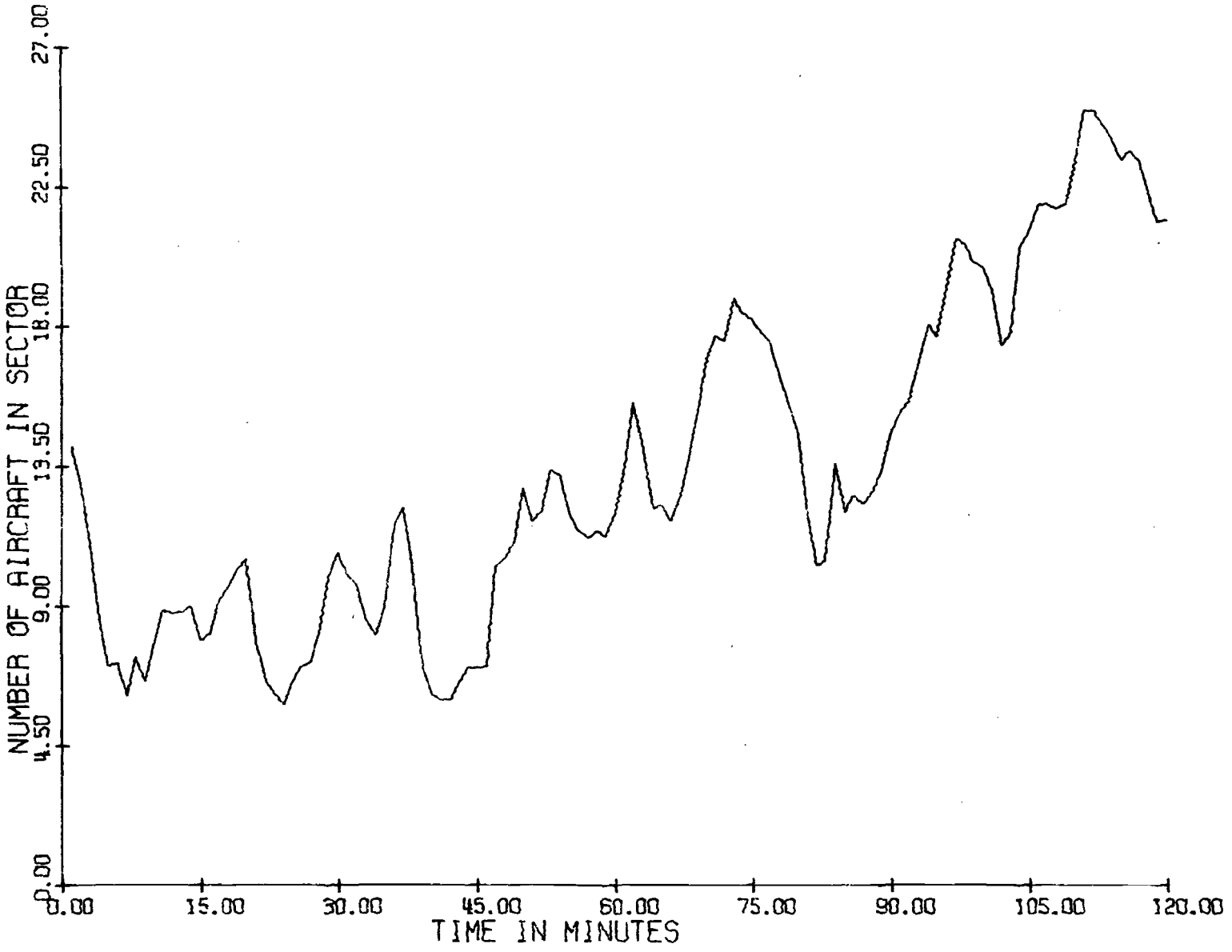

Figure 3.27 Simulated Aircraft Loading Time Series for N.Y. HI Function at 60 A/H and $\bar{K}$=0.9

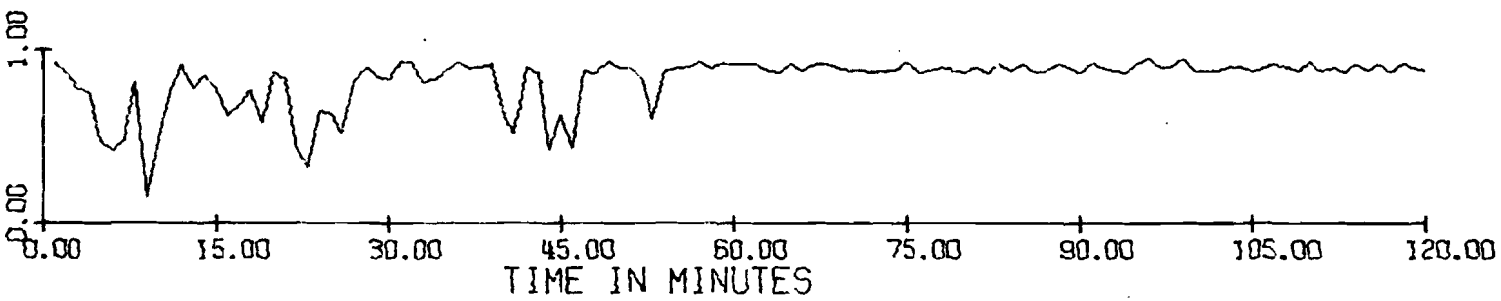

Figure 3.28 Simulated Channel Utilization Time Series for N.Y. HI Function at 60 A/H and $\tilde{K}$=0.9

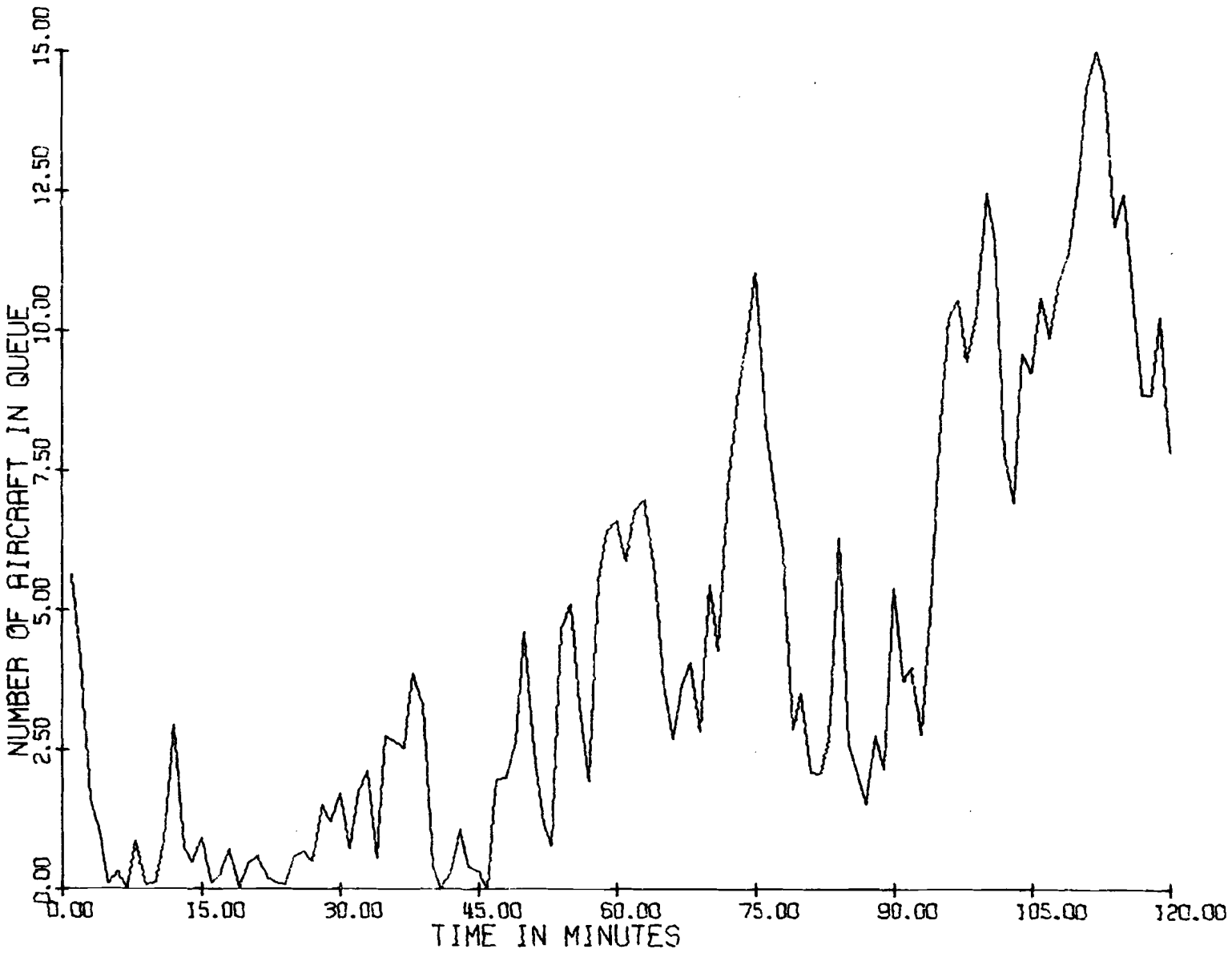

Figure 3.29 Simulated Queue Length Time Series for N.Y. HI Function at 60 A/H and $\tilde{K}$=0.9

Table 3.53 Summary Statistics of Simulations for the Changes

in the Expected #TR/CT ($\hat{K}$=0.7)

INPUT PARAMETERS - SECTOR FUNCTION HI

(1) AIRCRAFT INTERARRIVAL TIMES: EXPONENTIAL WITH MEAN = 60.000 SECONDS
(2) TRANSACTIONS PER AIRCRAFT: SHIFTED NEGATIVE BINOMIAL WITH K = 4.029 AND P = 0.579
(3) TRANSMISSIONS PER TRANSACTION: EMPIRICAL DISTRIBUTION
(4) TRANSMISSIONS LENGTHS: GAMMA WITH P = 1.3297 AND ALPHA = 3.6595
(NOTE: GAMMA PARAMETERS DETERMINED FROM EXPECTED ARRIVAL RATE)
(5) INTERCOMMUNICATION GAP LENGTHS ARE A FUNCTION OF TRANSACTIONS PER AIRCRAFT

SIMULATION RESPONSE - 2 HOUR ANALYSIS

(1) SECTOR AIRCRAFT LOADING
NUMBER OF AIRCRAFT IDENTIFIED IN SECTOR = 149
AVERAGE NUMBER OF AIRCRAFT PER SECOND = 10.260
MAXIMUM NUMBER OF AIRCRAFT PER SECOND = 19

(2) COMMUNICATIONS CHANNEL LOADING
AVERAGE CHANNEL UTILIZATION = .669
TOTAL NUMBER OF TRANSACTIONS = 728
AVERAGE LENGTH OF TRANSACTIONS = 6.618 SECONDS

(3) CHANNEL QUEUEING EFFECTS
AVERAGE TIME IN QUEUE = 12.222 SECONDS
AVERAGE TIME EXCLUDING ZERO ENTRIES = 17.492 SECONDS
TOTAL ENTRIES INTO QUEUE = 727
NUMBER OF ZERO ENTRIES (NON-WAITING) = 219
PERCENT OF ZERO ENTRIES = 30.1
AVERAGE NUMBER OF AIRCRAFT IN QUEUE = 1.234
MAXIMUM NUMBER OF AIRCRAFT IN QUEUE = 10

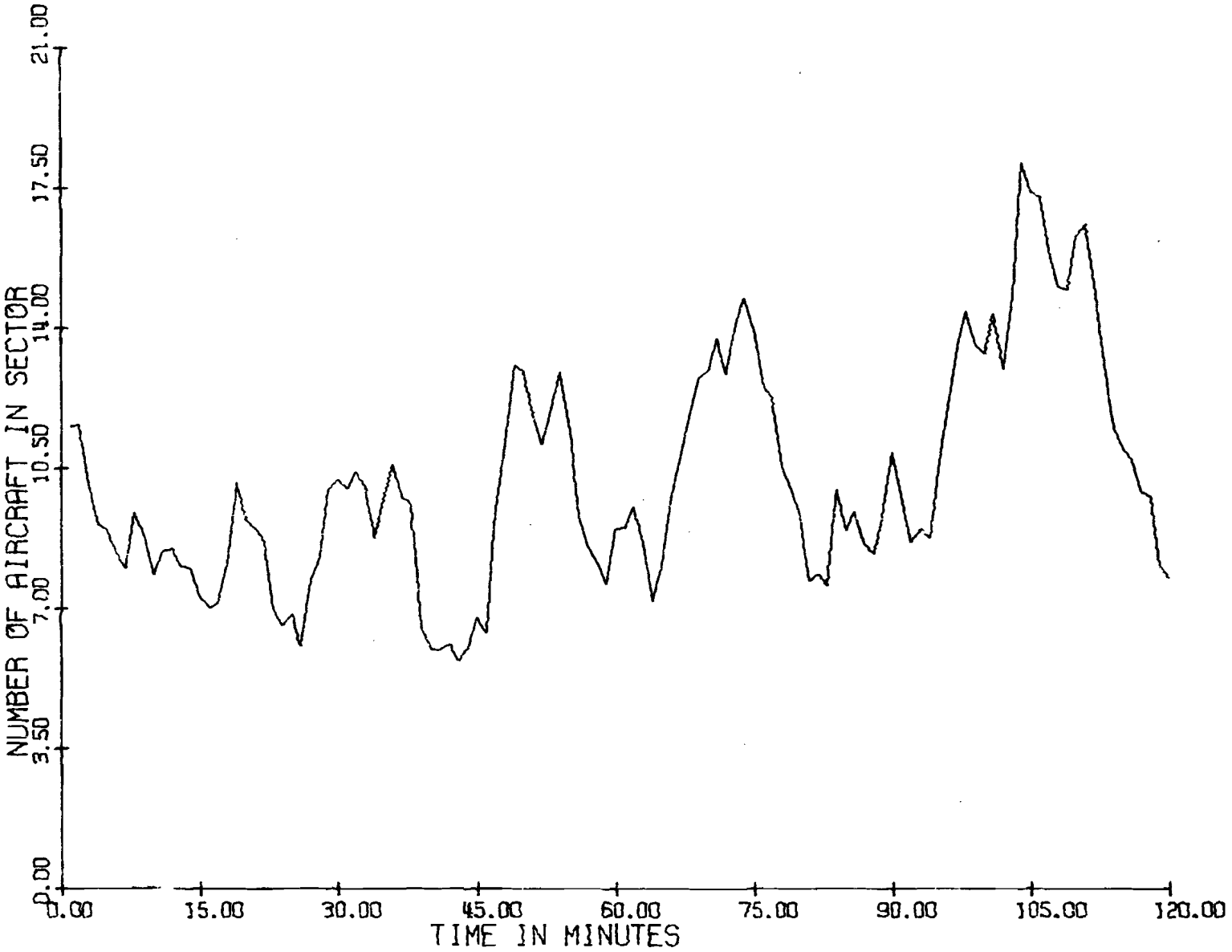

Figure 3.30 Simulated Aircraft Loading Time Series for N.Y. HI Function at 60 A/H and $\tilde{K}$=0.7

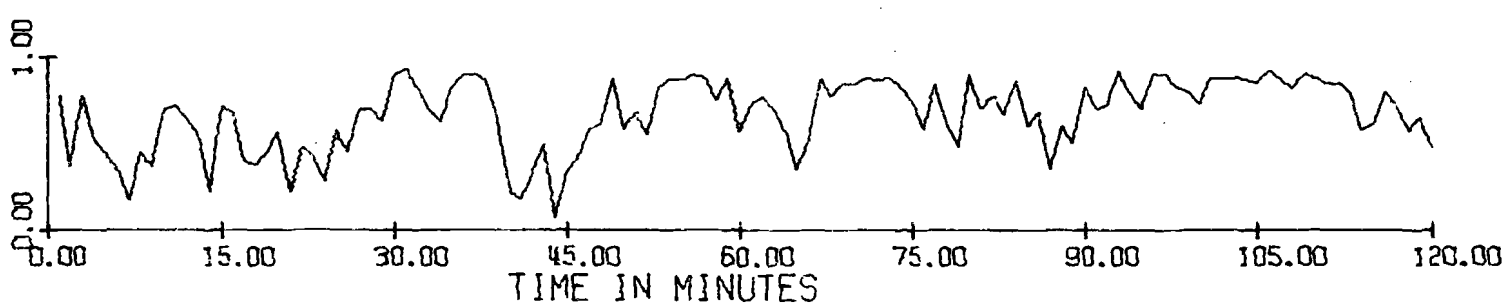

Figure 3.31 Simulated Channel Utilization Time Series for N.Y HI Function at 60 A/H and $\tilde{\tilde{K}}$=0.7

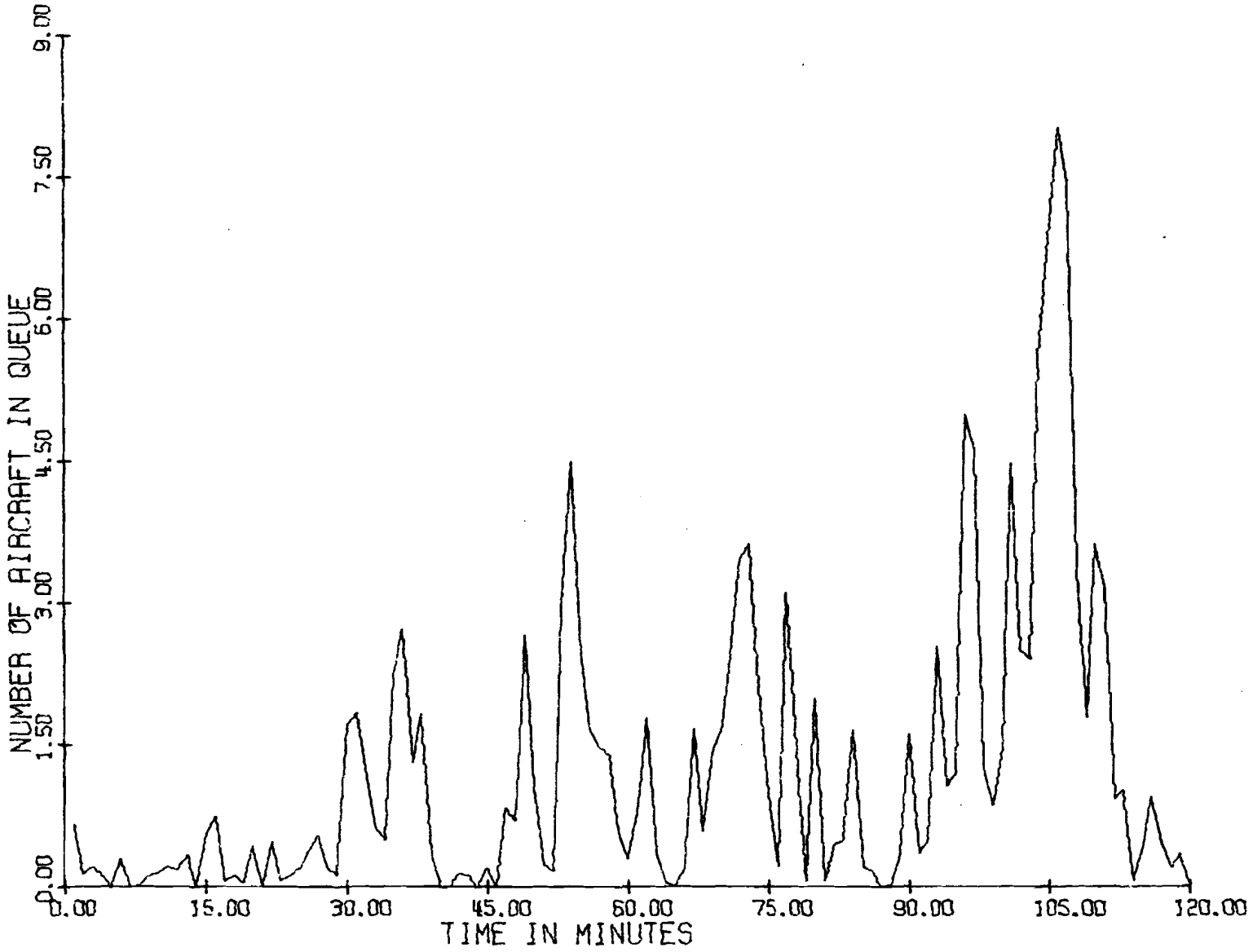

Figure 3.32 Simulated Queue Length Time Series for N.Y HI Function at 60 A/H and $\tilde{K}$=0.7

Table 3.54 Summary Statistics of Simulations for the Changes in the Expected #TR/CT ($\tilde{K}$=0.5)

INPUT PARAMETERS - SECTOR FUNCTION HI

(1) AIRCRAFT INTERARRIVAL TIMES: EXPONENTIAL WITH MEAN = 60.000 SECONDS
(2) TRANSACTIONS PER AIRCRAFT: SHIFTED NEGATIVE BINOMIAL WITH K = 4.029 AND P = 0.579
(3) TRANSMISSIONS PER TRANSACTION: EMPIRICAL DISTRIBUTION
(4) TRANSMISSIONS LENGTHS: GAMMA WITH P = 1.3297 AND ALPHA = 3.6595
(NOTE: GAMMA PARAMETERS DETERMINED FROM EXPECTED ARRIVAL RATE)
(5) INTERCOMMUNICATION GAP LENGTHS ARE A FUNCTION OF TRANSACTIONS PER AIRCRAFT

SIMULATION RESPONSE - 2 HOUR ANALYSIS

(1) SECTOR AIRCRAFT LOADING
NUMBER OF AIRCRAFT IDENTIFIED IN SECTOR = 145
AVERAGE NUMBER OF AIRCRAFT PER SECOND = 9.343
MAXIMUM NUMBER OF AIRCRAFT PER SECOND = 16

(2) COMMUNICATIONS CHANNEL LOADING
AVERAGE CHANNEL UTILIZATION = .475
TOTAL NUMBER OF TRANSACTIONS = 717
AVERAGE LENGTH OF TRANSACTIONS = 4.771 SECONDS

(3) CHANNEL QUEUEING EFFECTS
AVERAGE TIME IN QUEUE = 4.670 SECONDS
AVERAGE TIME EXCLUDING ZERO ENTRIES = 8.351 SECONDS
TOTAL ENTRIES INTO QUEUE = 717
NUMBER OF ZERO ENTRIES (NON-WAITING) = 316
PERCENT OF ZERO ENTRIES = 44.0
AVERAGE NUMBER OF AIRCRAFT IN QUEUE = .465
MAXIMUM NUMBER OF AIRCRAFT IN QUEUE = 5

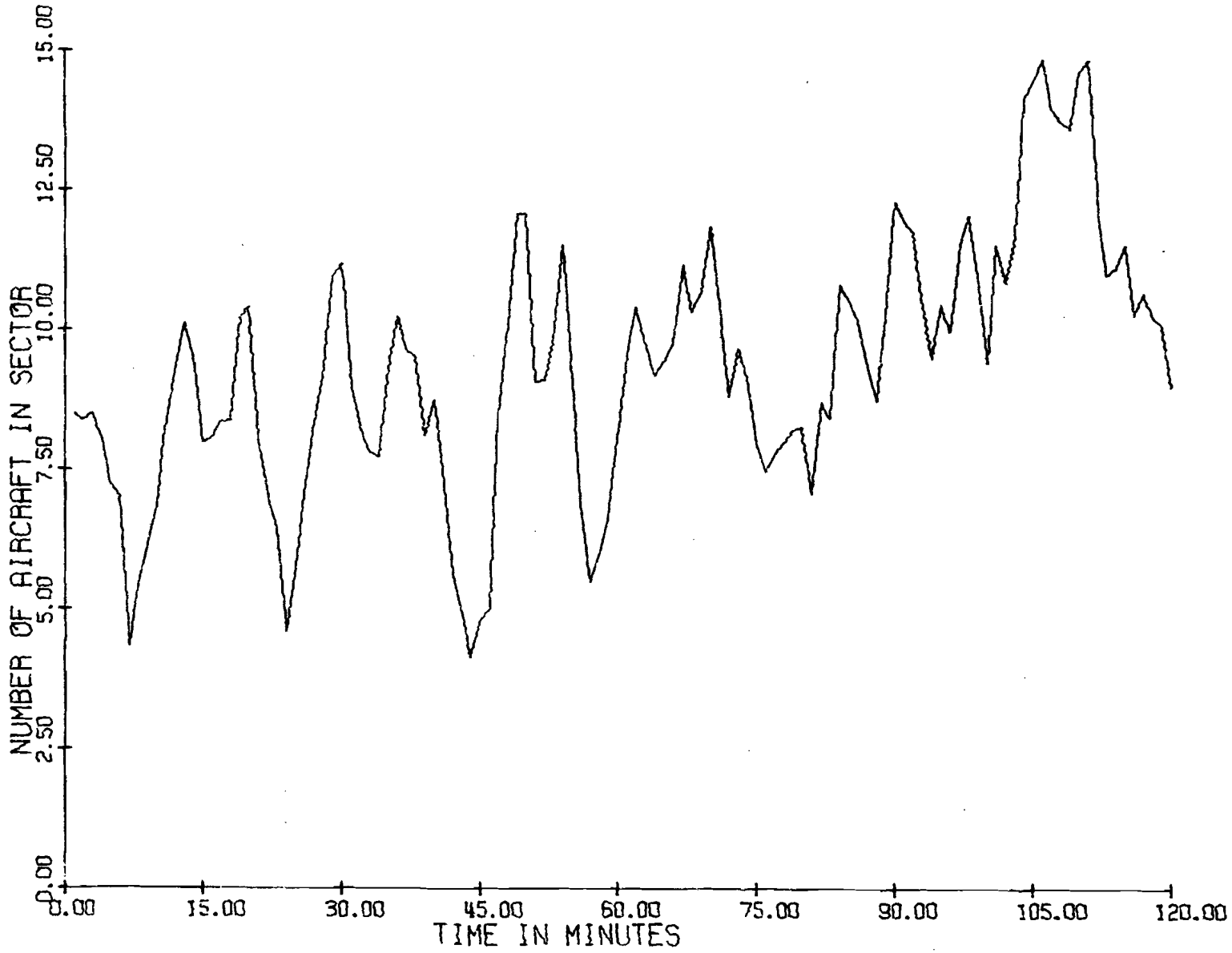

Figure 3.33 Simulated Aircraft Loading Time Series for N.Y. HI Function at 60 A/H and $\tilde{K}$=0.5

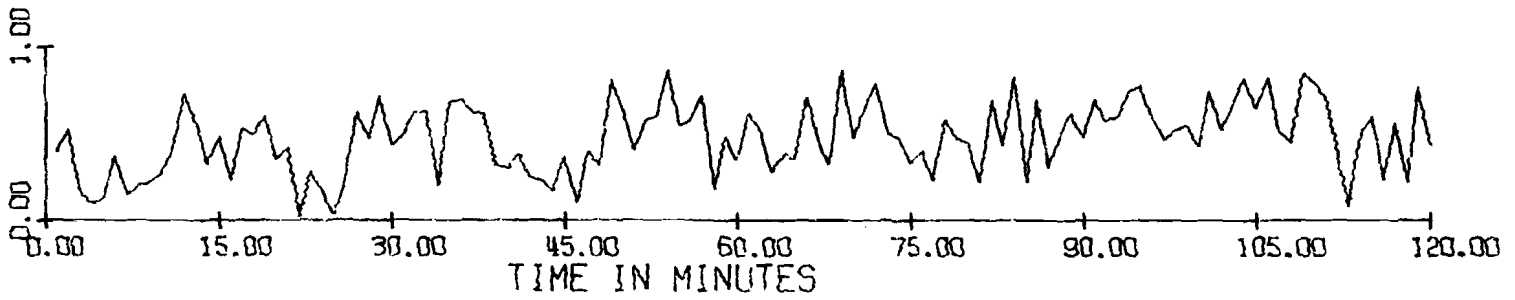

Figure 3.34 Simulated Channel Utilization Time Series for N.Y. HI Function at 60 A/H and $\tilde{K}$=0.5

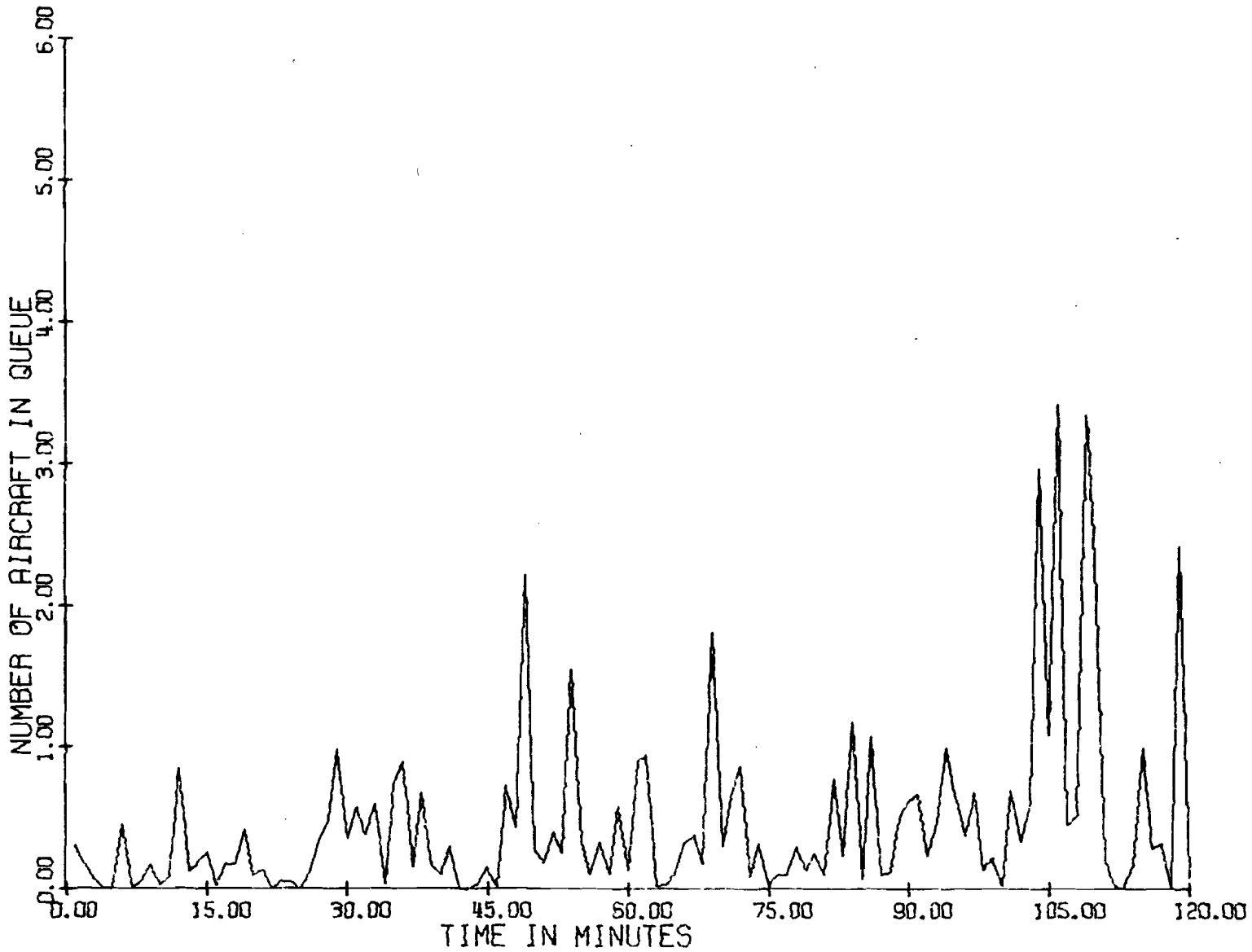

Figure 3.35 Simulated Queue Length Time Series for N.Y. HI Function at 60 A/H and $\tilde{K}$=0.5

CHAPTER 4

NETWORK MODELING - NETWORK STRUCTURE, AIRCRAFT ARRIVAL STREAMS, AND SECTOR SEQUENCES

4.1 Introduction

4.1.1 Motivation

The ATC voice communications study presented in previous Princeton reports has concentrated on the analysis and simulation of air-ground communications models for a single sector or sector function. The simulated sector is excited by a stream of traffic which is generated without regard to sector flows. Valuable insights regarding various responses such as queuing times, channel utilization, etc., have been gained by exercising the model in many different ways, but little consideration has yet been given to the important transfer phenomena of some significant events, such as traffic congestion, in a sequence of adjacent sectors. Indeed, a systematic study of a group of sectors as a network remains to be done.

This chapter presents the results of research conducted into various aspects of a network composed from a group of ATC enroute sectors, based upon the New York ARTCC data file. This chapter could form the basis for a more comprehensive study aimed at providing valuable information regarding the interrelationships of the ATC activities among the sectors in a network which might lead to the suggestions of methods useful for the improvement of the communications efficiency of the network as a whole.

The selection of the enroute sectors was suggested by a number of considerations. As a group, these sectors appear to be the most homogeneous, in terms of the probability distributions used to describe the major communication variables, and in the type of traffic pattern handled. The traffic flows among these sectors are the most diffuse when compared with the sector groups, due to the large number of paths passing through each sector. Further, enroute sectors are felt to be analogous to oceanic sectors where network analysis and simulations may have applications. The ultimate goal of this study is to integrate the single-sector simulation into a general network model which will be useful for the purposesjust mentioned.

4.1.2 Scope of this Report

The three facets of the multiple-sector network on which this first report will concentrate relate to the mechanics of flow among the enroute sectors. The first section develops a formulation for a general ATC network

using terminology from graph theory which has commonly been applied to ground transportation systems. The next section discusses the specifications of traffic streams, considering sources and sinks for traffic in the network and characterizing movement of aircraft through sequences of sectors. The final section applies these techniques to a network of enroute sectors from the New York data file.

4.2 Network Structure

4.2.1 Attributes of the Network

A general ATC network consists of a set of sectors $\{N_k, k=1,2,\ldots,m\}$, each controlled by a single control position with its assigned radio frequency. Aircraft move among the various sectors as permitted by geographical proximity or functional relationship. Adopting the notation used by Ford and Fulkerson (1962), Hu (1969), Potts and Oliver (1972), and others, the network is defined by $G=[N;A]$ where N is the set of sectors or "nodes," and A is a set of "arcs" representing feasible transition paths between adjacent sectors.

It is convenient to define a super-source s and super-sink t to represent the points of entry and exit, respectively, for all traffic in the network. Then if (X,Y) is the set of all arcs from nodes in set X to nodes in set Y,

$$A = (s, N) \cup (N, N) \cup (N, t)$$

where $\cup$ is the symbol for set union.

For a network containing m sectors, A could contain as many as (m^2+2m) directed arcs, each representing flow in one direction between a pair of nodes. In most networks, however, the number of arcs is much less than the maximum possible since many pairs of sectors are not physically or functionally adjacent. To specify which arcs are present in a network, a node-node incidence matrix D of dimension (m x m) may be defined where element

$$d_{ij} = \begin{cases} 1, & \text{if flow is possible from node } i \text{ to node } j; \\ 0, & \text{otherwise}. \end{cases}$$

For convenience, it is assumed that all 2m arcs in (s, N) and (N, t) exist, which does not restrict the generality of the formulation since the probability of using infeasible arcs (or the capacity of such arcs) can be set to zero.

4.2.2 Defining Flow on the Network

Flow over the network is defined on the arcs in A. Let f be a real-valued function on A with dimensions of aircraft per unit time, henceforth called the "traffic flow rate." Then if the total rate of flow through the network is F,

$$F = \sum_{N_k \varepsilon N} f(s,N_k) = f(s,N). \tag{4.1}$$

Equivalently,

$$F = \sum_{N_k \varepsilon N} f(N_k,t) = f(N,t). \tag{4.2}$$

Actually, (4.1) and (4.2) are special cases of Kirchhoff's flow conservation law which states that in equilibrium the total flow directed into a node must equal the total flow directed outward. Thus

$$\sum_{N_k \varepsilon N} f(x,N_k) - \sum_{N_k \varepsilon N} f(N_k,x) = \begin{cases} F, & \text{if } x=s \\ 0, & \text{if } x \neq s,t \\ -F, & \text{if } x=t. \end{cases} \tag{4.3}$$

In determining flow rates in an actual network from data collected over a finite sample period, intuitive estimators may give rise to estimates which do not satisfy (4.3) and for which (4.1) and (4.2) are not equivalent. A common reason for this is unequal numbers of aircraft in each node (sector) at the beginning and end of the sample period. In order to arrive at estimates which satisfy (4.3), it is necessary to isolate separate streams of traffic and to estimate the rate of flow in each stream individually, or to characterize the traffic flow pattern more economically while generating consistent estimates. Sections 4.3 and 4.4 discuss this problem in more detail.

4.3 Network Arrivals

4.3.1 Arrival Sources

The arrivals of aircraft to the network G are considered to be generated at the super-source s. From s, entry to the network occurs over one of the m arcs in (s, N). In reality, the flow through s is a superposition of traffic streams from many sources, such as airports in the region or other ATC centers. Similarly, the flow through the super-sink t is a superposition of traffic streams bound for many destinations.

Denote the set of sources feeding traffic to the super-source by $\{s_i, i=1,2, \ldots, m_s\}$ and the set of sinks from the super-sink by $\{t_j, j=1,2, \ldots, m_t\}$. Then all flow through the network originates at some s_i, passes through the super-source s into the network, then exits through t to some destination t_j. Figure 4.1 is a schematic diagram of such a network with four sources and four sinks.

4.3.2 Determining Flow Rates on (s, N)

Assume that the rate of traffic generated at each source s_i is λ_i and that the rate of traffic attracted to each sink t_j is μ_j. Then an

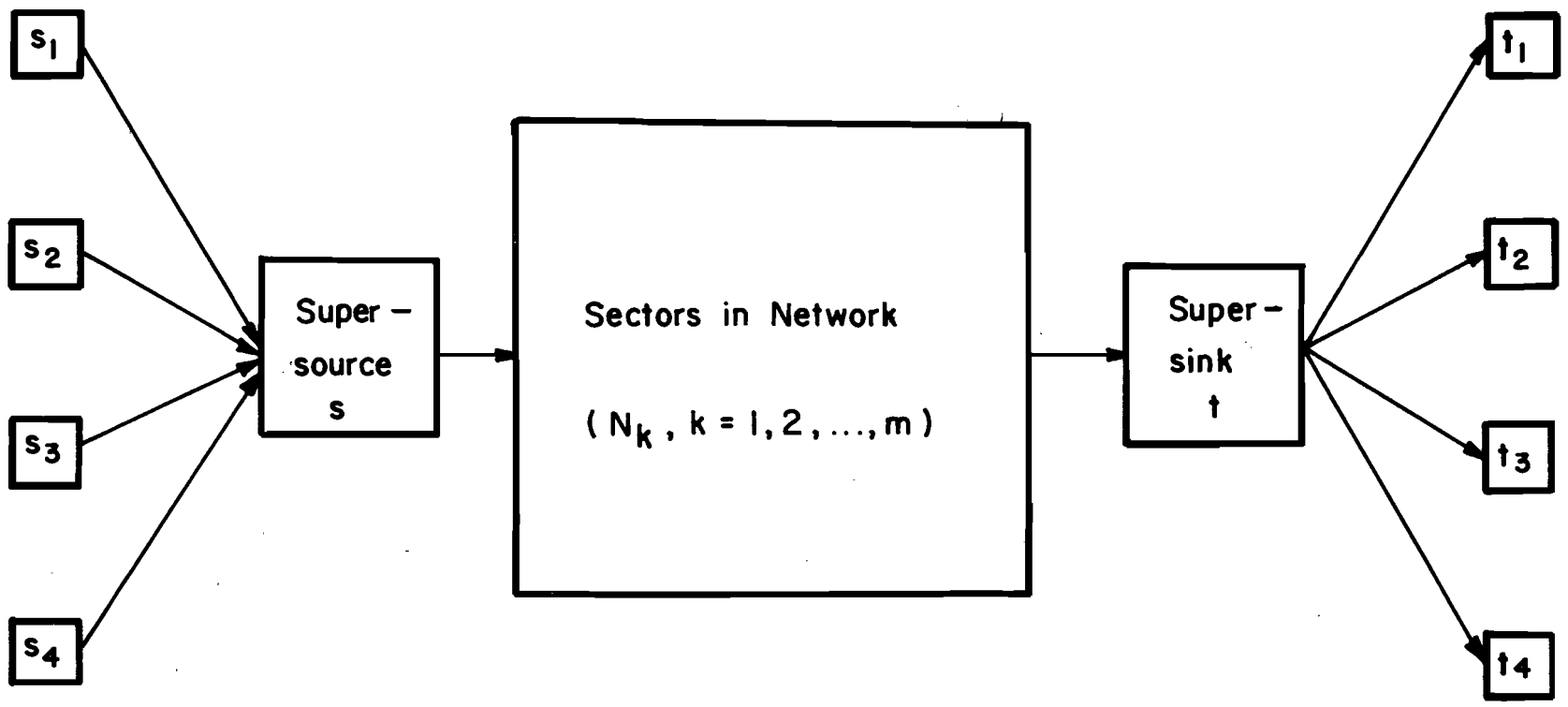

Figure 4.1 ATC Network Diagram

application of the flow conservation equation requires that

$$F = \sum_{i=1}^{m_s} \lambda_i = \sum_{j=1}^{m_t} \mu_j \tag{4.4}$$

where F is defined to be the rate of flow over the entire network (or equivalently the rate of flow from s to t). From (4.4), it is evident that the rate of flow over the arcs in (s, N) must equal both the sum of the generation rates λ_i and the sum of the attraction rates μ_j.

Given λ_i and μ_j, it is necessary to determine each $f(s, N_k)$ such that the above conservation equations are satisfied. To formulate the problem let

$$p_k = \Pr\text{ (an aircraft enters the network over arc } (s, N_k))$$

where Pr represents the probability and let

$$p_{k|i} = \Pr\text{ (an aircraft enters the network over arc } (s, N_k) \text{ given it was generated at source } i).$$

Then

$$f(s, N_k) = \sum_{i=1}^{m_s} p_{k|i}\, \lambda_i. \tag{4.5}$$

If the selection of entry arc from s does not depend on the source at which an aircraft was generated, then $p_{k|i} = p_k$ and

$$f(s, N_k) = p_k \sum_{i=1}^{m_s} \lambda_i \tag{4.6}$$

or equivalently

$$f(s, N_k) = p_k\, F. \tag{4.7}$$

The simple form of (4.7) will not be appropriate for most networks representing physical systems since the point of entry to the network will usually depend on the source of the arrival. For an ATC network, many $p_{k|i}$ will be equal to zero for positive p_k simply from geographical considerations. For example, a departure from an airport in the eastern part of the region can hardly enter the network at any sector in the western part. Thus (4.5) is normally required for specification of flow rates over the arcs in (s, N), and all $p_{k|i}$ must be determined.

A consideration which further complicates the situation is that the λ_i and μ_j are often functions of each other. In an analysis of the network, the specification of sink attraction rates may be more appropriate to the problem at hand than specification of source generation rates. It is even possible, as will be shown in a later section, that some combination of the λ_i's and μ_j's will be given, requiring that the others be determined. A discussion of techniques for solving this problem must be postponed until the specification of sector transition probabilities is given in section 4.4.

4.3.3 Estimation of Arrival Rate Parameters

Assume that a given traffic stream entering the super-source s has flow rate λ. Let $\{A(t),\ t > 0\}$ be the corresponding counting process for the number of aircraft in that stream passing a given point, such as the point of entry to s. Such a point may have a physical meaning or be simply an abstract reference. Then the structure of $\{A(t)\}$ will be important in determining an appropriate estimate for λ. The most frequent assumption, which has been applied successfully in the past for streams of aircraft, is that of a Poisson process. Parzen (1962) defines a Poisson process as a counting process such that

(i) $\{A(t),\ t>0\}$ has stationary independent increments; (4.8)

(ii) for any interval (t_1,t_2), $t_1>t_2$, $A(t_2)-A(t_1)$ has a Poisson distribution with mean $\lambda(t_2-t_1)$ where λ is the rate of occurrence per unit time of events being counted.

The Poisson process arises naturally in circumstances where events occur independently and has several interesting properties. Among the most commonly used is that the length of time between k events has a gamma distribution with parameters (k,λ). In particular, the time between consecutive arrivals (the "interarrival time") follows the exponential distribution with probability density function

$$f(x) = \lambda e^{-\lambda x}\ ,\ x > 0\ . \tag{4.9}$$

A second interesting property is that the superposition of n independent Poisson processes with rate parameters λ_i, $i = 1,2,\ldots,n$, is also a Poisson process with rate parameter

$$\lambda = \sum_{i=1}^{n} \lambda_i\ . \tag{4.10}$$

Consider the stream of traffic through the super-source s. If traffic generated at each of the sources s_i is a Poisson process with rate parameter λ_i and all the traffic streams are generated independently, then the stream through s is also Poisson with rate parameter

$$\lambda_s = \sum_{i=1}^{m_s} \lambda_i \quad . \tag{4.11}$$

Further, the joint distribution of arrivals per unit time at s from each of the sources s_i follows the multinomial distribution

$$P(x_1, x_2, \ldots, x_{m_s}) = \frac{x_s!}{x_1! x_2! \ldots x_{m_s}!} \left(\frac{\lambda_1}{\lambda_s}\right)^{x_1} \left(\frac{\lambda_2}{\lambda_s}\right)^{x_2} \cdots \left(\frac{\lambda_{m_s}}{\lambda_s}\right)^{x_{m_s}}$$

$$x_i = 0,1,2,\ldots \tag{4.12}$$

where $x_s = \sum_{i=1}^{m_s} x_i$ is the total number of arrivals at s in one unit of time.

Assume now that traffic in the network is observed during a finite period and that estimates are desired for each of the arc flow rates $f(s, N_k)$. Then from (4.5), we require estimates of the source generation rate parameters $\{\lambda_i, i = 1,2,\ldots,m\}$ and of the conditional probabilities $p_{k|i}$. For convenience the λ_i's can be represented by a vector of parameters $\underset{m_s x 1}{\underset{\sim}{\lambda}}$ and the conditional probabilities by a transition matrix $\underset{m_s x m}{\underset{\sim}{P}}$. All parameters are assumed to be constant over time.

Suppose that over the duration of the sample period we observe R arrivals through s. If the sample period consists of T discrete intervals of time, then for each arrival with entry time t_r, the data can be represented by $\{x_r(t), t=1,2,\ldots,T\}$ where

$$x_r(t) = \begin{cases} s_i & \text{if } t<t_r \text{ and the } r^{th} \text{ aircraft was generated at } s_i \\ N_k & \text{if } t \geq t_r \text{ and the } r^{th} \text{ aircraft entered the network over arc } (s,N_k). \end{cases}$$

We will show that the likelihood function of the parameter set $\theta = (\underset{\sim}{\lambda}, \underset{\sim}{P})$ given a sample X can be factored into two terms, one involving $\underset{\sim}{\lambda}$ only and the other involving $\underset{\sim}{P}$ only. The proof follows that of Duncan and Lin (1972) for Markov chains with stochastic entry.

For each observed arrival, no information is lost if $x_r(t)$ is replaced by the triplet (s_i, N_k, t_r). Then the sampling distribution can be written as

$$\begin{aligned} f_\theta(x) &= f_\theta(s, N, t) = f_\theta(N|s,t)\, f_\theta(s,t) \\ &= f_{\underset{\sim}{P}}(N|s,t)\, f_{\underset{\sim}{\lambda}}(s,t) \quad . \end{aligned} \tag{4.13}$$

Thus the likelihood function of the parameters given X can be written

$$L_X(\theta) = L_{N|s,t}(\underset{\sim}{P}) \cdot L_{s,t}(\underset{\sim}{\lambda}) \ . \tag{4.14}$$

If the transition probabilities $p_{k|i}$ are constant over time, then (4.14) reduces to

$$L_X(\theta) = L_{N|s}(\underset{\sim}{P}) \cdot L_{s,t}(\underset{\sim}{\lambda}) \ . \tag{4.15}$$

The consequence of (4.15) is that the overall likelihood function for θ is maximized when maximum likehood estimates are obtained separately for $\underset{\sim}{P}$ and $\underset{\sim}{\lambda}$. Further, the estimates of $\underset{\sim}{P}$ need involve only the number of aircraft entering each sector from each source, and the estimates of $\underset{\sim}{\lambda}$ require only knowledge of the time and source of each entry to s.

Suppose that in a sample period we observed a source-node entry count matrix ${}_{m_s}C_{xm}$ with elements defined by

c_{ik} = # of aircraft generated at source s_i which entered sector N_k.

Then the total number of aircraft generated at source s_i is given by

$$c_{i.} = \sum_{k=1}^{m} c_{ik}$$

and the number of aircraft entering the network over arc (s, N_k) is given by

$$c_{.k} = \sum_{i=1}^{m_s} c_{ik}.$$

Since the arrival streams from the individual sources are assumed to be independent Poisson processes, the maximum likelihood estimates of the source generation rate parameters are given by

$$\hat{\lambda}_i = \frac{c_{i.}}{T} \tag{4.16}$$

where T is the number of time units in the sample period, a well-known result.

Now since the conditional probabilities $P_{k|i}$ have been assumed to be constant over time, then given $c_{i.}$, the individual transition counts c_{ik} have a multinomial distribution. Thus the maximum likelihood estimates are simply

$$\hat{p}_{k|i} = \frac{c_{ik}}{c_{i.}} \ . \tag{4.17}$$

The estimate of the overall network flow rate F can be obtained using (4.4) and (4.16), and is

$$\hat{F} = \frac{\sum_{i=1}^{m_s} c_{i.}}{T} \tag{4.18}$$

which could be obtained directly by realizing that the flow through the super-source s is Poisson with rate given by (4.11). The estimates of the flow rates over the arcs in (s, N), using (4.5) and (4.17), are

$$\hat{f}(s, N_k) = \sum_{i=1}^{m_s} \frac{c_{ik}}{T} . \tag{4.19}$$

Since the $p_{k|i}$ are constant over time, these traffic streams are also Poisson. The estimate of the flow rate through s is given by

$$\hat{\lambda}_s = \sum_{i=1}^{m_s} \hat{\lambda}_i = \hat{F} . \tag{4.20}$$

4.3.4 Summary

The results of this section show that under two basic assumptions, the arrival rates at each sector of a network can be determined from the arrival rates at individual sources. The maximum likelihood estimates of traffic flow rates are easily obtained from observing entries to the network during a sample period. The basic assumptions required are:

(i) that the generation of aircraft at the sources are <u>independent Poisson</u> processes;
(ii) that the probability of an arrival from a given source entering a specific sector is constant over time.

When simulating the system, the number of aircraft generated at s per unit time will have the multinomial distribution given by (4.12) with whatever generation rates for the sources are desired. Thus only a single generator at s is required, not one for each source. Using the estimates of $p_{k|i}$ from (4.17), aircraft can then be assigned to the proper arcs in (s, N) in a random fashion. The movement of aircraft after they enter the initial sector is the subject of the next section.

4.4 Sector Sequences

4.4.1 Definition

As aircraft move through an ATC network, they pass from sector to sector (or from node to node) in sequences determined by their origin and destination. In a network of many sectors, the number of possible sequences is enormous, making the specification of the relative frequencies of all

sequences prohibitive. In order to reduce the complexity of the problem while still maintaining the general patterns of network flow, an approach based on Markov chains will be presented.

To state the problem formally, let $\{s_n(k),\ k = 0, 1, 2, \ldots\}$ be the sequence of sectors through which the nth aircraft in some index set passes, where

$$s_n(0) = \begin{cases} i, & \text{if the } n^{th} \text{ aircraft is a departure from the } i^{th} \text{ source} \end{cases}$$

$$s_n(k) = \begin{cases} r, & \text{if the } k^{th} \text{ sector entered by the } n^{th} \text{ aircraft is sector } r \end{cases}$$

$$1 \leq k \leq m_n$$

$$s_n(k) = \begin{cases} j, & \text{if the } n^{th} \text{ aircraft is an arrival at the } j^{th} \text{ sink} \end{cases}$$

$$k > m_n$$

where m_n is the number of network sectors in the sequence for the nth aircraft. Then the m nodes, m_s sources, and m_t sinks can be considered to be states of a Markov chain of unknown order from which $\{s_n(\cdot)\}$ is one possible observation.

It will be recognized that the nodes and sources are transient states, while the sinks are absorbing. Further, the nodes form a communicating class, accessible from the sources, but the sources (non-return states) are not accessible from any states in the chain.

The characterization of the sequences will thus involve state transition matrices of very special form. While all sequences begin in one of the source states, the probability of ever returning to those states must be zero. In describing the sequences, we state first the initial distribution of $s_n(0)$ and then discuss the state transition probabilities.

4.4.2 Initial Distribution of $s_n(0)$

The intial distribution of $s_n(0)$ has parameter set

$$\underset{\sim}{\theta} = \left[\frac{\lambda_1}{\lambda_s}, \frac{\lambda_2}{\lambda_s}, \ldots, \frac{\lambda_{m_s}}{\lambda_s}\right],$$

where

$$\Pr(s_n(0) = i) = \frac{\lambda_i}{\lambda_s} \tag{4.21}$$

and $\sum_{i=1}^{m_s} \lambda_i = \lambda_s$. Thus the relative generation rates at the sources determine the probability distribution for $s_n(0)$ in a natural way. Further, the properties of the Poisson model for source generation streams ensure that successive observations of $s_n(0)$ for n=1,2,..., will be independent.

4.4.3 Transition Probabilities

If the sector sequences $\{s_n(\cdot)\}$ can be regarded as realizations of a Markov chain of order q, then the distribution of $s_n(k)$ depends on the past history of the sequence only through $s_n(k-1)$, $s_n(k-2)$, ..., and $s_n(k-q)$. More explicitly, let

$$p_j = \Pr(s_n(k) = j) \tag{4.22}$$

$$p_{ij} = \Pr(s_n(k) = j \mid s_n(k-1) = i) \tag{4.23}$$

and

$$p_{hij} = \Pr(s_n(k) = j \mid s_n(k-1) = i,\ s_n(k-2) = h)\ . \tag{4.24}$$

Then if the sequences are zero-order Markov chains,

$$p_i = p_{ij} = p_{hij}. \tag{4.25}$$

For first order Markov chains,

$$p_i \neq p_{ij} = p_{hij}. \tag{4.26}$$

For second-order chains,

$$p_i \neq p_{ij} \neq p_{hij}\ . \tag{4.27}$$

The extension to higher orders is direct.

In studying sequences of sectors, it is therefore necessary to determine both the order of the chain and all relevant transition probabilities. This is most easily handled by defining a series of transition matrices $p^{(1)}$, $p^{(2)}$, ... where $p^{(q)}$, the "q-step transition matrix", has element

$$p_{ij} = \Pr\{s_n(k) = j \mid s_n(k-q) = i\} \tag{4.28}$$

$$q = 1,\ 2,\ \ldots\ .$$

For a zero-order Markov chain, (4.25) can be expressed by

$$p^{(q)} = [p_{ij}],\quad p_{ij} = p_i\ .$$

For first-order Markov chains, a consequence of (4.26) is that

$$p^{(q)} = [p^{(1)}]^q\ . \tag{4.30}$$

For second-order and higher Markov chains, no such simple representation is possible.

For an ATC network, it is instructive to determine what elements of the one-step transition matrix $p^{(1)}$ are non-zero. Figure 4.2 shows a sample network with two sources, two sinks, and five interior nodes. The location of all non-zero elements in the corresponding one-step transition matrix is shown in figure 4.3. The matrix has been partitioned into nine sections for ease of interpretation. The following observations are important:

(1) Since all flow from the sources and to the sinks is uni-directional, all elements in sections (i), (iv), (vii), (viii), and (ix) are zero. The same is true for all higher-step transition matrices.

(2) Since all flow in the network passes through at least one interior sector, all elements in section (iii) are zero. This is <u>not</u> true in higher step transition matrices. In fact, for large q, the only significant non-zero elements will be located in section (iii).

(3) Since transitions from any state to itself are not allowed, all elements on the main diagonal are zero.

(4) Since the interior nodes of the network allow flow in both directions between adjacent pairs, the non-zero elements in section (v) are symmetrically located about the main diagonal. This would not be true in general for all ATC networks.

The one-step transition matrix is closely related to the node-node incidence matrix D defined in section 4.2.1. The number of non-zero elements in the matrix is simply the number of arcs in the network and the location of the non-zero elements in section (v) is equivalent to the location of 1's in D.

Higher step transition matrices determine the accessibility of nodes in the network from each other. Since all flow originates at a source and ends at a sink, the only elements of the matrix which do not converge to zero as q becomes large are those in section (iii). Let the limiting values of the elements in section (iii) be given by

$$e_{ij} = \lim_{q \to \infty} p^{(q)}_{s_i t_j} \qquad (4.31)$$

$$i = 1, 2, \ldots, m_s$$
$$j = 1, 2, \ldots, m_t \ .$$

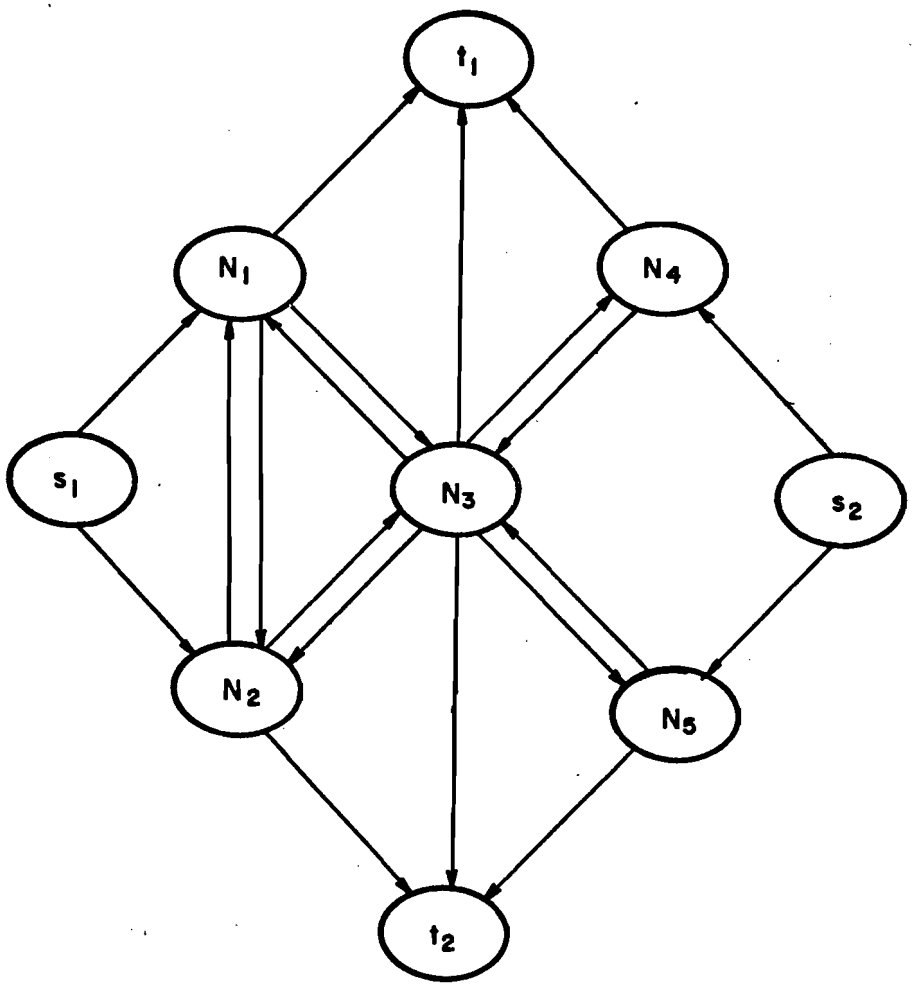

Figure 4.2 Sample ATC Network

	s_1	s_2	N_1	N_2	N_3	N_4	N_5	t_1	t_2
s_1	0		x	x	0	0	0	0	
s_2		(i)	0	0	0	x	x (ii)		(iii)
N_1			0	x	x	0	0	x	0
N_2			x	0	x	0	0	0	x
N_3	0		x	x	0	x	x	x	x
N_4			0	0	x	0	0	x	0
N_5		(iv)	0	0	x	0	0 (v)	0	x (vi)
t_1	0				0			0	
t_2		(vii)					(viii)		(ix)

x ≡ non-zero

Figure 4.3 One-Step Transition Matrix

Then the sink attraction rates are related to the source generation rates by

$$\mu_j = \sum_{i=1}^{m_s} \lambda_i \, e_{ij} \, . \tag{4.32}$$

To prove (4.32), sum both sides over all sinks, giving

$$\sum_{j=1}^{m_t} \mu_j = \sum_{j=1}^{m_t} \sum_{i=1}^{m_s} \lambda_i \, e_{ij} .$$

Exchanging summations on the right,

$$\sum_{j=1}^{m_t} \mu_j = \sum_{i=1}^{m_s} \lambda_i \sum_{j=1}^{m_t} e_{ij} .$$

Now $\sum_{j=1}^{m_t} e_{ij} = 1$ for all sources i, so that

$$\sum_{j=1}^{m_t} \mu_j = \sum_{i=1}^{m_s} \lambda_i \, .$$

But from (4.4), the sum of sink attraction rates and the sum of source generation rates are both equal to the total flow rate over the network, so that (4.32) must be true.

The importance of (4.32) is that if the e_{ij} are known, then knowledge of the sink attraction rates is equivalent to knowledge of the source generation rates. Thus the problem mentioned in section 4.3.2 of knowing some μ's and some λ's (together with the e_{ij}) will give an inconsistent solution to (4.32) except in very special circumstances. Luckily, one such circumstance which arises naturally for an ATC network is where all μ's and λ's refer to distinct streams of aircraft. A practical example of this is discussed in section 4.5.6.

4.4.4 Estimation of Transition Probabilities

The estimation of transition probabilities in Markov chains has been studied in detail by Anderson and Goodman (1957) and other authors. Their results are applicable to the analysis of sector sequences with only minor modifications.

Suppose there are available records of c independent sector sequences, each assumed to be a random observation from a qth order Markov chain with M states. Let n_{jk} be the number of times an aircraft enters state k from state j, n_{ijk} be the number of times an aircraft enters state

k from state j having entered j from state i, and so forth. Equivalently,

$$n_k = \sum_{n=1}^{c} \sum_{m=0}^{m_n} I_k\,(s_n(m)) \tag{4.33}$$

where $I_k(x)$ is an indicator function such that

$$I_k(x) = \begin{cases} 1, \text{ if } x = k\,; \\ 0, \text{ otherwise.} \end{cases}$$

Similarly,

$$n_{jk} = \sum_{n=1}^{c} \sum_{m=1}^{m_n} I_{jk}\,(s_n(m-1),\ s_k(m)) \tag{4.34}$$

where $I_{jk}(x, y)$ is a two-dimensional indicator function which is equal to one if x=j and y=k and zero otherwise. Generalizing in a similar manner,

$$n_{ijk} = \sum_{n=1}^{c} \sum_{m=2}^{m_n} I_{ijk}(s_n(m-2),\ s_n(m-1),\ s_n(m)). \tag{4.35}$$

Assuming stationary transition probabilities, Anderson and Goodman show that if the Markov chain is first order, then the n_{jk} form a set of sufficient statistics for the state transition probabilities. For a second order Markov chain, the n_{ijk} are sufficient. The results can be generalized to higher-order chains.

The maximum likelihood estimates of the transition probabilities depend on the order of the Markov chain. For a second-order chain, $s_n(0)$ and $s_n(1)$ are assumed to be nonrandom, while $s_n(k)$, $k \geq 2$, are assumed to be random variables. Then the maximum likelihood estimates of (4.24), (4.23) and (4.22)are given by

$$\hat{p}_{ijk} = \frac{n_{ijk}}{\sum_{\ell=1}^{M} n_{ij\ell}} \tag{4.36}$$

$$\hat{p}_{jk} = \frac{\sum_{i=1}^{M} n_{ijk}}{\sum_{i=1}^{M} \sum_{\ell=1}^{M} n_{ij\ell}} \tag{4.37}$$

$$\hat{p}_{k} = \frac{\sum_{i=1}^{M} \sum_{j=1}^{M} n_{ijk}}{\sum_{i=1}^{M} \sum_{j=1}^{M} \sum_{\ell=1}^{M} n_{ij\ell}}\ . \tag{4.38}$$

Notice that since $s_n(0)$ and $s_n(1)$ are assumed to be nonrandom, the estimates of the transition probabilities involve summations over n_{ijk} rather than using n_{jk} and n_k directly (the results are <u>not</u> equivalent).

It should be remarked that a second order Markov chain of M states can be reformulated as a first-order Markov chain of M^2 states by defining a state in the new chain to be a transition between two particular states in the original chain. This is equivalent in network terms to considering the arcs of the network to be states rather than the nodes. The increase in number of states is in practice much less than a factor of M since many possible arcs do not exist. Further, the one-step transition matrix of the new chain has many zeros. This change of formulation is illustrated in detail in section 4.5.4.

4.4.5 Determining the Appropriate Order of Markov Chain

Using (4.37) and (4.38), a likelihood ratio test was derived by Anderson and Goodman (1957) for testing the null hypothesis that a first-order Markov chain is sufficient to characterize a set of observations against the alternative of a second-order chain. The test criterion is

$$\lambda = \prod_{i,j,k=1}^{M} \left(\frac{\hat{p}_{jk}}{\hat{p}_{ijk}} \right)^{n_{ijk}} . \tag{4.39}$$

Then if the null hypothesis is true, the quantity $-2 \log\lambda$ has an asymptotic χ^2-distribution with $M(M-1)^2$ degrees of freedom. Similar tests were given for testing the null hypothesis that a chain is of $(r-1)^{th}$ order against the alternative that it is of rth order. If some of the p_{jk} are known a priori to be zero, then the degrees of freedom should be adjusted downward appropriately.

This technique can be applied effectively to ATC sector sequences only if the number of sectors is small and the number of observed sector sequences quite large. For other situations, a graphical technique based on information theory given by Chatfield (1973) (which can be related to the likelihood ratio test) is all that the data will support. The technique involves plotting the "conditional uncertainty" remaining in the data as successively higher order Markov chains are entertained.

The concept of conditional uncertainty is defined via Shannon's measure of information. Given an event with M mutually exclusive and exhaustive outcomes, each with probability p_k (k=1, 2, ..., M), then the average amount of information provided by one observation is given by

$$H = E(-\log p) = - \sum_{k=1}^{M} p_k \log p_k . \tag{4.40}$$

Similarly, the average information about pairs of successive events provided by a single experiment is given by

$$H(\text{pairs}) = - \sum_{j=1}^{M} \sum_{k=1}^{M} p_{jk} \log p_{jk}. \tag{4.41}$$

The difference between H(pairs) and H is

$$H_2 = H(\text{pairs}) - H , \tag{4.42}$$

termed the average conditional uncertainty about an event given the preceding event. The concepts are easily extended to determining H_3, the average conditional uncertainty about an event given the two previous events and so forth.

The information theory technique for determining the order of a Markov chain involves plotting consecutively the average conditional uncertainties about an event given no knowledge of the previous event, given knowledge only of the previous event, knowing the two previous events, and so on. The resulting sequence $\{\log M, H, H_2, H_3, \ldots\}$ will be monotonically decreasing, and its structure will help to indicate the order of Markov chain appropriate.

In order that the estimated conditional uncertainties will add together in the appropriate manner, it is necessary to first determine how many values will be required, and then to determine all estimates from sequences of the same length. For example, if the chain is thought to be of second order, the first conditional uncertainty expected to be insignificant is that involving two previous events, H_3. Wishing to plot values up to H_4, it is therefore necessary to compute n_{hijk} and estimate the conditional uncertainties using summations involving n_{hijk}. The analogy with the maximum likelihood estimates in section 4.4.4 is direct, treating the first three events in the sequence as nonrandom. This technique is illustrated in more detail in section 4.5.5.

4.4.6 Summary

The use of Markov chain models to characterize sequences of sectors over which aircraft pass provides a convenient formulation for traffic through ATC networks. It eliminates the need to specify the relative frequency of all possible sequences while maintaining the basic integrity of streams through the network. The estimation of transition probabilities, together with estimates of traffic generation rates of the sources to the network, completely describe the passage of traffic through the network on a sector-to-sector basis. Sector transit times and resultant network transit times will be considered in a future report.

A further note is appropriate about the likely order of Markov chain needed to describe sector sequences. It is obvious that since aircraft are unlikely to return to sectors from which they have just departed, first order Markov chain models will not be appropriate. The second-order model, however, would be sufficient to preserve straight line streams through individual sectors and might well prove adequate to describe the important aspects of the network flow patterns. Higher order models would probably gain little in terms of reality while sacrificing much in terms of simplicity and reliable estimation. Only very extensive data samples could clearly support models of higher than second order.

It thus remains to apply these techniques to an actual ATC network. The following section makes use of a data sample from the New York ARTCC which has been analyzed extensively in Hunter et al. (1973) and Hunter et al. (1974). The applicability of the methods to this point will be readily apparent.

4.5 Analysis of the New York Enroute Network

4.5.1 Network Structure

The New York enroute sectors consist of 32 control positions: 9 high altitude enroute (HI) sectors, 11 low altitude enroute (LE) sectors, and 12 low altitude transitional (LT) sectors (see table 4.1). These sectors cover a geographical area consisting of the entire states of New Jersey and Delaware and parts of New York, Pennsylvania, Connecticut, and Maryland (see figure 4.4). The relative position of the various sectors can be seen in figures 4.5 and 4.6. The HI sectors control traffic at and above 24,000 ft while the LE and LT sectors handle traffic at altitudes of less than 24,000 ft.

In describing the network of enroute sectors, there are m=32 nodes plus a super-source and super-sink. The node-node incidence matrix D, displayed in figure 4.7, indicates 152 arcs between sectors in the network. With an additional 32 arcs in (s,N) and 32 arcs in (N,t), there are 212 arcs in total (of a possible 1088).

There are 12 airports in the region covered by the New York enroute sectors which contributed at least five aircraft to the network flow observed during a 2 -hour sample period. These airports are listed in table 4.2 with the number of arrivals and departures observed through the network. These airports are commonly referred to by their standard three-letter codes.

Figure 4.8 illustrates the general flow of aircraft through the network. From the data base, it was possible to distinguish four classes of traffic:

Table 4.1

Identification of N.Y. Enroute Sectors

Sector #	Sector Type	Sector Ident. Code	
451	LT	R 5	ESR
453	LT	R 7	OOD
454	LT	R11	SBJ
455	LT	R12	ARD
456	LT	R15	COL
457	LT	R16	COL
458	LT	R17	7ID
459	LT	R23	BDR
460	LT	R24	RVH
461	LT	R25	SAX
462	LT	R27	HPN
463	LT	R28	HPN
464	LE	R 2	ABE
465	LE	R 3	SEG
466	LE	R 4	HAR
467	LE	R 8	CYN
468	LE	R 9	SBY
469	LE	R18	7HP
470	LE	R20	IPT
471	LE	R21	BGM
472	LE	R26	STW
473	LE	R29	HUO
474	LE	R30	IGN
475	HI	R 1	PSB
476	HI	10A	CYN
477	HI	10B	SIE
478	HI	R13	ARD
479	HI	R14	HAR
480	HI	R19	HUO
481	HI	R22	CMK
482	HI	R35	7HP
483	HI	R36	JFK

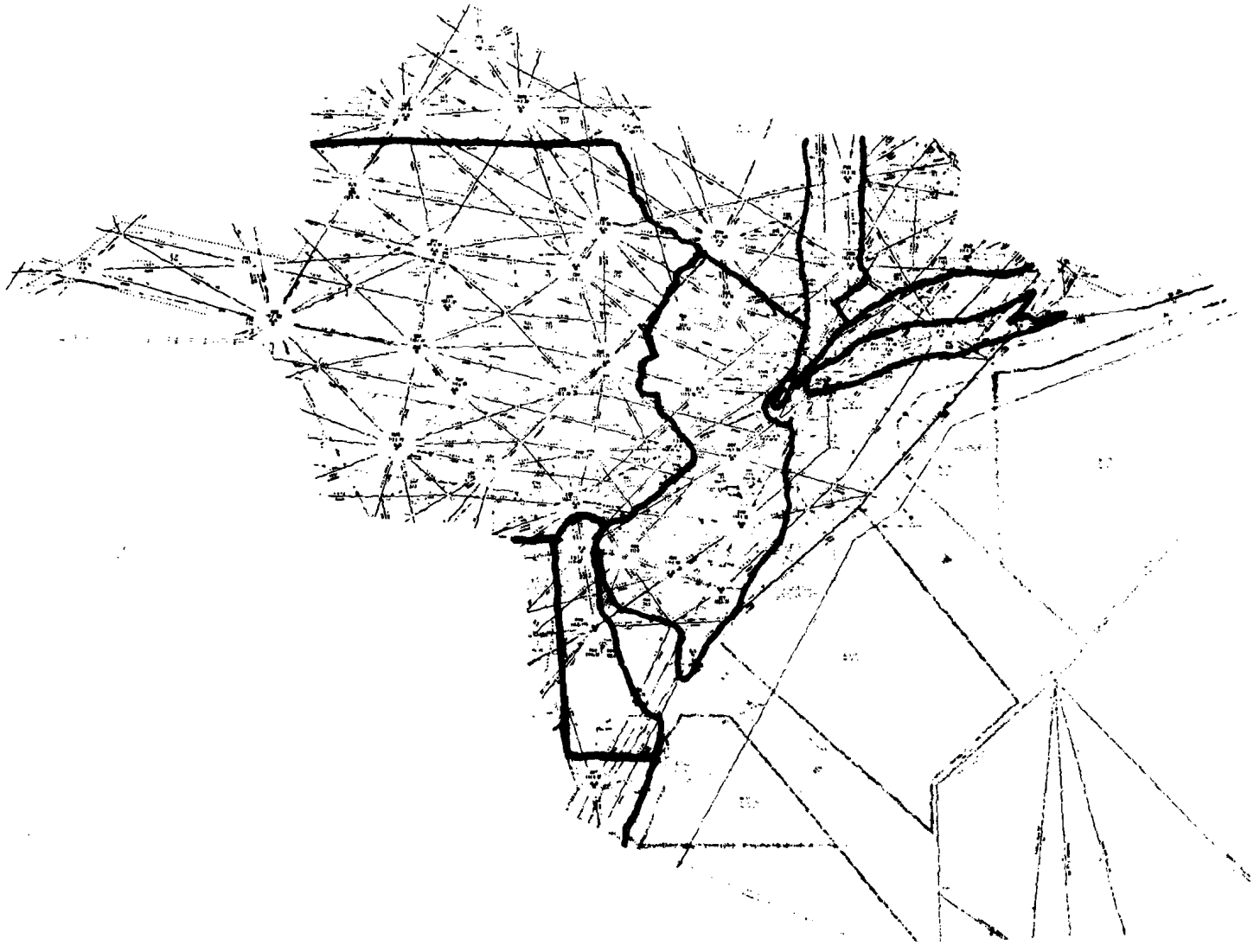

Figure 4.4 The New York ARTCC (1969)

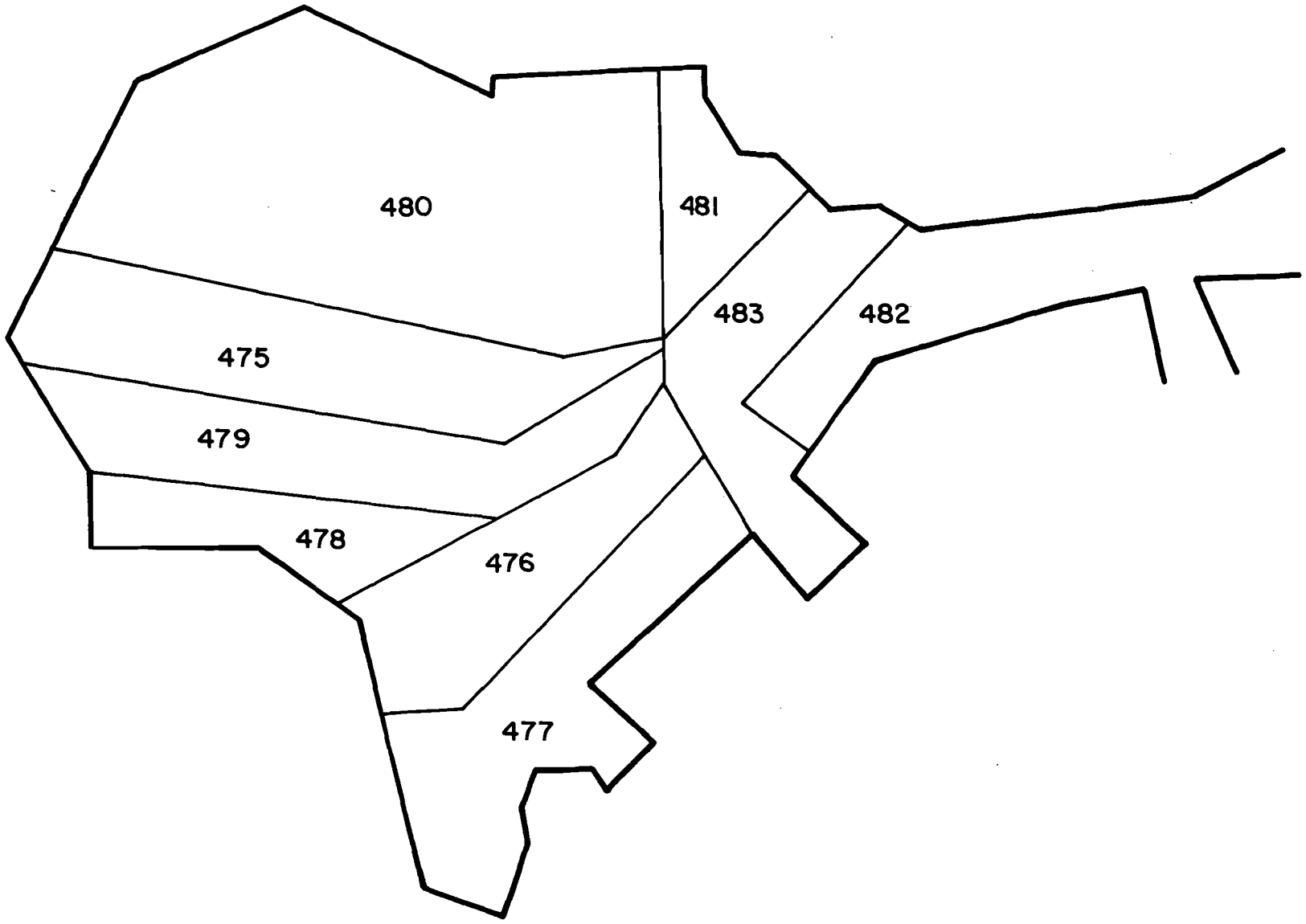

Figure 4.5 New York ARTCC Sector Control Boundaries—High Altitude (4/19/68)

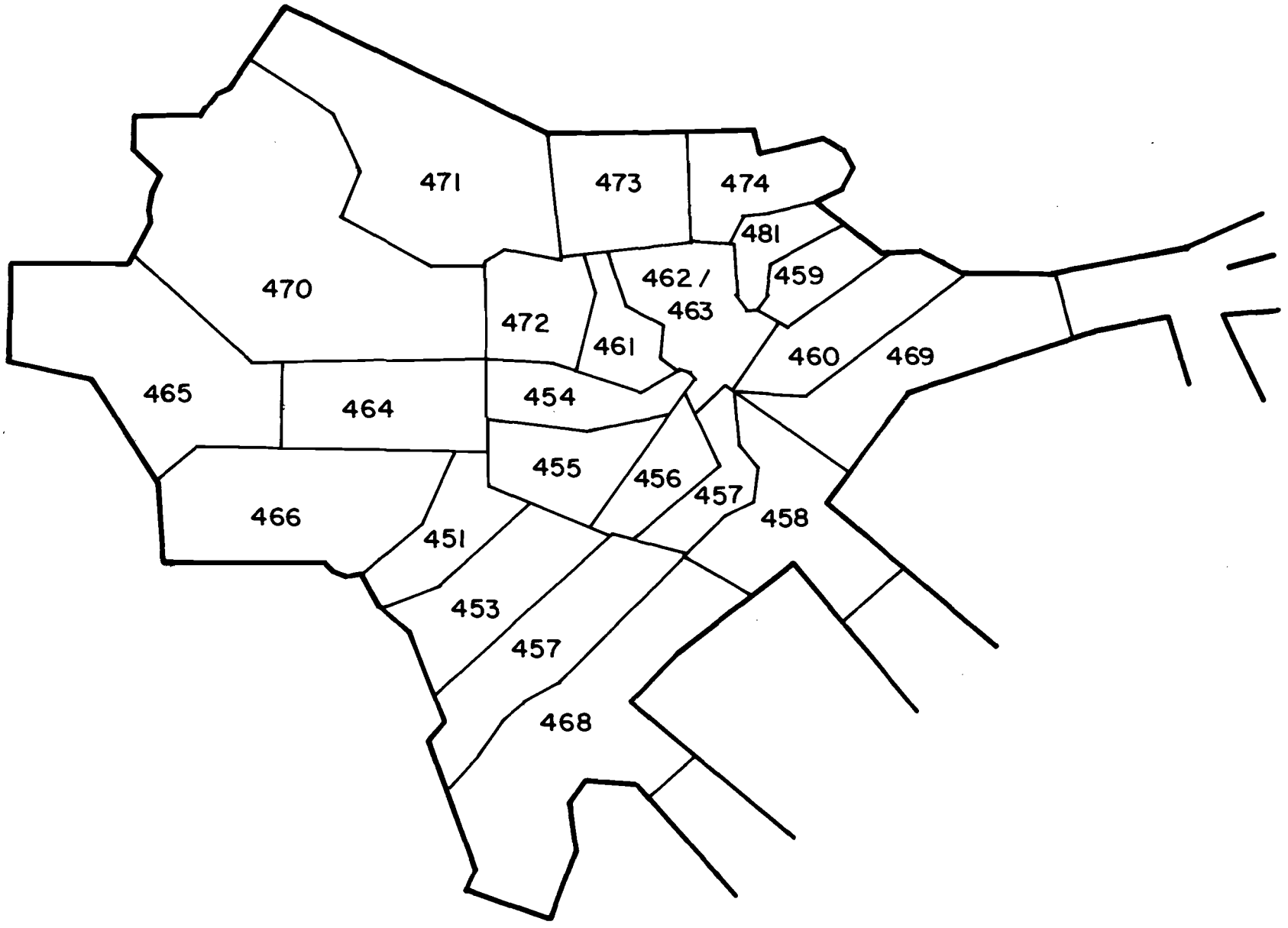

Figure 4.6 New York ARTCC Sector Control Boundaries — Low Altitude and Low Transitional (4/19/68)

SECTOR	451	53	54	55	56	57	58	59	60	61	62	63	64	65	66	67	68	69	70	71	72	73	74	75	76	77	78	79	80	81	82	83
451	0	1	0	1	0	0	0	0	0	0	0	0	1	0	1	0	0	0	0	0	0	0	0	0	0	0	0	1	0	0	0	0
453	1	0	0	1	1	1	0	0	0	0	0	0	0	0	1	1	0	0	0	0	0	0	0	0	0	0	0	1	0	0	0	0
454	1	0	0	1	1	0	0	0	0	0	0	0	0	0	0	0	0	0	0	0	1	0	0	0	0	0	0	0	0	0	0	0
455	1	0	0	0	0	0	0	0	0	0	0	0	1	0	0	0	0	1	0	0	0	0	0	0	0	0	0	0	0	0	0	0
456	1	0	0	0	0	0	0	0	0	0	0	0	0	0	0	0	0	0	0	0	0	0	0	0	1	0	0	0	0	0	0	0
457	0	0	0	0	1	0	0	0	0	0	0	0	0	0	0	0	0	0	0	0	0	0	0	0	0	0	0	0	0	0	0	0
458	0	0	0	1	1	0	0	0	0	0	0	0	0	0	0	1	1	1	0	0	0	0	0	0	0	1	0	0	0	0	1	1
459	0	0	0	0	0	0	0	0	1	1	0	0	0	0	0	0	0	0	0	0	0	1	1	0	0	0	0	0	1	0	0	0
460	0	0	0	0	0	0	1	1	0	0	0	0	0	0	0	0	0	1	0	0	0	0	0	0	0	0	0	0	0	0	0	0
461	0	0	1	1	1	0	0	0	0	0	1	1	0	0	0	0	0	0	0	1	1	1	0	0	0	0	1	0	0	0	0	0
462	0	0	0	0	0	0	0	0	0	1	0	1	0	0	0	0	0	0	0	0	0	1	0	0	0	0	0	0	0	0	0	0
453	0	0	0	0	0	0	0	0	0	1	0	0	0	0	0	0	0	0	0	1	0	1	0	0	0	0	0	0	1	0	0	0
464	1	0	1	1	0	1	0	0	0	1	0	0	0	1	1	0	0	0	1	0	1	0	0	1	0	0	0	0	1	0	0	0
465	0	0	0	0	0	0	0	0	0	0	0	0	1	0	1	0	0	0	1	0	0	0	0	0	0	0	0	0	0	0	0	0
455	1	0	0	0	0	0	0	0	0	0	0	0	1	1	0	0	0	0	0	0	0	0	0	0	0	0	0	0	0	0	0	0
467	0	1	0	0	0	1	1	0	0	0	0	0	0	0	0	1	1	0	0	0	0	0	0	0	0	1	0	0	0	0	0	0
468	0	1	0	0	0	0	1	0	0	0	0	0	0	0	0	1	0	0	0	0	0	0	0	0	0	1	0	0	0	0	0	0
469	0	0	0	0	0	0	1	0	1	0	0	0	0	0	0	0	0	0	0	0	0	0	0	0	0	0	0	0	0	0	0	1
470	0	0	0	0	0	0	0	0	0	0	0	0	1	1	0	0	0	0	0	1	1	0	0	0	0	0	0	0	0	0	0	0
471	0	0	0	0	0	0	0	0	0	0	0	0	0	0	0	0	0	0	1	0	1	1	0	0	0	0	0	0	1	0	0	0
472	0	0	0	0	0	0	0	0	0	0	1	1	1	0	0	0	0	0	1	1	0	1	0	1	0	0	0	0	1	0	0	0
473	0	0	0	0	0	0	0	0	0	0	1	1	0	0	0	0	0	0	0	1	1	1	1	0	0	0	0	0	0	1	0	0
474	0	0	0	0	0	0	0	0	0	0	0	1	0	0	0	0	0	0	0	0	0	1	0	0	0	0	0	0	1	1	0	0
475	0	0	0	0	0	0	0	0	0	0	0	0	1	0	1	0	0	0	0	0	1	0	0	1	0	0	1	1	1	0	0	0
476	0	1	0	1	1	0	0	0	0	0	0	0	0	0	0	0	0	0	0	0	0	0	0	0	0	1	0	0	0	0	1	0
477	0	0	0	0	0	0	0	0	0	0	0	0	0	0	0	1	1	0	0	0	0	0	0	0	1	0	0	1	0	0	0	1
478	0	0	0	0	1	0	0	0	0	0	0	0	0	0	0	0	0	0	0	0	0	0	0	1	0	0	0	0	0	0	0	0
479	0	0	0	0	0	0	0	0	0	0	0	0	0	0	1	0	0	0	0	0	0	0	0	1	0	0	1	1	0	0	0	0
480	0	0	0	0	0	0	0	1	0	0	0	0	0	0	0	0	0	0	0	1	1	1	0	1	0	0	0	0	0	1	0	0
481	0	0	0	0	0	0	0	0	1	0	1	1	0	0	0	0	0	0	0	0	0	0	1	0	0	0	0	0	1	0	0	1
482	0	0	0	0	0	0	1	0	0	0	0	0	0	0	0	0	1	0	0	0	0	0	0	0	0	0	0	0	0	0	0	1
483	0	0	0	0	0	0	0	0	1	0	0	0	0	0	0	0	0	1	0	0	0	0	0	0	0	1	0	0	0	0	0	0

Figure 4.7 Node-node Incidence Matrix in New York Enroute Network

(i) aircraft departing from airports within the region covered by the New York enroute sectors and bound for destinations beyond the network boundaries;

(ii) aircraft arriving from outside the region and bound for airports within the region;

(iii) aircraft both departing from and arriving at airports within the region;

(iv) traffic passing through the enroute sectors which were neither arrivals nor departures from airports in the region.

Table 4.2

Traffic from Airports within the New York Region

	Airport	Code	Departures through enroute network	Arrivals through enroute network
1.	Newark	EWR	53	40
2.	John F. Kennedy	JFK	52	64
3.	LaGuardia	LGA	58	56
4.	Philadelphia	PHL	36	40
5.	Atlantic City	ACY	9	5
6.	Wilmington	ILG	5	9
7.	Wilkes-Barre	AVP	3	2
8.	Binghamton	BGM	3	5
9.	Harrisburg	HAR	12	0
10.	Allentown	ABE	8	3
11.	Elmira	ELM	7	3
12.	Westchester	HPN	7	11
			253	238

Table 4.3

Traffic Breakdown by Class

		No. observed in sample period
(i)	Source in N.Y. region	237
(ii)	Terminus in N.Y. region	222
(iii)	Source and terminus in N.Y. region	16
(iv)	Through traffic	90

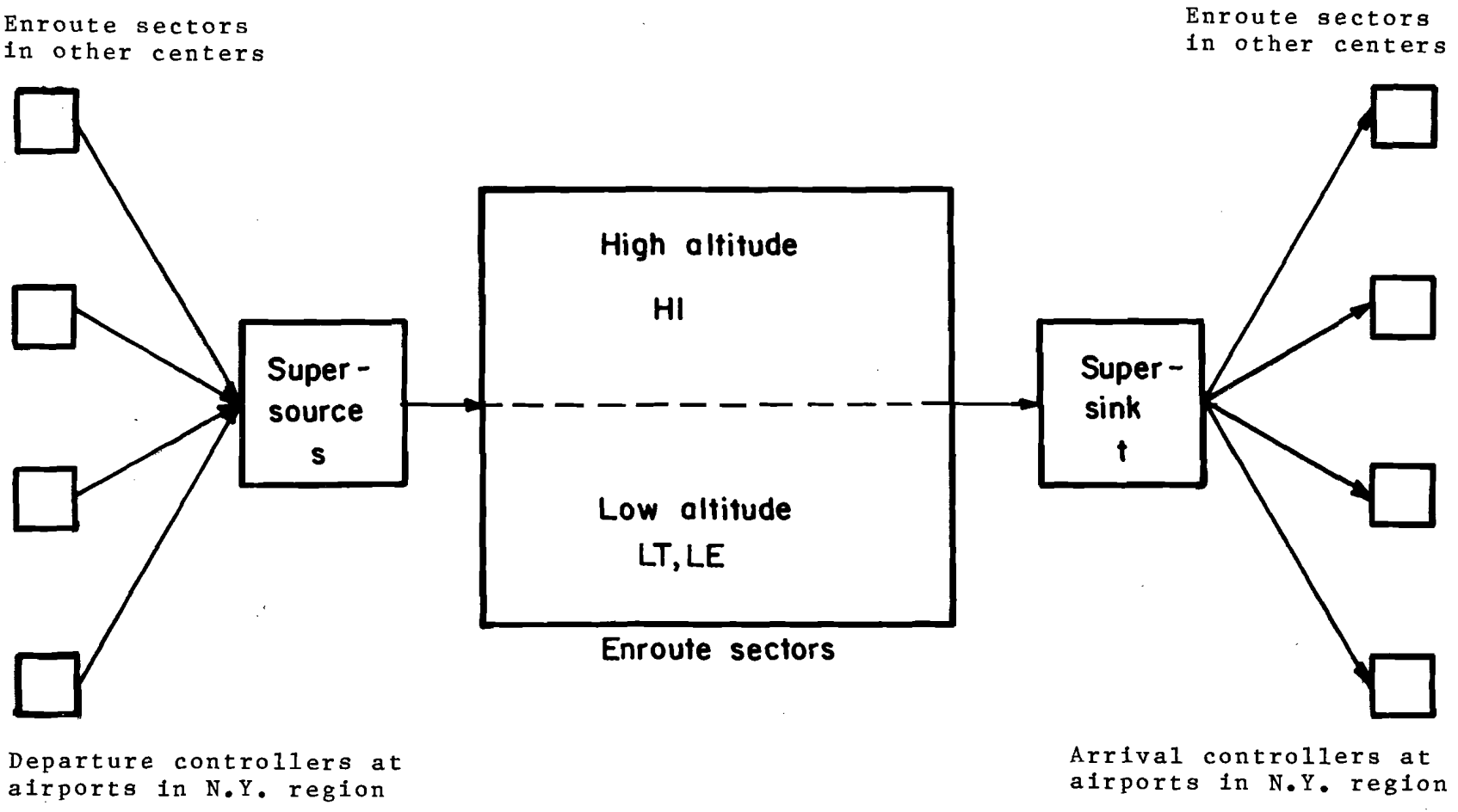

Figure 4.8 Schematic Diagram of Enroute Network Traffic Flow

A breakdown of the traffic observed during the sample period is given in table 4.3. Of the four classes, (i) and (ii) make up the bulk of the traffic observed. Class (iii) appears to be of little significance in determining total flow.

Appendix 4-A describes the tabulation of traffic in the enroute network during the sample period. Each aircraft is classified as a departure from an airport in the region, an arrival to an airport, through - traffic, or unidentifiable because its sector sequence was incomplete at the end of the sample period. Those 16 aircraft which both arrived at and departed from airports in the region are classified as departures but indicated by asterisks.

The count of all transitions between the sources, sinks, and nodes of the network is presented in table 4.4. The form of the table is that of a one-step transition matrix as discussed in section 4.4.3, only transition probabilities have been replaced by the counts n_{ij}. For a first-order Markov chain, the table gives all the information needed to estimate transition probabilities.

4.5.2 Modeling Network Arrivals

To apply the techniques of section 4.3 to the N.Y. enroute network, it is necessary to show that the streams from each of the sources to the network are well-represented by independent Poisson processes and that the conditional probabilities of an arrival entering over any of the 32 arcs in (s,N) given its source remains constant over time.

For purposes of analysis, it is convenient to consider 25 sources of traffic. Twelve of these sources represent departures from airports in the region. Another 12 represent the attraction of aircraft to each of the airports in the region. The final source represents all through-traffic.

It is reasonable to assume that if any of the traffic streams from the various sources deviate greatly from the structure of a Poisson process, it is likely to be those of the major airports (EWR, JFK, LGA, PHL) where scheduling of the heavy traffic may reduce the variance of the interarrival or interdeparture times. It is important to recognize that the structure of the streams is relevant upon entry to the enroute network, <u>not</u> upon takeoff and landing. For the departure streams, this requires looking at the streams as they leave the radar departure controllers. The arrival streams are harder to identify upon entry to the network since they originate through many arcs in (s,N), but it is reasonable to assume that if they appear to be Poisson upon leaving the network and entering

Table 4.4 Counts of Departures, Arrivals and Transitions in New York Network

	469	470	471	472	473	474	475	476	477	478	479	480	481	482	483	TOTAL
EWR	0	0	0	25	0	0	0	0	0	0	0	0	0	0	0	53
JFK	4	0	0	0	0	0	0	0	0	0	0	0	0	0	0	52
LGA	0	0	0	0	0	0	0	0	0	0	0	0	0	0	0	58
PHL	0	0	0	0	0	0	0	0	0	0	0	0	0	0	0	36
ACY	0	0	0	0	0	0	0	0	0	0	0	0	0	0	0	6
TLG	0	0	0	0	0	0	0	0	0	0	0	0	0	0	0	5
AVP	0	3	0	0	0	0	0	0	0	0	0	0	0	0	0	3
BGM	0	0	3	0	0	0	0	0	0	0	0	0	0	0	0	3
HAR	0	0	0	0	0	0	0	0	0	0	0	0	0	0	0	12
ABT	0	0	0	0	0	0	0	0	0	0	0	0	0	0	0	8
ELM	0	5	2	0	0	0	0	0	0	0	0	0	0	0	0	7
HPN	0	0	0	0	0	0	0	0	0	0	0	0	0	0	0	7
000	6	11	17	2	5	21	31	24	13	22	25	16	29	8	13	373
451	0	0	0	0	0	0	0	0	0	0	10	0	0	0	0	55
453	0	0	0	0	0	0	0	0	0	0	1	0	0	0	0	55
454	0	0	0	1	0	0	0	0	0	0	0	0	0	0	0	55
455	1	0	0	0	0	0	0	0	0	0	0	0	0	0	0	42
456	0	0	0	0	0	0	0	7	0	0	0	0	0	0	0	42
457	0	0	0	0	0	0	0	0	0	0	0	0	0	0	0	26
458	4	0	0	0	0	0	0	0	20	0	0	0	0	7	1	50
459	0	0	0	0	3	4	0	0	0	0	0	1	0	0	0	32
460	1	0	0	0	0	0	0	0	0	0	0	0	0	0	0	47
461	0	0	2	11	2	0	0	0	0	1	0	0	0	0	0	53
462	0	0	0	0	6	0	0	0	0	0	0	0	0	0	0	40
463	0	0	5	0	18	0	0	0	0	0	0	24	0	0	0	52
464	0	4	0	13	0	0	1	0	0	0	0	2	0	0	0	72
465	0	7	0	0	0	0	0	0	0	0	0	0	0	0	0	31
466	0	0	0	0	0	0	0	0	0	0	0	0	0	0	0	56
467	0	0	0	0	0	0	0	0	2	0	0	0	0	0	0	56
468	0	0	0	0	0	0	0	0	3	0	0	0	0	0	0	40
469	0	0	0	0	0	0	0	0	0	0	0	0	0	0	3	28
470	0	0	10	2	0	0	0	0	0	0	0	0	0	0	0	42
471	0	10	0	3	7	0	0	0	0	0	0	1	0	0	0	38
472	0	5	1	0	10	0	5	0	0	0	0	20	0	0	0	65
473	0	0	5	4	1	18	0	0	0	0	0	0	15	0	0	65
474	0	0	0	0	8	0	0	0	0	0	0	2	6	0	0	43
475	0	0	0	4	0	0	1	0	0	11	1	4	0	0	0	65
476	0	0	0	0	0	0	0	0	8	0	0	0	0	1	0	36
477	0	0	0	0	0	0	0	7	0	0	12	0	0	0	8	52
478	0	0	0	0	0	0	2	0	0	0	0	0	0	0	0	36
479	0	0	0	0	0	0	3	0	0	1	1	0	0	0	0	48
480	0	0	1	1	3	0	21	0	0	0	0	0	7	0	0	75
481	0	0	0	0	0	2	0	0	0	0	0	2	0	0	2	56
482	0	0	0	0	0	0	0	0	0	0	0	0	0	0	7	18
483	10	0	0	0	0	0	0	0	6	0	0	0	0	0	0	29
TOTAL	26	45	46	66	63	45	64	38	52	35	50	72	57	16	34	2126

Table 4.4 Counts of Departures, Arrivals and Transitions in New York Network (cont.)

	EWR	JFK	LGA	PHL	ACY	ILG	AVP	BGM	HAR	ABE	ELM	HPN	000	451	453
EWR	0	0	0	0	0	0	0	0	0	0	0	0	0	0	0
JFK	0	0	0	0	0	0	0	0	0	0	0	0	0	0	0
LGA	0	0	0	0	0	0	0	0	0	0	0	0	0	0	0
PHL	0	0	0	0	0	0	0	0	0	0	0	0	0	22	1
ACY	0	0	0	0	0	0	0	0	0	0	0	0	0	0	0
ILG	0	0	0	0	0	0	0	0	0	0	0	0	0	0	2
AVP	0	0	0	0	0	0	0	0	0	0	0	0	0	0	0
BGM	0	0	0	0	0	0	0	0	0	0	0	0	0	0	0
HAR	0	0	0	0	0	0	0	0	0	0	0	0	0	0	0
ABE	0	0	0	0	0	0	0	0	0	0	0	0	0	0	0
ELM	0	0	0	0	0	0	0	0	0	0	0	0	0	0	0
HPN	0	0	0	0	0	0	0	0	0	0	0	0	0	0	0
000	0	0	0	0	0	0	0	0	0	0	0	0	0	6	28
451	0	0	0	0	0	1	1	0	0	0	0	0	24	0	3
453	0	0	0	5	1	1	0	0	0	0	0	0	6	2	0
454	1	0	18	7	0	0	0	0	0	0	0	0	3	20	0
455	30	0	3	0	0	0	0	0	0	0	0	0	4	3	0
456	0	30	0	0	0	0	0	0	0	0	0	0	3	2	0
457	0	6	16	0	0	0	0	0	0	0	0	0	3	0	0
458	0	0	0	0	0	0	0	0	0	0	0	0	5	0	0
459	0	0	0	0	0	0	0	0	0	0	0	0	13	0	0
460	0	28	0	0	0	0	0	0	0	0	0	0	15	0	0
461	4	0	0	0	0	0	0	0	0	0	0	0	1	0	0
462	0	0	0	0	0	0	0	0	0	0	0	0	0	0	0
463	0	0	0	0	0	0	0	0	0	0	0	0	1	0	0
464	0	0	0	0	0	0	0	0	0	2	0	0	4	1	0
465	0	0	0	0	0	0	0	0	0	0	0	0	17	0	0
466	0	0	0	20	0	1	0	0	0	0	0	0	18	3	0
467	0	0	0	8	3	5	0	0	0	0	0	0	18	0	9
468	0	0	0	0	1	1	0	0	0	0	0	0	24	0	1
469	0	0	0	0	0	0	0	0	0	0	0	0	15	0	0
470	0	0	0	0	0	0	1	0	0	0	2	0	18	0	0
471	0	0	0	0	0	0	0	5	0	0	1	0	11	0	0
472	5	0	0	0	0	0	0	0	0	1	0	0	3	0	0
473	0	0	1	0	0	0	0	0	0	0	0	6	13	0	0
474	0	0	0	0	0	0	0	0	0	0	0	3	23	0	0
475	0	0	0	0	0	0	0	0	0	0	0	0	11	0	0
476	0	0	0	0	0	0	0	0	0	0	0	0	3	0	12
477	0	0	0	0	0	0	0	0	0	0	0	0	16	0	0
478	0	0	0	0	0	0	0	0	0	0	0	0	14	0	0
479	0	0	0	0	0	0	0	0	0	0	0	0	27	0	0
480	0	0	0	0	0	0	0	0	0	0	0	0	41	0	0
481	0	0	18	0	0	0	0	0	0	0	0	2	5	0	0
482	0	0	0	0	0	0	0	0	0	0	0	0	7	0	0
483	0	0	0	0	0	0	0	0	0	0	0	0	7	0	0
TOTAL	40	64	56	40	5	9	2	5	0	3	3	11	373	59	56

Table 4.4 Counts of Departures, Arrivals and Transitions in New York Network (cont.)

	454	455	456	457	458	459	460	461	462	463	464	465	466	467	468
EWR	18	0	0	0	0	0	0	10	0	0	0	0	0	0	0
JFK	0	0	0	0	31	3	0	0	3	11	0	0	0	0	0
LGA	0	0	0	0	0	16	0	20	22	0	0	0	0	0	0
PHL	0	0	0	1	0	0	0	0	0	0	1	0	0	11	0
ACY	0	0	0	1	0	0	0	0	0	0	0	0	0	0	8
ILG	0	0	0	0	0	0	0	0	0	0	0	0	0	3	0
AVP	0	0	0	0	0	0	0	0	0	0	0	0	0	0	0
BGM	0	0	0	0	0	0	0	0	0	0	0	0	0	0	0
HAR	0	0	0	0	0	0	0	0	0	0	2	1	9	0	0
ABE	0	0	0	0	0	0	0	0	0	0	8	0	0	0	0
ELM	0	0	0	0	0	0	0	0	0	0	0	0	0	0	0
HPN	0	0	0	0	0	4	0	0	3	0	0	0	0	0	0
000	2	3	0	1	1	5	18	2	0	1	0	10	16	19	18
451	0	1	0	0	0	0	0	0	0	0	8	0	7	0	0
453	0	16	2	17	0	0	0	0	0	0	0	0	1	3	0
454	0	1	4	0	0	0	0	0	0	0	0	0	0	0	0
455	0	0	0	0	0	0	0	0	0	0	1	0	0	0	0
456	0	0	0	0	0	0	0	0	0	0	0	0	0	0	0
457	0	0	1	0	0	0	0	0	0	0	0	0	0	0	0
458	0	1	2	0	0	0	0	0	0	0	0	0	0	6	4
459	0	0	0	0	0	0	10	1	0	0	0	0	0	0	0
460	0	0	0	0	1	2	0	0	0	0	0	0	0	0	0
461	18	3	5	0	0	0	0	0	2	4	0	0	0	0	0
462	0	0	0	0	0	0	0	13	0	21	0	0	0	0	0
463	0	0	0	0	0	0	0	4	0	0	0	0	0	0	0
464	20	15	0	2	0	0	0	1	0	0	0	3	4	0	0
465	0	0	0	0	0	0	0	0	0	0	6	0	1	0	0
466	0	0	0	0	0	0	0	0	0	0	7	7	0	0	0
467	0	0	0	2	4	0	0	0	0	0	0	0	0	1	4
468	0	0	0	0	2	0	0	0	0	0	0	0	0	8	0
469	0	0	0	0	7	0	3	0	0	0	0	0	0	0	0
470	0	0	0	0	0	0	0	0	0	0	3	6	0	0	0
471	0	0	0	0	0	0	0	0	0	0	0	0	0	0	0
472	0	0	0	0	0	0	0	0	1	9	5	0	0	0	0
473	0	0	0	0	0	0	0	0	2	0	0	0	0	0	0
474	0	0	0	0	0	0	0	0	0	1	0	0	0	0	0
475	0	0	0	0	0	0	0	0	0	0	31	0	2	0	0
476	0	1	11	0	0	0	0	0	0	0	0	0	0	0	0
477	0	0	0	0	0	0	0	0	0	0	0	0	0	5	4
478	0	0	20	0	0	0	0	0	0	0	0	0	0	0	0
479	0	0	0	0	0	0	0	0	0	0	0	0	16	0	0
480	0	0	0	0	0	1	0	0	0	0	0	0	0	0	0
481	0	0	0	0	0	0	12	0	9	4	0	0	0	0	0
482	0	0	0	0	3	0	0	0	0	0	0	0	0	0	1
483	0	0	0	0	0	0	6	0	0	0	0	0	0	0	0
TOTAL	58	41	45	24	49	31	49	51	42	51	72	27	56	56	39

the radar arrival controllers, they are likely to be Poisson at their original entry to the network.

Figures 4.9 - 4.16 are histograms of the empirical interarrival time distributions for the departure and arrival streams at the four major airports. If the underlying streams are Poisson, then the interarrival and interdeparture time distributions should be exponential. Table 4.5 lists various statistics calculated from the empirical distributions. In judging whether the distributions are exponential, one should remember that the mean and standard deviation of the exponential distribution are equal.

Since we observed the traffic streams over a time period T of 2 hours at intervals of 1 second each, it is best in estimating the flow rate parameters to use (4.16), the number of events observed divided by the length of the sample period. This estimator is known to be the minimum variance unbiased estimator for a Poisson distribution, satisfying the Cramer-Rao lower bound. Table 4.5 includes these estimates for λ with the appropriate upper and lower 95 per cent confidence limits given by

$$2\lambda_{\ell} = \frac{1}{2}\chi^2_{2n,\alpha/2} \tag{4.43}$$

$$2\lambda_{u} = \frac{1}{2}\chi^2_{2(n+1),\ 1-\alpha/2} \tag{4.44}$$

where n is the number of events observed in the 2 -hour sample (Johnson and Kotz, 1969). For x>100, the normal approximation to the χ^2 - distribution was used.

In testing whether the arrival and departure traffic streams might be reasonably represented by Poisson processes, goodness-of-fit tests were performed on the empirical interarrival and interdeparture time distributions against hypothesized exponentials. The first test performed was a chi-square goodness-of-fit test, based on the classes represented in the empirical histograms (with an open class to the right beyond the fourth or fifth interval of 60 seconds). The test statistic calculated was

$$\chi^2 = \sum_{i=1}^{k} \frac{(N_i - E_i)^2}{E_i} \tag{4.45}$$

where N_i was the observed number of interarrival times falling in each of the k classes and E_i was the expected number given that the true distribution was exponential with parameter λ. If the null hypothesis is correct, then χ^2 will have a chi-square distribution with k-2 degrees of freedom if λ is estimated from the grouped data (the estimates obtained from the

EWR DEPARTURE STREAM

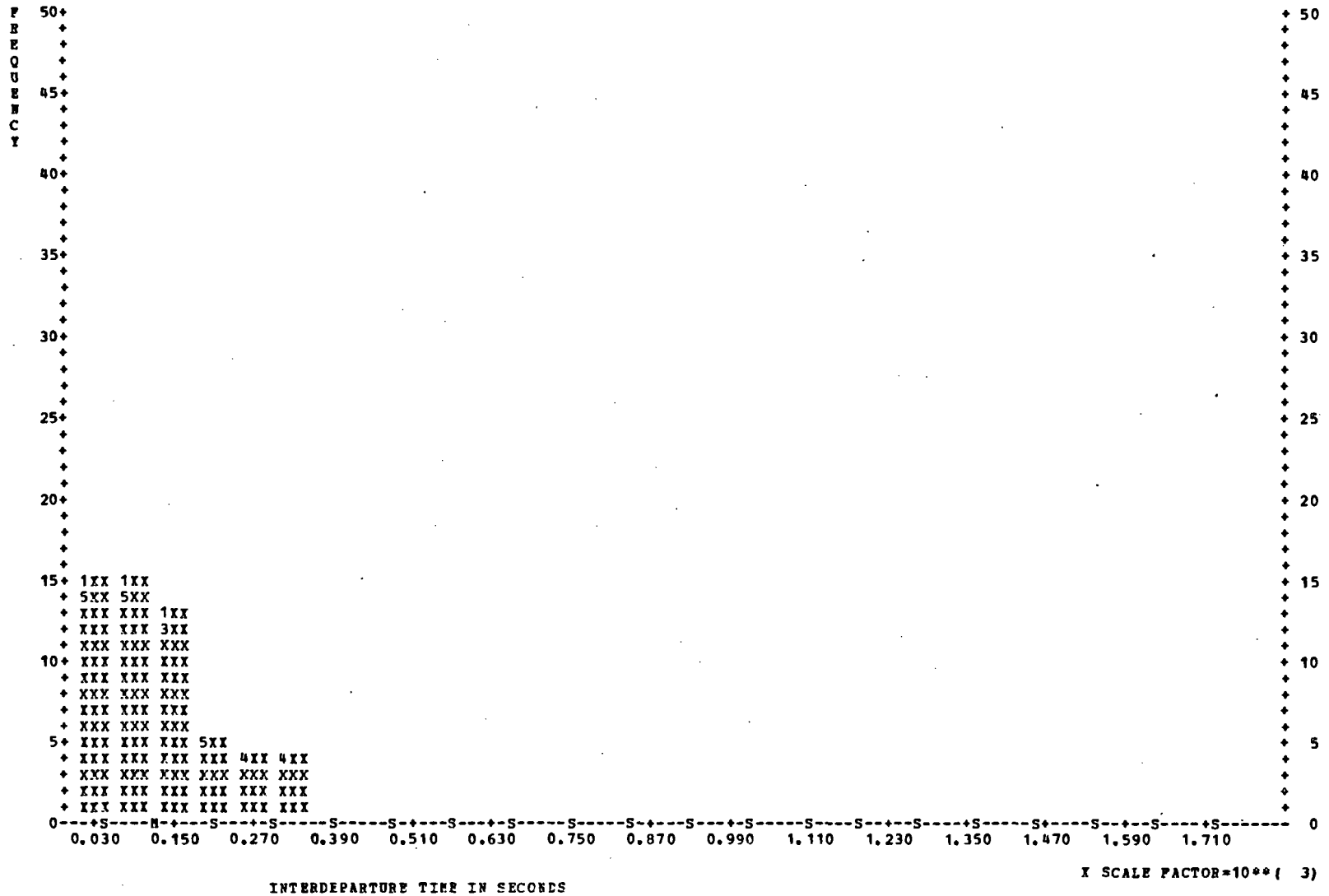

INTERDEPARTURE TIME IN SECONDS

NUMBER OF CLASSES= 30 DATA POINTS ON GRAPH= 56 DATA POINTS OFF GRAPH= 0

MEAN	VARIANCE	ST. DEV.	SKEWNESS	KURTOSIS	ST. SKEW.	ST. KURT.
126.8571	7885.8750	88.8024	0.7011	-0.2607	2.1420	-0.3982

Figure 4.9 Histogram of Interdeparture Times at EWR

EWR ARRIVAL STREAM

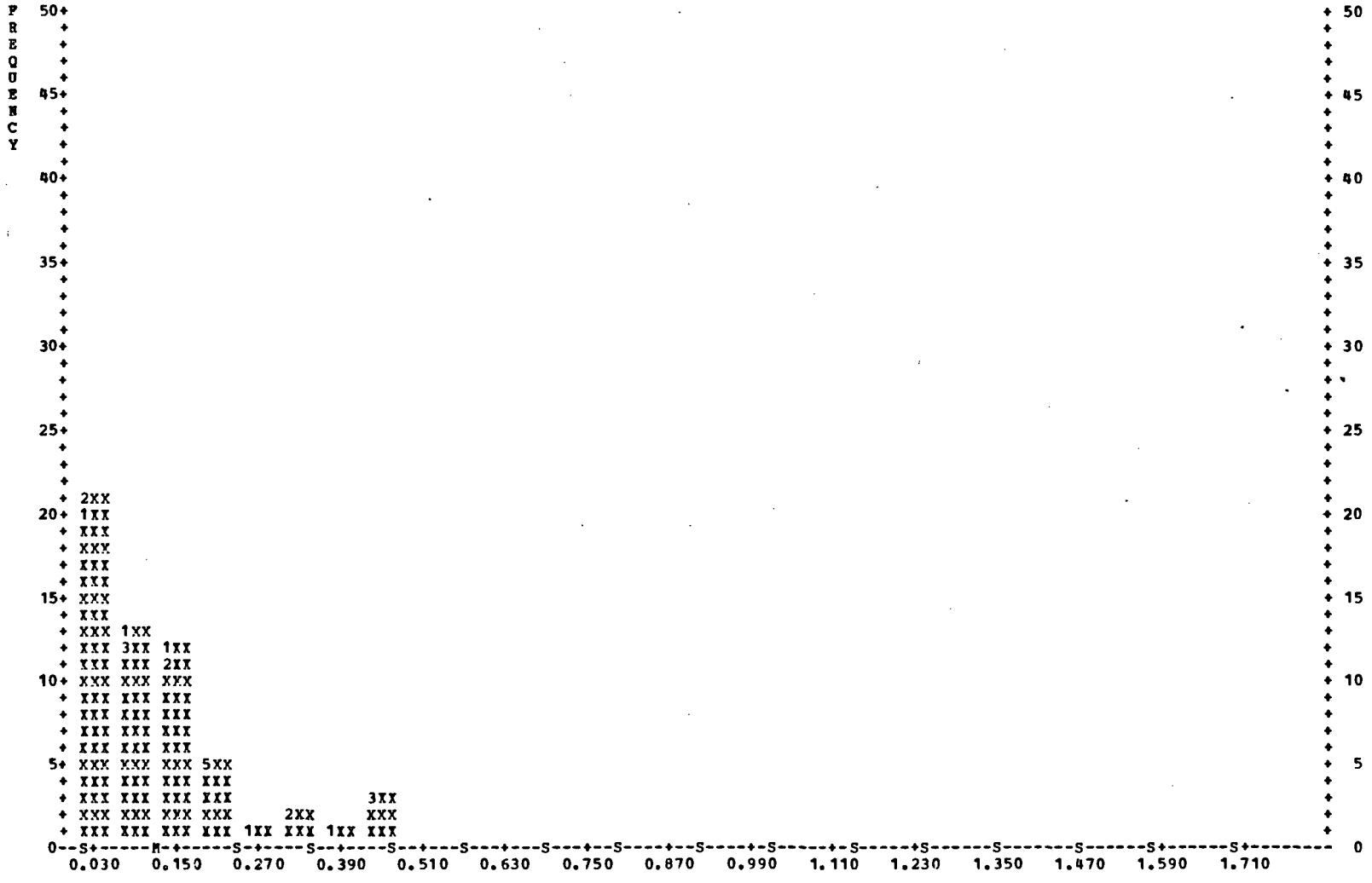

INTERARRIVAL TIME IN SECONDS

NUMBER OF CLASSES= 30 DATA POINTS ON GRAPH= 58 DATA POINTS OFF GRAPH= 0

MEAN	VARIANCE	ST. DEV.	SKEWNESS	KURTOSIS	ST. SKEW.	ST. KURT.
121.3793	12627.5703	112.3725	1.4490	1.4891	4.5052	2.3149

Figure 4.10 Histogram of Interarrival Times at EWR

JFK DEPARTURE STREAM

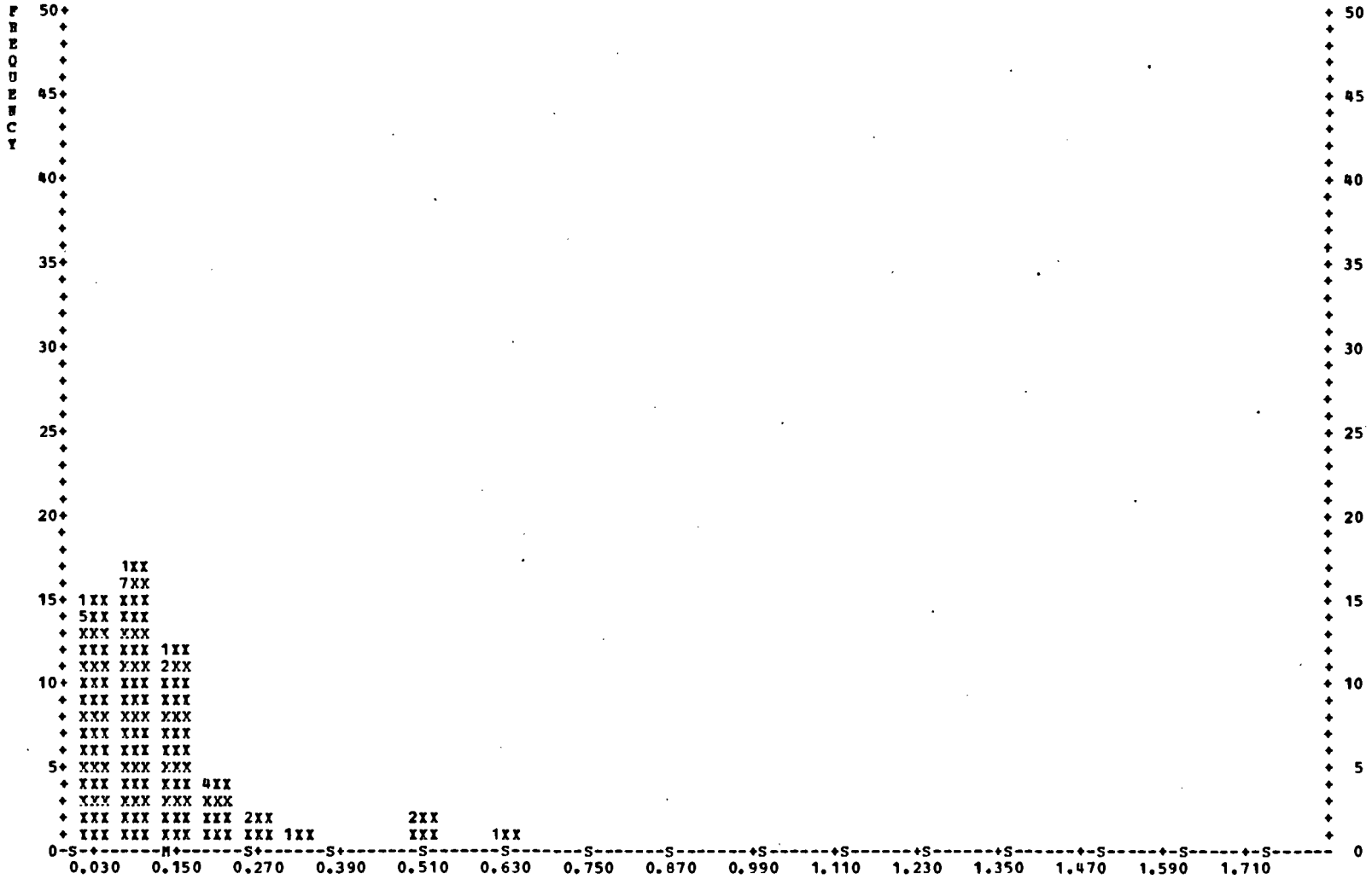

INTERDEPARTURE TIME IN SECONDS

NUMBER OF CLASSES= 30 DATA POINTS ON GRAPH= 54 DATA POINTS OFF GRAPH= 0

MEAN	VARIANCE	ST. DEV.	SKEWNESS	KURTOSIS	ST. SKEW.	ST. KURT.
131.2037	15343.0234	123.8670	2.1892	5.1084	6.5676	7.6626

Figure 4.11 Histogram of Interdeparture Times at JFK

JFK ARRIVAL STREAM

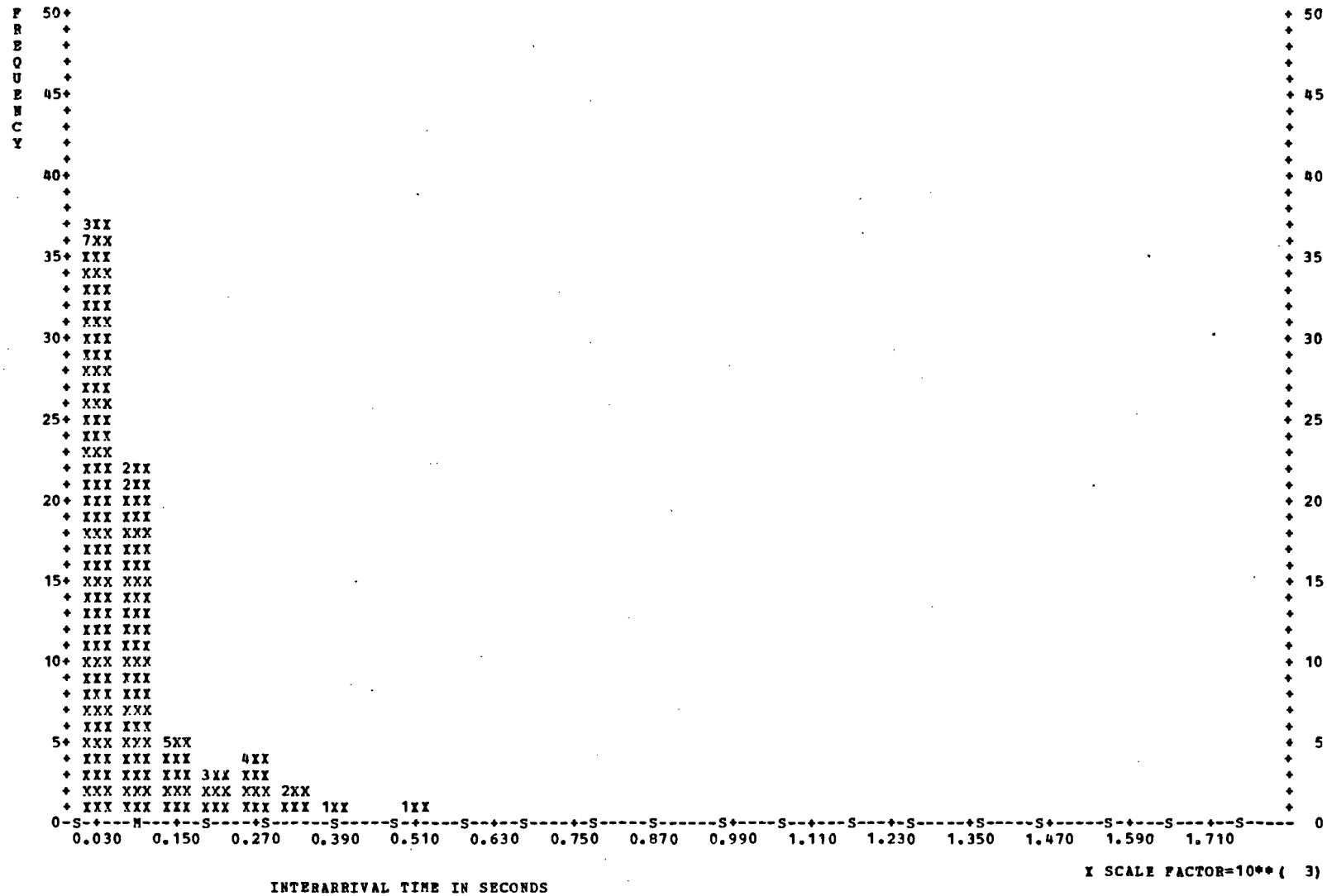

INTERARRIVAL TIME IN SECONDS

NUMBER OF CLASSES= 30 DATA POINTS ON GRAPH= 75 DATA POINTS OFF GRAPH= 0

MEAN	VARIANCE	ST. DEV.	SKEWNESS	KURTOSIS	ST. SKEW.	ST. KURT.
93.7867	9518.1875	97.5612	1.8720	3.4400	6.6184	6.0811

Figure 4.12 Histogram of Interarrival Times at JFK

LGA DEPARTURE STREAM

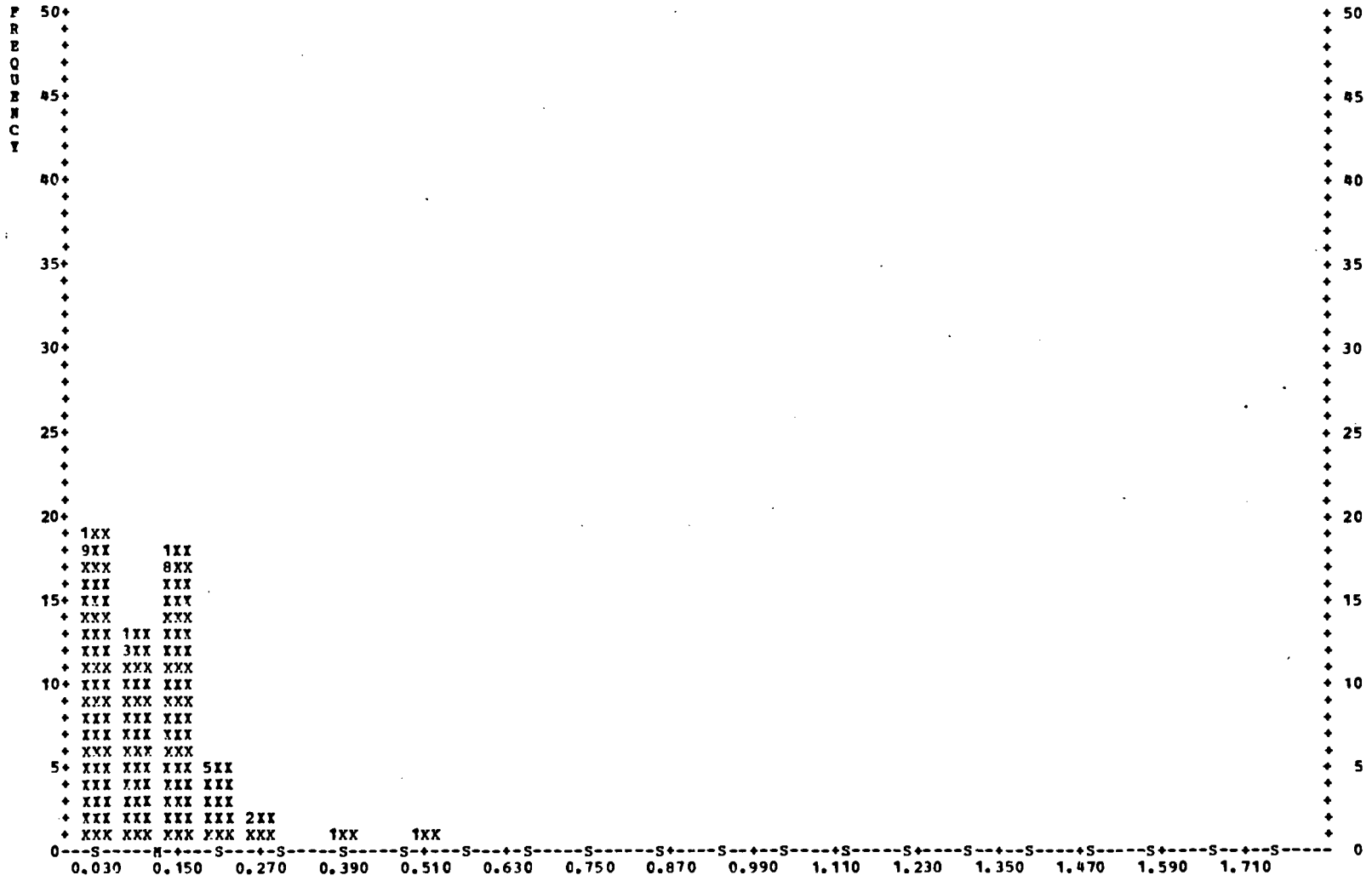

X SCALE FACTOR=10**(3)

INTERDEPARTURE TIME IN SECONDS

NUMBER OF CLASSES= 30 DATA POINTS ON GRAPH= 59 DATA POINTS OFF GRAPH= 0

MEAN	VARIANCE	ST. DEV.	SKEWNESS	KURTOSIS	ST. SKEW.	ST. KURT.
119.4068	8297.1758	91.0888	1.8329	5.1885	5.7475	8.1351

Figure 4.13 Histogram of Interdeparture Times at LGA

LGA ARRIVAL STREAM

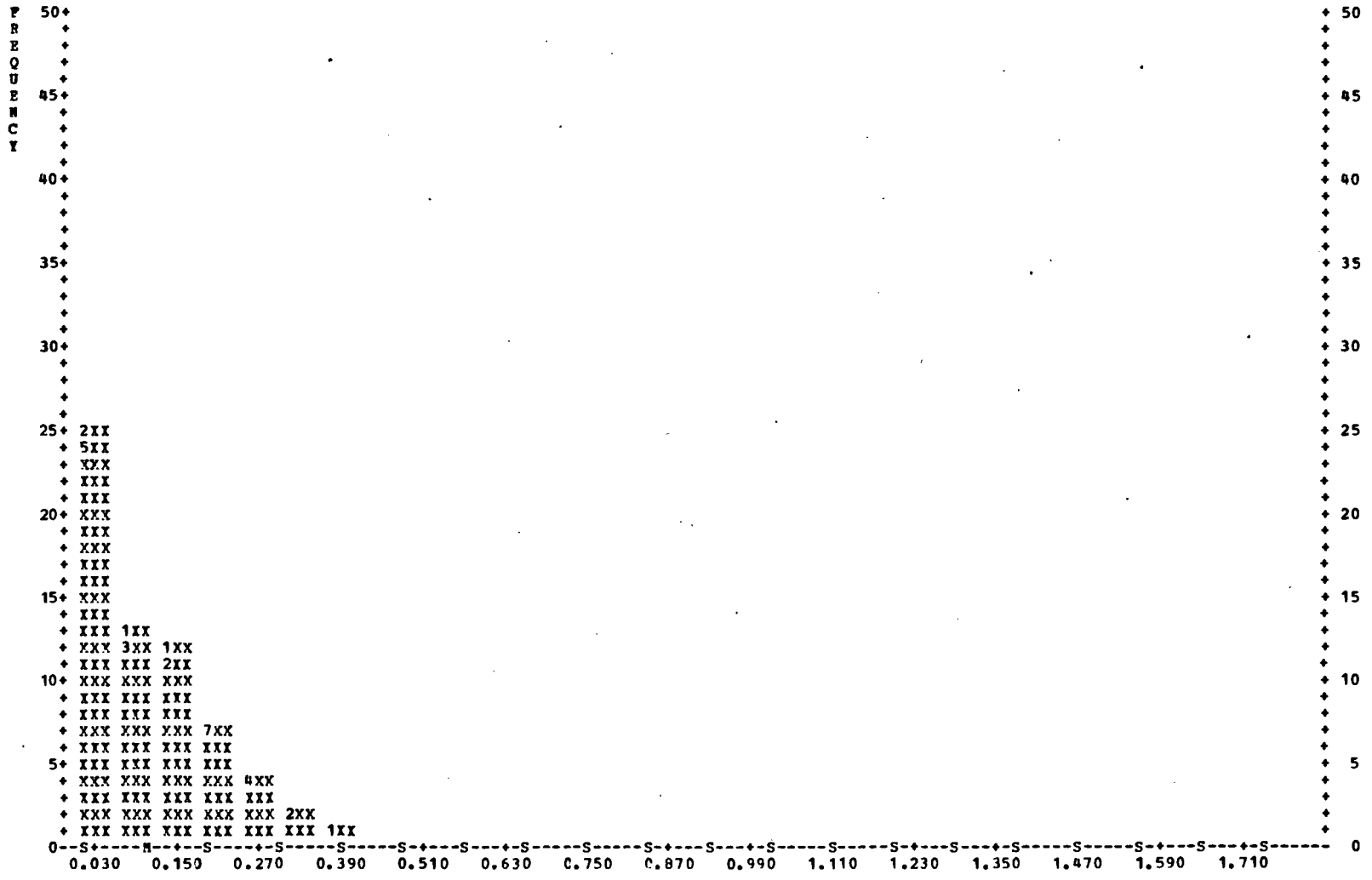

NUMBER OF CLASSES= 30 DATA POINTS ON GRAPH= 64 DATA POINTS OFF GRAPH= 0

MEAN	VARIANCE	ST. DEV.	SKEWNESS	KURTOSIS	ST. SKEW.	ST. KURT.
111.8125	8222.5938	90.6785	0.9586	0.2138	3.1309	0.3492

Figure 4.14 Histogram of Interarrival Times at LGA

PHL DEPARTURE STREAM

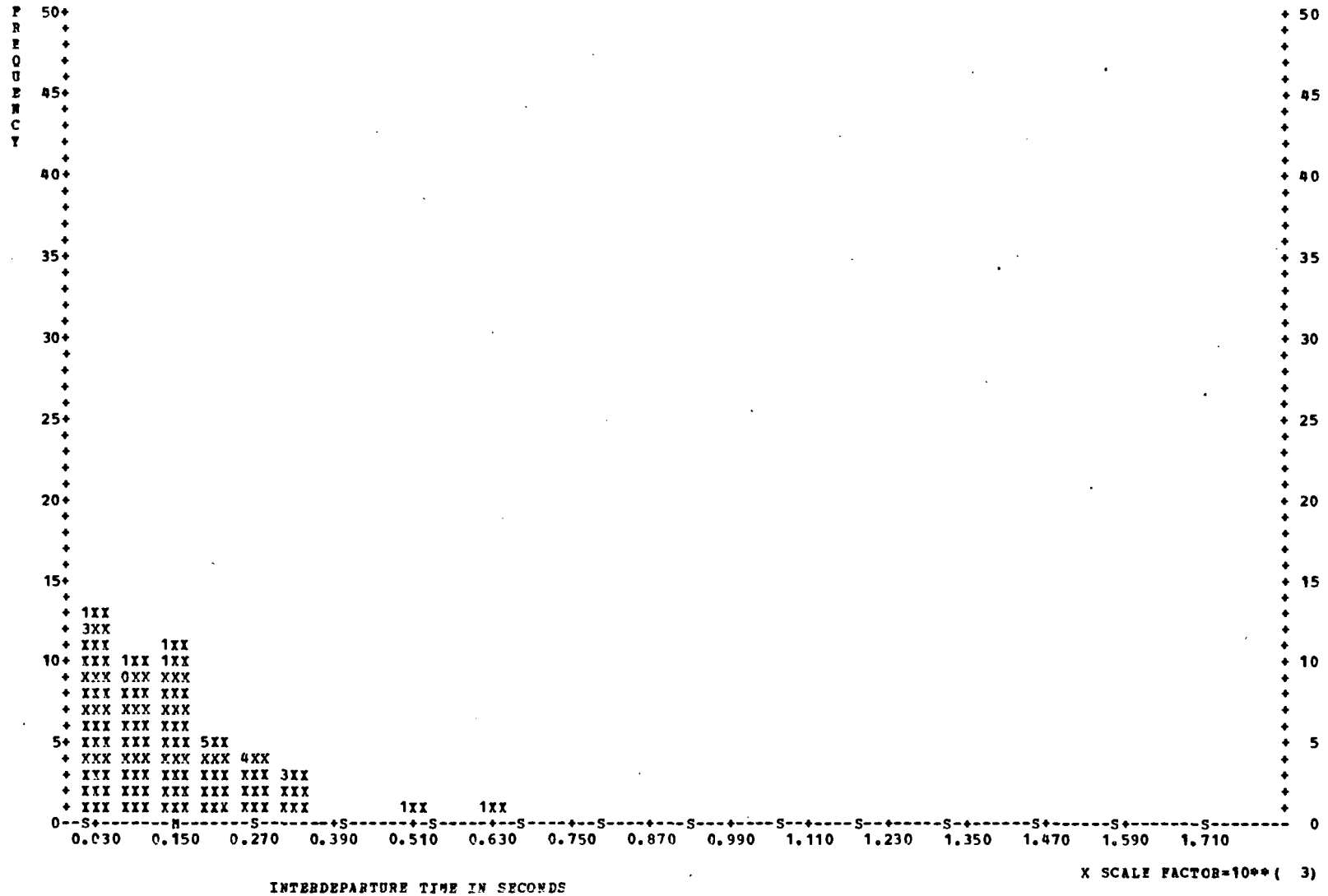

NUMBER OF CLASSES= 30 DATA POINTS ON GRAPH= 48 DATA POINTS OFF GRAPH= 0

MEAN	VARIANCE	ST. DEV.	SKEWNESS	KURTOSIS	ST. SKEW.	ST. KURT.
146.9583	17002.9414	130.3953	1.6029	3.5593	4.5337	5.0336

Figure 4.15 Histogram of Interdeparture Times at PHL

PHL ARRIVAL STREAM

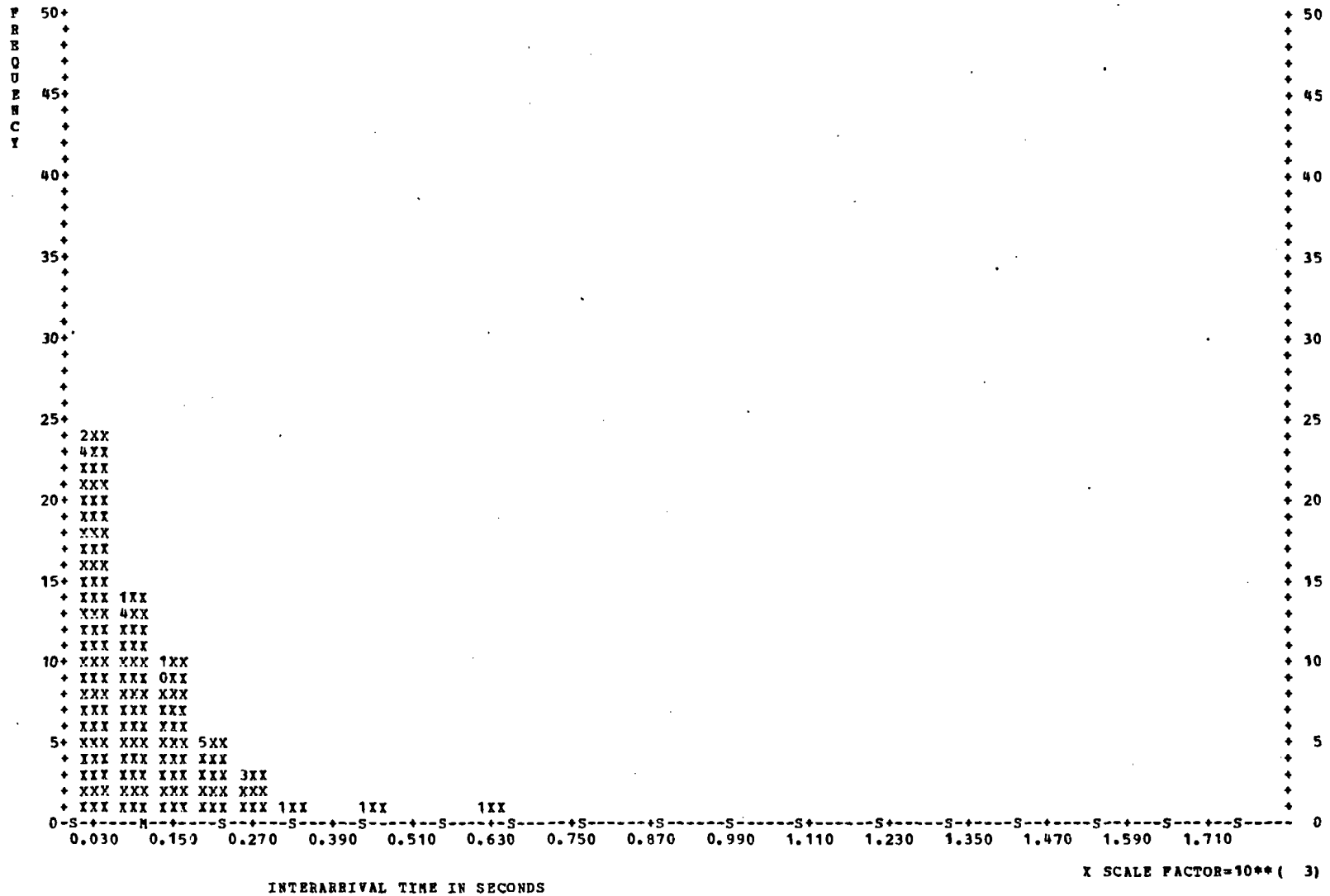

INTERARRIVAL TIME IN SECONDS

NUMBER OF CLASSES= 30 DATA POINTS ON GRAPH= 59 DATA POINTS OFF GRAPH= 0

MEAN	VARIANCE	ST. DEV.	SKEWNESS	KURTOSIS	ST. SKEW.	ST. KURT.
111.4576	12087.8008	109.9445	2.3818	7.3736	7.4688	11.5611

Figure 4.16 Histogram of Interarrival Times at PHL

Table 4.5

Statistics for Arrival and Departure Streams at Major Airports in the New York Region

Departure Streams:

Terminal	No. of Departures	(1) $\hat{\lambda}$	(1) Approximate 95% Conf. Limits λ_ℓ	λ_u	(2) Interdeparture Times $\bar{x}$	s	D_n	$D_n \alpha = .10$	$D_n \alpha = .05$	$D_n \alpha = .01$	$\hat{\hat{\lambda}}^{-1}$	χ^2	d.f
EWR	57	28.50	21.47	36.80	126.86	88.80	.1495*	.1271	.1404	.1656	133.458	5.350	4
JFK	55	27.50	20.60	35.67	131.20	123.87	.1311	.1294	.1429	.1685	123.356	5.489	3
LGA	60	30.00	22.78	38.49	119.41	91.09	.1336	.1239	.1368	.1614	114.223	12.735**	3
PHL	49	24.50	18.13	32.39	146.96	130.40	.1321	.1371	.1514	.1786	150.328	3.170	4

Arrival Streams:

Terminal	No. of Arrivals	$\hat{\mu}$	95% Conf. Limits $\hat{\mu}_{lower}$	$\hat{\mu}_{upper}$	Interarrival Times $\bar{x}$	s	D_n	$D_n \alpha = .10$	$D_n \alpha = .05$	$D_n \alpha = .01$	$\hat{\hat{\mu}}^{-1}$	χ^2	d.f
EWR	59	29.50	22.34	37.93	121.38	112.37	.0727	.1250	.1380	.1627	121.204	1.776	3
JFK	76	38.00	29.83	47.44	93.79	97.56	.0865	.1101	.1216	.1434	91.443	4.877	4
LGA	65	32.50	24.97	41.30	111.81	90.68	.0798	.1191	.1315	.1550	114.529	2.603	4
PHL	60	30.00	22.78	38.49	111.46	109.94	.1066	.1239	.1368	.1614	109.492	1.074	3

(1) In aircraft per hour

(2) In seconds

* Significant at $\alpha = .05$

** Significant at $\alpha = .01$

actual data values are "super-efficient" and could give misleading results). If $0=X_0<X_1<\ldots<X_{k-1}<\infty$ are the dividing points of the k classes (for this example, 0.0, 59.5, 119.5, ...), Johnson and Kotz (1970) quote a result from Kuldorf (1961) that the maximum likelihood estimator for λ is given by the unique solution to

$$\sum_{i=1}^{k-1} \frac{N_i(X_i-X_{i-1})}{e^{\hat{\lambda}(X_i-X_{i-1})}} - \sum_{i=2}^{k} N_i X_{i-1} = 0 \quad . \tag{4.46}$$

Solving (4.46) numerically, the estimates $\hat{\lambda}$ can be used to calculate E_i and to obtain the solution to (4.45). Table 4.5 includes the values of χ^2 from this procedure. Only one departure stream and no arrival streams showed significant lack-of-fit at the α=.05 significance level.

The second goodness-of-fit test performed was a one-sample Kolmogorov-Smirnov test. This test compares an empirical distribution $S_n(X)$ with a hypothesized distribution F(X) using the statistic

$$D_n = \sup_x \{|S_n(X) - F(X)|\}. \tag{4.47}$$

When F(x) is exponential but the parameter λ is unknown, then Monte Carlo studies have shown that the standard tables for the critical values of D_n are extremely conservative. Lilliefors (1969) in a Monte Carlo study suggested that values obtained from standard tables such as Massey (1957) for α=.20 were approximately α=.05 critical values when λ was estimated from the data. For sample sizes over N=30, he notes that approximate 5 per cent critical values are given by $D_n=1.06/\sqrt{N}$, 10 per cent values by $.96/\sqrt{N}$, and 1 per cent values by $1.25/\sqrt{N}$.

Comparing these critical values to the values of D_n calculated for the arrival and departure streams, no arrival streams appear to be significant at α=.10 or lower, but one departure stream is significant at α=.05 and three at α=.10.

The various tests conducted indicate that the Poisson model for aircraft arriving at the major airports is adequate but that the model is slightly questionable for the departure streams. The small size of the samples, however, makes it difficult to determine an alternative representation for the streams. Further, the magnitude of the scheduling in the departure streams, which reduces the variance of interdeparture times, will have only a negligible effect on the streams over the arcs in (s,N) which handle some fraction of the aircraft from several sources. These streams are considered further in section 4.5.3.

The assumption that the streams from the various sources are independent is more difficult to test. However, there is no convincing

reason why the streams should be dependent, at least under the assumption of constant traffic generation and flow rates. In fact, the real value of the model lies in being able to manipulate the various source generation rates separately. A more serious question of independence arises in section 4.5.4.

4.5.3 Modeling of Traffic Entering Sectors

The streams of traffic entering the network over each of the arcs in (s, N) are under the assumptions of section 4.3, Poisson processes. The maximum likelihood estimates of the flow rates $f(s, N_k)$ from (4.19) are simply the total number of entries to the sectors divided by the length of the sample period. Table 4.6 gives the number of entries observed in a 2 -hour sample and the corresponding flow rate estimates for each of the 32 arcs in (s, N).

It was argued in section 4.5.2 that the effects of scheduling in the departure streams would no longer be apparent in the streams entering the sectors of the network. In order to test this conjecture, the empirical distributions of interarrival times to the 32 sectors of the network were tested against hypothesized exponentials with the parameter estimates in table 4.6. Using Kolmogorov's statistic D_n with the adjusted critical values of Lilliefors (1969), it was found that of 28 sectors with greater than five arrivals during the sample period, 2 were significant at the α=.01 significance level, but the other 26 were within the 90 per cent confidence limits for the null hypothesis. Since occasional significant values will occur even if the null hypothesis is correct, the overall conjecture that the streams over the arcs in (s, N) are Poisson appears to be fairly adequate and will be adopted.

4.5.4 Source-Node Transition Probabilities

Once the streams of traffic through the network have been identified and the flow rates estimated, all traffic can be considered to originate at the super-source. Under the assumptions of section 4.3, the flow through s per unit time will have a Poisson distribution with rate parameter equal to the sum of the individual stream parameters. Conditionally on k arrivals at s in a given interval, the distribution of the k aircraft over the various sources will have the multinomial distribution of (4.12).

In determining where arrivals at the super-source actually enter the network, it is necessary to estimate source-node transition probabilities $p_{k|i}$ defined in section 4.3.3. It will be recalled that the estimates of the source-node transition probabilities are given in (4.17) to be

$$\hat{p}_{k|i} = \frac{c_{ik}}{c_{i.}} ,$$

Table 4.6 Test Statistics for Poisson Arrivals at Enroute Sectors

Sector	No. of arrivals	$\hat{f}(s,N_k)$	Interarrival times $\bar{x}$	Interarrival times s	D_n
451	28	14.0	262.6	249.6	0.1344
453	32	16.0	226.7	217.6	0.0844
454	20	10.0	349.7	219.4	0.3039**
455	3	1.5			
456	0	0.0			
457	3	1.5			
458	32	16.0	225.8	170.8	0.1554
459	28	14.0	254.6	282.5	0.0609
460	18	9.0	402.3	350.4	0.0963
461	33	16.5	220.7	145.9	0.1655
462	28	14.0	258.3	192.1	0.2580**
463	12	6.0	474.5	568.9	0.1824
464	11	5.5	541.4	665.9	0.2029
465	12	6.0	538.5	459.9	0.1490
466	36	18.0	276.0	241.6	0.1525
467	34	17.0	206.8	218.9	0.1428
468	27	13.5	267.8	284.2	0.1332
469	10	5.0	730.6	619.1	0.1937
470	20	10.0	336.5	385.2	0.1422
471	22	11.0	300.9	257.7	0.1495
472	27	13.5	253.2	197.0	0.1152
473	8	4.0	915.4	944.4	0.2202
474	21	10.5	306.1	304.7	0.1662
475	31	15.5	224.9	198.6	0.0667
476	24	12.0	282.0	236.7	0.0860
477	13	6.5	554.5	633.9	0.1772
478	22	11.0	301.0	373.2	0.1737
479	26	13.0	251.4	217.2	0.1159
480	17	8.5	428.4	487.2	0.1262
481	28	14.0	251.4	255.6	0.0973
482	8	4.0	638.3	529.6	0.0789
483	13	6.5	531.7	346.9	0.2185

** stat. sig. at α=.01

$\hat{f}(s,N_k)$ is in aircraft/hour

$\bar{x}$, s given in seconds

where $c_{i.}$ is the number of aircraft generated at source i during the sample period and c_{ik} is the number of aircraft generated at s_i which entered the network through sector N_k. Table 4.7 lists the estimates of $p_{k|i}$ obtained from the number of aircraft at each source which entered each sector of the network.

The assumption that the transition probabilities are constant over time can be tested in part by determining whether the selection of sectors entered by aircraft in a source stream are independent or whether some attempt is made to alternate the sectors entered. This is related to the question of independence among the traffic streams entering nodes in the network and requires a more detailed look at individual sources of traffic.

The most likely areas in which the streams would fail to be independent is where several LT and LE sectors are fed by the same departure controller at a major terminal. The following sectors fall into such a category:

From EWR	454,461,472
From JFK	458,463,others
From LGA	459,461,462
From PHL	451,467,others.

If the transition probabilities are constant over time, then the probability that any given exit will go to a selected enroute sector would not depend on the sector to which the previous exit was directed. For example, consider a departure controller feeding three enroute sectors labelled N_1, N_2, and N_3. Now let p_j be the unconditional probability that a given exit from the departure sector enters the jth enroute sector, and let p_{ij} be the conditional probability of entering the jth enroute sector given that the last exit entered the ith sector. Then if the selection of enroute sectors is independent,

$$p_{ij} = p_j \quad . \tag{4.48}$$

The problem of testing whether (4.48) is true is similar to that encountered in the analysis of Markov chains in determining whether successive events are independent. Using the notation adopted by Chatfield (1973), let n_{ij} be the number of times an exit to the ith sector was followed by an exit to the jth sector. If as is often done in testing random numbers, the process is made circular by considering the last exit to be followed by the first, then estimates of p_j are given by

$$\hat{p}_j = \frac{\sum_i n_{ij}}{N} \tag{4.49}$$

Table 4.7 Estimates of Source-Node Transition Probabilities

	451	453	454	455	456	457	458	459	460	461	462	463	464	465	466	467
EWR			.339							.189						
JFK							.596	.058			.058	.211				
LGA								.276		.345	.379					
PHL	.611	.028				.028							.028			.305
ACY						.111										
ILG		.400														.600
AVP																
BGM																
HAR													.167	.083	.750	
ABE													1.00			
ELM																
HPN								.571			.429					
000	.0161	.0751	.0054	.0080		.0027	.0027	.0134	.0483	.0054		.0027		.0268	.0429	.0509

Table 4.7 Estimates of Source-Node Transition Probabilities (cont.)

	468	469	470	471	472	473	474	475	476	477	478	479	480	481	482	483
EWR					.472											
JFK		.077														
LGA																
PHL																
ACY	.889															
ILG																
AVP			1.00													
BGM				1.00												
HAR																
ABE																
ELM			.714	.286												
HPN																
000	.0483	.0161	.0295	.0456	.0054	.0134	.0563	.0831	.0643	.0348	.0590	.0670	.0429	.0777	.0214	.0348

where the total number of exits is

$$N = \sum_i \sum_j n_{ij}.$$

Then if successive exits are independent, the expected number of times an exit to sector i will be followed by an exit to sector j is

$$e_{ij} = N\, p_i p_j \,. \tag{4.50}$$

Using (4.49) the estimates of e_{ij} are given by

$$\hat{e}_{ij} = \frac{\sum_i n_{ij} \sum_j n_{ij}}{N} \,. \tag{4.51}$$

Anderson and Goodman (1957) have shown that if the assumption of independence is correct, then

$$\chi^2 = \sum_{i,j} (n_{ij} - \hat{e}_{ij})^2 / \hat{e}_{ij} \tag{4.52}$$

is asymptotically distributed as χ^2 with $(c-1)^2$ degrees of freedom where c is the number of enroute sectors fed from the single departure sector.

Table 4.8 gives the estimates $\hat{p}_j$ determined for each of the departure controllers at the four major airports, the expected values from (4.50), estimates from (4.51), and χ^2 values from (4.52). A significant χ^2 value was obtained for LGA, where successive departures tended to alternate between sectors 461 and 462. No such interdependence was observed among departure streams from the other terminals.

On the basis of this analysis, there is no compelling evidence that the streams of traffic over the arcs in (s, N) are dependent. In particular, the assumption of constant source-node transition probabilities appears adequate, at least at the level of analysis for which the model would be appropriate.

4.5.5 Characterization of Sector Sequences

The sector sequences discussed in appendix 4-A describe the movement of aircraft through the network. A visual picture of this traffic has previously been presented in figures 7.13 - 7.15 of volume II, which displayed the number of transitions between all pairs of high altitude sectors, pairs of low altitude sectors, and pairs of high and low sectors respectively.

Table 4.8 Tests for Interdependence in Departure Streams

EWR

Observed

1st \ 2nd	454	461	472	
454	4	5	9	18
461	4	1	5	10
472	10	4	11	25
	18	10	25	53

Expected

1st \ 2nd	454	461	472
454	6.11	3.40	8.49
461	3.40	1.89	4.72
472	8.49	4.72	11.79

$\chi^2_4 = 2.49$

JFK

Observed

1st \ 2nd	458	463	other	
458	17	6	8	31
463	6	4	1	11
other	8	1	1	10
	31	11	10	52

Expected

1st \ 2nd	458	463	other
458	18.48	6.56	5.96
463	6.56	2.33	2.11
other	5.96	2.11	1.92

$\chi^2_4 = 4.43$

LGA

Observed

1st \ 2nd	459	461	462	
459	4	6	6	16
461	4	3	13	20
462	8	11	3	22
	16	20	22	58

Expected

1st \ 2nd	459	461	462
459	4.41	5.52	6.07
461	5.52	6.90	7.59
462	6.07	7.59	8.35

$\chi^2_4 = 12.14^*$

PHL

Observed

1st \ 2nd	451	467	other	
451	12	8	2	22
467	8	2	1	11
other	2	1	0	3
	22	11	3	36

Expected

1st \ 2nd	451	467	other
451	13.44	6.72	1.83
467	6.72	3.36	0.92
other	1.83	0.92	0.25

$\chi^2_4 = 1.49$

*Significant at α=.05

A more comprehensive summary of observed transitions among the enroute sectors is given in table 4.9, a part of the one-step transition matrix of counts presented earlier.

In order to determine what order of Markov chain would be appropriate to describe the sector sequences, the information theory approach described by Chatfield (1973) was selected.

Figure 4.17 is a plot of the estimated conditional uncertainties in the sector sequences, using all observed quadruplets in the sample. From the data in appendix 4-A, $N_4 = 777$ quadruplets were tabulated. The following formulas were used to calculate the conditional uncertainties:

$$H_o = \log 44 \qquad \text{(44 states in chain)}$$

$$H_1 = \log N_4 - N_4^{-1} \sum_i n_{i\ldots} \log n_{i\ldots}$$

$$H_2 = N_4^{-1} \left[\sum_i n_{i\ldots} \log n_{i\ldots} - \sum_{i,j} n_{ij..} \log n_{ij..} \right]$$

$$H_3 = N_4^{-1} \left[\sum_{i,j} n_{ij..} \log n_{ij..} - \sum_{i,j,k} n_{ijk.} \log n_{ijk.} \right]$$

$$H_4 = N_4^{-1} \left[\sum_{i,j,k} n_{ijk.} \log n_{ijk.} - \sum_{i,j,k,\ell} n_{ijk\ell} \log n_{ijk\ell} \right] .$$

It will be noticed that sharp drops occur until H_3, which is typical of second-order chains. The drop from H_3 to H_4 may or may not be significant, but it does not appear to be as important as the earlier drops. No rigorous statistical tests such as discussed in section 4.5 were performed because of the large number of states in the chain and the consequently small number of counts for all observed pairs, triplets, and higher sequences during the 2-hour sample period.

On the basis of the above analysis, it was decided that second order Markov chains would be sufficient to describe the patterns observed in the sector sequences. It will be recalled from section 4.4.4 that second order Markov chains on the nodes of a network can be expressed by equivalent first order chains on the arcs. Intuitively, if the sector which an aircraft enters depends on the previous two sectors through which it passed, an equivalent statement is that the arc through which the aircraft leaves a particular sector depends upon the arc by which it entered that sector, but beyond that the past history of arcs is irrelevant.

Table 4.10 presents the first-order transition matrices on the arcs of the network, a separate matrix for each enroute sector. The maximum likelihood estimates of p_{ijk} in (4.36) can all be derived from the table, since the element in the ith row and k^{th} column of the matrix for the jth sector is n_{ijk}, and the total of the

Table 4.9 New York Enroute Network Transition Counts

SECTOR	451	53	54	55	56	57	58	59	60	61	62	63	64	65	66	67	68	69	70	71	72	73	74	75	76	77	78	79	80	81	82	83	OUT	TOTAL
IN	28	32	20	3	0	3	32	28	18	33	28	12	11	12	26	34	27	10	20	22	27	8	21	31	24	13	22	26	17	28	8	13		637
451	0	3	0	1	0	0	0	0	0	0	0	0	8	0	7	0	0	0	0	0	0	0	0	0	0	0	0	10	0	0	0	0	28	57
453	2	0	0	16	2	17	0	0	0	0	0	0	0	0	1	3	0	0	0	0	0	0	0	0	0	0	0	1	0	0	0	0	14	56
454	20	0	0	1	4	0	0	0	0	0	0	0	0	0	0	0	0	0	0	0	1	0	0	0	0	0	0	0	0	0	0	0	30	56
455	3	0	0	0	0	0	0	0	0	0	0	0	1	0	0	0	0	1	0	0	0	0	0	0	0	0	0	0	0	0	0	0	37	42
456	2	0	0	0	0	0	0	0	0	0	0	0	0	0	0	0	0	0	0	0	0	0	0	0	7	0	0	0	0	0	0	0	33	42
457	0	0	0	0	1	0	0	0	0	0	0	0	0	0	0	0	0	0	0	0	0	0	0	0	0	0	0	0	0	0	0	0	24	25
458	0	0	0	1	2	0	0	0	0	0	0	0	0	0	0	6	4	4	0	0	0	0	0	0	0	20	0	0	0	0	7	1	5	50
459	0	0	0	0	0	0	0	0	10	1	0	0	0	0	0	0	0	0	0	0	0	3	4	0	0	0	0	0	1	0	0	0	13	32
460	0	0	0	0	0	0	1	2	0	0	0	0	0	0	0	0	0	1	0	0	0	0	0	0	0	0	0	0	0	0	0	0	44	48
461	0	0	18	3	5	0	0	0	0	0	2	4	0	0	0	0	0	0	0	2	11	2	0	0	0	0	1	0	0	0	0	0	5	53
462	0	0	0	0	0	0	0	0	0	13	0	21	0	0	0	0	0	0	0	0	0	6	0	0	0	0	0	0	0	0	0	0	0	40
463	0	0	0	0	0	0	0	0	0	4	0	0	0	0	0	0	0	0	0	5	0	17	0	0	0	0	0	0	24	0	0	0	2	52
464	1	0	20	15	0	2	0	0	0	1	0	0	0	3	4	0	0	0	4	0	13	0	0	1	0	0	0	0	2	0	0	0	6	72
465	0	0	0	0	0	0	0	0	0	0	0	0	6	0	1	0	0	0	7	0	0	0	0	0	0	0	0	0	0	0	0	0	17	31
466	3	0	0	0	0	0	0	0	0	0	0	0	7	7	0	0	0	0	0	0	0	0	0	0	0	0	0	0	0	0	0	0	39	56
467	0	9	0	0	0	2	4	0	0	0	0	0	0	0	0	1	4	0	0	0	0	0	0	0	0	2	0	0	0	0	0	0	34	56
468	0	1	0	0	0	0	2	0	0	0	0	0	0	0	0	8	0	0	0	0	0	0	0	0	0	3	0	0	0	0	0	0	27	41
469	0	0	0	0	0	0	7	0	3	0	0	0	0	0	0	0	0	0	0	0	0	0	0	0	0	0	0	0	0	0	0	3	15	28
470	0	0	0	0	0	0	0	0	0	0	0	0	3	5	0	0	0	0	0	10	2	0	0	0	0	0	0	0	0	0	0	0	22	42
471	0	0	0	0	0	0	0	0	0	0	0	0	0	0	0	0	0	0	9	0	3	7	0	0	0	0	0	0	1	0	0	0	20	40
472	0	0	0	0	0	0	0	0	0	0	1	9	5	0	0	0	0	0	5	1	0	10	0	5	0	0	0	0	20	0	0	0	9	65
473	0	0	0	0	0	0	0	0	0	0	2	1	0	0	0	0	0	0	0	5	4	1	18	0	0	0	0	0	0	16	0	0	18	65
474	0	0	0	0	0	0	0	0	0	0	0	1	0	0	0	0	0	0	0	0	0	8	0	0	0	0	0	0	2	6	0	0	26	43
475	0	0	0	0	0	0	0	0	0	0	0	0	31	0	2	0	0	0	0	0	4	0	0	1	0	0	11	1	4	0	0	0	11	65
476	0	12	0	1	11	0	0	0	0	0	0	0	0	0	0	0	0	0	0	0	0	0	0	0	0	8	0	0	0	0	1	0	3	36
477	0	0	0	0	0	0	0	0	0	0	0	0	0	0	0	5	4	0	0	0	0	0	0	0	7	0	0	12	0	0	0	8	18	54
478	0	0	0	0	20	0	0	0	0	0	0	0	0	0	0	0	0	0	0	0	0	0	0	2	0	0	0	0	0	0	0	0	14	36
479	0	0	0	0	0	0	0	0	0	0	0	0	0	0	16	0	0	0	0	0	0	0	0	3	0	0	1	1	0	0	0	0	29	50
480	0	0	0	0	0	0	0	1	0	0	0	0	0	0	0	0	0	0	0	1	1	3	0	21	0	0	0	0	0	7	0	0	42	76
481	0	0	0	0	0	0	0	0	12	0	9	4	0	0	0	0	0	0	0	0	0	0	2	0	0	0	0	0	2	0	0	2	25	56
482	0	0	0	0	0	0	3	0	0	0	0	0	0	0	0	0	1	0	0	0	0	0	0	0	0	0	0	0	0	0	0	7	8	19
483	0	0	0	0	0	0	0	0	6	0	0	0	0	0	0	0	0	10	0	0	0	0	0	0	0	6	0	0	0	0	0	0	7	29
TOTAL	59	57	58	41	45	24	49	31	49	52	42	52	72	27	57	57	40	26	45	46	66	65	45	64	38	52	35	51	73	57	16	34	625	

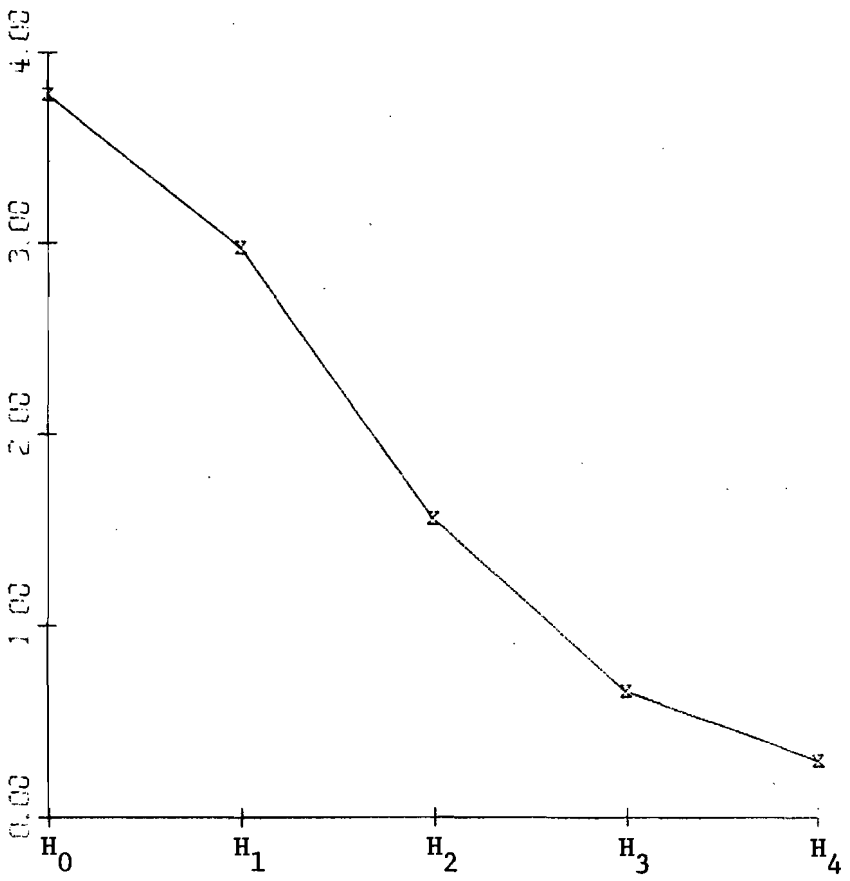

H_0 = 3.784

H_1 = 2.981

H_2 = 1.557

H_3 = 0.664

H_4 = 0.304

Figure 4.17 Plot of Conditional Uncertainties in Sector Sequences

Table 4.10 Arc-arc Transition Matrices with Counts in New York Enroute Network

ARC-ARC TRANSITION MATRIX FOR SECTOR 451

	000	453	455	464	466	479	ILG	AVP	TOT
000	1	0	1	0	2	0	0	1	5
453	0	0	0	2	0	0	0	0	2
454	15	2	0	0	0	0	0	0	17
455	3	0	0	0	0	0	0	0	3
456	1	0	0	0	0	0	0	0	1
464	0	1	0	0	0	0	0	0	1
466	1	0	0	0	0	0	1	0	2
PHL	0	0	0	6	5	10	0	0	21
TOT	21	3	1	8	7	10	1	1	52

ARC-ARC TRANSITION MATRIX FOR SECTOR 453

	000	451	455	456	457	466	467	479	PHL	ACY	ILG	TOT
000	2	1	5	1	9	0	1	1	4	1	1	26
451	1	0	0	0	0	0	2	0	0	0	0	3
467	0	0	3	0	3	1	0	0	0	0	0	7
468	0	1	0	0	0	0	0	0	0	0	0	1
476	0	0	7	0	5	0	0	0	0	0	0	12
PHL	1	0	0	0	0	0	0	0	0	0	0	1
ILG	2	0	0	0	0	0	0	0	0	0	0	2
TOT	6	2	15	1	17	1	3	1	4	1	1	52

ARC-ARC TRANSITION MATRIX FOR SECTOR 454

	000	451	455	456	472	EWR	LGA	PHL	TOT
000	0	1	0	0	1	0	0	0	2
461	1	10	0	0	0	0	1	5	17
464	0	0	1	0	0	1	17	0	19
EWR	2	8	0	4	0	0	0	2	16
TOT	3	19	1	4	1	1	18	7	54

Table 4.10 Arc-arc Transition Matrices with Counts in New York Enroute Network (cont.)

ARC-ARC TRANSITION MATRIX FOR SECTOR 455

	000	451	464	469	EWR	LGA	TOT
000	1	0	1	0	1	0	3
451	1	0	0	0	0	0	1
453	0	0	0	0	15	0	15
454	0	0	0	0	0	1	1
458	0	0	0	1	0	0	1
461	0	3	0	0	0	0	3
464	0	0	0	0	13	2	15
476	0	0	0	0	1	0	1
TOT	2	3	1	1	30	3	40

ARC-ARC TRANSITION MATRIX FOR SECTOR 456

	000	451	476	JFK	TOT
453	1	0	0	1	2
454	0	0	4	0	4
457	0	0	0	1	1
458	0	0	0	2	2
461	0	2	3	0	5
476	0	0	0	10	10
478	0	0	0	16	16
TOT	1	2	7	30	40

ARC-ARC TRANSITION MATRIX FOR SECTOR 457

	456	JFK	LGA	TOT
000	0	0	1	1
453	0	1	15	16
464	1	1	0	2
467	0	2	0	2
PHL	0	1	0	1
ACY	0	1	0	1
TOT	1	6	16	23

Table 4.10 Arc-arc Transition Matrices with Counts in New York Enroute Network (cont.)

ARC-ARC TRANSITION MATRIX FOR SECTOR 458

	000	455	456	467	468	469	477	482	483	TOT
000	0	0	0	0	0	1	0	0	0	1
460	0	0	0	0	1	0	0	0	0	1
467	0	1	0	0	0	2	0	0	0	3
468	0	0	0	0	0	1	0	0	1	2
469	3	0	0	2	1	0	1	0	0	7
482	0	0	2	0	0	0	0	0	0	2
JFK	1	0	0	3	2	0	17	6	0	29
TOT	4	1	2	5	4	4	18	6	1	45

ARC-ARC TRANSITION MATRIX FOR SECTOR 459

	000	460	473	474	480	TOT
000	0	3	1	0	0	4
460	0	0	1	0	0	1
480	1	0	0	0	0	1
JFK	1	1	0	1	0	3
LGA	7	5	0	3	0	15
HPN	2	0	1	0	1	4
TOT	11	9	3	4	1	28

ARC-ARC TRANSITION MATRIX FOR SECTOR 460

	000	458	459	469	JFK	TOT
000	2	1	2	0	11	16
459	8	0	0	1	1	10
469	0	0	0	0	3	3
481	1	0	0	0	10	11
483	0	0	0	0	2	2
TOT	11	1	2	1	27	42

Table 4.10 Arc-arc Transition Matrices with Counts in New York Enroute Network (cont.)

ARC-ARC TRANSITION MATRIX FOR SECTOR 461

	000	454	455	456	462	463	471	472	473	478	EWR	TOT
000	0	1	0	0	0	0	1	0	0	0	0	2
459	0	1	0	0	0	0	0	0	0	0	0	1
462	1	5	1	1	0	0	0	1	0	0	4	13
463	0	4	0	0	0	0	0	0	0	0	0	4
464	0	0	0	0	0	0	0	0	0	1	0	1
EWR	0	0	0	0	2	3	1	3	1	0	0	10
LGA	0	7	1	4	0	0	0	6	1	0	0	19
TOT	1	18	2	5	2	3	2	10	2	1	4	50

ARC-ARC TRANSITION MATRIX FOR SECTOR 462

	461	463	473	TOT
461	0	0	2	2
473	2	0	0	2
481	8	0	0	8
JFK	0	0	3	3
LGA	0	21	0	21
HPN	3	0	0	3
TOT	13	21	5	39

ARC-ARC TRANSITION MATRIX FOR SECTOR 463

	000	461	471	473	480	TOT
000	0	0	0	1	0	1
461	0	0	0	4	0	4
462	0	0	4	2	14	20
472	0	0	0	9	0	9
474	1	0	0	0	0	1
481	0	4	0	0	0	4
JFK	0	0	1	0	10	11
TOT	1	4	5	16	24	50

Table 4.10 Arc-arc Transition Matrices with Counts in New York Enroute Network (cont.)

ARC-ARC TRANSITION MATRIX FOR SECTOR 464

	000	451	454	455	457	461	465	466	470	472	475	480	ABE	TOT
451	0	0	0	0	0	1	0	0	3	4	0	0	0	8
455	0	0	0	0	0	0	0	0	1	0	0	0	0	1
465	0	0	2	2	2	0	0	0	0	0	0	0	0	6
466	0	0	0	0	0	0	0	0	0	5	0	0	0	5
470	0	0	1	0	0	0	0	0	0	0	0	0	1	2
472	1	0	0	0	0	0	0	3	0	0	0	0	0	4
475	0	0	17	11	0	0	0	0	0	0	0	0	1	29
PHL	0	1	0	0	0	0	0	0	0	0	0	0	0	1
HAR	0	0	0	1	0	0	0	0	0	1	0	0	0	2
ABE	0	0	0	0	0	0	2	1	0	2	1	2	0	8
TOT	1	1	20	14	2	1	2	4	4	12	1	2	2	66

ARC-ARC TRANSITION MATRIX FOR SECTOR 465

	000	464	466	470	TOT
000	2	4	0	3	9
464	2	0	0	0	2
466	3	0	0	4	7
470	5	0	1	0	6
HAR	1	0	0	0	1
TOT	13	4	1	7	25

ARC-ARC TRANSITION MATRIX FOR SECTOR 466

	000	451	464	465	PHL	ILG	TOT
000	0	0	5	3	6	1	15
451	3	1	0	1	0	0	5
453	1	0	0	0	0	0	1
464	3	0	0	0	0	0	3
465	1	0	0	0	0	0	1
475	1	0	0	0	0	0	1
479	1	1	0	0	14	0	16
HAR	5	1	1	1	0	0	8
TOT	15	3	6	5	20	1	50

Table 4.10 Arc-arc Transition Matrices with Counts in New York Enroute Network (cont.)

ARC-ARC TRANSITION MATRIX FOR SECTOR 467

	000	453	457	458	467	468	PHL	ACY	ILG	TOT
000	5	1	2	0	1	1	2	1	3	16
453	1	0	0	0	0	0	0	2	0	3
458	1	1	0	0	0	0	2	0	2	6
467	1	0	0	0	0	0	0	0	0	1
468	1	2	0	0	0	0	4	0	0	7
477	1	4	0	0	0	0	0	0	0	5
PHL	5	0	0	4	0	3	0	0	0	12
ILG	2	0	0	0	0	0	0	0	0	2
TOT	17	8	2	4	1	4	8	3	5	52

ARC-ARC TRANSITION MATRIX FOR SECTOR 468

	000	458	467	477	ACY	ILG	TOT
000	6	0	6	2	1	1	16
458	4	0	0	0	0	0	4
467	4	0	0	0	0	0	4
477	2	0	0	0	0	0	2
482	1	0	0	0	0	0	1
ACY	3	1	2	0	0	0	6
TOT	20	1	8	2	1	1	33

ARC-ARC TRANSITION MATRIX FOR SECTOR 469

	000	458	460	483	TOT
000	1	3	0	0	4
455	1	0	0	0	1
458	3	0	0	1	4
460	0	1	0	0	1
483	6	1	2	0	9
JFK	2	0	0	2	4
TOT	13	5	2	3	23

Table 4.10 Arc-arc Transition Matrices with Counts in New York Enroute Network (cont.)

ARC-ARC TRANSITION MATRIX FOR SECTOR 470

	000	464	465	471	472	AVP	ELM	TOT
000	2	1	0	6	1	0	0	10
464	1	0	0	2	0	1	0	4
465	3	0	0	2	0	0	2	7
471	3	2	2	0	0	0	0	7
472	1	0	3	0	0	0	0	4
AVP	1	0	1	0	1	0	0	3
ELM	4	0	0	0	0	0	0	4
TOT	15	3	6	10	2	1	2	39

ARC-ARC TRANSITION MATRIX FOR SECTOR 471

	000	470	472	473	480	BGM	ELM	TOT
000	2	5	1	3	1	1	1	14
461	0	0	0	0	0	2	0	2
463	2	0	0	0	0	1	0	3
470	4	0	0	3	0	0	0	7
472	1	0	0	0	0	0	0	1
473	1	2	0	0	0	1	0	4
480	0	0	1	0	0	0	0	1
BGM	0	2	0	1	0	0	0	3
ELM	1	0	1	0	0	0	0	2
TOT	11	9	3	7	1	5	1	37

ARC-ARC TRANSITION MATRIX FOR SECTOR 472

	000	462	463	464	470	471	473	475	480	EWR	TOT
000	2	0	0	0	0	0	0	0	0	0	2
454	0	1	0	0	0	0	0	0	0	0	1
461	0	0	0	1	1	1	0	1	6	0	10
464	0	0	4	0	0	0	9	0	0	0	13
470	0	0	0	0	0	0	0	0	0	2	2
471	0	0	0	0	0	0	0	0	0	3	3
473	0	0	0	1	0	0	0	0	0	0	1
475	0	0	3	0	0	0	1	0	0	0	4
480	0	0	1	0	0	0	0	0	0	0	1
EWR	0	0	0	3	3	0	0	3	14	0	23
TOT	2	1	8	5	4	1	10	4	20	5	60

Table 4.10 Arc-arc Transition Matrices with Counts in New York Enroute Network (cont.)

ARC-ARC TRANSITION MATRIX FOR SECTOR 473

	000	462	471	472	473	474	481	HPN	TOT
000	1	0	1	1	0	0	1	0	4
459	1	0	1	1	0	0	0	0	3
461	2	0	0	0	0	0	0	0	2
462	1	0	1	0	0	3	0	0	5
463	4	0	0	0	0	4	3	5	16
471	1	0	0	0	0	1	5	0	7
472	2	0	0	0	0	6	1	1	10
473	0	0	0	0	0	1	0	0	1
474	0	2	2	2	0	0	0	0	6
480	0	0	0	0	1	0	2	0	3
TOT	12	2	5	4	1	15	12	6	57

ARC-ARC TRANSITION MATRIX FOR SECTOR 474

	000	463	473	480	481	HPN	TOT
000	2	0	8	2	5	3	20
459	4	0	0	0	0	0	4
473	14	1	0	0	0	0	15
481	2	0	0	0	0	0	2
TOT	22	1	8	2	5	3	41

ARC-ARC TRANSITION MATRIX FOR SECTOR 475

	000	464	466	472	475	478	479	480	TOT
000	0	25	0	2	0	0	0	1	28
464	1	0	0	0	0	0	0	0	1
472	1	0	0	0	0	4	0	0	5
475	1	0	0	0	0	0	0	0	1
478	0	0	0	1	0	0	0	1	2
479	0	0	0	1	0	0	0	2	3
480	7	1	2	0	1	7	1	0	19
TOT	10	26	2	4	1	11	1	4	59

Table 4.10 Arc-arc Transition Matrices with Counts in New York Enroute Network (cont.)

ARC-ARC TRANSITION MATRIX FOR SECTOR 476

	000	453	455	456	477	482	TOT
000	0	12	1	4	4	1	22
456	3	0	0	0	4	0	7
477	0	0	0	6	0	0	6
TOT	3	12	1	10	8	1	35

ARC-ARC TRANSITION MATRIX FOR SECTOR 477

	000	467	468	476	479	483	TOT
000	2	3	0	6	0	0	11
458	6	0	1	0	11	0	18
467	1	0	0	0	0	1	2
468	0	0	0	0	0	2	2
476	2	0	0	0	0	4	6
483	0	1	3	0	1	0	5
TOT	11	4	4	6	12	7	44

ARC-ARC TRANSITION MATRIX FOR SECTOR 478

	000	456	475	TOT
000	1	17	1	19
461	1	0	0	1
475	11	0	0	11
479	0	0	1	1
TOT	13	17	2	32

Table 4.10 Arc-arc Transition Matrices with Counts in New York Enroute Network (cont.)

ARC-ARC TRANSITION MATRIX FOR SECTOR 479

	000	466	475	478	479	TOT
000	3	14	3	1	1	22
451	8	0	0	0	0	8
475	1	0	0	0	0	1
477	11	0	0	0	0	11
479	1	0	0	0	0	1
TOT	24	14	3	1	1	43

ARC-ARC TRANSITION MATRIX FOR SECTOR 480

	000	459	471	472	473	475	481	TOT
000	3	0	1	0	2	5	4	15
459	0	0	0	0	0	1	0	1
463	17	0	0	0	0	2	0	19
464	2	0	0	0	0	0	0	2
471	0	0	0	0	0	1	0	1
472	8	0	0	0	0	9	0	17
474	2	0	0	0	0	0	0	2
475	0	1	0	1	1	0	1	4
481	0	0	0	0	0	2	0	2
TOT	32	1	1	1	3	20	5	63

ARC-ARC TRANSITION MATRIX FOR SECTOR 481

	000	460	462	463	474	480	483	LGA	HPN	TOT
000	1	3	7	4	0	2	1	8	0	26
473	1	4	0	0	1	0	0	7	2	15
474	0	1	0	0	1	0	0	3	0	5
480	1	3	0	0	0	0	1	0	0	5
TOT	3	11	7	4	2	2	2	18	2	51

Table 4.10 Arc-arc Transition Matrices with Counts in New York Enroute Network (cont.)

ARC-ARC TRANSITION MATRIX FOR SECTOR 482

	000	458	483	TOT
COC	1	1	6	8
458	5	0	0	5
476	0	0	1	1
TOT	6	1	7	14

ARC-ARC TRANSITION MATRIX FOR SECTOR 483

	000	460	469	477	TOT
000	0	2	4	6	12
458	1	0	0	0	1
469	3	0	0	0	3
477	2	0	6	0	8
481	0	1	0	0	1
482	1	3	0	0	4
TOT	7	6	10	6	29

i^{th} row is $\sum_{\ell} n_{ij\ell}$. Then

$$\hat{p}_{ijk} = \frac{n_{ijk}}{\sum_{\ell=1}^{c} n_{ij\ell}}$$

where c is the number of columns in the ith matrix.

Tables 4.6, 4.7, and 4.10 thus completely describe the sequence of sectors through which aircraft move. Given λ_i for all sources, $p_{k|i}$ for the probability of aircraft generated at each source entering the network over arc (s,N_k), and the probabilities p_{ijk} for moving aircraft through the network, the traffic is completely specified.

4.5.6 Relating Sink Attraction Rates to Source Generation Rates

The problem described earlier for determining source generation rates from sink attractions can now be solved under the assumption that class (iii) traffic is insignificant. (Class (iii) is the traffic that both departs and arrives at airports in the region.) In the data sample, this class represented less than 3 per cent of the traffic through the network.

If it is assumed that class (iii) traffic is not significant, then all traffic attracted to the airports in the region can be considered to enter the sector through the enroute source. Thus

$$\lambda_e = \lambda_{\leftrightarrow} + \sum_{j=1}^{m_t} \mu_j \tag{4.53}$$

where $\lambda_{\leftrightarrow}$ is the rate of through-traffic passing through the network. If $\lambda_{\leftrightarrow}$ and the μ's are used to determine λ_e, equation (4.32) will be consistent.

The final problem involves determining the conditional probability $p_{k|s_e}$ for entry to the network from the enroute source. The solution proposed is to specify the sink attraction rates μ_j and then backsolve using the transitional probabilities p_{ijk} to determine the arrival components of $p_{k|s_e}$. The through-components would be the weighted difference between the arrival components and the estimates of $p_{k|s_e}$ determined from all traffic at the enroute source.

4.5.7 Summary

The formulation presented in this chapter could be applied to a general ATC network to determine the flow patterns over the network given specified rates of traffic arriving and departing from sources and sinks to the network. An extensive data base is needed if all transition probabilities are to be estimated, but for specified probabilities the techniques are easily applied.

It should be recognized that the aspects of the network studied in this report only give a microscopic description of traffic flow. Important variables such as transit times and communication measures have yet to be studied. The attempt here has been to formulate the ATC system in network terms and to describe the general patterns of flow in such a way that a simulation model could be easily constructed.

The New York enroute network example was perhaps a more complicated network than would usually be studied. For oceanic systems, the number of sectors will be much smaller and the traffic patterns much simpler. The same sort of analysis as was applied to the N.Y. enroute network in this report could thus be applied with much less effort to these simpler networks, yet the possible conclusions would be at least as powerful.

Finally, it is felt that while the network model at this level of sophistication could produce interesting conclusions about the locations of heavy traffic flow in networks, stronger statements will be possible after transit times and communication requirements are introduced.

APPENDIX 4-A

TABULATION OF ENROUTE SECTOR TRAFFIC

Technical report PU-42 includes a list of all traffic observed through the N.Y. enroute sectors during a 2 -hour sample period. The list, which provided the raw data for use in this chapter, includes the following information:

*1 Classification of aircraft type

*2 Aircraft identification code

*3 Entry and exit movement patterns

4 Sample entry and exit times in seconds (0-7200)

5 Traffic class

a. ARV - arrival from an airport in the region
b. DEP - departure from an airport in the region
c. (blank) - through-traffic
d. - - - - - - unidentifiable since sector sequence is cut by end of sample period

6 Sector sequence in order of entry times.

* For description, see Hunter et al.(1973)

The following sectors were held to indicate arrivals and departures from airports in the region:

EWR-ARV	546,547,548	EWR-DEP	534
JFK-ARV	549,550,551	JFK-DEP	535
LGA-ARV	552,553,554	LGA-DEP	536
PHL-ARV	555,556	PHL-DEP	537,538
ACY-ARV	545	ACY-DEP	533
ILG-ARV	511,543	ILG-DEP	511,543
AVP-ARV	525,539	AVP-DEP	525,539
BGM-ARV	526,540	BGM-DEP	526,540
HAR-ARV	509,541,542	HAR-DEP	509,541,542
ABE-ARV	524,529	ABE-DEP	524,529
ELM-ARV	527,530	ELM-DEP	527,530
HPN-ARV	510,531	HPN-DEP	510,531

APPENDIX 4-B

LIST OF NOTATIONS

Notation

m	=	# of sectors (nodes) in a network G
N_k	=	sector k $(k=1,2,\ldots, m)$
G	=	network
N	=	set of nodes in G
A	=	set of arcs in G
s	=	super-source
t	=	super-sink
D	=	node-node incidence matrix
d_{ij}	=	element in i^{th} row and j^{th} column of D
F	=	traffic flow rate from s to t
(X,Y)	=	set of arcs from nodes in set X to nodes in set Y
$f(X,Y)$	=	traffic flow rate over arcs in (X,Y)
s_i	=	source i $(i = 1,2, \ldots, m_s)$
m_s	=	# of sources with arcs to s
t_j	=	sink j $(j = 1, 2, \ldots, m_t)$
m_t	=	# of sinks with arcs from t
λ_i	=	traffic generation rate at source i
μ_j	=	traffic attraction rate at sink j
p_k	=	prob. that aircraft enters network at sector k
$p_{k\|i}$	=	prob. that aircraft generated at source i enters network at sector k
λ_s	=	traffic flow rate through s

$\underset{\sim}{\lambda}$ = $(m_s x\ 1)$ vector of source generation rates

$\underset{\sim}{P}$ = $(m_s x m)$ matrix of source-node entry probabilities $P_{k|i}$

C = source-node entry count matrix

c_{ik} = element of C equal to the number of aircraft which were generated at source i and entered the network over arc (s,N_k)

c_i = number of aircraft generated at source i during the sample period

T = number of time units in the sample period

$\{S_n(k),\ k=0,1,2,\ \ldots\}$ = sequence of sectors traversed by n^{th} aircraft

m_n = number of network sectors traversed by n^{th} aircraft

$P^{(q)}$ = q-step transition matrix

$p_{ij}^{(q)}$ = prob. of going from sector i to sector j in q-steps

e_{ij} = probability of an arrival from source i ending up at sink j

$n_k,\ n_{jk},\ n_{ijk}$ = counts of observed transitions between sectors in a sample of sector sequences

$I_k(x),\ I_{jk}(x,y),\ I_{ijk}(x,y,z)$ = indicator functions for sector sequences

$p_k,\ p_{jk},\ p_{ijk}$ = state transition probabilities

$\lambda_{\leftrightarrow}$ = flow rate of through-traffic in G

λ_e = arrival rate of enroute traffic

$p_{k|s_e}$ = conditional probability of entering the network over arc (s,N_k) given generation at the enroute source.

APPENDIX 4-C

REFERENCES OF CHAPTER 4

Anderson, T.W. and Goodman, L.A., "Statistical Inference about Markov Chains," Annals of Mathematical Statistics, 28, No. 1 (1957), 89-110.

Chatfield, C., "Statistical Inference Regarding Markov Chain Models," Applied Statistics, 22, No. 1 (1973), 7-20.

Duncan, G.T. and Lin, L.G., "Inference for Markov Chains Having Stochastic Entry and Exit," Journal of the American Statistical Association, 67, No. 340 (1972), 761-767.

Ford, L.R. and Fulkerson, D.R., Flows in Networks, Princeton University Press, 1962, Princeton, N.J.

Hu, T.C., Integer Programming and Network Flows, Addison Wesley, 1969, Reading, Mass.

Hunter, J.S. (et. al.), "Modeling Air Traffic Performance Measures," vol. II, "Initial Data Analyses and Simulations"(1973), vol. III, "Simulation Model for N.Y. ATC Communications,"Federal Aviation Administration report no. DOT FA72NA-741, Princeton University, Princeton, N.J.

Johnson, N.L. and Kotz, S., Continuous Univariate Distributions - 1, Houghton Mifflin Co., (1970), Boston, Mass.

Johnson, N.L. and Kotz, S., Discrete Distributions, Houghton Mifflin Co., (1969), Boston, Mass.

Kulldorf, G., Contributions to the Theory of Estimation from Grouped and Partially Grouped Samples, John Wiley & Sons, Inc., (1961) New York.

Lilliefors, H.W., "On the Kolmogorov-Smirnov Test for the Exponential Distribution with Mean Unknown," Journal of the American Statistical Association, 64, No. 325 (1969), 387-389.

Massey, L.H., "The Kolmogorov-Smirnov Test for Goodness-of-Fit," Journal of the American Statistical Association, 46 (1951), 68-78.

Parzen, E., Stochastic Processes, Holden-Day, 1962, San Francisco

Polhemus, N.W., "Modeling Aircraft Flow in Air Traffic Control Systems," Proceedings of the Transportation Research Forum, Oct., 1974.

Potts, R.B. and Oliver, R.M., Flows in Transportation Networks, Academic Press, 1972, New York.

CHAPTER 5

MISCELLANEOUS RELATED STUDIES

5.1 Introduction

As has been explained in previous chapters, in the ATC simulation model, seven input parameters plus a historical histogram are used to characterize the entire input system. Questions have been asked as to how much each of these variables contributes to the expected utilization of the communications channel. To answer this question a mathematical analysis has been carried out and reported in section 5.2.

In practical applications of the simulation model, particularly for measuring the operational stability of the ATC system, indices which are easy to understand and convenient for use are of great help. A proposal on the compilation of a triplet of three operational indices, each representing a major response, is given in section 5.3.

Continuing effort has been devoted to the exploration of the coupling of responses observed in adjacent sectors. Transfer function models which link the aircraft loading series at two functionally related sectors have been constructed using Box-Jenkins modeling techniques, and reported in section 5.4.

A statistical investigation on four sets of 8-hour data collected from New York center (Sectors 454LT, 515LC, 536DP and 554AR) was completed and results reported in section 5.5. This study will be useful for constructing a simulation model with unstable input flows, observed over long periods of time.

To pursue a statistical model satisfactorily describing the queuing time processes generated from a simulation model, a transformation technique was developed to make the series easier for parametric time series analysis. The resulting statistical model is useful for queuing time forecasting in a nonhomogeneous arrival system such as ATC communications. The potential usefulness of this study to ATC network simulations is elucidated and reported upon in section 5.6.

5.2 Sensitivity Analysis of the Expected ATC Communications Channel Utilization

In the simulation model which has been developed for ATC systems to date, seven initiating parameters plus one historical histogram are used to characterize the entire input system to the simulation framework. Questions have been asked about how important, relatively, each of these input parameters is to the overall expected channel utilization. To answer these questions a sensitivity analysis is developed and presented in this section.

5.2.1 Derivation of the Sensitivity Equations

As earlier demonstrated in the report, volume III, parameters of major importance in the simulation model are:

θ : number of aircraft arrivals per hour;

α, λ : parameters of a gamma distribution fitted to the transmission lengths;

p, k : the two parameters in a negative binomial distribution fitted to the number of CT's per aircraft (shifting the origin by two for the data of Enroute sectors, and by one for the remaining);

a_o, a_1 : regression coefficients for generating intercommunication gap lengths, depending on #CT/AC;

τ : the expected number of transmissions per communication transaction.

Important properties and relationships among these parameters are briefly reviewed and displayed in the following mathematical equations:

(i) E(TR) = expected transmission length (seconds)

$$= \alpha \cdot \lambda = b_o - b_1\theta = 3.70 - 0.0158\theta \text{ (for all except LC Sectors)}$$
$$= 2.97 - 0.0042\theta \text{ (for LC Sectors)}$$

(ii) E(#TR/CT) = expected number of transmissions per transaction = τ

(iii) E(#CT/AC) = expected number of transactions per aircraft

$= k(\frac{1}{p} - 1) + m$ where m=2, for Enroute sectors, and m=1, otherwise.

If we now assume the three variables TR, #TR/CT and #CT/AC are mutually independent and that the values of the parameters a_0 and a_1 are moderate, it can be shown that:

$$
\begin{aligned}
E(CU) &= \text{expected channel utilization, in seconds per hour} \\
&= \Theta \cdot E(TR) \cdot E(\#TR/CT) E(\#CT/AC) \\
&= \Theta \cdot (b_o - b_1\Theta) \cdot \tau \cdot [k(\tfrac{1}{p} - 1) + m] \\
&= b_o \cdot \Theta(1 - b_1\Theta/b_o) \cdot \tau \cdot [k(\tfrac{1}{p} - 1) + m] \qquad (5.1)
\end{aligned}
$$

Let y = E(CU) and x be any variable on the right side of Equation (5.1). The elasticity η, that is, the percentage change in y resulting from a one percent change in x, is then defined as

$$
\eta_x = \frac{\partial \log y}{\partial \log x} = \frac{d \log y}{dy} \cdot \frac{\partial y}{\partial x} \cdot \frac{dx}{d\log x}
$$

$$
= \frac{\partial y}{y} \Big/ \frac{\partial x}{x} .
$$

From Equation (5.1), taking logarithms on both sides, we find that

$$
\log y = \log b_o + \log \Theta + \log (1 - \frac{b_1}{b_o}\Theta) + \log \tau + \log [k(\frac{1}{p} - 1) + m]
$$

To reduce notation, let $w = [k(\frac{1}{p} - 1) + m]$, then the elasticities of the expected channel utilization with respect to τ, w and Θ are

$$
\eta_\tau = \frac{\partial \log y}{\partial \log \tau} = 1 \qquad (5.2)
$$

$$
\eta_w = \frac{\partial \log y}{\partial \log w} = 1 \qquad (5.3)
$$

and

$$
\eta_\Theta = 1 - \frac{\Theta}{(b_o/b_1) - \Theta} = \frac{(b_o/b_1) - 2\Theta}{(b_o/b_1) - \Theta} \qquad (5.4)
$$

Using Equation (5.2) and (5.3) we note that a 1- percent change in either $E(\#TR/CT) = \tau$ or $E(\#CT/AC) = w$, but not both, will generate a 1-per cent change in the value of E(CU), given all the other elements in the equation being held constant. On the other hand, Equation (5.4) tells us that the relative change in E(CU) is always smaller than unity, when the traffic density, Θ, is changed. In other words, when the traffic density is reduced (increased) by 50 per cent, the channel utilization will drop (rise) by less than 50 per cent.

Furthermore, to pursue the elasticity measure η_w one more step, we find

$$
\eta_k = k \cdot [k(\frac{1}{p} - 1) + m]^{-1} (\frac{1}{p} - 1) \qquad (5.5)
$$

$$
\eta_p = -[k(\frac{1}{p} - 1) + m]^{-1} (k/p) \qquad (5.6)
$$

Though the physical meanings of η_k and η_p are difficult to express, a numerical illustration will be illuminating. Using the N.Y. HI sector function as an example we calculate the elasticities η_Θ, η_k and η_p for values of Θ, k and p, close to those observed in the historical data. The resulting curves are displayed in figures 5.1-5.3. (In figures 5.2 and 5.3 since the estimates of (k,p) for the HI sector function are (k=4.03, p=0.58), we computed η_k at p=0.58 and computed η_p at k=4.03). Computations for other sector functions can be similarly performed.

5.2.2 Concluding Remarks on the Sensitivity Analysis

In the discussion presented above we have ignored the influence of the driving variables upon queuing. It is naive to judge the influence of a variable solely based on the expected channel utilization. A sensitivity analysis for the queuing response requires large scale simulation experiments and is postponed for a future study.

5.3 Construction of Operational Indicies for ATC Communication Performance

A characterization of various major responses in ATC communication channels has been presented in earlier reports. In volume III sophisticated statistical techniques are used: to construct a simulation model, to validate the simulated responses, and to detect operational instability under heavy traffic situations. However, much of this material is mathematical, containing expressions usually not of great value to those with the responsibility of actually operating ATC processes. In this study we explore some equivalent, but simple, indicators of the operational soundness (stability) of ATC communications performance. The objective is to stimulate interest in experimenting with the ATC communication simulation model by ATC personnel.

As discussed in chapter 3 of this volume, communication capacities of ATC communications functions were measured by the average responses generated from a series of simulation exercises, along with a nonstationarity detector defined as $P_r(\xi>1)$, imposed upon the aircraft loading time series. To express the operational stability or soundness of an ATC channel in a simple and informative manner, ideas that produced the measurements of many physical phenomena such as temperature, humidity, etc., can be of great use. For instance, the boiling temperature of water under the normal pressure of gravity was set equal to 100° in the Celsius scale. In this case, the number "100" is used to indicate a critical condition of water transformations. Similarly, the operation of an ATC system can be expressed and quantified in the way temperature is represented by a thermometer. Using such a system the communication performance can be read and understood at the instant a measurement is made. However, the determination of a critical point, such as the 100° design for a Celsius thermometer, for an ATC system depends on the system conditions, the ability of a controller, etc. More information and understanding is needed to formulate these measurements. Some behavior

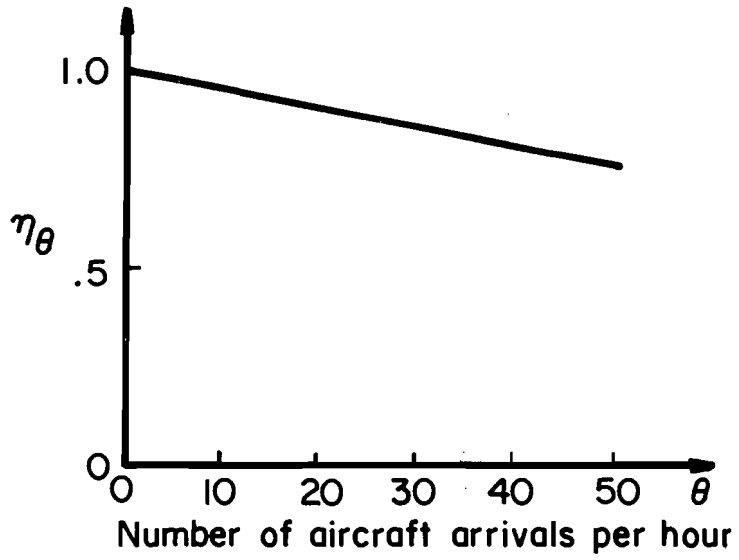

Figure 5.1 Elasticity Measure η_θ (N.Y. HI Function)

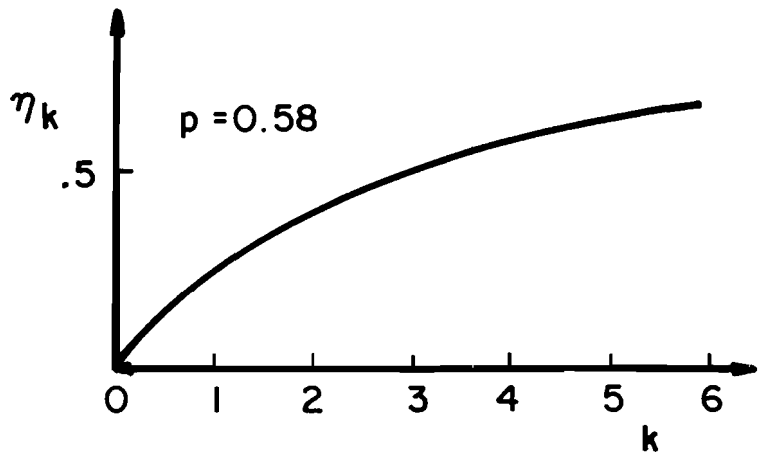

Figure 5.2 Elasticity Measure η_k (N.Y. HI Function)

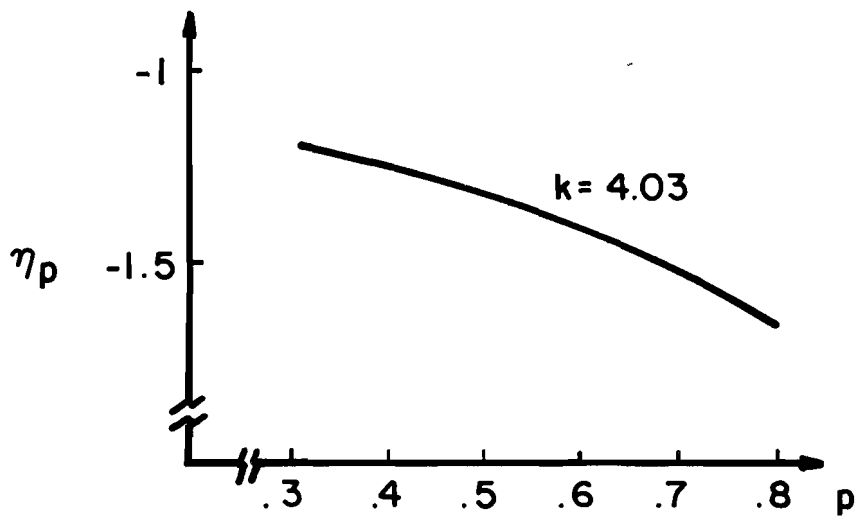

Figure 5.3 Elasticity Measure η_p (N.Y. HI Function)

inherent to the ATC systems is first described in the first subsection with some analogies from physical sciences. Numerical illustrations are then provided in the subsequent subsection for examples previously studied.

5.3.1 Some Basic Considerations

Physics tells us that when the concentration of a solvent in the solution tends closer to its saturation point, an exponential increase in time or pressure, is required to achieve each incremental gain in concentration. Further, many physical phenomena are multivariate in aspect, requiring the simultaneous monitoring of several responses. Similarly, in a communications channel, when the percentage channel utilization approaches its ceiling, say 85 per cent, the demands made upon a controller are not proportionally but, instead, exponentially related to incremental changes in channel utilization. And further, variables in addition to channel utilization are necessary to characterize sector communications loading.

Following this reasoning, we have selected exponential models for the construction of three separate operation indices to represent communications loading. An index is compiled for each of three major responses: aircraft loading, channel utilization and communications queuing. For the reasons just stated in an analogy of Celsius thermometer the number 100 is selected to be used as a critical value for each index. Thus, when a response yields an index close to 100, that response is about to become unstable and unsatisfactory operation of the channel destined to ensue.

5.3.2 Operational Indices for ATC Communications

The simulation model for ATC communications within a sector, described in volume III, can be exercised by varying any of the following parameters previously defined, either singly or in combination: θ, p, k, α, λ, a_o, a_1, and the distribution of #TR/CT. Further, by using the message element dictionaries, additional modifications in the number and lengths of transmissions are possible. For any particular setting of these input parameters three time series responses are generated in the simulation representing the burden of air traffic and communications in the sector:

n_t : number of aircraft present per minute,

c_t : channel utilization per minute,

q_t : number of aircraft in communications queue per minute.

A series equivalent to $\{q_t\}$ is :

Q_i : communications queuing times per CT, where i means "for the ith CT attempted"

A second order autoregressive time series model was found adequate for describing the series $\{n_t\}$. Furthermore, overall averages of channel utilization or queuing time can be calculated from entire series of $\{c_t\}$ or $\{Q_i\}$.

In volume III, chapter 4, the aircraft arrival rate θ was experimentally varied to determine the effect upon the three responses. Much valuable information was gained from a close study of the three time series responses. The information can now be encapsulated by the three indices I_a, I_b, I_c.

Let the multivariate aspects of the sector communications loading be written as a triplet of three indices I_a, I_b, I_c

where I_a : an index which indicates the stability of the aircraft loading time series;

I_b : an index determined from the recorded channel utilization, as a fraction;

I_c : an index on communication queuing times generated from the simulation model.

Useful functional forms which express these three indices are:

$$I_a = f_1(x) = 100\ e^{(1.645 - x)}$$

$$I_b = f_2(y) = 100\ e^{\left(\frac{0.20}{1-y} - 1\right)}$$

$$I_c = f_3(z) = 100\ e^{(z/50 - 1)} \qquad (5.7)$$

Although the constants in these index models are somewhat arbitrary, the results of indexing applied to some data generated by simulations, appears consistent with our a priori judgment. The quantities x,y, and z are

$x = \hat{\xi}/\hat{\phi}_\xi$ where $\hat{\xi}=1-\hat{\phi}_1-\hat{\phi}_2$ and where $\hat{\phi}_1$ and $\hat{\phi}_2$ are the autoregressive parameters of the aircraft loading time series generated from the simulation model and $\hat{\sigma}_\xi$ is the associated standard deviation;

$y =$ overall channel utilization with the value between zero and one;

$z =$ average queuing time (seconds) per communications transaction.

Plots of the indices I_a, I_b and I_c as functions of x, y, and z are displayed in figures 5.4 - 5.6. Numerical illustrations using various examples demonstrated in volume III are provided in tables 5.1 and 5.2. More specifically, table 5.1 presents the movements of the indices at different traffic densities while table 5.2 provides a set of indices for various functions exercised at the historical traffic densities.

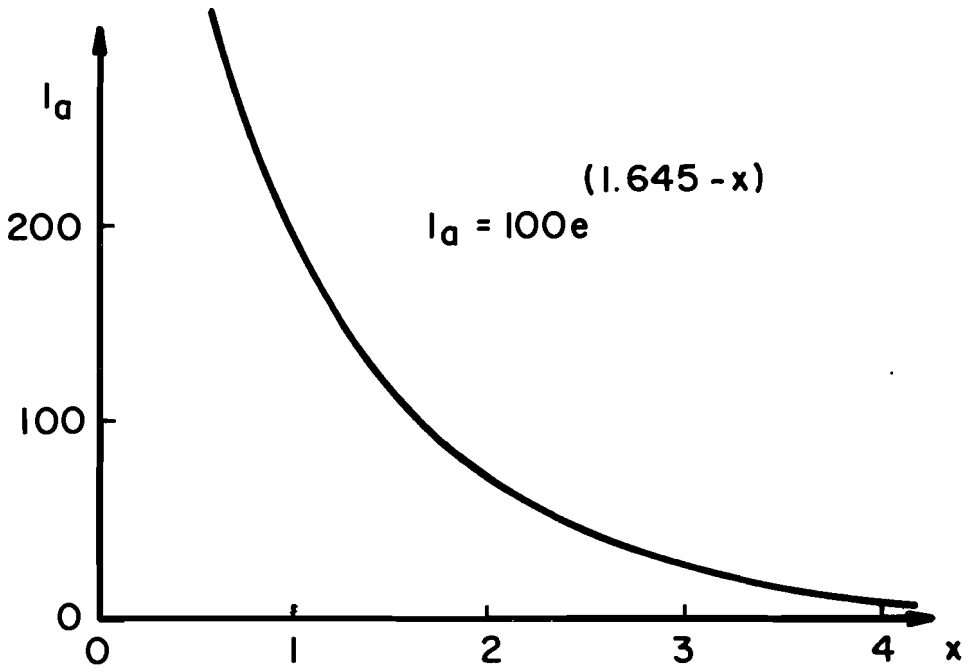

Figure 5.4 Operational Index I_a for Aircraft Loading Time Series

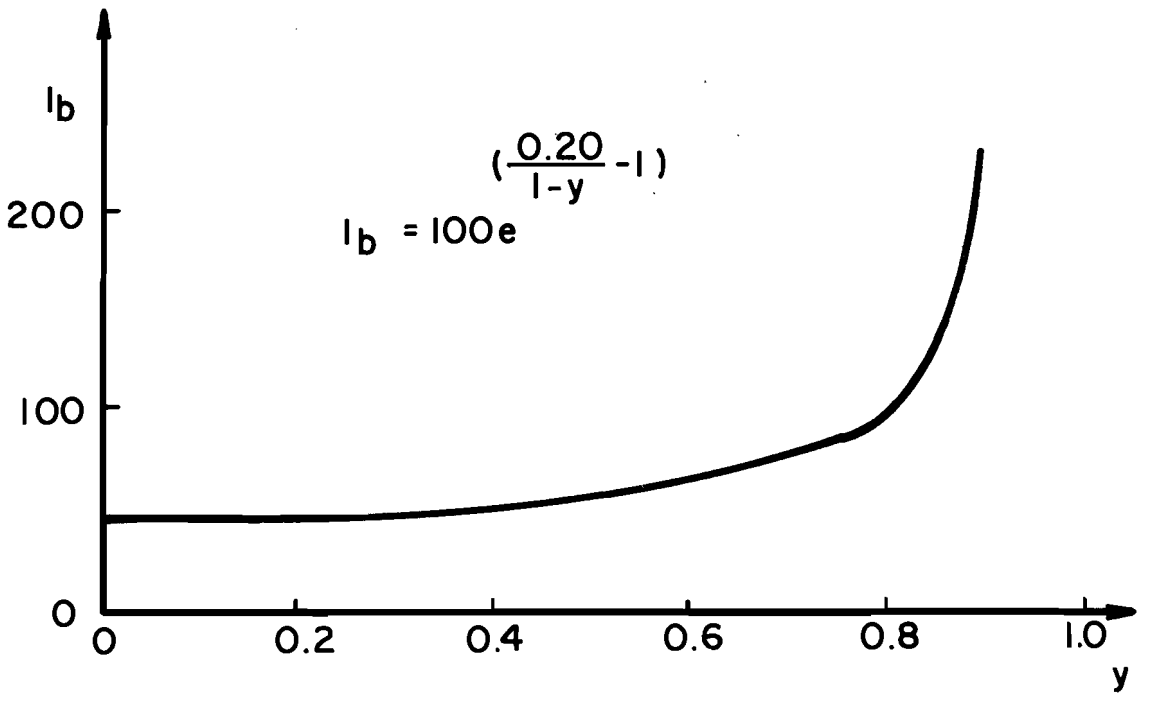

Figure 5.5 Operational Index I_b for Channel Utilization

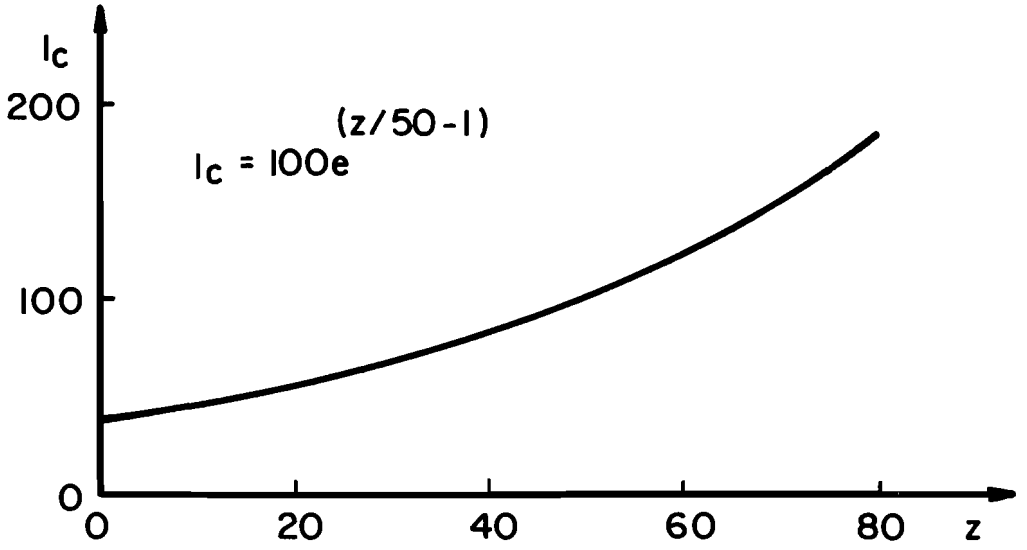

Figure 5.6 Operational Index I_c for Queuing Time

Table 5.1 ATCC Operational Indices for N. Y. Sector 475 HI at Various Experimental Traffic Densities

Traffic density	x	y	z (sec.)	(I_a, I_b, I_c)
50%	4.4	0.3290	3.861	(6, 50, 40)
100%	4.0	0.5631	10.428	(9, 58, 45)
125%	3.6	0.6976	20.526	(14, 71, 55)
150%	1.6	0.8353	56.818	(105,124,115)

Traffic density 100% = 33 aircraft arrivals/hour.

Table 5.2 ATCC Operational Indices for Eight N. Y. Sectors at Historical Traffic Densities

Sector ID	x	y	z (seconds)	(I_a, I_b, I_c)
453 LT	2.100	0.53	12.530	(63, 56, 47)
475 HI	3.965	0.56	10.430	(9, 58, 45)
504 GN	2.700	0.47	15.405	(35, 54, 50)
510 LC	2.415	0.47	7.215	(46, 54, 42)
524 LG	1.895	0.34	9.021	(78, 50, 44)
534 DP	2.515	0.47	6.782	(42, 54, 42)
543 AD	2.475	0.46	16.691	(44, 53, 51)
553 AR	1.940	0.59	12.680	(74, 60, 47)

5.3.3 Concluding Remarks on Operational Indices

A composite index can, of course, be computed by simply averaging the three sub-indices, or by using a weighting function for averaging. Future experience should develop the indices discussed in this section into a more mature form.

It is hoped that experimentation with the simulation model will be stimulated through the use of these indices of ATC communications performance.

5.4 A Transfer Function Model for Aircraft Flows at Adjacent ATC Sectors

In extending the ATC sector communications simulation model to describe a general ATC network, it is important to characterize the flow of traffic in a sequence of functionally related sectors. This section considers a transfer function model which links the time series of aircraft loading indices in a sector with that in the next, in a single stream of traffic. Box and Jenkins' methods for identification and estimation of transfer function models, discussed in Time Series Analysis, Forecasting and Control, are applied to the modeling of responses generated by a traffic flow from a local control sector to a radar departure control sector, both handling traffic leaving JFK International Airport.

5.4.1 Transfer Functions Representing Dynamic Relationships in a Sequence of Traffic Flow

The dynamic relationship of responses in two adjacent sectors of a single stream of traffic can be represented by figure 5.7, where the "input" series X_t measures the response in the first sector, and the "output" series Y_t measures the response in the second sector. The "dynamic system" is the mechanism by which response in one sector is translated into response in the next.

While the traffic stream is inherently continuous in time, observations are generally available only at discrete intervals. The relationship between Y_t and X_t might thus be approximated by a linear filter of the form

$$\begin{aligned} Y_t &= \nu_0 X_t + \nu_1 X_{t-1} + \nu_2 X_{t-2} + \ldots \\ &= (\nu_0 + \nu_1 B + \nu_2 B^2 + \ldots) X_t = \nu(B) X_t \end{aligned} \tag{5.8}$$

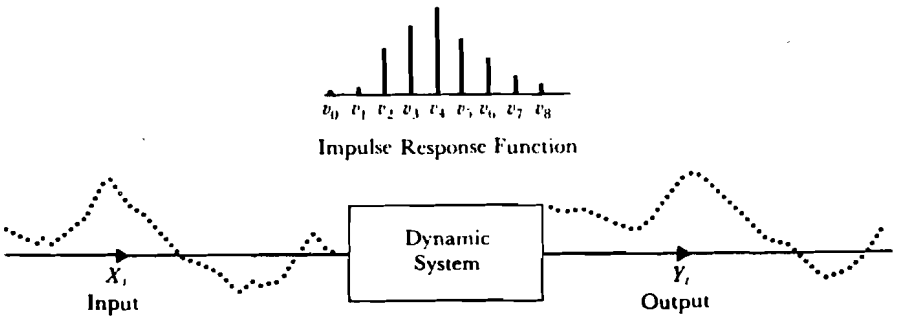

Figure 5.7 A Traffic Stream Through two ATC Sectors

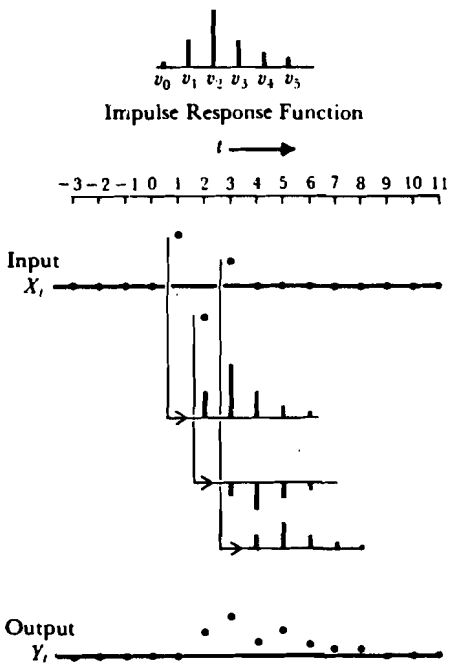

Figure 5.8 Application of the Impulse Response Function

where B is the backwards operator such that $BX_t = X_{t-1}$. The operator $\nu(B)$ is called the "transfer function" of the filter, and the individual weights $\nu_0, \nu_1, \ldots,$ form the "impulse response function". If there are b whole periods of delay before a deviation in the input series affects the output, then $\nu_0, \nu_1, \ldots, \nu_{b-1}$ will be equal to zero. Figure 5.8 shows how the impulse response function translates the input series X_t into the output series Y_t.

The superposition of several traffic streams entering a given sector could be represented as a sum of several transfer functions. For example, if the output sector was fed by two traffic streams, then the combined effect Y_t^* would be

$$Y_t^* = \nu_1(B)X_{1,t} + \nu_2(B)X_{2,t}.$$

In general, an output series can be represented by

$$Y_t^* = \nu_1(B)X_{1,t} + N_t$$

where N_t is noise which may be autocorrelated and is usually assumed to be independent of $X_{1,t}$.

5.4.2 Parameterization of the Model

Just as continuous dynamic systems are often representable by linear differential equations, discrete dynamic systems can often be represented by linear difference equations of the form

$$(1 + \xi_1\nabla + \ldots + \xi_r\nabla^r)Y_t = g(1 + \eta_1 V + \ldots + \eta_s V^s)X_{t-b} \qquad (5.9)$$

where ∇ is the backward difference operator, g is the steady-state gain of the system, and b is the number of time units of delay between input and output. In terms of the backwards operator $B=1-\nabla$, Equation (5.9) can be written as

$$(1 - \delta_1 B - \ldots - \delta_r B^r)Y_t = (\omega_0 - \omega_1 B - \ldots - \omega_s B^s)\, B^b X_t \qquad (5.10)$$

Equation (5.9) or (5.10) defines a transfer function model of order (r,s). The transfer function $\nu(B)$ is given by

$$\nu(B) = \delta^{-1}(B)\ \omega(B)B^b \qquad (5.11)$$

where $\delta(B)$ and $\omega(B)$ are polynomials in B.

The problem of fitting the transfer function model includes determining the order of the polynomials, identifying the delay parameter b, and estimating the parameters. Box and Jenkins have suggested methods useful for these purposes, and the corresponding computer programs are available for use. In the next subsection, the Box-Jenkins techniques are applied to the analysis of responses in two adjacent ATC sectors through which a stream of traffic is passed.

5.4.3 An Example of Modeling

The traffic stream selected for this example is that of departing aircraft from JFK during a 2-hour sample period. At that time, two local control sectors (LC) were in operation, one of which was handling solely departures and fed all traffic to a radar departure controller (DP). The data represent about 48 aircraft in the 2-hour period. The departure controller also handled a small amount of additional traffic from other sources.

The model appropriate to this problem is thus

$$Y_t = \nu(B)X_t + N_t \tag{5.12}$$

where shocks N_t are structured and

$$N_t = \phi^{-1}(B)\,\theta(B)a_t \tag{5.13}$$

where a_t instead are independent identically distributed normal variables with mean zero and variance equal to σ^2 (see Box and Jenkins for reference). The series Y_t is the deviation of the aircraft loading series in the DP sector about its mean level, X_t is a similar quantity for the LC sector, and N_t represents deviations due to additional traffic and random noise. Both aircraft loading series are shown in figure 5.9. The following results from the analysis were obtained:

(1) Both the input and output series, when modeled separately, were well fitted by second order autoregressive models.

Input:

$$X_t = 0.867X_{t-1} - 0.176X_{t-2} + a_t \qquad \bar{X} = 1.153$$

Variance of original series = 0.513
Residual mean square = 0.235

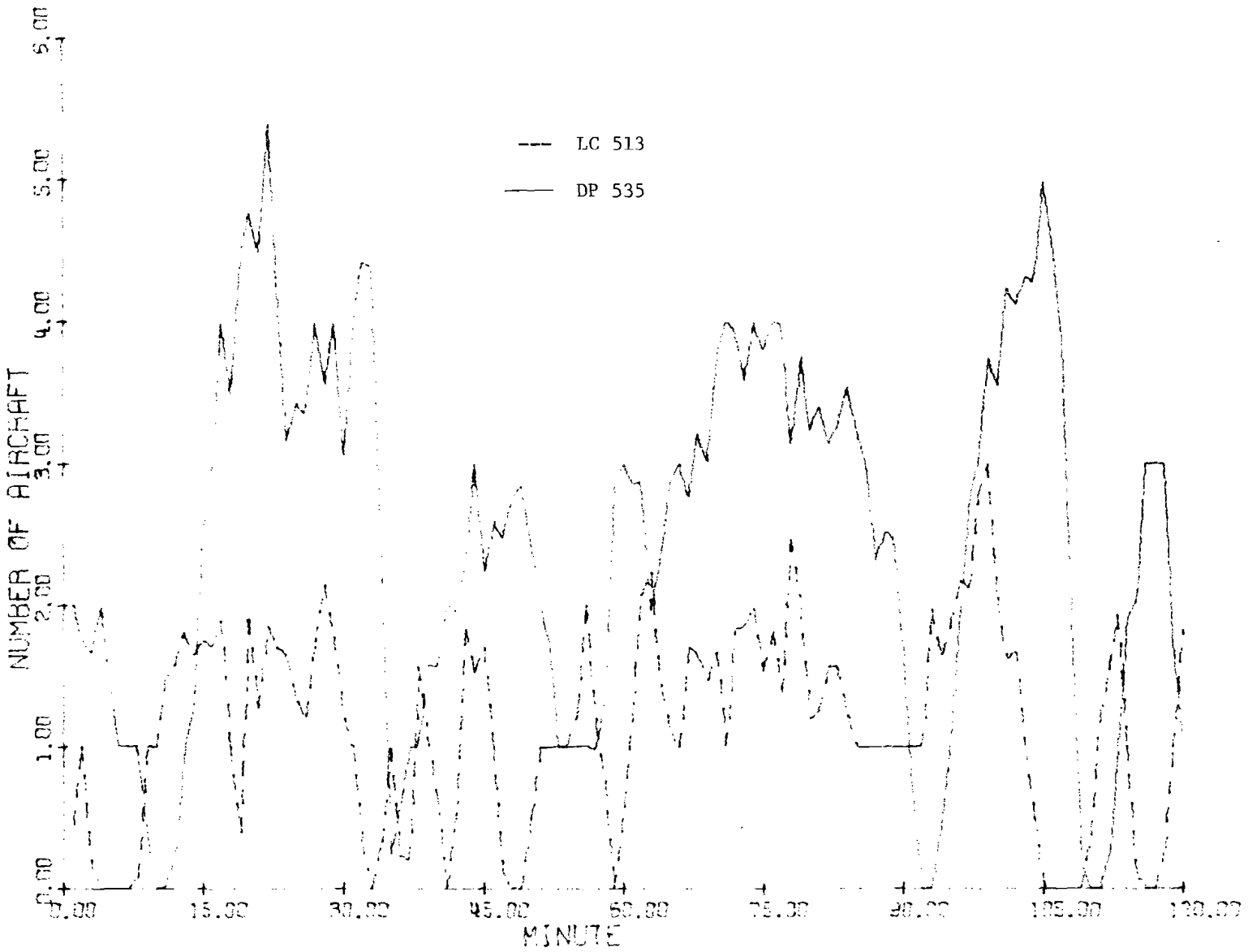

Figure 5.9 Aircraft Loading Time Series for N.Y. LC Sector 513 and DP Sector 535

Output:

$$Y_t = 1.172Y_{t-1} - 0.322Y_{t-2} + b_t \qquad \bar{Y} = 2.463$$

Variance of original series = 1.803
Residual mean square = 0.366

(2) After applying the prewhitening transformation estimated from the above model for the input series, significant cross-correlation was observed between the prewhitened input and output series beginning at a lag of 2 or 3 minutes. The pattern of the estimated impulse response weights suggested a model of order (2,2) or lower; the exact order is discussed below. In addition, the noise remaining in the output series after applying the estimated transfer function was well characterized by an AR (2) model.

(3) In experimenting with various models, the following was observed:

(a) Models with r=2 gave adequate transfer functions for b=2 and b=3. Estimated parameters for s>0 did not appear to be significant in either case. The following model appeared to be appropriate:

$$Y_t = \frac{0.231}{(1-1.58B+.715B^2)} X_{t-2} + \frac{1}{(1-.802B+.118B^2)} a_t$$

Residual mean square = 0.263
(Gain = 1.71)

The impulse response function for this model has weights equal to zero at lags 0 and 1 and then decays as a damped sine wave, eventually satisfying

$$\nu_j - 1.58\nu_{j-1} + .715\nu_{j-2} = 0 \qquad j>2.$$

(b) Models with r=1 and b=2 gave good results. However, with r=1 and b=3, the estimation of the parameters in the non-linear least squares routine was highly unstable, suggesting that a probable factorization existed to a simpler model with r=0.

(c) Models with r=0 gave adequate transfer functions for s=3 beginning at lag 3 and for s=4 at lag 2. These models have impulse response functions with zero values at lags up to b-1 and s+1 values $\nu_b, \nu_{b+1}, \ldots, \nu_{b+s}$ which follow no fixed pattern. The fitted model for b=2 is.

$$Y_t = (.205+.389B+.359B^2+.513B^3+.384B^4)X_{t-2} + \frac{1}{(1-.866B+.164B^2)} a_t$$

Residual mean square = 0.286
(Gain = 1.85)

(d) The parameter estimates for the AR(2) noise model were relatively insensitive to the transfer function selected, at least for those models which appeared to be adequate.

On the basis of this analysis, it appears that series of longer length may be required to discriminate among the various possible transfer function models. Analysis of traffic in sectors for which the transit time is longer might also help to clarify the appropriate form of model. The main advantages of models with r>0 over those with r=0 are: (i) they need fewer parameters; (ii) the impulse response decays smoothly, while the weights in the models with r=0 appear to be very irregular. Confirmation of the values of s selected is also needed.

5.5 Analysis of New York Eight-Hour Data

The analysis of the ATC verbal communications system reported in this and earlier volumes has been largely based on a 2-hour sample of 101 air traffic control positions in the New York metroplex. For more thorough studies on longer periods of time, additional 6 hours of data were obtained for four of these positions. With this additional data, it is possible to investigate more closely some of the behavior inherent to the input stream and to obtain more reliable estimates of system parameters. (For the purpose of illustration only the data and analysis of the traffic flow of an LC sector are included in this section.)

The analysis of data over the 8-hour sample periods, as expected, generates new problems for study. A basic assumption in all of the modeling to date is that the system was approximately stationary throughout the period of observation. This assumption is not tenable for the longer sample period, as is immediately evident from a plot of the 8-hour aircraft loading series for N.Y. sector 515LC shown in figure 5.10. As has been observed by many researchers in the transportation field, transportation systems simply do not remain stationary (even approximately) for more than a couple of hours at a time.

From visual inspection of the aircraft loading series in the four ATC sectors, there appear to be both trends and step shifts in the level of the process. The most likely explanation for such nonstationary behavior lies in the arrival and departure rates of aircraft from the sectors. In particular, the assumption of homogeneous Poisson streams of aircraft entering and leaving the sectors is extremely dubious for the

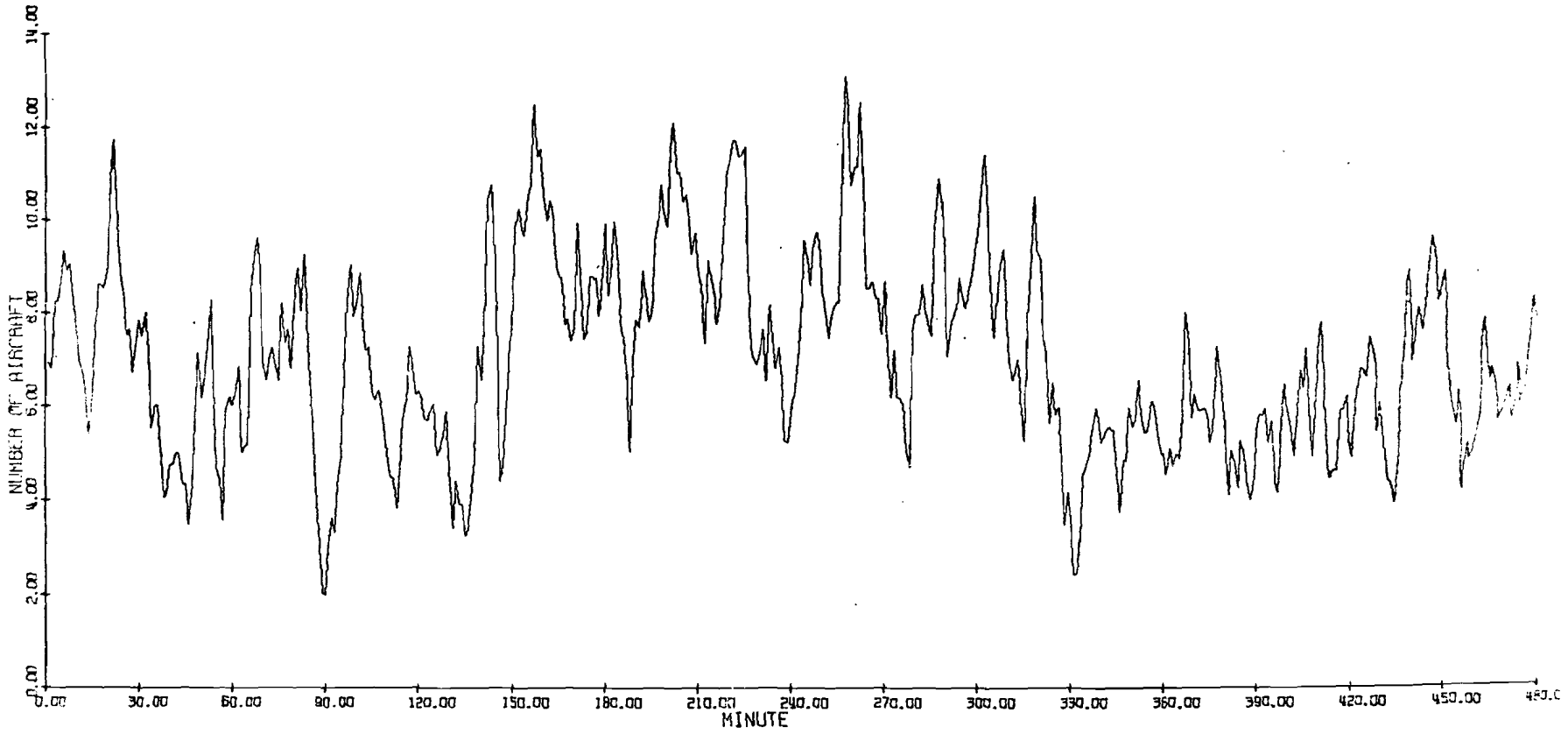

Figure 5.10 Eight-Hour Aircraft Loading Time Series for N.Y. LC Sector 515

entire 8-hour periods. Since these streams are the fundamental driving variables in the system, a careful analysis of their structure over time is of primary importance.

Models of traffic streams, expressed as point processes have been extensively studied over the last 40 years. As early as 1936, Adams (1936, see appendix 5-A for references), postulated a Poisson model for the distribution of counts of vehicles on a highway passing a point in fixed intervals of time. Breiman (1969) formulated a general model for a traffic stream in the time-space domain. He considered the paths of vehicles in a stream over time and space as a "trajectory process" and defined the process to be homogeneous in the direction of a unit vector c if its stochastic properties were invariant under translation along the vector.

Now since most observations of traffic streams are performed by collecting data at a specific point in space or at a specific point in time, streams are commonly studied as point processes along lines parallel to either the time or space axis. It is then only necessary to assume homogeneity in time or space, depending upon the perspective of the observer. In the literature, much analysis of the distribution of vehicles in the stream is based on assuming that the observed point process is stationary.

In the case of streams of aircraft through ATC sectors, the concept of trajectories in the time-space domain does not have as precise a physical meaning as it does in highway traffic. In particular, it is necessary to adopt the meaning of "space" so that all trajectories of aircraft through the sector are considered to originate at a common "point of arrival" and to terminate at a common "point of departure." The slope of individual trajectories, considered to be straight lines connecting an aircraft's point of arrival with its point of departure, represents the aircraft's rate of passage through the sector rather than an actual physical velocity.

In studying each 8-hour stream of aircraft, two point processes will be considered. An "arrival stream" will be considered to be a point process evolving in time where an event occurs at the moment an aircraft initiates the first communication with the sector controller. The "departure stream" will be considered to be a point process evolving in time where an event occurs at the moment an aircraft concludes its final communication with the sector controller. These two streams will have the same stochastic properties if the underlying trajectory process is homogeneous in space.

There are many ways of representing an observed point process graphically. Two of the most useful are shown in figures 5.11 - 5.14 for the arrival and departure streams observed in a local control sector. In each pair of figures displayed on the same page, the top graph plots the cumulative number of events from the start of the sample period against time. The bottom graph shows counts of aircraft arrivals in fixed

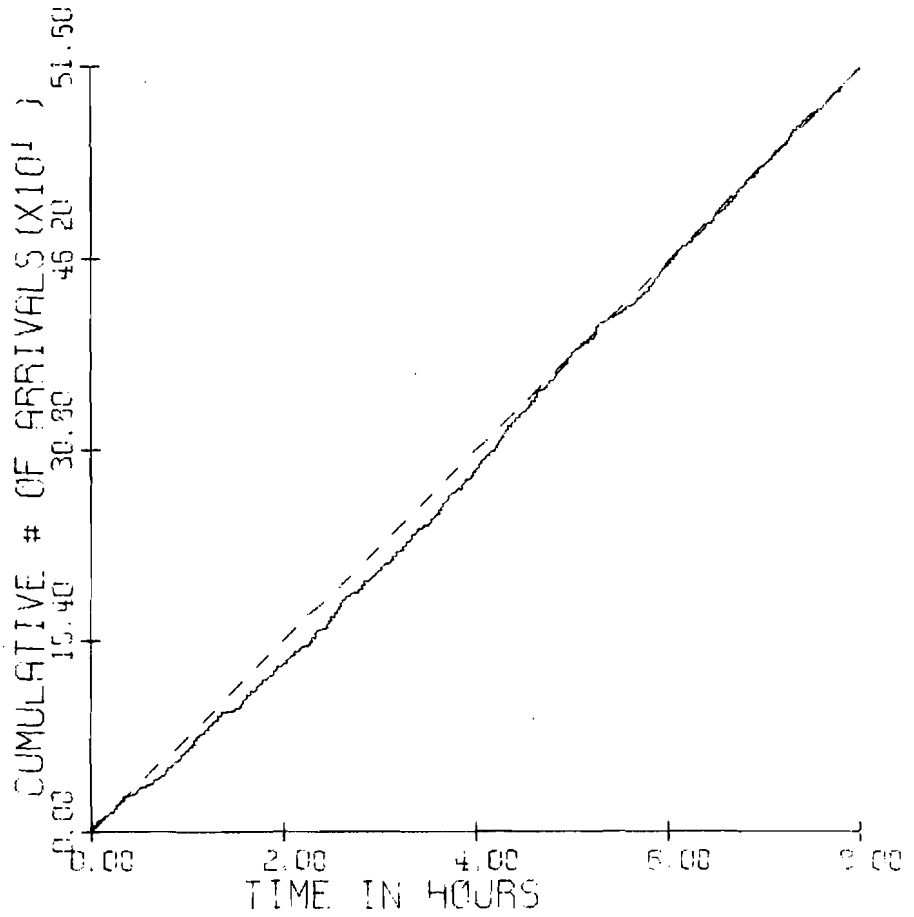

Figure 5.11 Plot of Cumulative Arrival Count vs. Time for LC Sector 515

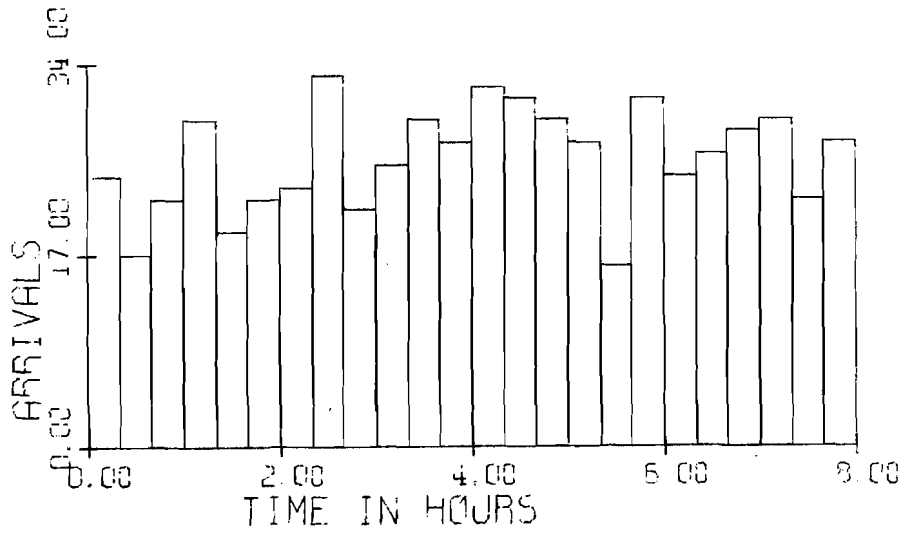

Figure 5.12 Plot of Arrival Count in Twenty-Minute Intervals for LC Sector 515

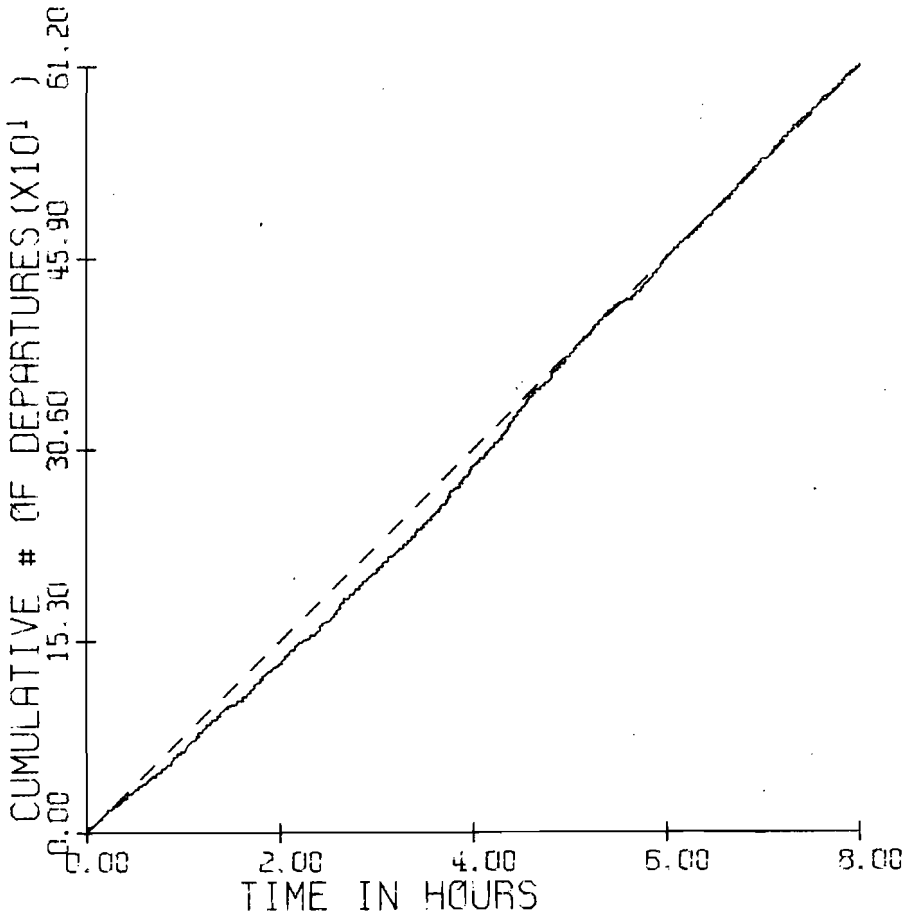

Figure 5.13 Plot of Cumulative Departure Count versus Time for LC Sector 515

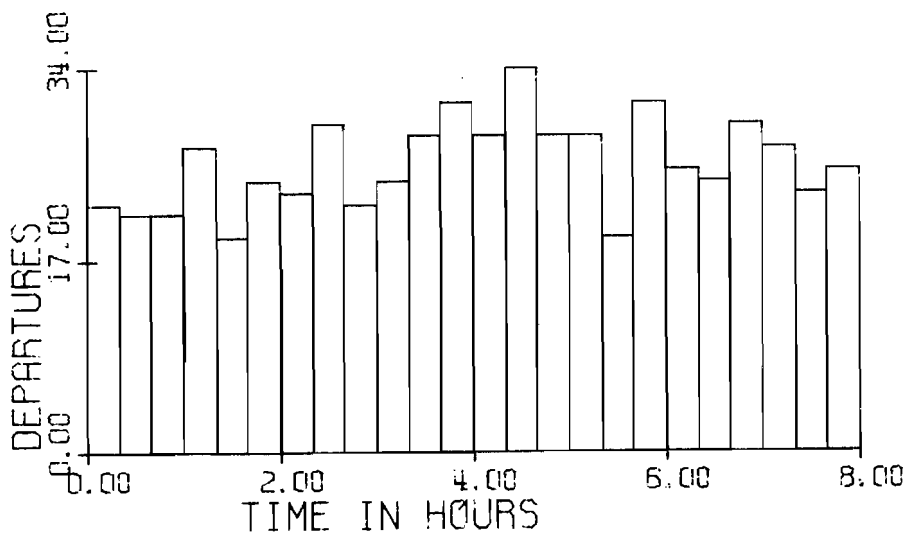

Figure 5.14 Plot of Departure Count in Twenty-Minute Intervals for LC Sector 515

intervals of 20 minutes. The slope of the cumulative count curve and the level of the counts in the bottom graph represent the rate at which aircraft are arriving or departing from the sectors.

Superimposed on the cumulative count graphs is a dotted line which gives the theoretical line for a homogeneous process with an expected number of counts equal to the total number observed. Systematic departure of the observed counts from this theoretical curve indicates nonhomogeneity in the arrival (departure) rate. An investigation of the graphs displayed is being conducted to determine if there is a statistically significant change in rate over the 8-hour periods and to formulate mathematical models for that change.

Another way of studying point processes is to consider the distance in time or space between successive events. Such distances are commonly termed "headways" and in this analysis represent the times between the successive arrivals or departures of aircraft for an ATC sector. The consideration of headways does not involve the arbitrary selection of an interval length which complicates the analysis of counts.

Many models for the distributions of headways have been proposed, all of which assume that the underlying point process is stationary. Edie (1974) has given a general summary of many of these models, which includes renewal models and semi-Markov processes. Taylor et al. (1974) have recently compared several Poisson clustering models, which are a special case of branching renewal processes on one hand and doubly stochastic Poisson processes on the other.

In studying headways, it is important to determine whether successive headways are independent. Significant serial correlation can sometimes be detected by visual inspection of a plot depicting the location of paired values of successive headways. Such plots for the aircraft traffic streams are given in figures 5.15 and 5.17. No significant patterns of serial correlation are easily detectable, but a thorough statistical investigation has not been completed.

An important function related to the distribution of headways is the survivor function $R(x)$ defined by $R(x)=1-F(x)$, where $F(x)$ is the distribution function of the headways. For a homogeneous Poisson process $F(x)$ is the negative exponential distribution and $\log R(x)$ is linear in x. Log survivor functions which are convex correspond to headway distributions which are underdispersed with respect to the negative exponential, while concave log survivor functions correspond to overdispersed headway distributions. The graphs in figures 5.16 and 5.18 show the empirical log survivor functions for the aircraft arrival and departure streams.

It is very important to note that the analysis of alternative models for headways, and for other facets of the ATC requires that the underlying process be stationary, at least to the second order. It is thus important either to be able to isolate periods in which the traffic

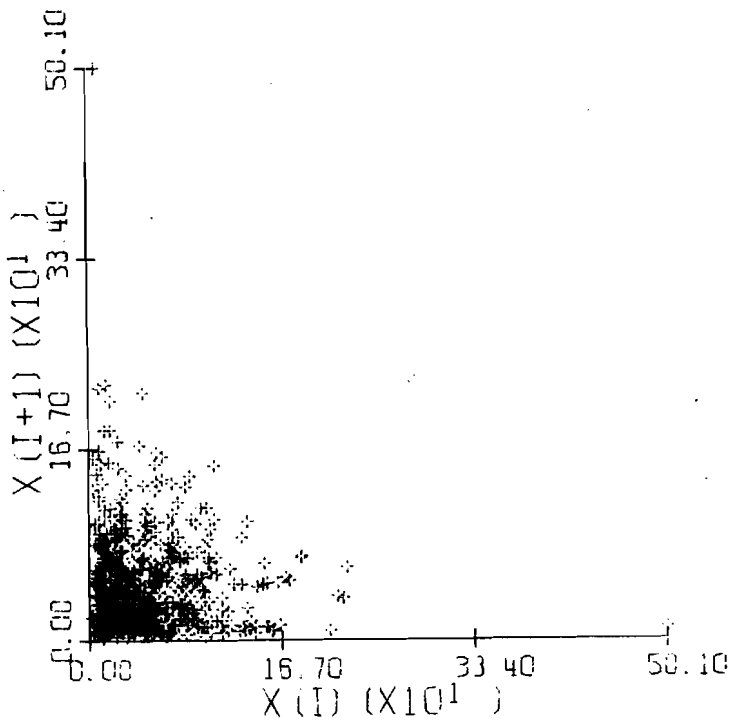

Figure 5.15 Scatter Plot of Pairs of Consecutive Headways in LC Sector 515 Arrival Stream

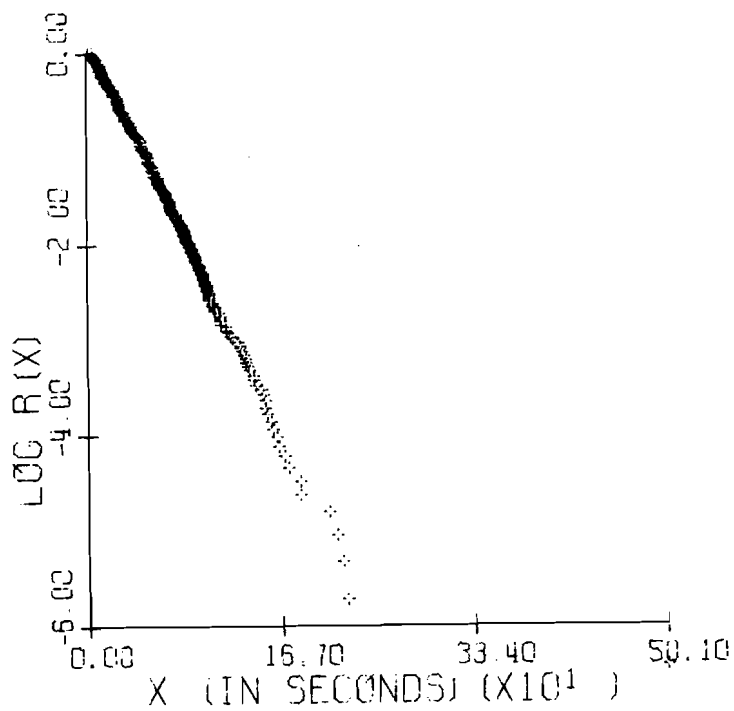

Figure 5.16 Log Survivor Function for Headways in LC Sector 515 Arrival Stream

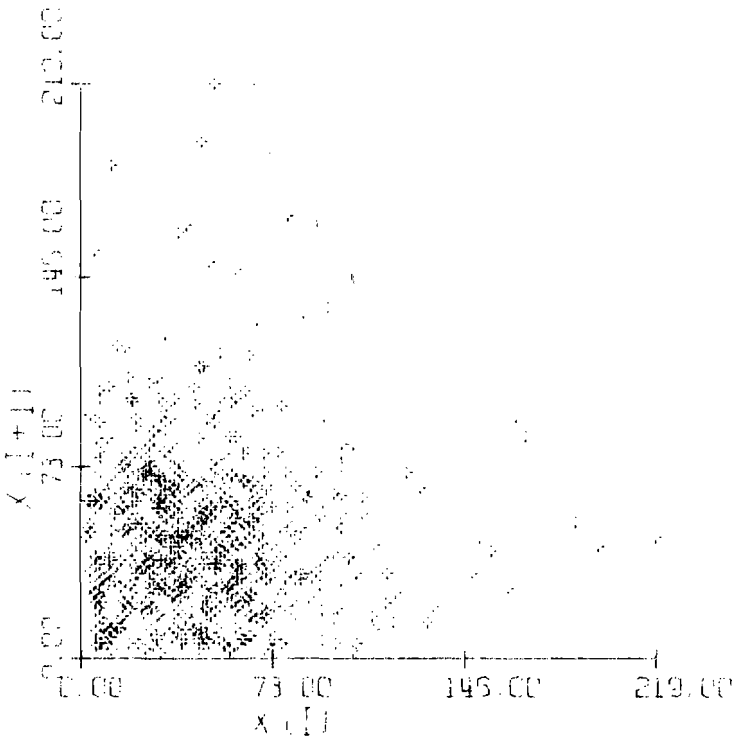

Figure 5.17 Scatter Plot of Pairs of Consecutive Headways in LC Sector 515 Departure Stream

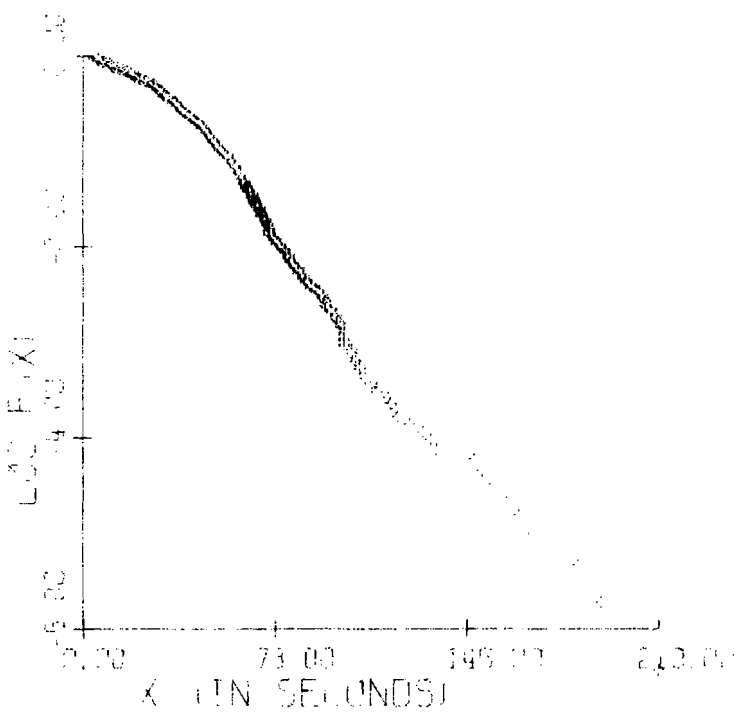

Figure 5.18 Log Survivor Function for Headways in LC Sector 515 Departure Stream

streams are approximately stationary or to manipulate the point process in such a way as to achieve stationarity in a transformed metric. Current research is being conducted in both of these areas. Results from the studies of the 8 -hour sample data can provide much valuable information to the operation of ATC simulations for a longer period of time in the future.

5.6 Queuing Time Analysis and Forecasting for ATC Communications

In section 3.2 we have pointed out some applications, as well as the limitations of the usefulness, of the conventional queuing theory to the analysis of ATC communications. It was found that the expected queuing time per communication transaction derived from the theoretical results can only provide an approximate lower bound to the value realized in an ATC system. Although information obtained from analytic solutions is helpful for selecting the range for simulation experimentation, it is not adequate for providing final estimations.

To pursue further the analysis of the ATC queuing, and to perform forecasting which may be useful for network simulations in the future, in this section a transformation technique useful for modelling queuing time processes is first introduced. Applications of this technique are then illustrated for two simulated ATC communications responses.

A portion of the material presented in this section has been described in more detail in an article by Hsu (D. -A. Hsu, "Queuing Time Forecasting," Civil Engineering Research Report #75-TR-7, Princeton University, July 1975). Readers are referred to this article for technical references and discussions.

5.6.1 Times in System and a Transformation Technique

Although the series of queuing times, recorded in the order of arrivals, of each communication transaction, is an important variable for study, some difficulties are inherent to the analysis of this variable. One of the causes is that the queuing time variable has a nonzero probability at the point of zero. This makes the distribution function difficult to express and unsuitable for analysis. In order to avoid this problem, we select another variable which is closely related to the variable in question for analysis. That is the process of times in system of each communication transaction, defined as the sum of the queuing time and the CT length associated with each communication transaction. Let this series be denoted by $\{W_t^*\}$, where t indicates the arriving order of the CT's.

A preliminary analysis of general processes of times in system suggests that a first order autoregressive model AR(1) is a natural process

for an independent homogeneous arrival system, given certain transformations being made. However, as has been pointed out in an earlier analysis (see subsection 3.2.1), the CT arrivals, in general, do not conform to the independency requirement imposed. Therefore, a general class of models, such as those of autoregressive or moving average or the mixture of both, suggested by Box and Jenkins, should be considered in the modelling of the $\{W_t^*\}$ series just mentioned. Nevertheless, in a recursive transformation procedure, an AR(1) model is still a good starting model. The model can be refined after the transformation having reached an intermediate stage. In mathematical form, an AR(1) model is expressed as

$$(W_t^* - \mu) - \phi(W_{t-1}^* - \mu) = a_t \tag{5.14}$$

where μ is the overall mean of the series W_t^* and a_t is an independent, identically distributed normal variable.

A transformation procedure, useful for the analysis of the series of $\{W_t^*\}$ generated from the ATC simulation model, consists of the following stages:

(a) Fit the time series model specified by Equation (5.14), using the least square estimator for ϕ, to the data generated from a simulation experiment (the simulation run provides a sufficiently large number of observations, with a given set of input parameters), and compute the residuals using the following formula.

$$\hat{a}_t = (W_t^* - \hat{\mu}) - \hat{\phi}(W_{t-1}^* - \hat{\mu}) \quad , \quad t=2, 3, \ldots, N \tag{5.15}$$

where

$$\hat{\mu} = \sum_{t=1}^{N} W_t^*/N$$

$$\hat{\phi} = \frac{\sum_{t=2}^{N} (W_t^* - \hat{\mu})(W_{t-1}^* - \hat{\mu})}{\sum_{t=1}^{N-1} (W_t^* - \hat{\mu})^2}$$

and N = the number of observations contained in the series.

(b) Separate the set of data $\{W_t^*\}$ into, say, 10 equal-size groups in order of their magnitude (i.e. divide the data at the i x 10% quantiles for i = 1,2, ...,10) and label these observations by the ordinal number of the group to which the observations belong. Then classify the $\hat{a}_t$'s into the groups according to the label assigned to W_t^*. (For instance, if W_{15}^* is labeled "5", the a_{15} should be assigned to the fifth group.) Then compute the following:

$$\hat{\sigma}_a^2 = \frac{\sum_{t=2}^{N} \hat{a}_t^2}{N-1} \tag{5.16}$$

and

$$\hat{\sigma}_i^2 = \frac{\sum_{j \varepsilon I_i} \hat{a}_j^2}{N/10} \tag{5.17}$$

where I_i contains the elements which belong to the ith group. Let us further define that

$$R_i = \hat{\sigma}_i / \hat{\sigma}_a \tag{5.18}$$

Then, denoting the transformed values as W_t, the following transformation is suggested:

$$W_t = W_t^* / R_1 \qquad \text{for } t \varepsilon I_1 \tag{5.19}$$

$$W_t = \max_{t' \varepsilon I_{i-1}} \{W_{t'}\} + \left[W_t^* - \max_{t' \varepsilon I_{i-1}} \{W_{t'}^*\}\right] / R_i \text{ for } t \varepsilon I_i, \quad i = 2,3,\ldots$$

(c) Again fit the first order autoregressive model to the series of W_t and obtain a new set of residuals. The distribution of residuals is then examined using the conventional measurements of skewness and kurtosis, i.e. $\hat{\gamma}_1 = \hat{\mu}_3 / \hat{\mu}_4^{1.5}$ and $\hat{\gamma}_2 = (\hat{\mu}_4 / \hat{\mu}_3) - 3$ where $\hat{\mu}_i = 1,2,3,4$, are the ith central moments (with respect to the mean) computed from the data observed. If the value of γ_1 is significantly different from zero (tables and graphs compiled for the tests of $\hat{\gamma}_1$ and $\hat{\gamma}_2$ are available in Snedecor and Cochran, Statistical Method, 1970), the procedure specified by Equations (5.16) - (5.19) and then again (5.15) using the last set of transformed data is suggested to be recursively operated until the value of $\hat{\gamma}_1$ is brought to a satisfactory level.

To examine the adequacy of the expression specified in Equation (5.14), the methods for diagnostic checking suggested by Box and Jenkins in time series modeling can be employed to investigate the nonexistence of the serial correlation in the final residuals. (In the case where a_t is far away from normality these methods should be used with caution. Further study should be performed to investigate the influence of nonnormality upon the testing statistics.) The test statistics available are (i) $r_k^*(\hat{a}_t) = r_k(\hat{a}_t)/\sqrt{n}$, where $r_k(\hat{a}_t)$ is the sample autocorrelation function of the final residuals at lag k and n is the relevant sample size; and (ii) $Q = n \sum_{k=1}^{K} r_k^2(\hat{a}_t)$, where K is a constant which can be adequately determined for each specific case. The first test statistic $r_k^*(\hat{a}_t)$ useful for testing individual autocorrelation coefficients is normally distributed with mean zero and variance one, if the coefficient is virtually zero. In

addition, the second statistic Q is distributed, in our case of first order autoregressive process, as a χ^2 (K-1) variable, where K-1 represents the degree of freedom, and useful as a portmanteau test of all relevant autocorrelation coefficients.

Model modification can then be proceeded using Box-Jenkins techniques. Diagnostic instruments described in the last paragraph can again be used to provide information helpful for identifying the lack of fit and suggesting the direction of modifications.

5.6.2 Examples from ATC Simulations

Two examples are provided in this subsection to illustrate the modeling procedure described earlier in this section. Extensions of the resulting models to the queuing time forecasting are finally mentioned.

Example 1: The series of times in system for each of the communication transactions, denoted by $\{W_t^*\}$ was collected from a simulation exercise of 2-hour period for New York Sector 524 LG (ABE airport) at the historical traffic density (θ = 25 aircraft arrivals/hour). Totally 230 observations were used in the following modeling procedure.

Stage (i): The entire series of $\{W_t^*\}$ were separated into 10 groups, each with size 23, according to their magnitudes in seconds. The 10 partition points are: (4.69, 7.53, 9.53, 12.01, 14.36, 17.03, 21.06, 27.94, 43.23, 98.19), where the last value is the maximum value observed from the sample. An AR(1) model was then fitted to this data. Results of fitting are: $\hat{\phi}$ = 0.8453, $\hat{\sigma}_a^2$ = 96.1309, $\hat{\mu}$ = 20.0514, $\hat{\gamma}_1(\hat{a}_t)$ = 0.3766 and $\hat{\gamma}_2(\hat{a}_t)$= 1.6135. Both $\hat{\gamma}_1(\hat{a}_t)$ and $\hat{\gamma}_2(\hat{a}_t)$ significantly depart from normality. A transformation is therefore needed.

Stage (ii): From Equations (5.16) - (5.18), values of R_i were calculated and found: $(R_1, R_2, \ldots R_{10})$ = (0.8327, 1.1978, 1.4508, 1.2657, 1.7133, 1.6064, 1.4860, 0.8126, 0.8449, 0.6058). These values indicate that the transformation function is convex at the lower range of the W_t^* value and is concave at the higher range. Following the transformation specified by Equation (5.19), we transformed $\{W_t^*\}$ into $\{W_t\}$ and again fitted the AR(1) model into the new set of data. It was found that the new results are: $\hat{\phi}$ = 0.7595, $\hat{\sigma}_a^2$ = 110.4477, $\hat{\mu}$ = 21. 2753, $\hat{\gamma}_1(\hat{a}_t)$ = 0.0623 and $\hat{\gamma}_2(\hat{a}_t)$ = -0.0617. This time both $\hat{\gamma}_1(\hat{a}_t)$ and $\gamma_2(\hat{a}_t)$ conform to the conditions for normality.

Stage (iii): Further examination on the sample autocorrelation function calculated from the residuals indicated that the value of $r_7^*(\hat{a}_t)$ is equal to 3.34 and is significantly different from zero at the 0.01 level. In addition the value of Q, based on the first 24 autocorrelation coefficients, is $Q(a_t) = 230 \sum_{k=1}^{24} r_k^2 (a_t) = 40.23$ being greater than the .025 significance level of a χ^2 variable with 23 degrees of freedom. A mixed autoregressive and moving average model, with the moving average parameter being at the seventh order, was then tried on the data of W_t. The new

estimates of the parameters are: $\hat{\phi} = 0.7400$, $\hat{\theta} = 0.1847$, $\hat{\sigma}_a^2 = 107.4800$, $\hat{\mu} = 21.0410$, $\hat{\gamma}_1(\hat{a}_t) = 0.0511$ and $\hat{\gamma}_2(\hat{a}_t) = -0.0655$. The estimate $\hat{\theta}_7$ is significantly different from zero at the 0.01 level. A further check on the residual autocorrelation function indicated that the value of $r_7^*(\hat{a}_t)$ has been reduced to 0.61 and the value of Q has been brought down to 23.81 which is well below a critical point. The transformation function and the last set of parameter estimates are the essential information for constructing a predictive procedure for queuing times, as will be pointed out in the concluding remarks of this section.

Example 2: A similar series of W_t^* was also collected from a simulation run for New York sector 553 AR (La Guardia airport) at a traffic density equal to 21 aircraft arrivals per hour. Results of modeling on the total of 370 observations are briefly reported below:

Stage (i): The 10 partition points are (6.43, 9.96, 13.39, 16.26, 19.81, 23.32, 27.69, 35.76, 45.11, 131.61). The first fitting of the AR(1) model gave results: $\hat{\phi} = 0.7590$, $\hat{\sigma}_a^2 = 159.3731$, $\hat{\mu} = 24.4667$, $\hat{\gamma}_1(\hat{a}_t) = -0.0942$, and $\hat{\gamma}_2(\hat{a}_t) = 2.4327$. The value of $\hat{\gamma}_2(\hat{a}_t)$ is much too high to be from a normal distribution. Transformations were therefore pursued.

Stage (ii): Estimates of R_i are: $(R_1, R_2, \ldots, R_{10}) = (0.6923, 1.2136, 1.4175, 1.4746, 1.2576, 1.4486, 1.2812, 1.3633, 0.9306, 0.5921)$. The new set of estimates of parameters in the AR(1) model, for the transformed data, are : $\hat{\phi} = 0.6984$, $\hat{\sigma}_a^2 = 185.3221$, $\hat{\mu} = 25.9928$, $\hat{\gamma}_1(a_t) = -0.1811$ and $\hat{\gamma}_2(\hat{a}_t) = 0.3540$. The values of $\hat{\gamma}_2(\hat{a}_t)$ has been substantially reduced and is now well below a critical point.

Stage (iii): Checks on the residual autocorrelation function showed that all $r_k^*(\hat{a}_t)$'s for k = 1, 2, ... 24 are within -2.0 and 2.0, and Q = 15.58. No model modification is proved necessary from these evidences.

5.6.3 Concluding Remarks on Queuing Time Analysis

Given the parameter values of an autoregressive model or a moving average model or the mixture of both, the forecasting of variables generated from the process is a straightforward matter. Confidence limits for forecasts obtained from Box-Jenkins procedure can be transformed back to an original scale using the inverse transformation function determined by $\{R_i\}$. Applications of the procedure illustrated above to queuing network simulations are natural extensions of this work.

APPENDIX 5-A

REFERENCES FOR SECTION 5.5

Adams, W.F. (1936) "Road Traffic Considered as a Random Series," J. Inst. Civil Engrs. 4, pp. 121-130.

Breiman, L. (1969) "Point and Trajectory Processes in One-Way Traffic Flow," Transportation Research 3, pp. 251-264.

Edie, L.C. (1974) "Flow Theories," In Traffic Science, D.C. Gazis, ed. New York, Wiley-Interscience, pp. 1-108.

Taylor, M.A.P., A.J. Miller and K.W. Ogden (1974) "A Comparison of Some Bunching Models in Rural Traffic Flow," Transportation Research 8, pp. 1-10.

CHAPTER 6

CONCLUSIONS AND RECOMMENDATIONS

Discussions on many subjects of interest concerning the properties and the applications of the simulation model of Air Traffic Control Communications have been provided in detail in the previous chapters. However, conclusions scattered over individual chapters or sections need to be gathered to form a complete piece of picture which represents our effort devoted in this volume. Further, recommendations adequately drawn from the research results are also helpful in suggesting future pursuit on the subject of ATC communications. For these reasons we present in the following sections the overview and the outlined recommendations.

6.1 Conclusions

In this volume we have demonstrated the general applicability of the simulation model of ATC communications in both distinct geographical areas and different types of studies. We have compared the communications data of New York versus Houston ARTCC and found that only one or two of the sensitive input variables, most likely the number of communication transactions per aircraft, need to be adjusted in order to perform communications simulations in different geographical areas. Further, we have illustrated the competence of the model in answering many questions of practical interest. The questions investigated include the evaluations of: (i) the communication capacity of a typical sector performing a particular function; (ii) the effects of a tone-burst scheme on delaying communications performance; (iii) the influences of reducing the number of transmissions per communication transaction upon the communication responses. On the first subject, we have determined the communication capacities of nine sector functions in the New York area through the simulation experiments and a special statistical technique in detecting the onset of unstable performance. For the second problem we have evaluated the reduction of communication capacity and the induced extra communications delay at various combined values of the tone duration and the expected number of aircraft arrivals. Finally, for the third question, we are able to provide numerical answers to the relative changes of the communications responses at various rates of reduction on the number of transmissions per communication transaction.

In addition to the research effort devoted to the studies of the communications in a single sector, a network formulation of enroute control sectors has been proposed and a second order Markov chain model is used to describe the transferring of an aircraft from one sector to the next for the New York ARTCC. Estimations of the aircraft arrival rates, the transition patterns, and the flow rates have been studied and empirically illustrated using the New York data. This network modelling effort has prepared for the simulation of ATC communications of a network as a whole.

Other subjects also explored in this volume are: (i) a sensitivity analysis of the expected ATC communications channel utilization with respect to various input variables; (ii) the construction of operational indices for ATC communications performance that simplify the presentation of various responses; (iii) a transfer function model for aircraft flows at adjacent ATC sectors describing the dynamic relationship between the aircraft loadings in two consecutive sectors; (iv) an analysis of New York air traffic data of an 8-hour period in which the traffic density is apparently nonhomogeneous; and (v) a queuing-time analysis and forecasting for ATC communications with potential applications to the simulation of network communications.

6.2 Recommendations

As logical results of the conclusions presented above, several recommendations concerning potential applications of the simulation model in future investigations of ATC communications are provided as the following:

(i) As has been pointed out earlier in section 5.3 of volume III and section 4.1 of this volume, to investigate the ATC communications performance in a metropolitan area such as New York as a whole, which consists of a network of control sectors, is a natural extension of our effort to date. Simulations of a sequence of sectors, each simulation being executed using the constructed model, can be accomplished in accordance with the geographical or functional adjacencies of the sectors. In other words, the aircraft departure stream of one sector is to be used as inputs to the next sector (or several sectors) which is (are) functionally related. Such a network study would be useful in the evaluation of the present performance of a facility and the prediction of performance in hypothetical environments. Thus, experimental results generated from network simulations could serve as valuable aids in decision making processes concerned with changes in the rules of communication operations, the introduction of new communication techniques, expansions or constructions of airports, etc.

(ii) Air Traffic Control performance in distinct geographical areas may be different in one aspect or another, as has been shown in a comparison of New York versus Houston data presented in chapter 2 of this volume. Whether these differences warrant discriminatory requirements on the ATC performance is a question requiring further studies. Here we recommend that the simulation model can help answer the question empirically and comprehensibly.

(iii) As has been illustrated in section 3.4 of this volume, the simulation model provides certain insights about the effectiveness of a change in a performance parameter upon various responses of concern. This type of study, to a certain extent, provides a basis to the cost and benefit analysis of an improvement measure and may serve as a concrete motive to certain government actions.

(iv) Questions concerning the effect of access control techniques, channel allocation methods, etc., upon air/ground communications are being raised by those engaged in the study of satellite mobile communications/surveillance systems. Investigations of the efficiency, flexibility, and capacity of proposed alternatives can be supported by simulation experiments using methodology developed in the present work.

It is the belief of those who have participated in the investigations presented in the four volumes that the simulation model and related extensions can serve as a very powerful tool in analyzing various outcomes associated with many future governmental decisions of concern.